

The Crocodylian, Bird and Turtle Fauna from the Late Eocene Na Duong Basin of Vietnam

Dissertation

der Mathematisch-Naturwissenschaftlichen Fakultät
der Eberhard Karls Universität Tübingen
zur Erlangung des Grades eines
Doktors der Naturwissenschaften
(Dr. rer. nat.)

vorgelegt von
M.Sc Tobias Massonne
aus Saarlouis

Tübingen
2023

Gedruckt mit Genehmigung der Mathematisch-Naturwissenschaftlichen Fakultät der
Eberhard Karls Universität Tübingen.

Tag der mündlichen Qualifikation:

11.06.2024

Dekan:

Prof. Dr. Thilo Stehle

1. Berichterstatter/-in:

Prof. Dr. Madelaine Böhme

2. Berichterstatter/-in:

Prof. Dr. Hervé Bocherens

Acknowledgements

First and foremost, I would like to thank my two supervisors, Prof. Dr. Madelaine Böhme and Prof. Dr. Hervé Bocherens for supervising of my PhD. Without Prof. Dr. Böhme in particular, my thesis would have been absolutely impossible. Not only was she the one who led the excavation that brought to light all the well-preserved fossils I have been privileged to work with over the past few years, but she also made my thesis possible by providing the financial support I needed to complete it. In addition, she has always been an approachable supervisor with interesting ideas and has continued to encourage me to explore new things as my thesis has developed. I will always be grateful to her for those half hour, one-minute discussions. Although not that involved in the subject, Prof Dr. Bocherens was always there for me when there were problems. He was easily accessible and was a great mediator, especially during a problematic period at the beginning of my PhD. He was also a valuable member of my Everest TAC committee, helping me organise the PhD and advising me on postdoctoral plans. Although he was not a direct supervisor of my thesis, I would also like to mention Dr. Erich Weber in this paragraph. He not only supervised my Master's thesis and was a member of the TAC committee. But without him, I probably would not have changed my subject from zoology to palaeontology. We also spent a lot of time discussing science and other things on several field trips. His expertise in many different areas of zoology helped me a lot in my palaeontology research.

In addition to my supervisors, there have been several other important people who have helped me along the way to completing my PhD, supported me during the publication process and kept me on track with my publications. Here I would like to thank four people in particular, in alphabetical order. First and foremost, there is Dr. Felix J. Augustin. Although he is younger than me, I consider him a senior in academia, with his experience in writing and publishing papers. His workload inspired me to work harder as well. Also, his comments on the projects helped me to improve my writing style. Secondly, I am very grateful to PD Dr. Andreas T. Matzke. He really helped me to get on the right track with his writing experience. He does not mince his words and more than once tried to force me to focus on the essentials, which I would say he succeeded in about half of the time. I would also like to thank Dr. Márton Rabi, who supported me in the supervision of my Master's thesis and the first paper of my PhD. His eye for detail was a great help in the past and his open ear for discussion, especially about phylogeny, is still very helpful today. Last but not least, I would like to thank PD Dr. Davit Vasilyan, who also helped me with the supervision of my Master's thesis and the first paper of my PhD. It is thanks to him and Dr. Weber that I switched from zoology to palaeontology. Without his offer to supervise my Master's thesis, I would not have worked on the fossils of the Na Duong Basin at all, and probably would not have done my PhD in palaeontology.

Fortunately, I was also blessed with an amazing working group. We spent a lot of time together, had lunches, drinks in the evenings and talked about all sorts of things.

Nevertheless, most of the time the focus was on science, where I felt encouraged by the others. I hope I was able to give as much back to them as they gave to me. Over the years, people come and go, but I would especially like to thank the following members of the group with whom I spent most of my time, in alphabetical order: Dr. Anna Ayvazyan, Christian Dietzel, Agnes Fatz, Josephina Hartung, Panagiotis Kampouridis, Dr. Uwe Kirscher, Christina Kyriakouli, Dr. Gabriel Ferreira, Dr. Thomas Lechner and Adrian Tröscher. In this context, I would also like to thank Dr. Gustavo Darlim and Jules D. Walter for the great discussions about crocodylians over the past years and Mareike Keysan for her help with office work.

Other people I would like to thank are PD Dr. Ingmar Werneburg, who gave me access to the fossil collection and comparison material for my studies here in Tübingen, and Dr. Alexander Kupfer from the Naturkundemuseum of Stuttgart, who lent me extant specimens under his care for the entire duration of my PhD, which were very helpful as comparison material. I would also like to thank Regina Ellenbracht and Henrik Stöhr, who prepared all of the material I worked with, and especially the latter, who was also never tired of repairing parts of the precious fossils. Moreover, I want to thank Wolfgang Gerber, who helped me with some photos of the fossils and Jürgen Rösinger, who helped me with material from the zoological collection. Another person I would like to thank in this paragraph is a co-author of one of my papers, Dr. Gerald Mayr, whose expertise on birds was an immense help in writing the article on the only bird fossil from the Na Duong Basin. I would also like to thank Dr. Chris Baumann and Dr. Sophie G. Habinger for spell-checking my thesis. Several international scientists have helped me with photographs of comparative material and their expertise, without which this work would have been much more problematic, if not impossible. In particular, I am indebted to the following people, in alphabetical order: Prof. Dr. Christopher A. Brochu, Prof. Dr. Walter G. Joyce and Dr. Jeremy E. Martin.

Finally, I would like to thank all of my countless friends. It is hard for me not to thank everyone personally, as much as I would like to, but please bear in mind that I have to spend money on the copies of this thesis and I would prefer not to go bankrupt because of all the pages I would have to write. I am very grateful for the time we spent together, which helped me a lot to recharge my energy to work on my PhD. I hope that I have been able to return the favour and that you have enjoyed your time with me. Last but not least, I would of course like to thank my family. My parents, who have always given me the opportunity to follow my dreams and do what I want to do, and who have supported me in more ways than I can list here, and my sister, who has always had an open ear for my problems!

It was very difficult for me to put all the people in the 'right' place in this acknowledgement, as I also consider some of my colleagues also to be good friends, and other people on the list are not 'just' friends or colleagues, but have also helped me with my work. But I hope I have found a good balance without making anyone unhappy. Thank you all for this great time!

Table of Contents

Summary	1
Zusammenfassung	3
List of Publications	5
1. Introduction	8
1.1 Geological settings	8
1.1.1 Age of the Na Duong Basin.....	11
1.1.2 Fossils of the Na Duong Basin	12
1.1.3 Ecosystem of the Na Duong Basin	14
1.1.4 Palaeoclimate of the Na Duong Basin.....	16
1.2 Archelosauria of the Na Duong Basin	17
1.2.1 Crocodylians	18
1.2.2 Birds.....	26
1.2.3 Turtles.....	28
1.3 Institutional abbreviations	32
1.4 Objectives	33
2 Results & Discussion	34
2.1 A new species from the Eocene of Vietnam highlights a Southeast Asian alligatoroid lineage and its origin	34
2.2 A new species of <i>Maomingosuchus</i> from the Eocene of Vietnam highlights the phylogenetic relationship of tomistomines and their dispersal from Europe to Asia	40
2.3 A tarsometatarsus from the Eocene of Na Duong – the first Palaeogene fossil bird from Vietnam	46
2.4 A new cryptodire from the Eocene of Vietnam sheds new light on <i>Pan-Trionychidae</i> from Southeast Asia	50
3. Conclusion	57
References	63
Appendix	81

Summary

At the end of the Eocene, there was a major cooling of the Earth, which subsequently led to a great mass extinction, the so-called 'Grande Coupure'. To learn more about the faunal exchange during this extinction event, fossil ecosystems, especially those that existed immediately before and after the cooling at the end of the Eocene, are of enormous importance. The Na Duong Basin in northeastern Vietnam is ideally suited for such a study. The basin is now an active open-cast coal mine, but in the late Eocene it contained small ponds that were in transition to an anoxic lake. A large number of well-preserved fossils of many different plant and animal species have been found in the Na Duong Basin. However, as very little is known about the reptiles and birds of the basin, an important piece of the puzzle to reconstruct this ecosystem was still missing. The main objective of this thesis was therefore to add to the existing knowledge on this aspect. However, the results have not only had the expected impact on the knowledge of the Na Duong Basin as such, but have also improved our understanding of the relationships of crocodylians and turtles of the Palaeogene of East Asia and the ecological connection of three late Eocene basins in Vietnam, Thailand and China.

The first project focused on several individuals of a small alligatoroid of just under 2 m in length. After the description of the material and an intensive phylogenetic analysis, it was possible to show that the fossil was a new species (*Orientalosuchus naduongensis*) and that *O. naduongensis* was the missing link to unite a total of six species that lived in East Asia from the Cretaceous to the Eocene into a new clade: Orientalosuchina. Within this group, the closest relatives of *O. naduongensis* were species from the two late Eocene basins of Maoming (China) and Krabi (Thailand). The results of the phylogeny also allow conclusions to be drawn about the distribution of early alligatoroids at the end of the Cretaceous.

The second project of the thesis focused on the apex predator of the Na Duong Basin, a tomistomine about 3.5 m long. The new species (*Maomingosuchus acutirostris*) was placed in the genus *Maomingosuchus* after a detailed description of the holotype, an almost completely preserved individual, and a comparison with fossil members of the group. Previously, this genus was only known from the Maoming and Krabi basins. The phylogenetic analysis also revealed a much more basal position of *Maomingosuchus* than previously postulated. The new result correlates much better with the age of the genus and also allows the conclusion that representatives of the tomistomines must have reached East Asia at least three times independently of each other.

The third project focused on a tarsometatarsus from an unknown chicken-sized bird species, which was described and compared with extant specimens. The characteristic appearance of the bone is not comparable with any known species. The fossil is one of the few known birds from the Palaeogene of East Asia the only one from the Palaeogene of Vietnam. Thus, despite its incompleteness and relatively poor preservation, the fossil makes an important contribution to our knowledge of the Palaeogene avifauna of East Asia.

The last project described several individuals of a new species of *Pan-Trionychidae* named *Striatochelys baba*. The species is a relatively small representative of *Pan-Trionychidae* with a carapace length of slightly less than 30 cm. Comparison with

extant and fossil representatives of the group as well as a phylogenetic analysis suggests a relationship with the purely Asian extant genus *Nilssonina*. However, *S. baba* shows the greatest similarity to a fossil species from the Maoming Basin.

The results of the thesis show that the three East Asian basins of Na Duong, Maoming and Krabi had a closely related crocodylian and turtle fauna. Representatives of Orientalosuchina and the genus *Maomingosuchus* were found in each of these basins, and the turtle genus *Striatochelys* was represented at least in Na Duong and Maoming. These results indicate that at some point in the Palaeogene there must have been a connection between the three basins, allowing faunal exchange. On the other hand, the results also suggest that either there must have been some kind of physical barrier before the end of the Eocene that allowed the basins to be separated and resulting in the divergence of the herpetofauna. Alternatively, the closely related species may be chronospecies.

With regard to the faunal exchange of the Reptilia groups studied, a definite conclusion is limited by the lack of East Asian assemblages that can be dated with certainty immediately after the 'Grande Coupure'. Orientalosuchina occur only from the Late Cretaceous to the late Eocene, but are absent from Miocene assemblages, possibly indicating, that this group did not survive the 'Grande Coupure' and was possibly replaced by the genus *Alligator*, which dispersed from North America towards Asia around this time. Tomistomines have survived to the present day, but the *Maomingosuchus* lineage is not found in Miocene assemblages, instead much larger tomistomines such as *Penghusuchus pani* are present in East Asia at this time, probably from a second dispersal event from Europe. *Striatochelys baba* may represent a stem member of the extant *Nilssonina*, as indicated by direct comparison with extant species and the phylogenetic analysis. If this is true, this species or close relatives survived the cooling at the beginning of the Oligocene. Unfortunately, the bird fossil is too poorly preserved and other fossils from East Asia are too sparse to draw any conclusions about its survival of the 'Grande Coupure'.

Zusammenfassung

Am Ende des Eozäns gab es eine starke Abkühlung der Erde, was im Anschluss zu einem großen Massenaussterben, dem sogenannten „Grande Coupure“ führte. Um mehr über den Faunenaustausch, der ihm Zuge dieses Aussterbeereignisses stattfand, herauszufinden, sind fossile Ökosysteme, insbesondere diejenigen die unmittelbar vor und nach der Abkühlung am Ende des Eozäns existierten, immens wichtig. Eine Untersuchung eben jenes Zeitraumes ermöglicht das Na Duong Becken im Nordosten Vietnams. Heutzutage ist das Becken ein aktiver Kohletagebau, im späten Eozän erstreckten sich hier allerdings kleine Tümpel, die sich im Übergang zu einem anoxischen See befanden. Im Na Duong Becken wurde eine große Anzahl gut erhaltener Fossilien von zahlreichen verschiedenen Pflanzen- und Tierarten gefunden. Da bislang jedoch nur sehr wenig über die Reptilien und Vögel des Beckens bekannt ist, fehlten noch wichtige Puzzlestücke zur Rekonstruktion dieses Ökosystems. Das Hauptziel der vorliegenden Thesis war es deshalb das vorhandene Wissen in diesem Aspekt zu erweitern. Die Ergebnisse hatten jedoch nicht nur einen erwarteten Effekt auf das Wissen über das Na Duong Becken als solches, sondern erweiterten ebenfalls unser Verständnis über die Verwandtschaftsverhältnisse der Krokodile und Schildkröten des Paläogens Ostasiens und außerdem die ökologische Verbindung dreier späteoziäner Becken Vietnams, Thailands und Chinas.

Das erste Projekt beschäftigte sich mit mehreren Individuen eines kleinen Alligatoroiden von gerade einmal knapp 2 m Länge. Nach der Beschreibung des Materials und einer intensiven phylogenetischen Analyse konnte gezeigt werden, dass es sich bei dem Fossil um eine neue Art (*Orientalosuchus naduongensis*) handelte und dass *O. naduongensis* das fehlende Bindeglied darstellte mit dem sechs Arten, die von der Kreidezeit bis ins Eozän Ostasiens lebten, zu einer neuen Gruppe zusammengeführt werden konnten, den Orientalosuchina. Innerhalb dieser Gruppe waren die nächsten Verwandten von *O. naduongensis*, Arten aus den beiden ebenfalls späteoziänen Becken von Maoming (China) und Krabi (Thailand). Die Ergebnisse der Phylogenie ermöglichen des Weiteren Rückschlüsse auf die Verbreitung der frühen Alligatoroiden am Ende der Kreidezeit.

Das zweite Projekt der Thesis beschäftigte sich mit dem Apex Prädator des Na Duong Beckens, einem etwa 3,5 m langem Tomistominen. Die neue Art (*Maomingosuchus acutirostris*) konnte nach einer intensiven Beschreibung des Holotypus, bei dem es sich um ein nahezu vollständig erhaltenes Individuum handelt, und einem Vergleich mit fossilen Vertretern der Gruppe, der Gattung *Maomingosuchus* zugeordnet werden. Vertreter dieser Gattung waren zuvor nur aus dem Maoming und Krabi Becken bekannt. Die phylogenetische Analyse konnte des Weiteren eine wesentlich basalere Stellung von *Maomingosuchus* feststellen, als früher postuliert wurde. Das neue Ergebnis passt dabei wesentlich besser zum Alter der Gattung und ermöglicht zusätzlich die Schlussfolgerung, dass Vertreter der Tomistomine Ostasiens mindestens dreimal unabhängig voneinander erreicht haben müssen.

Das dritte Projekt behandelte einen Tarsometatarsus einer unbekanntes Vogelart, von der Größe eines Huhns, der beschrieben und mit rezenten Vertretern verglichen wurde. Das charakteristische Aussehen des Knochens ist dabei mit keiner bislang bekannten Art vergleichbar. Bei dem Fossil handelt es sich um einen der wenigen Vögel die aus dem Paläogens Ostasiens bekannt sind und stellt gleichzeitig das einzige Individuum aus dem Paläogen Vietnams dar. Dadurch liefert das Fossil trotz

seiner Unvollständigkeit und der relativ schlechten Erhaltung einen wichtigen Beitrag zu unserem Wissen über die paläogene Vogelwelt Ostasiens.

Das letzte Projekt beschrieb mehrere Individuen einer neuen Art von *Pan-Trionychidae* mit dem Namen *Striatochelys baba*. Bei der Art handelt es sich um einen relativ kleinen Vertreter der *Pan-Trionychidae* mit einer Carapaxlänge von etwas unter 30 cm. Der Vergleich mit rezenten und fossilen Vertretern der Gruppe sowie eine phylogenetische Analyse legen eine Verwandtschaft mit der rein asiatischen rezenten Gattung *Nilssonina* nahe. Die größte Ähnlichkeit weist *S. baba* aber mit einer fossilen Art des Maoming Beckens auf.

Die Gesamtheit der Ergebnisse der Thesis zeigen, dass die drei ostasiatischen Becken von Na Duong, Maoming und Krabi eine nahverwandte Krokodil- und Schildkrötenfauna besaßen. In jedem dieser Becken, existierten Vertreter der *Orientalosuchina* und der Gattung *Maomingosuchus* und die Schildkrötengattung *Striatochelys* ließ sich bislang zumindest in Na Duong und Maoming nachweisen. Diese Ergebnisse deuten darauf hin, dass es irgendwann im Paläogen eine Verbindung zwischen den drei Becken gegeben haben muss durch die ein Faunenaustausch möglich war. Auf der anderen Seite bedeuten die Ergebnisse aber auch, dass es vor dem Ende des Eozäns entweder physische Barrieren gegeben haben muss, die eine Separierung der Becken gefolgt von einer Spezifizierung der Herpetofauna ermöglicht haben, oder dass es sich bei den nah verwandten Arten um Chronospezies handelt.

Was den Faunenaustausch der untersuchten Gruppen der Reptilia angeht, so ist eine eindeutige Schlussfolgerung durch das weitestgehende Fehlen ostasiatischer Fundstellen, die mit Sicherheit auf die Zeit unmittelbar nach dem „Grande Coupure“ datiert werden können, begrenzt. *Orientalosuchina* kommen nur von der späten Kreidezeit bis zum späten Eozän vor, fehlen aber in miozänen Fundstellen, was möglicherweise darauf hindeutet, dass diese Gruppe den „Grande Coupure“ nicht überlebte und möglicherweise durch die Gattung *Alligator* ersetzt wurde, die wahrscheinlich etwa zu dieser Zeit von Nordamerika nach Asien einwanderte. Tomistomine haben zwar bis heute überlebt, aber die *Maomingosuchus* Linie ist in miozänen Fundstellen nicht mehr vertreten. Stattdessen sind viel größere Vertreter der Gruppe wie *Penghusuchus pani* zu dieser Zeit in Ostasien anzutreffen, die wahrscheinlich von einem zweiten Einwanderungsereignis aus Europa stammen. Basierend auf der phylogenetischen Analyse und dem Vergleich mit rezenten Vertretern, könnte es sich bei *S. baba* um eine Stammart der heutigen *Nilssonina* handeln. Wenn das zutrifft, hat diese Art oder zumindest nahe Verwandte die Abkühlung am Anfang des Oligozäns überlebt. Leider ist das Vogelfossil zu schlecht erhalten und andere Fossilien aus Ostasien sind zu spärlich, um Rückschlüsse auf das Überleben des Vogels nach dem „Grande Coupure“ zu ziehen.

List of Publications

Publications included in this thesis

The following publications have been published by peer reviewed international journals and can be found in the Supplementary part of this thesis. The papers are listed here and in the Supplementary in chronological order.

- 1) **Massonne, T.**, Vasilyan, D., Rabi, M. & Böhme, M. 2019. A new alligatoroid from the Eocene of Vietnam highlights an extinct Asian clade independent from extant *Alligator sinensis*. *PeerJ* **7**:e7562, 1–60.

<http://dx.doi.org/10.7717/peerj.7562>

- 2) **Massonne, T.**, Augustin, F. J., Matzke, A. T., Weber, E. & Böhme, M. 2021. A new species of *Maomingosuchus* from the Eocene of the Na Duong Basin (northern Vietnam) sheds new light on the phylogenetic relationships of tomistomine crocodylians and their dispersal from Europe to Asia. *Journal of Systematic Palaeontology*, **19**(22), 1551–1585.

<https://doi.org/10.1080/14772019.2022.2054372>

- 3) **Massonne, T.**, Böhme, M. & Mayr, G. 2022. A tarsometatarsus from the upper Eocene Na Duong Basin – the first Palaeogene fossil bird from Vietnam. *Alcheringa: An Australasian Journal of Palaeontology*, **46**(3-4), 291–296.

<https://doi.org/10.1080/03115518.2022.2126010>

- 4) **Massonne, T.**, Augustin, F. J., Matzke, A. T. & Böhme, M. 2023. A new cryptodire from the Eocene of the Na Duong Basin (northern Vietnam) sheds new light on *Pan-Trionychidae* from Southeast Asia. *Journal of Systematic Palaeontology*, **21**(1), 2217505, 1–25.

<https://doi.org/10.1080/14772019.2023.2217505>



Erklärung nach § 5 Abs. 2 Nr. 8 der Promotionsordnung der Math.-Nat. Fakultät

-Anteil an gemeinschaftlichen Veröffentlichungen-

Nur bei kumulativer Dissertation erforderlich!

Declaration according to § 5 Abs. 2 No. 8 of the PhD regulations of the Faculty of Science

-Collaborative Publications-

For Cumulative Theses Only!

Last Name, First Name: Massonne, Tobias

List of Publications

1. Massonne, T., Vasilyan, D., Rabi, M. & Böhme, M. 2019. A new alligatoroid from the Eocene of Vietnam highlights an extinct Asian clade independent from extant *Alligator sinensis*. *PeerJ* 7:e7562, 1–60.
2. Massonne, T., Augustin, F. J., Matzke, A. T., Weber, E. & Böhme, M. 2021. A new species of *Maomingosuchus* from the Eocene of the Na Duong Basin (northern Vietnam) sheds new light on the phylogenetic relationship of tomistomine crocodylians and their dispersal from Europe to Asia. *Journal of Systematic Palaeontology*, 19(22), 1551–1585.
3. Massonne, T., Böhme, M. & Mayr, G. 2022. A tarsometatarsus from the upper Eocene Na Duong Basin – the first Palaeogene fossil bird from Vietnam. *Alcheringa: An Australasian Journal of Palaeontology*, 46(3-4), 291–296.
4. Massonne, T., Augustin, F. J., Matzke, A. T. & Böhme, M. 2023. A new cryptodire from the Eocene of the Na Duong Basin (northern Vietnam) sheds new light on *Pan-Trionychidae* from Southeast Asia. *Journal of Systematic Palaeontology*, 21(1), 2217505, 1–25.

Nr.	Accepted publication yes/no	List of authors	Position of candidate in list of authors	Scientific ideas by the candidate (%)	Data generation by the candidate (%)	Analysis and Interpretation by the candidate (%)	Paper writing done by the candidate (%)
1	yes	4	1	70	80	80	70
2	yes	5	1	90	90	80	80
3	yes	3	1	80	70	70	80
4	yes	4	1	80	80	90	90

I confirm that the above-stated is correct.

Date, Signature of the candidate

I/We certify that the above-stated is correct.

Date, Signature of the doctoral committee or at least of one of the supervisors

Further Publications not included in this thesis but written during the PhD

The following publications have been published by peer reviewed international journals and are listed here in chronological order.

- 5) Walter, J., Darlim, G., **Massonne, T.**, Aase, A., Frey, E. & Rabi, M. 2022. On the origin of Caimaninae: insights from new fossils of *Tsoabichi greenriverensis* and a review of the evidence. *Historical Biology*, **34**(4), 580–595.

<https://doi.org/10.1080/08912963.2021.1938563>

- 6) **Massonne, T.** & Böhme, M. 2022. Re-evaluation of the morphology and phylogeny of *Diplocynodon levantinum* Huene & Nikoloff, 1963 and the stratigraphic age of the West Maritsa coal field (Upper Thrace Basin, Bulgaria). *PeerJ* **10**:e14167, 1–35.

<http://dx.doi.org/10.7717/peerJ.14167>

1. Introduction

In recent decades, we have been confronted with a global mass extinction, probably the sixth major mass extinction event in Earth's history, affecting almost all groups of animals and plants (Wagler, 2011 and references therein). Although all parts of the world are affected, some areas are of particular conservation value because they have a much greater biodiversity than other regions of comparable size. These regions are known as biodiversity hotspots. The term was first used by Myers (1988), who considered only 10 special areas. Since then, the number of hotspots has steadily increased and currently includes 36 areas (Myers, 1990; Myers et al., 2000, Mittermeier et al., 2011; Noss et al., 2015). One of these hotspots is located in Southeast Asia and includes the mainland countries of Cambodia, Laos, Malaysia, Myanmar, Thailand and Vietnam. Vietnam is the 25th most biodiverse country in the world, with more than 200 new plant species, more than 84 new vertebrate species and more than 500 new invertebrate species discovered between 1992 and 2004 (Sterling & Hurley, 2005 and references therein). But it was not only in historical times that Vietnam's flora and fauna showed such enormous biodiversity. Excavations between 2008 and 2012 in northeastern Vietnam uncovered a long-forgotten late Eocene ecosystem with several new taxa, opening a window into the period just before the 'Grande Coupure' at the Eocene-Oligocene boundary, the Na Duong Basin (Costa et al., 2011 and references therein; Böhme et al., 2011, 2013).

1.1 Geological settings

The geology of northern Vietnam is strongly influenced by the Red River Fault Zone (RRFZ) (also known as the Ailao-Shan-Red River Fault Zone, ASRRFZ), which separates the terranes of South China and Indochina. The RRFZ originates in Tibet and extends over 1000 km southeast into the Tonkin Gulf of the South China Sea (Tapponier et al., 1990; Leloup et al., 1995, 2001; Clift & Sun, 2006; Wysocka, 2009; Fyhn et al., 2018; Böhme et al., 2011; Wysocka et al., 2018, 2020, 2022). The fault zone was probably formed by the collision of the Indian subcontinent with Asia about 50 Ma ago and had a major phase of activity between the late Eocene and early Miocene (Tapponier et al., 1986, 1990; Leloup et al., 1995, 2001; Pubellier et al., 2003; Clift & Sun, 2006; Böhme et al., 2011; Mazur et al., 2012; Fyhn & Phach, 2015), but

see also Searle (2006) for a different time estimate. Although the RRFZ is the main fault zone in northern Vietnam, there are several smaller sub-parallel rift systems of similar age, e.g. the Cao Bang-Tien Yen Fault Zone (CB-TYFZ) (Pubellier et al., 2003; Wysocka, 2009; Böhme et al., 2011, 2013; Wysocka et al., 2020) (Fig. 1).

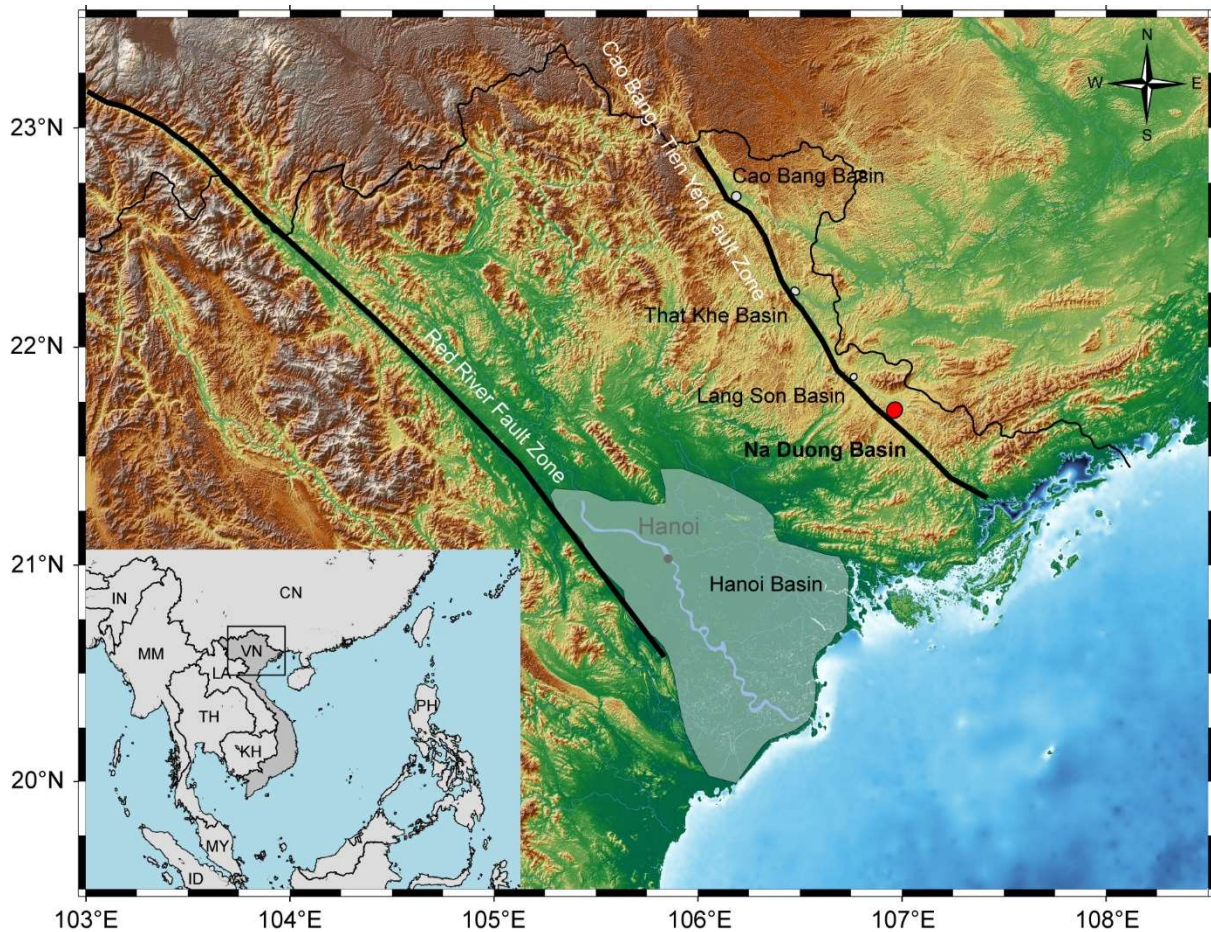


Figure 1. Map of northern Vietnam showing the Hanoi, Cao Bang, That Khe, Long Son and Na Duong Basin, as well as the Red River Fault Zone and the Cao-Bang-Tien Yen Fault Zone.

The CB-TYFZ is located about 150 km northeast of the RRFZ and consists of four Palaeogene sedimentary pull-apart basins, i.e. Cao Bang, That Khe, Lang Son and Na Duong (in order from northwest to southeast) (Wysocka, 2009; Böhme et al., 2011, 2013; Fyhn et al., 2018; Wysocka et al., 2018, 2020; Thanh et al., 2019) (Fig. 1). The basins have a base of Mesozoic and Palaeozoic rocks and are filled with series of different siliciclastic sediments (Böhme et al., 2011, 2013; Wysocka et al., 2020). The succession of basins can be divided into three formations: Cao Bang, Na Duong and Rin Chua (Böhme et al., 2011; Wysocka et al., 2020). These formations differ in composition, thickness and age. The Cao Bang Formation consists mainly of conglomerate, gravel and sandstone and has a maximum thickness of 150 m, while

the intermediate Na Duong Formation consists mainly of sandstone, siltstone, claystone and coal seams and has a maximum thickness of 240 m. The overlying Rin Chua Formation, on the other hand, consists mainly of claystone and siltstone and is 300 m thick (Wysocka, 2009; Böhme et al., 2011, 2013; Wysocka et al., 2018, 2020).

Both the Na Duong and Rin Chua Formations are most visible in the Na Duong Basin, which covers an area of 45 km² and is best accessed via the Na Duong Coal Mine (Fig. 2). In 2012, the upper 140 m of the Na Duong Formation and the lower 80 m of the Rin Chua Formation were exposed (Böhme et al., 2013). However, the thickness of these exposed areas is constantly changing due to active open pit mining. Böhme et al. (2011) reported only 120–135 m for the Na Duong Formation and 35–40 m for the Rin Chua Formation. In the Na Duong Formation, lignites, lignitic marls, carbonate,

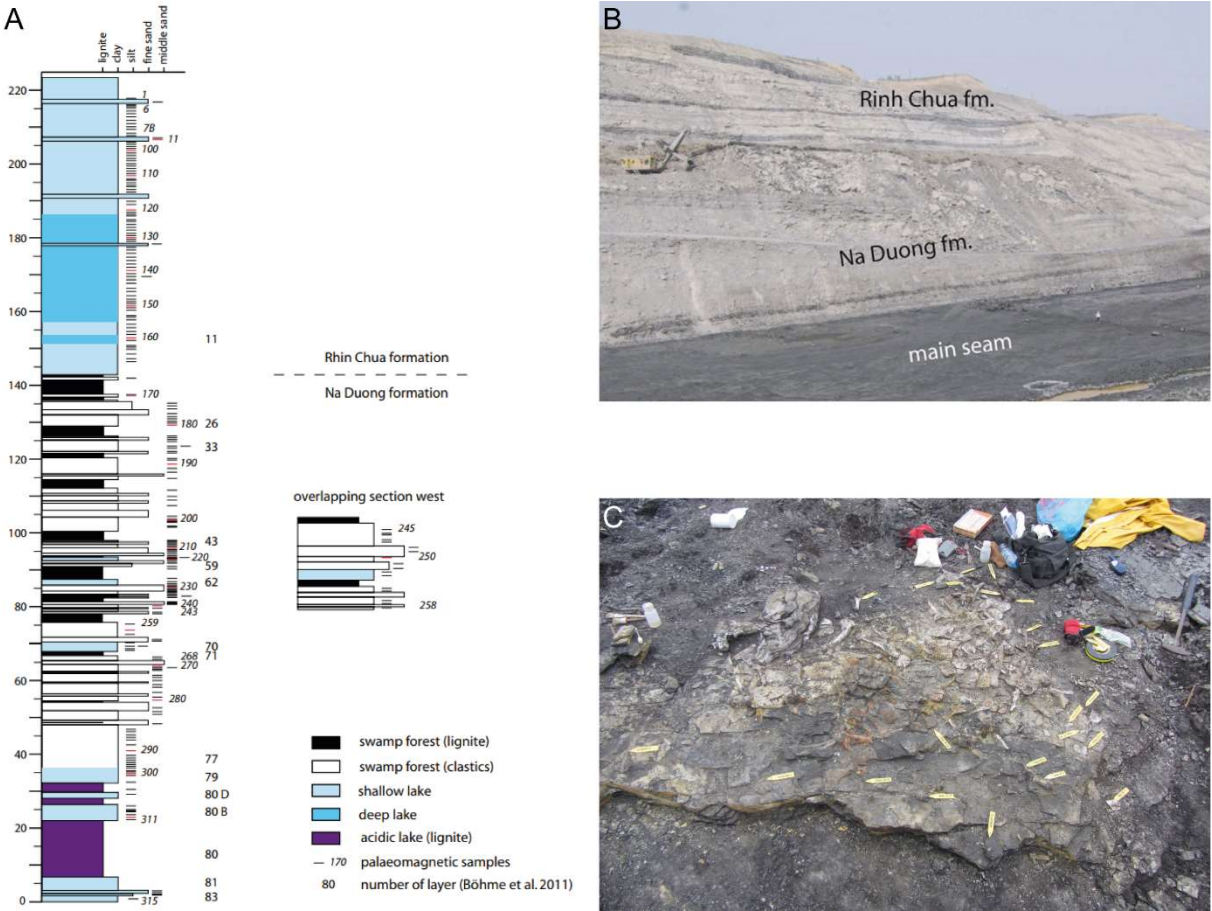


Figure 2. A, Sedimentology log of the Na Duong coal mine (Böhme et al., 2013). **B**, Overview of the Na Duong coal mine, showing the Na Duong formation with the overlying Rin Chua formation and the main coal seam (layer 80) (altered after Böhme et al., 2011). **C**, field photo taken during the excavation of a crocodylian (© Madelaine Böhme).

claystones, marls, marly siltstones and sandstones alternate, whereas in the Rin Chua Formation there are no lignite seams and claystones alternating with pyritic marls

dominate (Wysocka, 2009; Böhme et al., 2011, 2013). While the composition and thickness of the formations are well known, it is more difficult to estimate their age (Wysocka, 2009; Böhme et al., 2011, 2013; Wysocka et al., 2018, 2020).

1.1.1 Age of the Na Duong Basin

The age of the Cao Bang, Na Duong and Rin Chua Formations has been hotly debated in the past. Some authors argued for a Miocene to Pliocene age based on macroflora, molluscs and mammals (e.g. Dzanh, 1995, 1996; Wysocka, 2009), while Khúc et al. (2005 and references therein) dated the Cao Bang, Na Duong and Rin Chua Formations to the Eocene and Oligocene based on palynomorphs (spores and pollen). In the last decade, new studies focusing on age correlation with the origin of the RRFZ, as well as studies on biostratigraphy i.e. palynomorphs and macrofossils (macroflora and macrofauna), confirmed the older age estimate (late Eocene to early Oligocene) for the Na Duong and Rin Chua Formations (Böhme et al., 2011, 2013; Ducrocq et al., 2015; Fyhn & Phach, 2015; Fyhn et al., 2018; Wysocka et al., 2018, 2020). Based on the evolutionary status of a rhinocerotid and an anthracotheriid, Böhme et al. (2013) correlated the vertebrate-bearing horizon of the Na Duong Basin with the Naduan Chinese Land Mammal Age (NCLMA). The NCLMA is calibrated with palaeomagnetic data and belongs to the Ulangochuian at 40–37 Ma (Wang et al., 2019). This led to a correlation of the Na Duong Formation with the Bartonian to late Priabonian (39–35 Ma). Ducrocq et al. (2015) reached a similar conclusion based on anthracotheriids and dated the Na Duong Basin to the early/middle late Eocene. Another approach, based on palaeomagnetic studies by Böhme et al. (2013), could not provide results for the Na Duong Formation and the lower part of the Rin Chua Formation due to remagnetisation after tilting. The occurrence of this problem prevented any magnetostratigraphic interpretation, at least for the Na Duong section. In contrast, the results from the top 40 m of the Rin Chua Formation showed the original magnetisation and were in good agreement with an Eocene inclination. Wysocka et al. (2018) focused on palynomorphs from the Cao Bang Basin and found the most similarities with palynomorphs from the early Oligocene. Pollen assemblages from the Na Duong and Rin Chua Formations showed the greatest similarities with pollen from several Southeast Asian basins, especially

pollen from the Shangcun Formation of the Maoming Basin. This suggests an early Oligocene age for the Na Duong and Rin Chua Formations (Wysocka et al., 2020).

1.1.2 Fossils of the Na Duong Basin

In the Cao Bang Basin, fossil vertebrates are rather rare, with only disarticulated fish remains found along with five unionid and two gastropod species (Böhme et al., 2011; Neubauer et al., 2012; Schneider et al., 2013). The Rin Chua Formation is also largely devoid of vertebrates, with only fragmented fish remains of seven cyprinid taxa, but yields several gastropods and bivalves (Böhme et al., 2013). Most of the Na Duong Formation also has a relatively small number of vertebrate fossils (isolated fish remains and crocodylian teeth), as well as some invertebrates, i.e. bivalves (Unionidae) (Fig. 3) and one gastropod species (Pachychilidae) (Böhme et al., 2013). The biggest difference to the other formations, however, are the lignite deposits. Large tree trunks were found in the upper third of the 15 m thick main seam (layer 80) (Fig. 2 B), while many well-preserved fossil vertebrates were excavated at the bottom of the same seam (Böhme et al., 2011, 2013; Ducrocq et al., 2015; Chavasseau et al., 2019; Garbin et al., 2019; Tsubamoto et al., 2022) (Fig. 2 C).

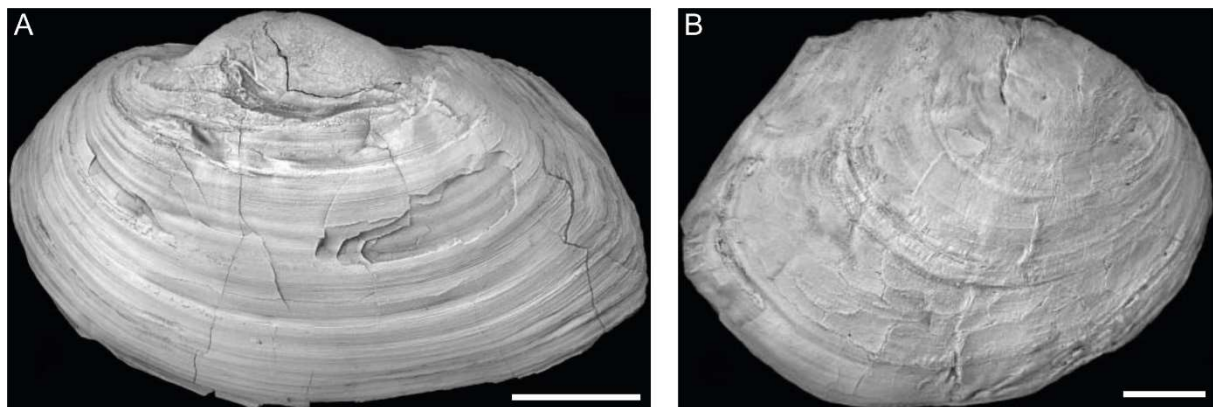


Figure 3. Unionids from the Na Duong Basin (Na Duong Formation), late Eocene, Vietnam. **A**, *?Nodularia cunhatia* Schneider et al., 2013 (BSPG 2011 XXI 13); **B**, *Christaria mothanica* Schneider et al., 2013 (GPIT/BI/5567). Scale bars = 1 cm (altered after Schneider et al., 2013).

The excavated vertebrates can be divided into three main groups: fishes, archelosaurids (see p. 17) and mammals. Based on pharyngeal teeth and disarticulated bones, Böhme et al. (2013) identified eight different fish species belonging to two families, i.e. Amiidae and Cyprinidae. While the Amiidae material could not be identified beyond the family level, the cyprinids belong to at least two

species of the subfamily Barbinae. The mammalian fauna is represented by anthracotherids, a rhinocerotid and a sivaladapid. Of the anthracotherids, only *Bakalovia orientalis* Böhme et al., 2013 (Fig. 4 A, B) is preserved with several individuals. The known material includes a complete skull and mandibles as well as postcranial bones.

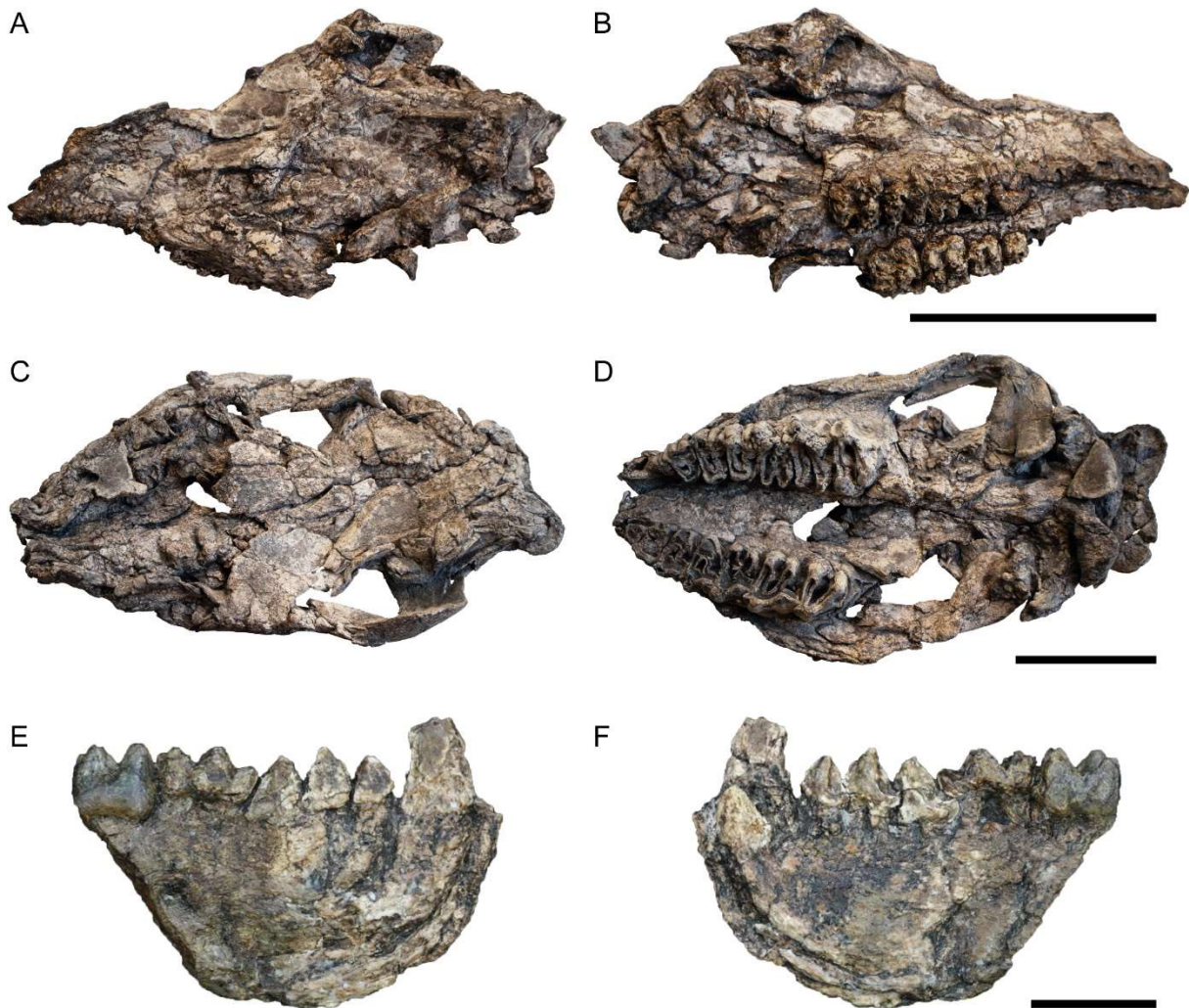


Figure 4. Mammals from the Na Duong Basin (Na Duong Formation), late Eocene, Vietnam. *Bakalovia orientalis* (SAU 3-21) in **A**, dorsolateral and **B**, ventrolateral view. *Epiaceratherium naduongense* (SAU 10) in **C**, dorsal and **D**, ventral view. *Anthradapis vietnamensis* (ND-2015-12-7) in **E**, lateral and **F**, lingual view. Scale bars = 10 cm (A–D) and 1 cm (E–F). (E–F altered after Chavasseau et al., 2019).

In contrast, three other species described by Ducrocq et al. (2015) (*Anthracokeryx naduongensis*, *Bothriogenys vietnamensis* and *Bothriogenys langsonensis*) are only preserved with fragments of the mandible and isolated teeth. Based on the known material, anthracotherids appear to have been relatively common in Na Duong and probably had a semi-aquatic lifestyle (Pickford, 2008; Böhme et al., 2013). In contrast, the much larger rhinocerotid *Epiaceratherium naduongense* Böhme et al., 2013 is only

known from a single skull (Fig. 4 C, D) and appears to have been more adapted to a terrestrial lifestyle (Böhme et al., 2013). Also quite rare is the sivaladapid *Anthradaptis vietnamensis* Chavasseau et al., 2019, known from a single mandible (Fig. 4 E, F) and representing the largest sivaladapid found to date (Chavasseau et al., 2019).

In addition to the numerous vertebrate and invertebrate fossils found in the Na Duong Basin, a large number of different plant species were also preserved, either as stems, leaves, resin, spores or pollen (Fig. 5). Based on the pollen, Wysocka et al. (2020) found a plant composition that varied slightly between layers. About 50-60% of the plants are angiosperms, followed by gymnosperms (40-50%) and spores (1-12%). The angiosperm flora was dominated by four plant genera, i.e. *Caryapollenites*, *Periporopollenites*, *Tricolporopollenites* and *Ulmipollenites*. Böhme et al. (2013) discovered a slightly different plant composition. Among the most common angiosperms were lianas (*Bauhinia*) and dipterocarps, which are now highly diverse in Southeast Asia, forming giant rainforest trees with canopy heights of over 70 m (Yamakura et al., 1986; Maury-Lechon & Curtet, 1998). In addition, Böhme et al. (2013) identified large royal ferns with stem lengths of one metre (known from layer 80) and aquatic plants of the genus *Nelumbo* (lotus) found directly below the main coal seam.

1.1.3 Ecosystem of the Na Duong Basin

The rich fossil record of fauna and flora as well as the geology allow a detailed reconstruction of the ecosystem of the Na Duong Basin during the late Eocene. Wysocka et al. (2009) found evidence for the presence of a wet forest swamp based on the high abundance of lignite and the abundance of clastic material possibly provided by fluvial distributions flowing through a swamp ecosystem into a lake. However, the absence of coal seams in the northern part of the Na Duong Basin suggests that the extent of the swamps was probably limited to the southern part.

The study of palynomorph assemblages by Wysocka et al (2020) further supports these findings. Studies by Böhme et al. (2013) came to the same conclusion: the presence of different facies types indicates that the Na Duong Basin was a swamp ecosystem with aquatic and terrestrial environments. The aquatic environment can be divided into three distinct environments characterised by different facies, i.e. shallow ponds (claystones), anoxic lakes (coaly shales), and streams and rivulets (fine- and medium-grained sandstones). While the main lignite seam (layer 80) was probably an



Figure 5. Fossilized plant remains from the Na Duong Basin (Na Duong Formation), late Eocene, Vietnam. **A**, fragment of a fern (GPIT/PL/619); **B**, seeds of *Nelumbo* sp. (GPIT/PL/609); **C**, unidentified leaf with relatively coarse teeth (GPIT/PL/618); **D**, unidentified leaf with widely spaced teeth (GPIT/PL/620). Scale bars = 1 cm (altered after Böhme et al., 2013).

anoxic lake during the late Eocene, the sediments directly above and below the seam likely represent a pond environment, inhabited by barbine fish, turtles and crocodylians and characterised by meadows of lotus plants (Böhme et al., 2013). The main vertebrate-bearing horizon, which developed during the transition from shallow ponds to an anoxic lake, has the greatest diversity of aquatic life (see above) and allows the

reconstruction of a food chain. Although not preserved, the presence of molluscs whose shells dissolved in the acidic environment of the anoxic lake seems likely (Schneider et al., 2013). They form the food source for fish and turtles, which in turn provide food for crocodylians (Böhme et al., 2013). The terrestrial environment around the lake was characterised by a swamp forest. This was indicated by lignites and clay to sandstones as well as by the results of a palaeomagnetic analysis, which found magnetite, again indicating a water-saturated soil (Böhme et al., 2013). Several tree stumps preserved in situ also allow conclusions about the tree density of the forest, which could be reconstructed to more than 600 trees per hectare and an estimated canopy height of 35 m based on trunk diameters. This is consistent with the tree density and height in modern peat swamp forests in Southeast Asia, which are also mainly dominated by dipterocarp species (Niklas, 1995; Gunawan et al., 2012; Engelhart et al., 2013; Böhme et al., 2013).

1.1.4 Palaeoclimate of the Na Duong Basin

Knowledge of the fossil plant composition of the Na Duong Basin also allows interpretation of the palaeoclimate. The ecosystem was dominated by dipterocarps, which are known to be sensitive to climate as their seeds do not normally germinate below 15°C and can therefore be used as a proxy for tropical or warm-subtropical climates (Tompsett, 1998; Böhme et al., 2013). This climate assessment is further supported by the presence of crocodylians in the basin. The lowest mean annual temperature for crocodylians today is above 14.2°C. However, environments with such low values are only inhabited by the genus *Alligator*, which is best adapted to cold conditions, while other crocodylian species prefer warmer conditions (Colbert et al., 1946; Hagan et al., 1983; Markwick, 1998a, b). Thus, the presence of crocodylians in Na Duong supports the conclusion based on the dominance of dipterocarps. On the other hand, the majority of leaves have serrated margins (Fig. 5 C, D), a feature commonly associated with more temperate climates (e.g. Bailey & Sinnott, 1916; Baker-Brosh & Peet, 1997; Wilf, 1997; Traiser et al., 2005; Peppe et al., 2011; Böhme et al., 2013; Wysocka et al., 2020). However, such leaves are now also found on tropical riverbanks and wet soils (Burnham et al., 2001; Greenwood, 2005; Böhme et al., 2013), ecosystems similar to those reconstructed for the Na Duong Basin in the late Eocene. In contrast to the climate estimates of Böhme et al. (2013), Wysocka et

al. (2020) argue for a slightly colder climate (warm temperate to subtropical) in the Na Duong Basin, based on differences in the plant composition studied. While Wysocka et al. (2020) also found species that can be associated with subtropical to tropical conditions, the pollen composition analysed in their study was dominated by species whose closest living relatives are found in temperate climates. However, the differences in climate estimates could be due to a collection bias in Wysocka et al. (2020), where only few pollen samples were collected from the Na Duong Formation.

1.2 Archelosauria of the Na Duong Basin

The subtropical climate of the forest and swamp ecosystem of the Na Duong Basin provided ideal conditions not only for invertebrates, fish and mammals, but also for crocodylians, turtles and birds. Böhme et al. (2013) provisionally identified three different crocodylian species with different morphologies, i.e. a brevirostrine morphotype, a longirostrine crocodyline morphotype and a longirostrine gavialoid morphotype, as well as five to six turtle species from the two families *Pan-Trionychidae* and *Pan-Geoemydidae* in the basin. However, of these species, only one turtle species (*Banhxeochelys trani*) from the group *Pan-Geoemydidae* has been described so far by Garbin et al. (2019) (Fig. 6).

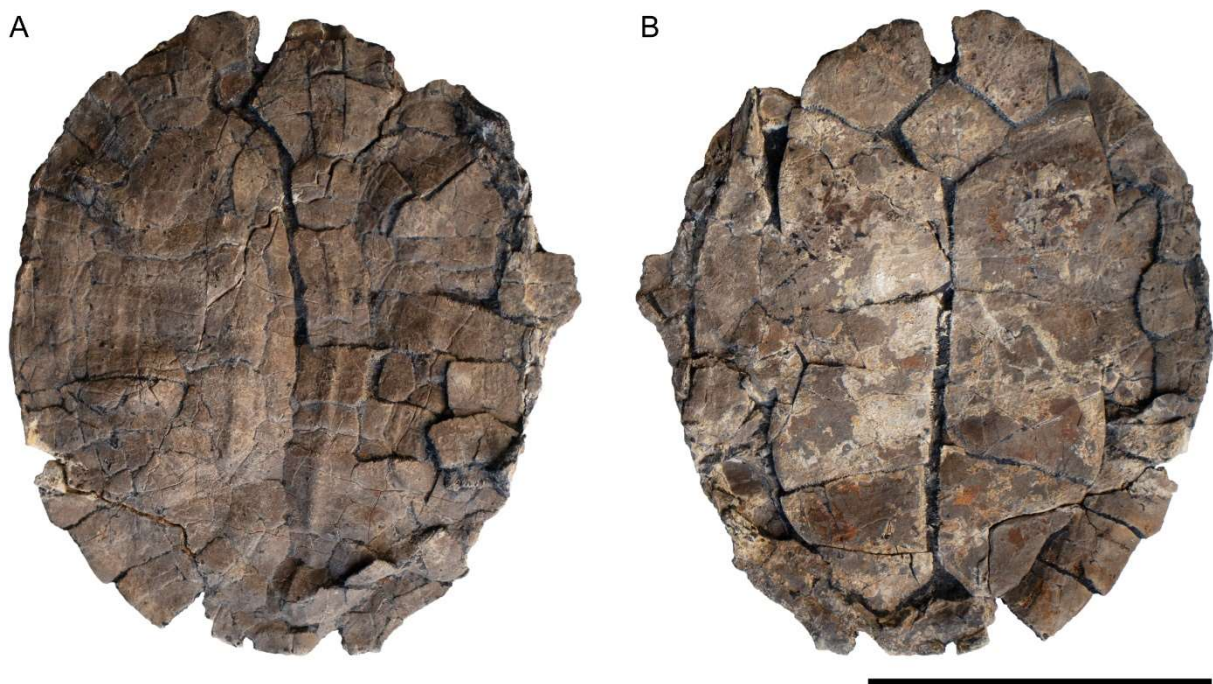


Figure 6. Pan-geoemydid *Banhxeochelys trani* (GPIT/RE/09743) from the Na Duong Basin (Na Duong Formation), late Eocene, Vietnam in **A**, dorsal and **B**, ventral view. Scale bar = 10 cm.

1.2.1 Crocodylians

The definition of Crocodylia has changed in recent decades. Previously, the group corresponded to the now more common term Crocodyliformes and included Protosuchia, Mesosuchia, and Eusuchia (e.g. Clark, 1986; Benton & Clark, 1988; Martin & Benton, 2008; Rio & Mannion, 2021), and some authors still advocate the use of Crocodylia in this broader sense (Martin & Benton, 2008 and references therein). Benton & Clark (1988) argued instead for the use of the term Crocodylia in the narrower sense. Brochu (2003) followed this view and defined Crocodylia as the last common ancestor of *Gavialis gangeticus* (Gmelin, 1789), *Alligator mississippiensis* (Daudin, 1802) and *Crocodylus niloticus* Laurenti, 1768 and all their descendants. In this thesis I will follow the definition of Brochu (2003).

There are two different ways of dividing Crocodylia into three main lineages, depending on whether morphological or molecular data are used (Fig. 7). These groups are defined as follows:

- a) Alligatoidea as *A. mississippiensis* and all crocodylians closer to it than to *C. niloticus* or *G. gangeticus* (Norell et al., 1994; Brochu, 1997a, 1999, 2003).
- b) Gavialoidea as *G. gangeticus* and all crocodylians more closely related to it than to *A. mississippiensis* or *C. niloticus* (Brochu, 2003).
- c) Crocodyloidea as *C. niloticus* and all crocodylians more closely related to it than to *A. mississippiensis* or *G. gangeticus* (Salisbury & Willis, 1996; Brochu, 2003).
- d) Longirostres as the last common ancestor of *C. niloticus* and *G. gangeticus* and all their descendants (Harshman et al., 2003; Brochu, 2003).

The main obstacle to the inner relationships of Crocodylia is the relationship between the gharial *G. gangeticus* and the false gharial *Tomistoma schlegelii* (Müller, 1838), which has been controversial for about 40 years (e.g. Densmore, 1983; Densmore & Dessauer, 1984; Clark, 1986; Densmore & Owen, 1989; Tarsitano et al., 1989; Hass et al., 1992; Brochu, 1997a, b, 2003; Gatesy et al., 2003; Harshman et al., 2003; Janke et al., 2005; Oaks, 2011; Lee & Yates, 2018; Rio & Mannion, 2021). Using morphological data alone, Gavialoidea are found at the base of Crocodylia (e.g. Brochu, 1999, 2007; Brochu & Gingerich, 2000; Delfino et al., 2005; Kobayashi et al., 2006; Jouve et al., 2008, 2015; Martin et al., 2014; Shan et al., 2017; Salas-Gismondi et al., 2019; Rio et al., 2020) (Fig. 7 A). On the other hand, *Gavialis* is found to be the sister genus of *Tomistoma* when only molecular data or a molecular backbone is used

(e.g. Densmore & Dessauer, 1984; Densmore & Owen, 1989; Harshman et al., 2003; McAliley et al., 2006; Willis, 2009; Oaks, 2011; Pan et al., 2021; Walter et al., 2022; Iijima et al., 2022) (Fig. 7 B). The close phylogenetic relationship between *Gavialis* and *Tomistoma* was further supported by studies using combined datasets of morphological and molecular data (Gatesy et al., 2003; Lee & Yates, 2018; Iijima & Kobayashi, 2019; Darlim et al., 2022) and, more recently, by studies using only morphological datasets alone (Sookias, 2020; Ristevski et al., 2020; 2023a; Rio & Mannion, 2021; Boerman et al., 2022).

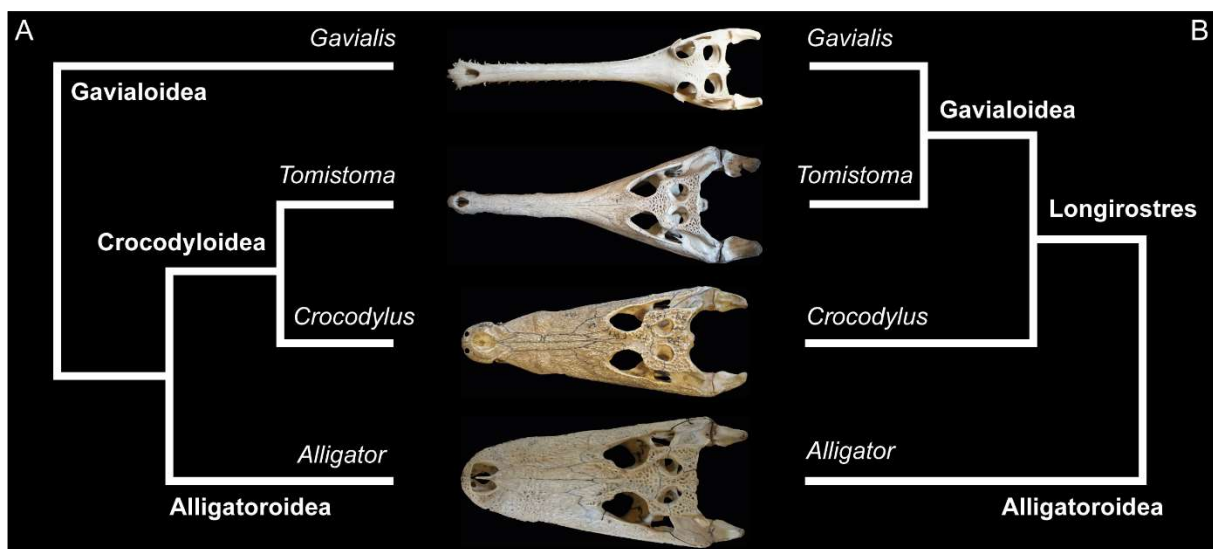


Figure 7. Simplified phylogenetic tree showing the inner relationship of Crocodylia. **A**, traditional tree based on morphological data only. **B**, tree based on molecular data, combined datasets or recently extended morphological datasets.

All of the above groups have survived to the present, but reached their greatest diversity in the early to middle Eocene and early to middle Miocene. Both are periods of maximum global mean temperature (e.g. Hutchison, 1982; Markwick, 1998a, b; Brochu, 2003). During the Eocene, crocodylians lived from Ellesmere Island in the north to Antarctica in the south (Estes & Hutchison, 1980; Willis & Stilwell, 2000; Brochu, 2003), whereas today they are found only in tropical and subtropical regions (e.g. Thorbjarnarson, 1992; Brochu, 1997b, 2003). Southeast Asia is one of only two hotspots for crocodylian diversity (Scheyer et al., 2013) with five species occurring in a historical time frame, i.e. *Crocodylus palustris* (Lesson, 1831), *Crocodylus siamensis* Schneider, 1801, *Crocodylus porosus* Schneider, 1801, *G. gangeticus* and *T. schlegelii*. However, their habitat has been greatly reduced in recent centuries (e.g. Platt & Tri, 2000; Thorbjarnarson, 1992; Thorbjarnarson et al., 2000;

Stuart et al., 2002; Stuebing et al., 2006; Vinh et al., 2006; Bezuijen et al., 2010, 2013, 2014, 2015; Webb et al., 2010, 2021). For example, the gharial population in Myanmar became extinct around 1927, and remnant populations now exist only in South Asia, inhabiting merely two percent of their former range (Whitaker et al., 2007; Stevenson & Whitaker, 2010), and the last sighting of *C. palustris* in Myanmar was in 1867-68 (Choudhury & de Silva, 2013). In Vietnam, the crocodylian fauna has also suffered severe losses in recent decades, and wild populations have collapsed. *Crocodylus porosus* probably became extinct in the wild 20 to 30 years ago (Thorbjarnarson et al., 2000; Stuart et al., 2002; Webb et al., 2010, 2021), and only a few relict populations of *C. siamensis* may remain in the southern part of the country (Platt & Tri, 2000; Stuart et al., 2002; Vinh et al., 2006; Bezuijen et al., 2013). The possible occurrence of *T. schlegelii* in Vietnam is questionable, as only a single record from 1967 is known, but the species may well have existed in Vietnam in historical times (Stuebing et al., 2006; Bezuijen et al., 2010, 2014). Although not directly known from Southeast Asia, a sixth species is worth mentioning here: *Hanyusuchus sinensis* Iijima et al., 2022. *Hanyusuchus sinensis* was a large gavialoid that lived in the region of southern China until historical times, before becoming extinct around 1630 (Iijima et al., 2022).

During the Late Cretaceous and Palaeogene, East and Southeast Asia was home to a large number of different crocodylian taxa. The vast majority of them were found in China (Sun et al., 1992), while some other well-preserved material is only known from sites in Myanmar, Thailand and Vietnam (Tsubamoto et al., 2006a, b; Martin & Lauprasert, 2010; Böhme et al., 2011, 2013; Martin et al., 2019a). The fossil record of crocodylians includes many different clades. Two species from China belong to a group called Planocraniidae, which also had two representatives in the Eocene of Europe and North America (Brochu, 2012). The position of the group on the phylogenetic tree is uncertain. Depending on which dataset is used, they are either considered a sister clade to Crocodyloidea + Alligatoidea, a sister clade to Longirostres, or even outside Crocodylia (Brochu, 2012; Lee & Yates, 2018; Rio & Mannion, 2021). *Planocrania datangensis* Li, 1976 and *Planocrania hengdongensis* Li, 1984 are both well-preserved fossils from southern China. The former is known from the Palaeocene Nongshan Formation of Guangdong Province and the latter from the Eocene Limuping Formation of Hunan Province (Li, 1976, 1984; Brochu, 2012).

The fossil record of Crocodyloidea is rather sparse and includes only two species from China: *Asiatosuchus grangeri* Mook, 1940 from the Eocene Irdin Manha Formation of Inner Mongolia and the recently described *Qianshanosuchus youngi* Boerman et al., 2022 from the Palaeocene Wanghudun Formation of Anhui Province. *Asiatosuchus grangeri* represents the holotype of *Asiatosuchus*, but is preserved with only one pair of mandibles, while the material from *Q. youngi* represents only a single juvenile individual (Mook, 1940; Berg, 1966; Sun et al., 1992; Boerman et al., 2022). Another possible crocodyloid is *Asiatosuchus nanlingensis* Young, 1964 from the Palaeocene Shanghu Formation in southern China's Guangdong Province. However, this material is very fragmentary and consists only of parts of a mandible, making assignment to a specific group almost impossible (Wang et al., 2016; Wu et al., 2018; Shan et al., 2021).

The largest fossil crocodylian group from East and Southeast Asia is Alligatoroidea with five known species from China and one from Thailand (Fig. 8), which lived from the Late Cretaceous to the late Eocene (Sun et al., 1992; Martin & Lauprasert, 2010; Skutschas et al., 2014; Wang et al., 2016; Li et al., 2019; Shan et al., 2021; Wu et al., 2023). The oldest individuals in the group are *Jiangxisuchus nankangensis* Li et al., 2019 (Fig. 8 A) from the Late Cretaceous Nanxiong Formation of Jiangxi Province (China), *Eurycephalosuchus gannaensis* Wu et al., 2023 (Fig. 8 B) from the Late Cretaceous Hekou Formation of Jiangxi Province (China), followed by the poorly preserved *Eoalligator chunyi* Young, 1964 (Fig. 8 C) from the Palaeocene Shanghu Formation of Guangdong Province (China) and *Protoalligator huiningensis* Yang, 1982 (Fig. 8 D) from the Palaeocene Wanghudun Formation of Anhui Province (China) (Wang et al., 2016). Finally, from the late Eocene, *Dongnanosuchus hsui* Shan et al., 2022 (Fig. 8 E) from the Youganwo Formation of the Maoming Basin in Guangdong Province (China) and *Krabisuchus siamogallicus* (Martin & Lauprasert, 2010) (Fig. 8 F) from the Krabi Basin in Thailand are known. Until 2019, the phylogenetic position of these taxa was unclear and some taxa (*J. nankangensis* and *E. chunyi*) were sometimes recovered as crocodyloids (Wang et al., 2016; Li et al., 2019). With the description of *Orientalosuchus naduongensis* Massonne et al., 2019 from the Na Duong Basin of Vietnam, these taxa were unified into a monophyletic group named Orientalosuchina (see Results & Discussion). The monophyly of the group was later supported by several authors (Shan et al., 2021; Ristevski et al., 2023b; Wu et al., 2023).

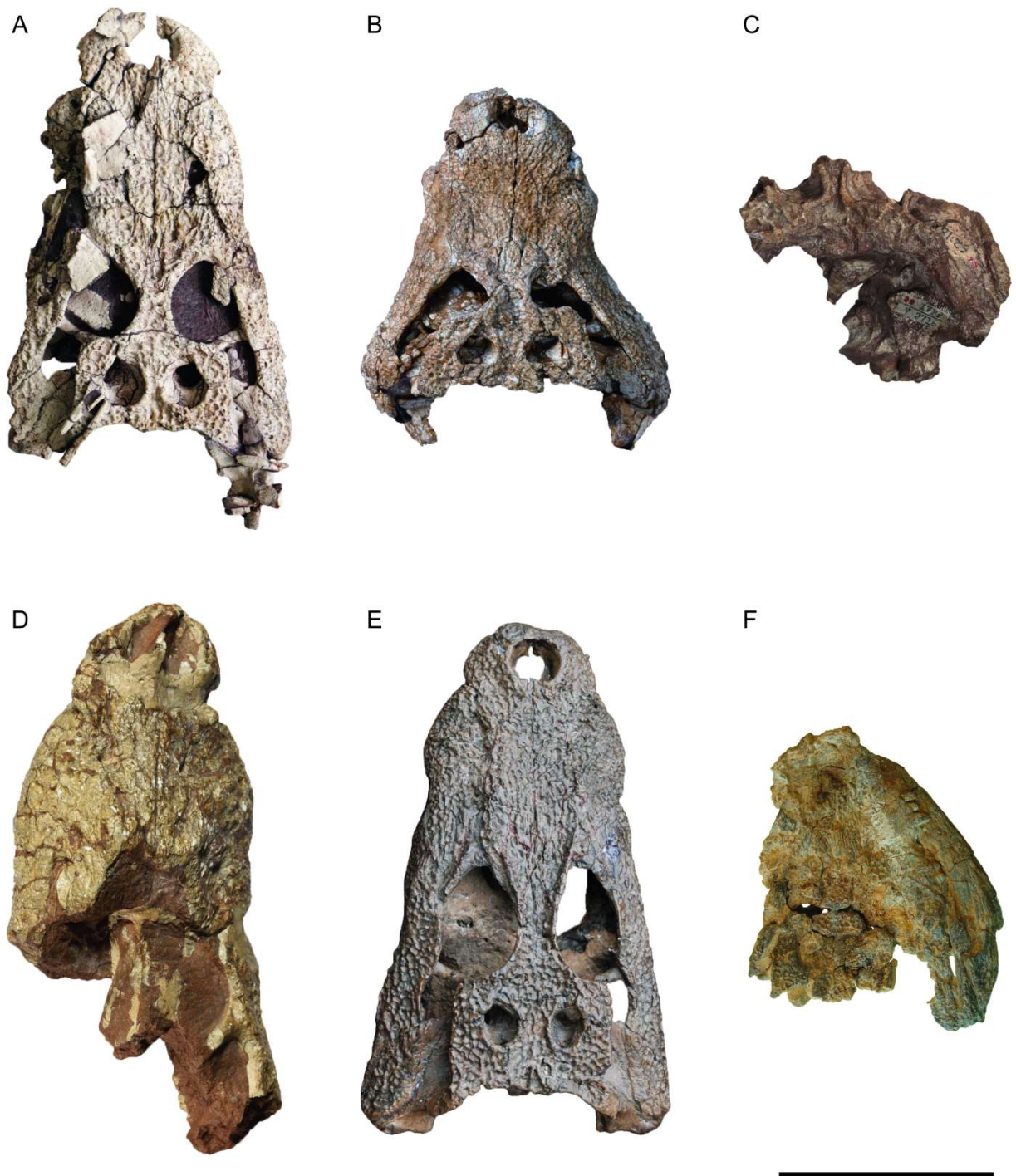


Figure 8. Comparison of orientalosuchines of East and Southeast Asia from the Late Cretaceous to the late Eocene. **A**, *Jiangxisuchus nankangensis* (IVPP V 19125) from the Late Cretaceous of China (altered after Li et al., 2019); **B**, *Eurycephalosuchus gannaensis* (IVPP V 31110) from the Late Cretaceous of China (altered after Wu et al., 2023); **C**, *Eoalligator chunyi* (IVPP V 2716-1.1) from the Palaeocene of China (altered after Wang et al., 2016); **D**, *Protoalligator huiningensis* (IVPP V 4058) from the Palaeocene of China (altered after Wang et al., 2016); **E**, *Dongnanosuchus hsui* (DM000001-F000001) from the Eocene of China (altered after Shan et al., 2022); **F**, *Krabisuchus siamogallicus* (Kr-C-012) from the Eocene of Thailand (© Jeremy E. Martin). Scale bar = 10 cm.

Compared to the alligatoroids, gavialoids of the tomistomine group are rare in the Palaeogene of Southeast Asia (Fig. 9). The only well-preserved material from China

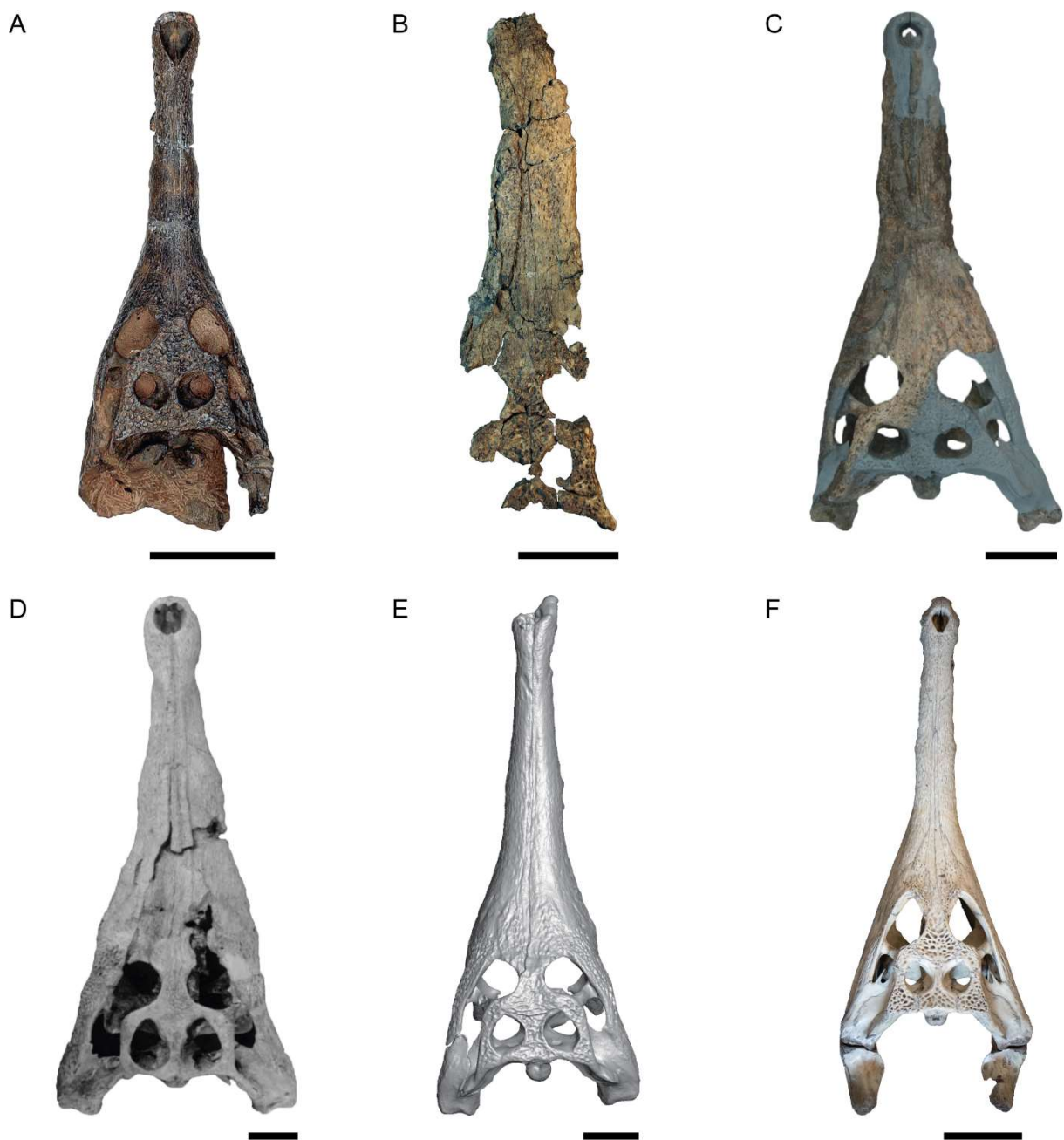


Figure 9. Comparison of tomistomines of East and Southeast Asia from the late Eocene to today. **A**, *Maomingosuchus petrolicus* (DM-F0001) from the Eocene of China (altered after Shan et al., 2017); **B**, *Maomingosuchus* sp. (PRC-1121) from the Eocene of Thailand (altered after Martin et al., 2019); **C**, *Penghusuchus pani* (NMNS-005645) from the Miocene of Taiwan (altered after Shan et al., 2009); **D**, *Toyotamaphimeia machikanensis* (MOU F00001) from the Pliocene/Pleistocene of Japan (altered after Katsura, 2004); **E**, *Hanyusuchus sinensis* (XM 12-1558) from the Bronze Age of China (altered after Iijima et al., 2022); **F**, *Tomistoma schlegelii* (SMNS 13023) from Indonesia, Malaysia and Brunei. Scale bar = 10 cm.

belongs to *Maomingosuchus petrolicus* (Yeh, 1958) (Fig. 9 A) from the Eocene Youganwo Formation of the Maoming Basin in Guangdong Province (Shan et al., 2017). Additional material of a tomistomine assigned to the genus *Maomingosuchus* (Fig. 9 B) is known from the Eocene Krabi Basin of Thailand

(Martin et al., 2019a). Tomistomines are more common from the Miocene onwards, with *Penghusuchus pani* Shan et al., 2009 (Fig. 9 C) from the Miocene Yuwentao Formation of Taiwan, and especially from the Pliocene onwards with giant species such as *Toyotamaphimeia machikanensis* (Kamei & Matsumoto, 1965) (Fig. 9 D) from several Pliocene/Pleistocene localities in Japan and Taiwan, fragmentary remains of *Toyotamaphimeia taiwanicus* (Shikama, 1972) from the Pleistocene of Taiwan, *H. sinensis* (Fig. 9 E) mainly from the Bronze Age of southern China and finally the extant *T. schlegelii* (Fig. 9 F) from Indonesia, Malaysia and Brunei (Katsura, 2004; Kobayashi et al., 2006; Bezuijen et al., 2010; Iijima et al., 2018, 2022; Ito et al., 2018; Cho & Tsai, 2023). These tomistomines vary widely in size. There is a rough pattern from small species in the late Eocene to much larger species from the Miocene onwards (Fig. 10). The rarity of tomistomines in the Palaeogene of East Asia is to be expected. The most basal taxa of the group are so far only known from the late Palaeocene/early Eocene of the western Tethys region of Africa and Europe (*Maroccosuchus zennaroii* Jonet & Wouters, 1977, *Kentisuchus spenceri* [Buckland, 1836] and *Kentisuchus astrei* Jouve, 2016) and their eastward dispersal occurred only in the Eocene (e.g. Brochu, 2007; Piras et al., 2007; Jouve et al., 2015; Jouve, 2016).

In addition to the above taxa, several other fossil crocodylians are known from East and Southeast Asia, but most are fragmentarily and cannot be assigned to any particular group. The majority of these fossils are from China (Sun et al., 1992), but further enigmatic material in the form of disarticulated postcranial bones, skull fragments and isolated teeth, belonging to at least two different crocodylian species have also been found in the late middle Eocene Pondaung Formation of Myanmar (Tsubamoto et al., 2006a, b). The material differs mainly in the morphology of the teeth. One tooth type has a typical crocodylian morphology, while the other has a ziphodont morphology, which is so far only known from a few crocodylian species (*Boverisuchus vorax* [Troxell, 1925], *Boverisuchus magnifrons* Kuhn, 1938 and *Quinkana* spp.) (Langston, 1975; Molnar, 1981; Willis, 1997; Brochu, 2012; Sobbe et al., 2013).

Three different morphotypes of crocodylians have been described from the Na Duong Basin in Vietnam (Böhme et al., 2013), belonging to two new species in different ontogenetic stages (see p. 40). The detailed description of these crocodylians, their position on the phylogenetic tree, their relationship to other species of East and Southeast Asia and the resulting palaeobiogeographical implications are one of the

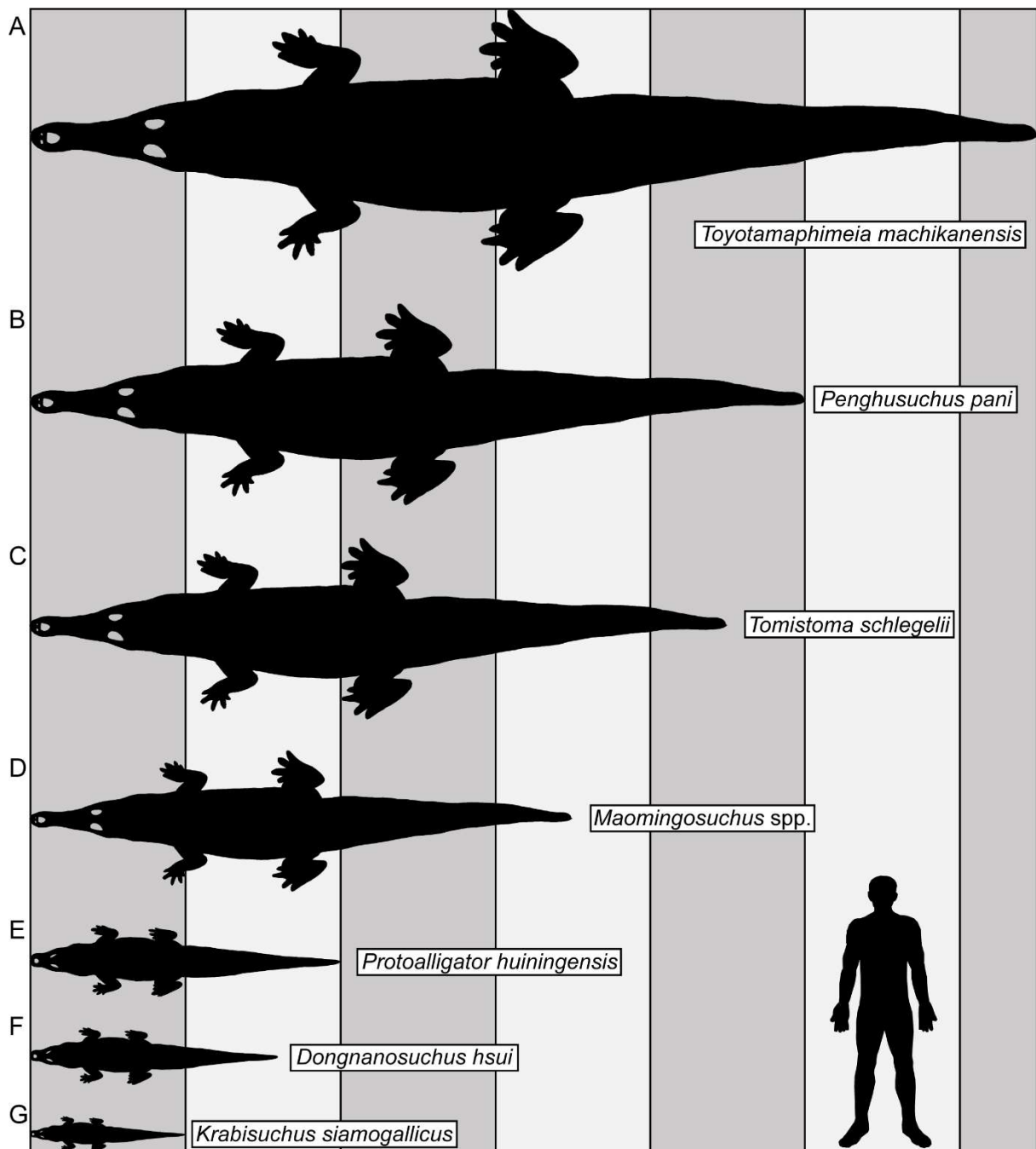


Figure 10. Size comparison of selected species of tomistomines (A-D) and orientalosuchines (E-G) with a human of 1.8 m. Column width = 1 m.

main tasks of this thesis. The description of the alligatoroid *Orientalosuchus naduongensis* gen. et sp. nov. and the discovery of a hitherto unknown crocodylian group (Orientalosuchina), which so far comprises seven different species, as well as the distribution of early alligatoroids are part of this thesis (see chapter 2.1). The description of a new tomistomine, *Maomingosuchus acutirostris* sp. nov. and the

discovery of several dispersal events of tomistomines from Europe to East Asia are also part of this thesis (see chapter 2.2).

1.2.2 Birds

Apart from crocodylians and turtles, birds are the only other group of Reptilia currently known from the Na Duong Basin, as no fossil rhynchocephalians and squamates have been found until now. While living birds are clearly identifiable as birds, when looking at fossils the exact definition of what a bird actually is becomes blurred, leading to several different definitions of the term 'bird' (Gauthier, 1986; Lee & Spencer, 1997; Gauthier & Queiroz, 2001; Modesto & Anderson, 2004). In this thesis I will use the definition given by Gauthier & Queiroz (2001, p.29): 'Aves refers to the crown clade stemming from the most recent common ancestor of Ratitae (*Struthio camelus* Linnaeus, 1758), Tinamidae (*Tetrao* [*Tinamus*] *major* Gmelin, 1789), and Neognathae (*Vultur gryphus* Linnaeus, 1758).'

There is further disagreement about the origin and diversification of modern birds. Their origin is sometime in the Cretaceous, but age estimates range from the Early Cretaceous (Cooper & Penny, 1997; Ericson et al., 2006; Haddrath & Baker, 2012; Jetz et al., 2012; Lee et al., 2014; Yonezawa et al., 2017) to the Late Cretaceous (Longrich et al., 2011; Claramunt & Cracraft, 2015; Prum et al., 2015). Furthermore, it is unclear when the diversification of bird groups occurred. Some authors argue for diversification during the Cretaceous (Cooper & Penny, 1997; Haddrath & Baker, 2012; Lee et al., 2014), while others consider diversification in the Palaeogene after the mass extinction at the end of the Cretaceous as most likely (Ericson et al., 2006; Longrich et al., 2011; Claramunt & Cracraft, 2015; Prum et al., 2015).

From the Late Cretaceous/Paleogene onwards, birds are represented by two major groups: Palaeognathae and Neognathae (Gussekkloo & Zweers, 1999; Mayr & Clarke, 2003; Sorenson et al., 2003; Livezey & Zusi, 2007; Claramunt & Cracraft, 2015; Yonezawa et al., 2017; Mayr, 2022). Palaeognaths comprise only a few lineages and are mainly characterised by a co-ossified palatine and pterygoid articulated with the skull via a basipterygoid process (Cracraft, 1973; Härlid & Arnason, 1999; Baker et al., 2014; Mitchell et al., 2014; Mayr, 2022). Neognaths, on the other hand, are characterised by a mobile joint between the palatine and pterygoid and an often reduced basipterygoid process (Hu et al., 2019; Mayr, 2022). Neognaths are again

divided into two groups: Galloanserae and Neoaves, the latter comprising the majority of all bird species (Erickson et al., 2006; Mayr, 2011, 2022; Jetz et al., 2012; Kuhl et al., 2014; Claramunt & Cracraft, 2015; Prum et al., 2015; Hu et al., 2019; Braun & Kimball, 2021).

While only a few species belong to palaeognaths, the majority of the approximately 10,000 living bird species belong to neognaths, making birds the most diverse group of terrestrial vertebrates (Härlid & Arnason, 1999; Gauthier & Queiroz, 2001; Erickson et al., 2006; Prum et al., 2015; Hu et al., 2019; Mayr, 2022). Most of these species are found in tropical rainforests (MacArthur & MacArthur, 1961; Loiselle & Blake, 1992; Sekercioglu, 2012). Today, Southeast Asia hosts a large number of different species (over 1300) and has the highest proportion of endemic species, thus living up to its name as a biodiversity hotspot (Sodhi et al., 2006; Robson, 2008). However, the number of fossils from the Palaeogene is very sparse in comparison.

While the avifauna of the Mesozoic, especially the Cretaceous, is relatively well sampled, studies of birds from the Palaeocene and Eocene of Southeast Asia are very limited (Kurochkin, 1976; Rich et al., 1986; Nessonov, 1992; Hou et al., 2003; Mayr, 2009, 2022; Zelenkov & Kurochkin, 2015; Hood et al., 2019). Better preserved fossils are mainly known from the Palaeocene and Eocene of India, Mongolia and China. They include species assigned to Anseriformes, Galiformes, Mirandornithes, Gruiformes and Strigiformes (Hwang et al., 2010; Mayr et al., 2010; Kurochkin & Dyke, 2011; Wang et al., 2012; Mayr et al., 2013; Stidham & Ni, 2014; Zhao et al., 2015; Hood et al., 2019; Zelenkov 2021 a, b). Other fragmentary material from the Eocene is known for Gastornithiformes (*Zhongyuanus xichuanensis* Hou, 1980) from China (Buffetaut, 2013), a member of Protoplotidae (*Protoplotus beauforti* Lambrecht, 1931) from Sumatra and a putative member of Threskiornithidae from the Pondaung Formation of Myanmar (Stidham et al., 2005). In addition to the neognaths fossils mentioned above, some palaeognaths assigned to Eogruidae and Ergilornithidae are known from the Eocene and early Oligocene of Mongolia (Clarke et al., 2005; Hood et al., 2019; Mayr & Zelenkov, 2021; Mayr, 2022). To date, however, no birds are known from the Palaeogene of Vietnam, and the only fossil remains of the country's avifauna are from the Pleistocene and represent modern taxa (Boev, 2022).

Given the rarity of fossil bird remains from the Palaeogene of Southeast Asia in general, and the complete lack of such discoveries from Vietnam in particular, even

fragmentary remains can make an important contribution to our knowledge of the avifauna of Southeast Asia. A single distal part of a tarsometatarsus of a presumed member of Neognathae was found in the Na Duong Basin. The description of this material and its comparison with extant aquatic, terrestrial and arboreal birds is part of this thesis (see chapter 2.3).

1.2.3 Turtles

The species richness of extant turtles far exceeds that of crocodylians. There are currently 486 taxa, divided into 357 species and 129 additional subspecies, occurring on all continents except Antarctica and in all warm and temperate oceans (Turtle Taxonomy Working Group, 2021).

Turtles or testudines are defined by Joyce et al. (2021, p.15) as ‘the smallest crown clade containing the pleurodire *Chelus* (originally *Testudo*) *fimbriatus* (Schneider, 1783), the trionychian *Trionyx* (originally *Testudo*) *triunguis* (Forskål, 1775), the americhelydian *Chelonia* (originally *Testudo*) *mydas* (Linnaeus, 1758), and the testudinoid *Testudo graeca* Linnaeus, 1758’. The turtles living today are divided into two suborders: *Cryptodira* and *Pleurodira* (Gaffney et al., 2006; Werneburg et al., 2015; Ferreira et al., 2018; Joyce et al., 2021; Turtle Taxonomy Working Group, 2021). *Cryptodira* is defined as ‘the smallest crown clade containing the testudinoid *Testudo graeca* Linnaeus, 1758, the chelonioid *Chelonia* (originally *Testudo*) *mydas* (Linnaeus, 1758), the trionychian *Trionyx* (originally *Testudo*) *triunguis* (Forskål, 1775), the kinosternoid *Kinosternon* (originally *Testudo*) *scorpioides* (Linnaeus, 1766) and the chelydrid *Chelydra* (originally *Testudo*) *serpentina* (Linnaeus, 1758)’ (Joyce et al., 2021, p.21). *Pleurodira*, in turn, is defined as ‘the smallest crown clade containing the chelid *Chelus* (originally *Testudo*) *fimbriatus* (Schneider, 1783), the pelomedusid *Pleomedusa* (originally *Testudo*) *subrufa* (Bonnaterre, 1789) and the podocnemid *Podocnemis* (originally *Emys*) *expansa* (Schweigger, 1912)’ (Joyce et al., 2021, p.15).

The fossil record of testudines extends well back into the Late Jurassic (Evers & Benson, 2018). The oldest member of *Pan-Pleurodira* was *Notoemys oxfordiensis* (Fuente & Iturralde-Vinent, 2001) from the Late Jurassic of Cuba (Joyce et al., 2013; Cadena & Joyce, 2015). The age of what is thought to be the oldest member of the *Pan-Cryptodira* (*Sinaspideretes wimani* Young & Chow, 1953 from

China) is more indeterminate, but time estimates range from the middle Jurassic to the Early Cretaceous (Meylan & Gaffney, 1992; Joyce et al., 2013; Tong et al., 2014; Evers & Benson, 2018). Crown pleurodires (*Teneremys lapparenti* Broin, 1980 from Niger) and crown cryptodires (fragmentary stem trionychid remains from Japan) appeared somewhat later in the middle Early Cretaceous (Gaffney et al., 2006; Joyce et al., 2013; Cadena & Joyce, 2015).

Cryptodires and pleurodires differ in two main ways related to neck retraction and pelvic girdle morphology (Gaffney et al., 2006; Werneburg et al., 2015; Wise & Stayton, 2016). While cryptodires move their neck in the vertical plane, pleurodires instead perform a horizontal movement (Werneburg et al., 2015; Anquetin et al., 2017). Furthermore, the pelvic girdle of cryptodires is loosely connected to the carapace and plastron by filaments, whereas the girdle of pleurodires is firmly attached to the shell (Gaffney et al., 2006; Mayerl et al., 2016; Wise & Stayton, 2016). Cryptodires are the more dominant of the two groups, accounting for more than 70% of extant species, and are found in freshwater, marine and terrestrial environments in the Americas, Asia, Africa and Europe, and with a single species (*Carettochelys insculpta* Ramsay, 1886) also in Australia (Wise & Stayton, 2016; Ferreira et al., 2018; Turtle Taxonomy Working Group, 2021). Pleurodires, on the other hand, live today only in freshwater habitats in the Southern Hemisphere, but were also native to other habitats, such as coastal areas, around the world during the Cretaceous and Cenozoic (Gaffney et al., 2006; Pérez-García, 2016; Wise & Stayton, 2016; Ferreira et al., 2018; Turtle Taxonomy Working Group, 2021).

Southeast Asia (more specifically the Indo-Burma hotspot from the Himalayas and the Ganges region through southern China to Indonesia) currently has the highest abundance of different turtle taxa with 50 species, 19 of which are endemic (Mittermeier et al., 2015; Turtle Taxonomy Working Group, 2021). Considering the size of the country, Vietnam has the highest diversity of terrestrial/freshwater turtles, with a total of 27 species from four families (*Geoemydidae*, *Platysternidae*, *Testudinidae*, *Trionychidae*), ranking eighth overall in the world (Mittermeier et al., 2015; Turtle Taxonomy Working Group, 2021).

Geoemydids are by far the dominant turtle group in Southeast Asia and Vietnam, followed at some distance by trionychids (softshell turtles) (Turtle Taxonomy Working Group, 2021). What makes the latter group special is their unique shell morphology. The carapace and plastron are greatly reduced, lacking

scutes, peripherals and pygals (Meylan, 1987; Vitek & Joyce, 2015; Joyce & Lyson, 2017). The carapace itself consists of two parts: an anteromedial bony disc part and a cartilaginous part at the margins (Meylan, 1987). The difference in size between these two parts varies greatly from species to species. In some species, e.g. *Lissemys punctata* (Lacépède, 1788), the cartilaginous part accounts for less than ten percent of the total carapace length, whereas in others, e.g. *Dogania subplana* (Geoffroy Saint-Hilaire, 1809), it occupies a much larger area of almost 50 percent of the total carapace length (Meylan, 1987).

Trionychidae are a highly aquatic group that is now found in all freshwater areas of Asia, Africa and North America (Joyce & Lyson, 2017; Turtle Taxonomy Working Group, 2021). However, in the past they were much more widespread, and also lived in Australia, Europe and South America (Böhme, 1995; Vitek & Joyce, 2015; Joyce & Lyson, 2017; Georgalis & Joyce, 2017; Georgalis, 2021). *Pan-Trionychidae* (*Trionychidae* including the stem taxa) can be divided into two extant lineages (*Pan-Cyclanorbinae* and *Pan-Trionychinae*) and a third lineage (*Plastomenidae*), which, however, became extinct in the Eocene (Joyce et al., 2009, 2016, 2018, 2021; Lyson et al., 2021; Jasinski et al., 2022). The oldest valid pan-trionychid taxa (*Trionyx* *kyrgyzensis* Nessov, 1995, *Perochelys lamadongensis* Li et al., 2015, *Perochelys hengshanensis* Brinkman et al., 2017) date to the Early Cretaceous of Asia (Danilov & Vitek, 2013; Brinkman et al., 2017), but their position on the phylogenetic tree has not been fully resolved (Brinkman et al., 2017; Georgalis & Joyce, 2017; Joyce et al., 2021). While there are a large number of fossil sites from the Upper Cretaceous of Central and Eastern Asia (e.g. Vitek & Danilov, 2010; 2012; Danilov & Vitek, 2013; Danilov et al., 2014; Brinkman et al., 2017; Georgalis & Joyce, 2017), sites and species from the Palaeogene are much rarer.

The only taxa not assigned to the genus '*Trionyx*' are *Kuhnemys palaeocenica* (Danilov et al., 2015) (Fig. 11 A) from the Thanetian (Late Palaeocene) of Mongolia and *Drazinderetes tethyensis* Head et al., 1999 (Fig. 11 B) from the Bartonian (Late Eocene) of Pakistan (Georgalis & Joyce, 2017). Six taxa are known from the genus '*Trionyx*', i.e. '*Trionyx* *gregarius*' (Gilmore, 1934) (Fig. 11 C), '*Trionyx* *johnsoni*' (Gilmore, 1931) (Fig. 11 D), '*Trionyx* *linchuensis*' (Yeh, 1962) (Fig. 11 E) and '*Trionyx* *impressus*' (Yeh, 1963) (Fig. 11 F) from the Eocene of China, as well as '*Trionyx* *ninae*' Chkhikvadze, 1971 (Fig. 11 G) from the Eocene and Oligocene of Kazakhstan and

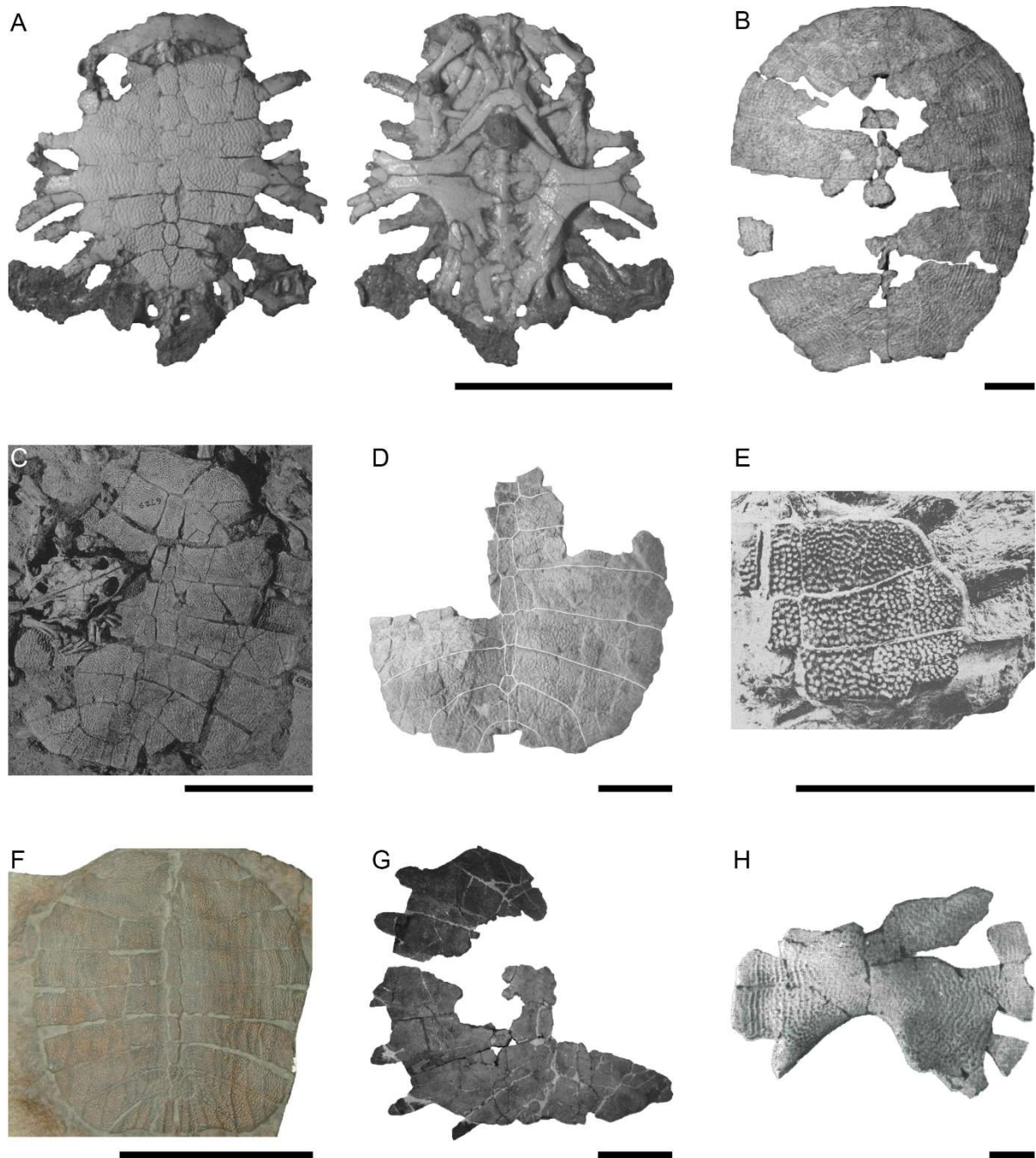


Figure 11. Comparison of pan-trionychids of East and Southeast Asia from the Palaeogene. **A**, *Kuhnemys palaeocenica* (PIN 3639/13) from the Palaeocene of Mongolia (altered after Danilov et al., 2015); **B**, *Drazinderetes tethyensis* (GSP-UM 3195) from the Eocene of Pakistan (altered after Head et al., 1999); **C**, '*Trionyx*' *gregarius* (AMNH 6729) from the Eocene of China (altered after Gilmore, 1934); **D**, *Trionyx*' *johnsoni* (AMNH 6357) from the Eocene of China (altered after Gilmore, 1931); **E**, '*Trionyx*' *linchuensis* (IVPP V1050) from the Eocene of China (altered after Yeh, 1962); **F**, '*Trionyx*' *impressus* from the Eocene of China (© Walter G. Joyce); **G**, '*Trionyx*' *ninae* (ZIN PH 1/155) from the Eocene/Oligocene of Kazakhstan (altered after Vitek & Danilov, 2015); **H**, '*Trionyx*' *minusculus* (IPGAS Z-13-1) from the Eocene of Kazakhstan (altered after Chkhikvadze, 1973). Scale bars = 10 cm (A-G) and 1 cm (H).

'*Trionyx*' *minusculus* (Chkhikvadze, 1973) (Fig. 11 H) from the Eocene of Kazakhstan (Vitek & Danilov, 2015; Georgalis & Joyce, 2017). '*Trionyx*' *impressus* from the

Maoming Basin of southern China, is only known from a single carapace imprint (Georgalis & Joyce, 2017), but it nevertheless represents the only taxon from the late Eocene (Bartonian to Priabonian) of East Asia to date. In contrast, all other named species and specimens from the late middle Eocene of Myanmar, eastern China (Zhejiang Province), or eastern central China (Henan Province) are poorly preserved and therefore can only be identified as *Pan-Trionychidae* indet. (Georgalis & Joyce, 2017).

As summarised above, the fossil record of pan-trionychids from the Palaeogene of East Asia is sparse. Our knowledge of the representatives of the group from the late Eocene is even more problematic, as the only named species is preserved with only a single imprint. In this respect, the Na Duong Basin offers a significant contribution to the turtle fauna by providing several well-preserved individuals of a new species of *Pan-Trionychidae*: *Striatochelys baba* gen. et sp. nov. The description of this new species, its position on the phylogenetic tree and its relationship to other (living and fossil) species of East and Southeast Asia is part of this thesis (see chapter 2.4).

1.3 Institutional abbreviations

AMNH American Museum of Natural History, New York, New York, USA; **BSPG** Bayerische Staatssammlung für Paläontologie und historische Geologie, Munich, Germany; **DM** Darwin Fossil Museum, Keelung, Taiwan; **GPIT** Geologisch-Paläontologisches Institut Tübingen, Tübingen, Germany; **GSP** Geological Survey of Pakistan, Islamabad, Pakistan; **IPGAS** Institute of Paleobiology, Georgian Academy of Sciences, Tbilisi, Georgia; **IVPP** Institute of Vertebrate Paleontology and Paleoanthropology, Beijing, China; **Kr-C** Krabi crocodylian, Sirindhorn Museum, Kalasin Province, Thailand; **MOU** Museum of Osaka University, Osaka, Japan; **ND** Na Duong Collections at the Institute of Marine Geology and Geophysics, Vietnam Academy of Science and Technology, Hanoi, Vietnam; **NMNH** National Museum of Natural History, Washington, DC, USA; **NMNS** National Museum of Natural Science, Taichung, Taiwan; **PIN** Paleontological Institute, Russian Academy of Sciences, Moscow, Russia; **PRC** Palaeontological Research and Education Centre, Mahasarakham University, Mahasarakham, Thailand; **SMF** Senckenberg Museum, Frankfurt am Main, Germany; **SMNS** Staatliches Museum für Naturkunde Stuttgart, Stuttgart, Germany; **XM** Xinhui Museum, Jiangmen, Guangdong, China;

ZIN PH Paleoherpertological Collection, Zoological Institute of the Russian Academy of Sciences, St. Petersburg, Russia.

1.4 Objectives

The late Eocene Na Duong Basin of Vietnam is one of only few Paleogene localities in Southeast Asia and therefore offers a unique opportunity to study a wide variety of animals and plants from the past in terms of their morphology, ecology, phylogeny and possible dispersal events. In the past decades, many studies have been published, focusing on basin age, palaeoclimate, biostratigraphy, vegetation reconstruction and animal description (unionids, mammals and a single reptile species) (Dzanh, 1996; Wysocka, 2009; Böhme et al., 2011, 2013; Schneider et al., 2013; Ducrocq et al., 2015; Chavasseau et al., 2019; Garbin et al., 2019; Wysocka et al., 2020; Tsubamoto et al., 2022).

The aim of this thesis is to expand our knowledge of the Na Duong ecosystem by focusing on the reptile- and avifauna of the basin. To this end, I examined all the Na Duong material currently housed at the Geological-Paleontological Institute of the Eberhard Karls University of Tübingen, which was excavated between 2009 and 2012 under the supervision of Prof. Dr. Madelaine Böhme. The reptile- and avifauna material includes two different crocodylian species with several individuals, two turtle species (one of which has already been described by Garbin et al., 2019) with several individuals and a single bird bone.

In addition to a morphological approach describing all the new species and comparing them with extant and fossil material to identify differences from existing species, another aim of the thesis was to carry out phylogenetic analyses (in the case of the two crocodylian and the turtle species). These analyses help to clarify the position of the taxa on the phylogenetic tree and to find out close relatives, as well as to discover new clades together with synapomorphies and new characters that can help in future analyses of different taxa. The results of the phylogeny will then be used to reveal possible dispersal events for the new species and help to learn more about the ecology of East and Southeast Asia.

2 Results & Discussion

This section summarises the main results of the four papers in the thesis. The complete papers can be found in their published versions in the appendix at the end of the thesis.

2.1 A new species from the Eocene of Vietnam highlights a Southeast Asian alligatoroid lineage and its origin

The first paper of this thesis is about a new species of Alligatoidea from the Na Duong Basin of Vietnam. A total of 29 specimens were collected during systematic surveys between 2009 and 2012 at the base of layer 80 in the Na Duong coal mine and subsequently prepared by the Geological-Paleontological Institute of the Eberhard Karls University of Tübingen (GPIT) (Böhme et al., 2012). The material includes several complete (Fig. 12), or nearly complete skulls, mandibles (Fig. 13) and associated postcranial material. For a list of specimens and a full description of the material, see Massonne et al. (2019) in the appendix. The overall state of preservation is good, but the skulls are dorsoventrally flattened and show deformed or crushed areas and weathered surfaces. The postcranial material was found disarticulated or fused to the matrix. The best-preserved individual, GPIT-PV-31631 (formerly GPIT-RE-09761), consists of a skull (Fig. 12) and associated postcranial material, representing an almost complete animal, and was therefore selected as the holotype of the new species: *Orientalosuchus naduongensis* gen. et sp. nov.

In the field, the material was assigned to an *Allognathosuchus*-like species. Subsequently, the hypothesis that it might represent a missing link in the history of *Alligator* was then investigated. However, after comparison with other alligatoroid species, it became clear that not only did the material represented a new species, but it also did not appear to be particularly close to either *Allognathosuchus* or *Alligator*. Instead, a closer comparison revealed a high degree of similarity with several taxa from East and Southeast Asia (i.e. *Krabisuchus siamogallicus*, *Protoalligator huiningensis*, *Eoalligator chunyii*, *Jiangxisuchus nankangensis* and an unnamed alligatoroid from Maoming).

Despite these similarities, *O. naduongensis* clearly represents a new species, diagnosed by a combination of characters not found in any other crocodylian species:

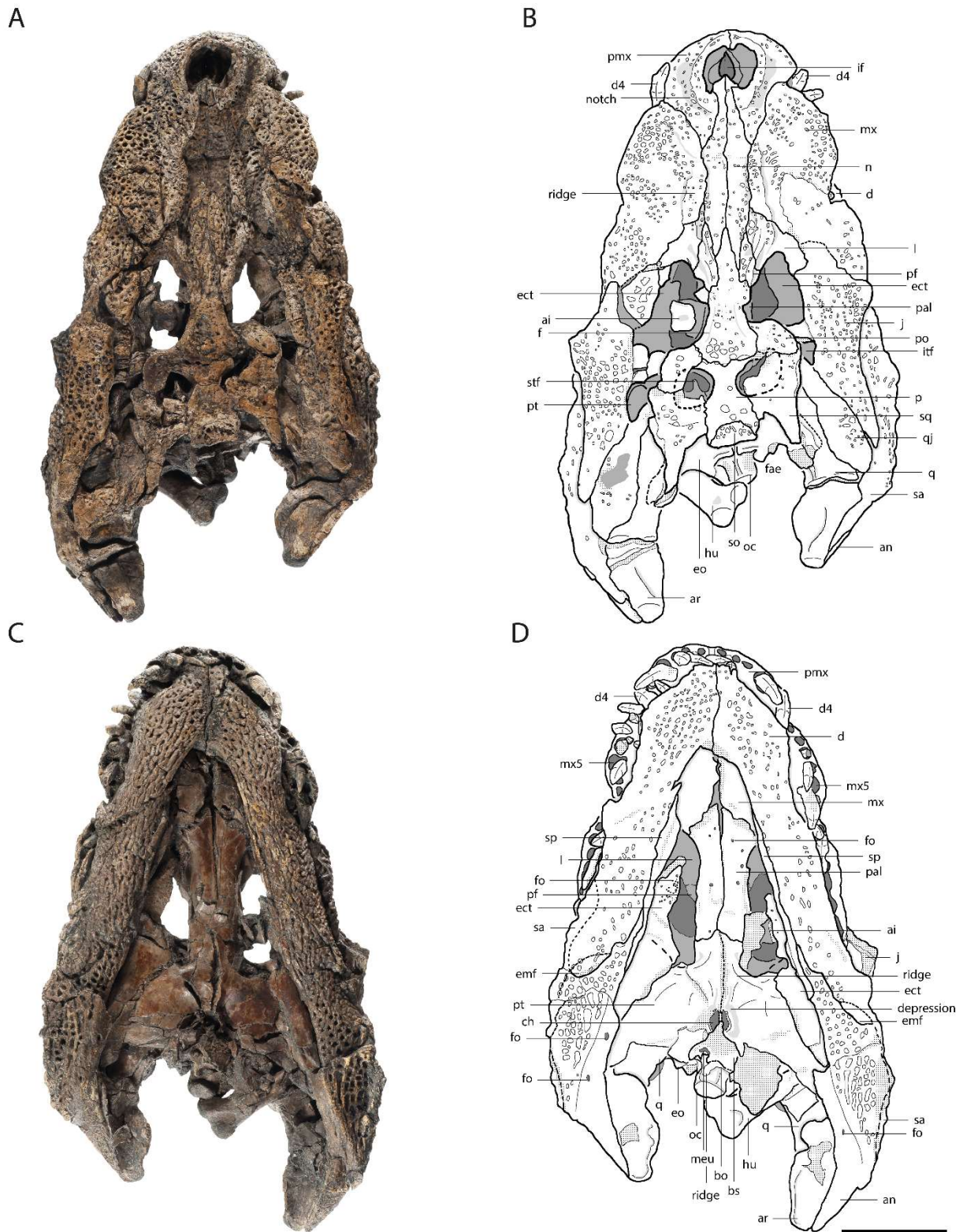


Figure 12. Skull of *Orientalosuchus naduongensis*, holotype, GPIT-PV-31631 (former GPIT-RE-09761), Na Duong Formation, late Eocene, Vietnam. Skull in **A, B**, dorsal and **C, D**, ventral view. **Abbreviations:** ai, atlas intercentrum; an, angular; ar, articular; bo, basioccipital; bs, basisphenoid; ch, choana; d, dentary; d4, dentary tooth 4; emf, external mandibular fenestra; eo, exoccipital; ect, ectopterygoid; f, frontal; fo, foramen; fae, foramen aerum; hu, humerus; if, incisive foramen; itf, infratemporal fenestra; j, jugal; l, lacrimal; mx, maxilla; mx5, maxilla tooth 5; n, nasal; oc, occipital condylus; p, parietal; pf, prefrontal; pal, palatine; pmx, premaxilla; po, postorbital; pt, pterygoid; q, quadratum; qj, quadratojugal; sa, surangular; so, supraoccipital; sp, splenial; sq, squamosal; stf, supratemporal fenestra. Scale bar = 5 cm. (altered after Massonne et al., 2019)

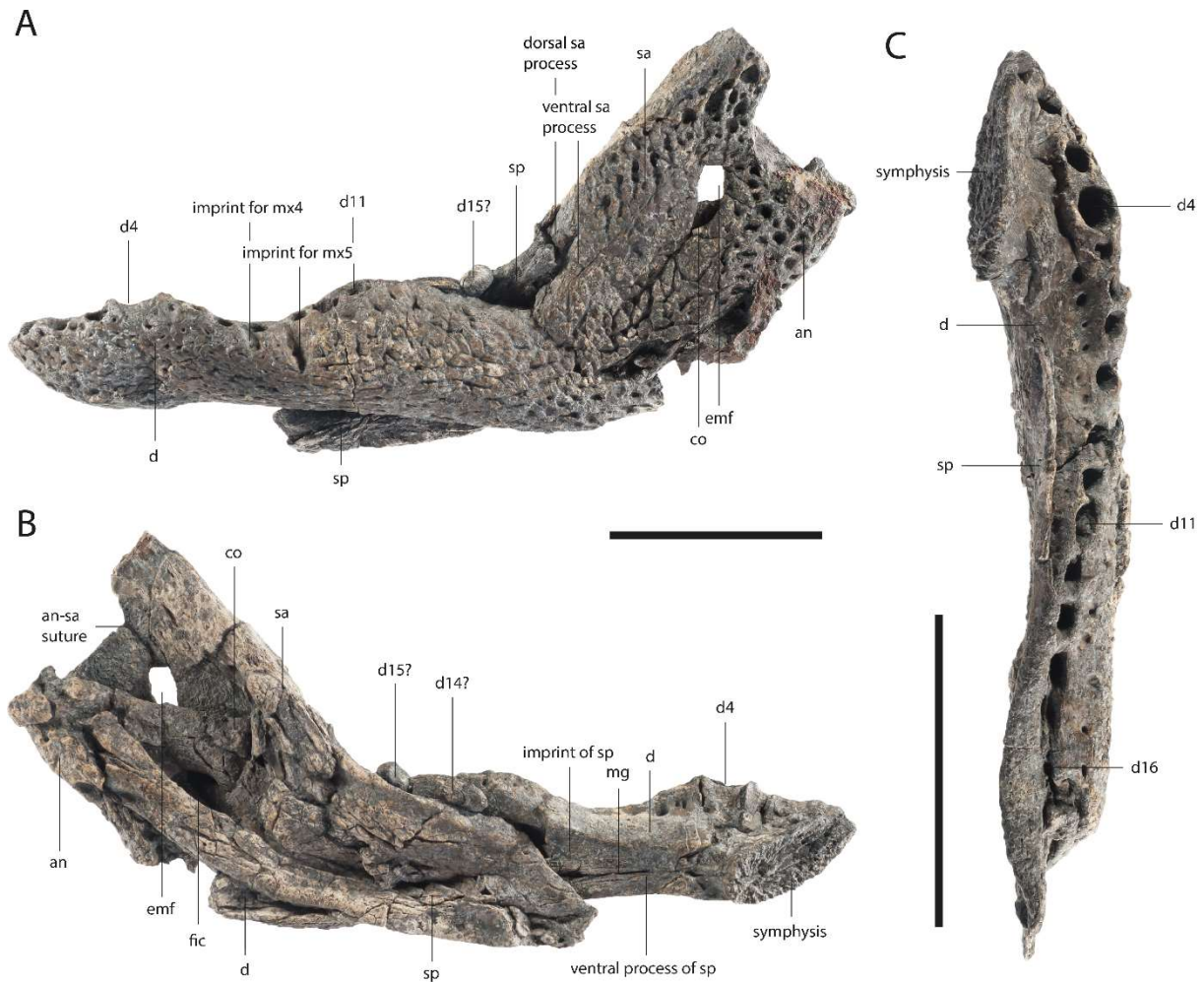


Figure 13. Lower jaw of *Orientalosuchus naduongensis*, GPIT-PV-31674 (former GPIT-RE-09728), Na Duong Formation, late Eocene, Vietnam. Lower jaw in **A**, lateral, **B**, medial and **C**, dorsal view. **Abbreviations:** an, angular; co, coronoid; d, dentary; d1-16, dentary tooth 1-16; emf, external mandibular fenestra; fic, foramen intermandibularis caudalis; mg, meckelian groove; mx4-5, maxilla tooth 4-5; sa, surangular; sp, splenial. Scale bar = 5 cm. (altered after Massonne et al., 2019)

(1) notch between the premaxilla and maxilla, (2) dominant maxillary ridge alongside the nasal, (3) the fifth maxillary tooth being the largest maxillary tooth, (4) anterior tip of frontal being acute and projects between the nasal bones, (5) small supratemporal fenestra, (6) large supraoccipital exposure preventing the parietal from reaching the posterior skull table in adults, (7) quadrate foramen aerum laying on the dorsomedial angle of the quadrate, (8) large suborbital fenestrae reaching anteriorly the level of the seventh to eighth maxillary tooth, (9) maxilla-palatine suture forming an obtuse angle and not reaching beyond the anterior end of the suborbital fenestra, (10) palatine-pterygoid suture laying anterior to the posterior end of the suborbital fenestra, (11) pterygoid forming a neck surrounding the choana, (12) dentary tooth row with only 16 teeth, (13) laterally compressed posterior teeth, (14) very small external mandibular

fenestra, (15) foramen aerum at the lingual margin of the retroarticular process, (16) axis with a hypapophysis that is located near the centre of the centrum, (17) coracoid with a very large glenoid, (18) iliac blade with a rectangular posterior outline and a dorsal indentation, and (19) dorsal osteoderms with no or only a modest ridge.

Orientalosuchus naduongensis is further distinguished from *K. siamogallicus* in having an inwardly pushed pterygoid around the choana, a neck surrounding the opening, and a very large supraoccipital exposure; from *E. chunyii*, among others, in having very prominent preorbital ridges, a very large supraoccipital exposure, and a smooth dorsal surface of the surangular; from *J. nankangensis*, among others, in having a small incisive foramen, prominent preorbital ridges and a frontoparietal suture entirely on the skull table, and from *P. huiningensis*, among others, in having a deeply curved dentary, laterally compressed posterior teeth, a deep notch lateral to the naris and very prominent preorbital ridges.

In order to clarify the relationships between these taxa from East and Southeast Asia and their position on the tree, a phylogenetic analysis was performed based on the dataset of Brochu & Storrs (2012). The dataset contained a total of 202 characters, nine of which were newly created for this analysis, and the total number of taxa was increased from 103 to 114. The newly added *O. naduongensis* was scored for 118 characters. For a full list of added characters and their descriptions, as well as a list of all added taxa and the exact methods used, see Massonne et al. (2019) in the appendix.

The results of the phylogenetic analysis (Fig. 14) show that the new species from Na Duong proved to be a serendipity for science, as for the first time it was possible to find a monophyletic group consisting of the above-mentioned East and Southeast Asian taxa. The new group is named Orientalosuchina and is defined as the most inclusive clade containing *Orientalosuchus naduongensis*, *Krabisuchus siamogallicus*, *Eoalligator chunyii*, *Jiangxisuchus nankangensis* and *Protoalligator huiningensis*, but not *Brachychampsa montana* Gilmore, 1911, *Stangerochampsa mccabei* Wu et al., 1996, *Leidyosuchus canadensis* Lambe, 1907, *Diplocynodon darwini* (Ludwig, 1877), *Bottosaurus harlani* von Meyer, 1832, or any species of recent Crocodylia. Within Orientalosuchina, there is a polytomy between *J. nankangensis*, *E. chunyii*, *P. huiningensis* and *O. naduongensis* + *K. siamogallicus*, which is not surprising since *E. chunyii*, *P. huiningensis* are poorly preserved, limiting the resolution

of the tree. Nevertheless, the analysis reveals a particularly close relationship between the two late Eocene species *O. naduongensis* and *K. siamogallicus*. The other Eocene taxon from the Maoming Basin had to be pruned for the analysis, as its particularly poor preservation would otherwise have led to a complete collapse of the tree. There are two alternative positions for this taxon. Either it is very closely related to the two aforementioned taxa, or it is closely related to crocodylines from the Miocene of Africa, which seems much less likely in direct comparison.

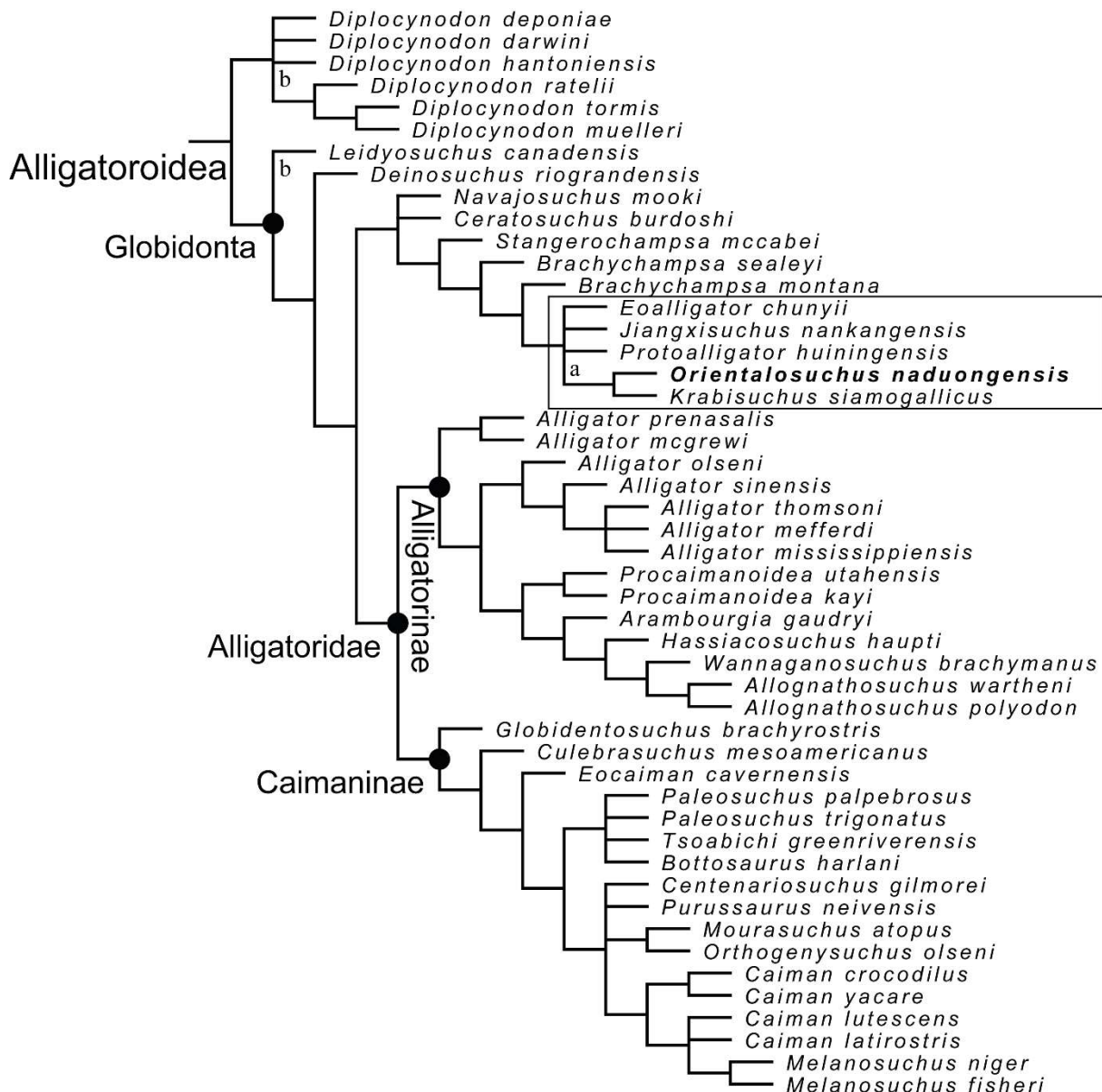


Figure 14. Reduced strict consensus tree of 2520 equally optimal trees, highlighting Alligatoroidea, obtained from the maximum parsimony analysis with 202 characters included; length: 926 steps; CI: 0.292 and RI: 0.759. 'a' indicates the alternative position of the pruned 'Maoming alligatoroid' (the alternative position lies inside Crocodylinae). 'b' indicates the alternative position of the pruned *Asiatosuchus nanlingensis*. The box highlights the monophyletic Orientalosuchina. (altered after Massonne et al., 2019)

Due to the aforementioned poor preservation of two basal taxa (i.e. *E. chunyii* and *P. huiningensis*), Orientalosuchina is supported by only one autapomorphy present on all trees: a short dentary symphysis extending to the height of the fourth to fifth alveolus (49-0). However, this character is also common in other alligatoroids, such as most species of *Alligator* and Caimaninae. One of the two species (*P. huiningensis* or *E. chunyii*) is found in the ancestral position of the group. Depending on the taxon, this has a major influence on the additional autapomorphies for Orientalosuchina. If *P. huiningensis* is in an ancestral position, there is a single additional autapomorphy for the group. If instead *E. chunyii* is recovered as the most basal taxon, the monophyly of Orientalosuchina is further supported by a total of seven autapomorphies. The full list of autapomorphies can be found in the appendix of Massonne et al. (2019).

The unclear position of *P. huiningensis* or *E. chunyii* also affects possible synapomorphies for *O. naduongensis* and *K. siamogallicus*. No characters are found in all trees, but five are found in some of them: the dentary curving deeply between the fourth and 10th dentary alveoli (50-1), the palatine-pterygoid-suture being situated far from the posterior angle of the suborbital fenestra (118-1), the frontoparietal suture laying entirely on the skull table (150-2), the anterior and medial teeth have dominant vertical ridges on their labial surface (198-1), and the intersupratemporal bar being similarly broad as the supratemporal fenestra (199-0).

The position of Orientalosuchina on the phylogenetic tree, their morphology, and their Late Cretaceous origin (*J. nankangensis* and *E. chunyii*) strongly suggest that they represent a relatively basal monophyletic clade of alligatoroids. The results suggest that East and Southeast Asia was colonised twice by alligatoroids: once by the ancestor of Orientalosuchina during the Late Cretaceous and once by an early member of the *A. sinensis* lineage during the Cenozoic (Brochu, 1999). For both lineages, dispersal across Beringia is most consistent with palaeogeography, climate, phylogeny, inferred stenohalinity, fossil record, and divergence dates (Taplin & Grigg, 1989; Brochu, 1999; Fiorillo, 2008; Oaks, 2011; Li et al., 2019). The presumed lower eustatic sea level in the late Maastrichtian (Kominz et al., 2008) would have favoured the dispersal of Orientalosuchina, consistent with the likely age of *J. nankangensis* and *E. chunyii*. Evidence for the dispersal of Late Cretaceous vertebrates from North America to Asia is otherwise sparse and includes only some tyrannosauroid, hadrosaurid and ceratopsian dinosaurs (Loewen et al., 2013; Farke et al., 2014; Prieto-Márquez et al., 2019).

2.2 A new species of *Maomingosuchus* from the Eocene of Vietnam highlights the phylogenetic relationship of tomistomines and their dispersal from Europe to Asia

The second paper of the thesis is about a new species of Tomistominae from the Na Duong Basin of Vietnam. All the material examined here belongs to a single individual (GPIT-PV-31657), found in 2011 at the base of layer 80 in the Na Duong coal mine and subsequently prepared by the Geological-Paleontological Institute of the Eberhard Karls University of Tübingen (GPIT) (Böhme et al., 2012). The bones are overall well-preserved, but disarticulated and dispersed over a small area of about 4 m². As all of the bones were found in close proximity to each other and have the same general size without duplication of elements, it is clear that GPIT-PV-31657 represents a single individual. The material consists of a skull with articulated mandibles (Fig. 15) and the almost completely disarticulated postcranial material (Fig. 16). The skull is compressed dorsolaterally, resulting in poorly preserved ventral and occipital regions. For a full description of the material, see Massonne et al. (2021) in the appendix.

In total, several skulls of different sizes of the new species were excavated, but only briefly examined and compared and not described in detail for the thesis. The initial hypothesis regarding these skulls was the existence of two different species. All of the medium to large skulls were assigned to an *Asiatosuchus*-like crocodylian, and only one skull of much smaller size was thought to represent a tomistomine. This primary assumption is reflected in the herpetofauna section of Böhme et al. (2012). However, a closer comparison of all the skulls revealed that the smaller skull represents a subadult individual and that all the existing differences can be explained by the earlier ontogenetic stage of this individual. Furthermore, all skulls showed a high similarity to a tomistomine from the Maoming Basin, which was named *Tomistoma petrolica* by Yeh (1958) and redescribed and renamed *Maomingosuchus petrolicus* by Shan et al. (2017) based on several newly discovered individuals. The result of the primary analysis is thus that, apart from *O. naduongensis* (see above), only one other species of Crocodylia existed in the Na Duong Basin and that it belongs to the longirostrine Tomistominae and is not closely related to *Asiatosuchus*. Based on the similarities, the new species from Na Duong is assigned to the same genus as the species from Maoming, but due to some distinct differences, such as the acute snout,

it represents a new species named *Maomingosuchus acutirostris* sp. nov. The new species is a small to medium-sized tomistomine with a skull length (premaxilla-supraoccipital) of 546 mm and an estimated total length of about 3.5 m, based on the skull-to-body length ratio of the extant *Tomistoma schlegelii* (1:6.4 according to Whitaker & Whitaker, 2008), which presumably has similar body proportions.

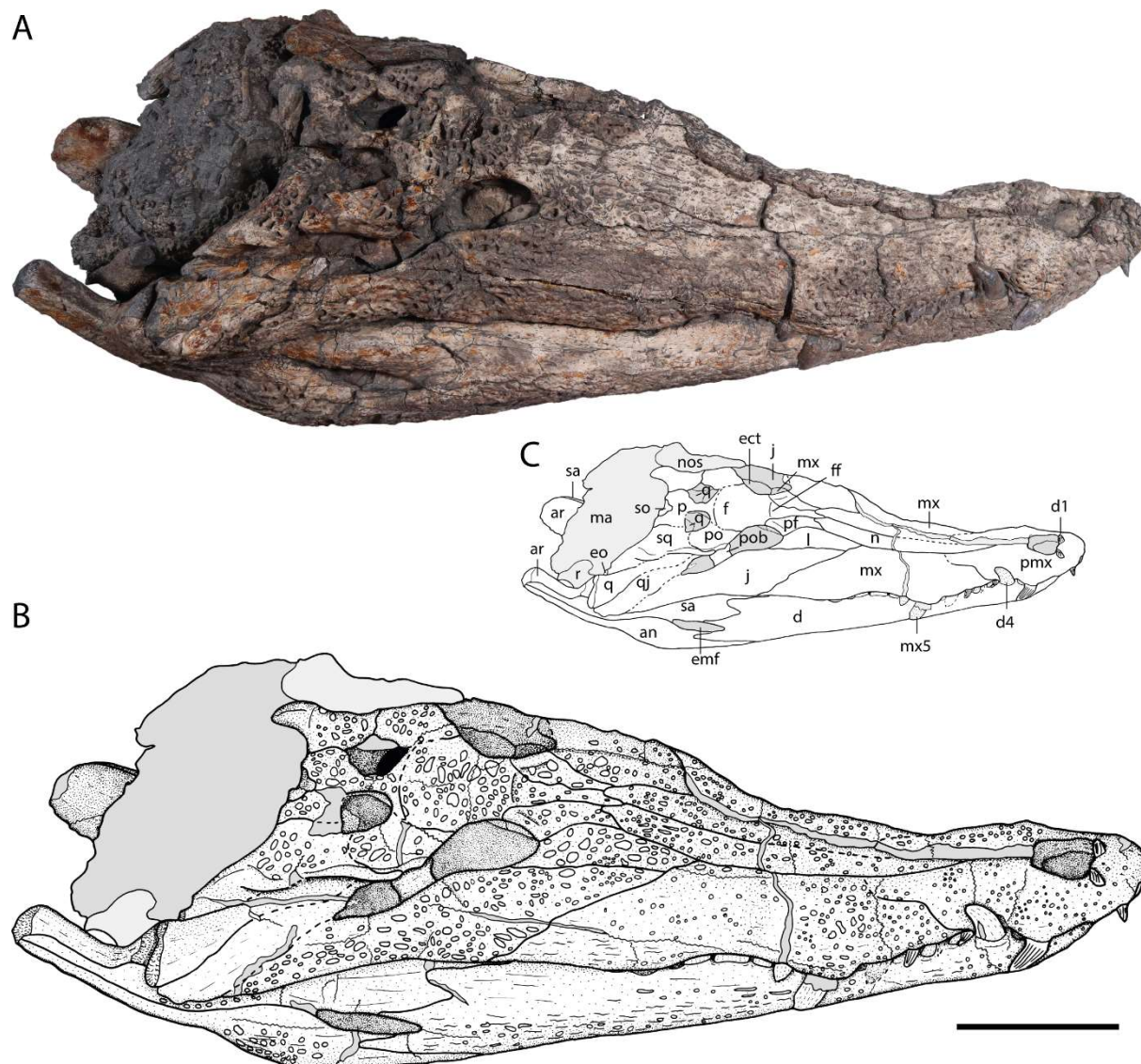


Figure 15. *Maomingosuchus acutirostris*, holotype, GPIT-PV-31657, Na Duong Formation, late Eocene, Vietnam. Skull in **A**, **B**, dorsolateral view and **C**, a sketch with the visible bones and characteristics. **Abbreviations:** an, angular; ar, articular; d, dental; d1, dentary tooth 1; d4, dentary tooth 4; ect, ectopterygoid; emf, external mandibular fenestra; eo, exoccipital; f, frontal; ff, frontal fossa; j, jugal; l, lacrimal; ma, matrix; mx, maxilla; mx5, maxillary tooth 5; n, nasal; nos, nuchal osteoderm; p, parietal; pf, prefrontal; pmx, premaxilla; po, postorbital; pob, postorbital bar; q, quadrate; qj, quadratojugal; r, rib; sa, surangular; so, supraoccipital; sq, squamosal. Scale bar = 10 cm. (Massonne et al., 2021)

In addition to *M. acutirostris* and *M. petrolicus*, a third individual (*Maomingosuchus* sp.) was described by Martin et al. (2019a) from the late Eocene

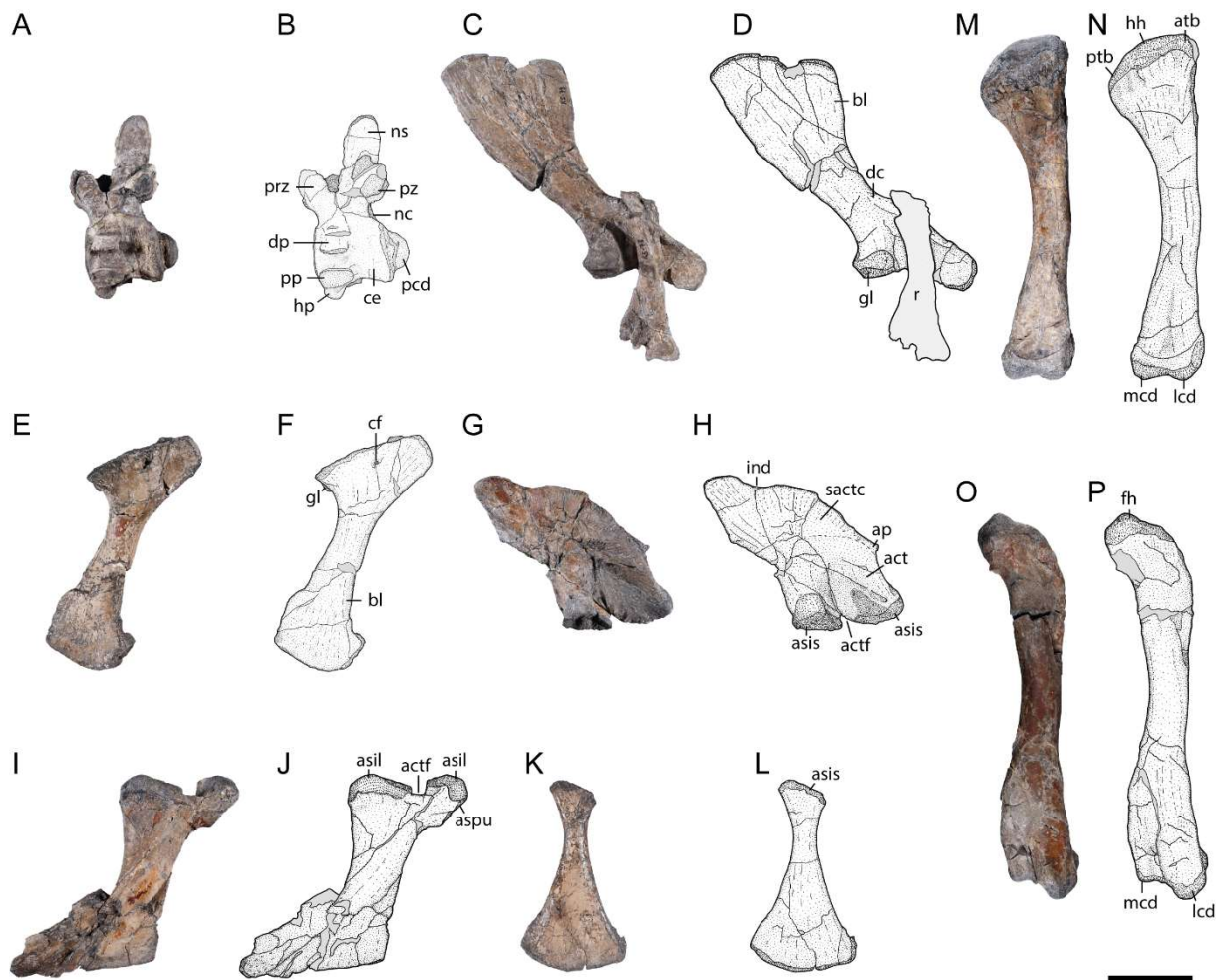


Figure 16. *Maomingosuchus acutirostris*, holotype, GPIT-PV-31657, Na Duong Formation, late Eocene, Vietnam. Cervical vertebra in **A, B**, lateral view; Scapula in **C, D**, lateral view; Coracoid in **E, F**, lateral view; Ilium in **G, H**, lateral view; Ishium in **I, J**, lateral view, pubis in **K, L**, lateral view; humerus in **M, N**, lateral view and Femur in **O, P**, lateral view. **Abbreviations:** **act**, acetabulum; **actf**, acetabulum foramen; **ap**, anterior process; **asil**, articular surface with ilium; **asis**, articular surface with ischium; **aspu**, articular surface with pubis; **atb**, anterior tubercle; **bl**, blade; **ce**, centrum; **cf**, coracoid foramen; **dc**, deltoid crest; **dp**, diapophysis; **fh**, femur head; **gl**, glenoid; **hh**, humerus head; **hp**, hypapophysis; **ind**, indentation; **lcd**, lateral condylus; **mcd**, medial condylus; **nc**, neural canal; **ns**, neural spine; **pcd**, posterior condylus; **pp**, parapophysis; **prz**, prezygapophysis; **ptb**, posterior tubercle; **pz**, postzygapophysis; **r**, rib; **sactc**, supraacetabular crest. Scale bar = 5 cm. (altered after Massonne et al., 2021)

Krabi Basin of Thailand based on a partially preserved skull and mandible. The authors refrained from erecting a new species for the Krabi-*Maomingosuchus* due to its fragmentary preservation and general similarity to *M. petrolicus*. In the current phylogenetic analysis (see p. 44), the Krabi-*Maomingosuchus* was found to be closely related to *M. petrolicus*, but with three autapomorphies that distinguish it from the other maomingosuchids. The Krabi-*Maomingosuchus* is therefore treated here as a provisionally valid but unnamed species of *Maomingosuchus*.

As there are now three species of *Maomingosuchus*, the diagnosis has changed slightly from previous studies, and the genus is now diagnosed by the unique combination of the following characters: (1) distinct dorsoventrally extending ridges on the lateral and mesial surfaces of the anterior teeth (shared with an indeterminate tomistomine from the Ikovo locality and some non-tomistomine taxa); (2) presence of a frontal fossa between the orbits, close to the posterior end of the prefrontals (shared with '*Crocodylus*' *affinis* Marsh, 1871 and *Prodiplocynodon langi* Mook, 1941); (3) a flat frontal margin between the orbits (shared with *Dollosuchoides*). Preserved only in *M. acutirostris* and *M. petrolicus* are: (4) perforations for the first dentary tooth anterior to the external naris (shared with *Kentisuchus spenceri*); (5) 15 maxillary teeth in total (shared with *Dollosuchoides densmorei* Brochu, 2007); and (6) exoccipital with ventrally projecting lamina hiding the entrance to the cranio-quadrangle passage (shared with gharials and basal eusuchians).

Maomingosuchus acutirostris can be diagnosed by the combination of the following characters: (1) relatively robust teeth, especially the 5th maxillary tooth and the 11th or 12th dentary teeth (similar to *Maroccosuchus zennaroi*); (2) anterior part of the prefrontal on the same level as anterior part of the frontal (shared with the Krabi-*Maomingosuchus*, some individuals of *M. petrolicus* and *Gavialosuchus eggenburgensis* [Toula & Kail, 1885]); (3) supraoccipital visible on dorsal skull table (shared with '*Tomistoma*' *cairensis* Müller, 1927, '*Tomistoma*' *coppensi* Pickford, 1994, *Paratomistoma courti* Brochu & Gingerich, 2000 and *M. petrolicus*); (4) atlantal rib with process on dorsal margin (shared with *Toyotamaphimeia machikanensis* and some non-tomistomines); and (5) ilium with a prominent anterior process (shared with *Penghusuchus pani* and *T. machikanensis*). In addition to the characters above, *M. acutirostris* can be further distinguished from *M. petrolicus* by, among other characters, an elongated premaxilla, anterior to the external naris and a ratio of the mediolateral width of the supratemporal fenestral bar to the width of the skull table at the same level of 0.100–0.175. Both *M. acutirostris* and *M. petrolicus* differ from the Krabi-*Maomingosuchus* by, among other characters, the first five maxillary teeth getting continuously larger posteriorly; the 7th and 8th maxillary teeth more widely spaced than other teeth and a surangular–dentary suture intersecting the external mandibular fenestra anterior to its posterior corner.

To clarify both the relationship between the *Maomingosuchus* taxa and their position within Tomistominae, a phylogenetic analysis was performed using the dataset of

Nicholl et al. (2020). *Maomingosuchus acutirostris* and the Krabi-*Maomingosuchus* were added to the dataset, which now consists of 72 taxa and 244 characters. The analysis followed the methods of Nicholl et al. (2020). *Maomingosuchus acutirostris* could be scored for 111 characters of the dataset. A detailed description of the methods used can be found in the appendix of Massonne et al. (2021).

The results of the phylogenetic analysis (Fig. 17) recover a monophyletic *Maomingosuchus* in a basal position within Tomistominae as a sister clade to *Tomistoma* + *Paratomistoma* + *Gavialosuchus* + *Melitosaurus*. Within *Maomingosuchus*, *M. acutirostris* is found as a sister taxon to *M. petrolicus* + Krabi-*Maomingosuchus*. The monophyly of *Maomingosuchus* is supported by three autapomorphies: a flush margin of the orbit with the skull surface (103–0), a ventral border of the exoccipital convex and ventrally projected (166–0) and a frontal ending at the same level as the anterior extension of the prefrontal (171–1). In previous analyses (Shan et al., 2017; Iijima et al., 2018; Nicholl et al., 2020), *M. petrolicus* was found in different positions among tomistomines, but usually in a derived position. Only Piras et al. (2007) obtained results similar to the current analysis. The analysis by Martin et al. (2019a) was the only one that included both *M. petrolicus* and Krabi-*Maomingosuchus* and recovered *Maomingosuchus* as a sister clade to the extant *T. schlegelii*. The reevaluation of some characters for *M. petrolicus* and Krabi-*Maomingosuchus* and the inclusion of *M. acutirostris* results in a more basal position of *Maomingosuchus* in the current analysis, which is more congruent with its late Eocene age.

Based on the phylogenetic analysis and previous phylogenies, most of the basal tomistomine taxa were excavated in the western Tethyan region. Therefore, it is most parsimonious to assume that they originated in this area before the early Eocene (as previously suggested by Jouve et al., 2015; Jouve, 2016; Shan et al., 2017; Iijima et al., 2018; Nicholl et al., 2020). Furthermore, the current analysis suggests that dispersal to Southeast Asia must have occurred several times independently. Accordingly, the first dispersal for the stem lineage of *Maomingosuchus* occurred no later than the late Eocene, while a second dispersal for the stem lineage of *Penghusuchus* + *Toyotamaphimeia* occurred no later than the early to middle Miocene, and a third dispersal for the stem lineage of the extant *T. schlegelii* occurred during the Neogene (Fig. 16). Based on palaeogeographical reconstructions, two different

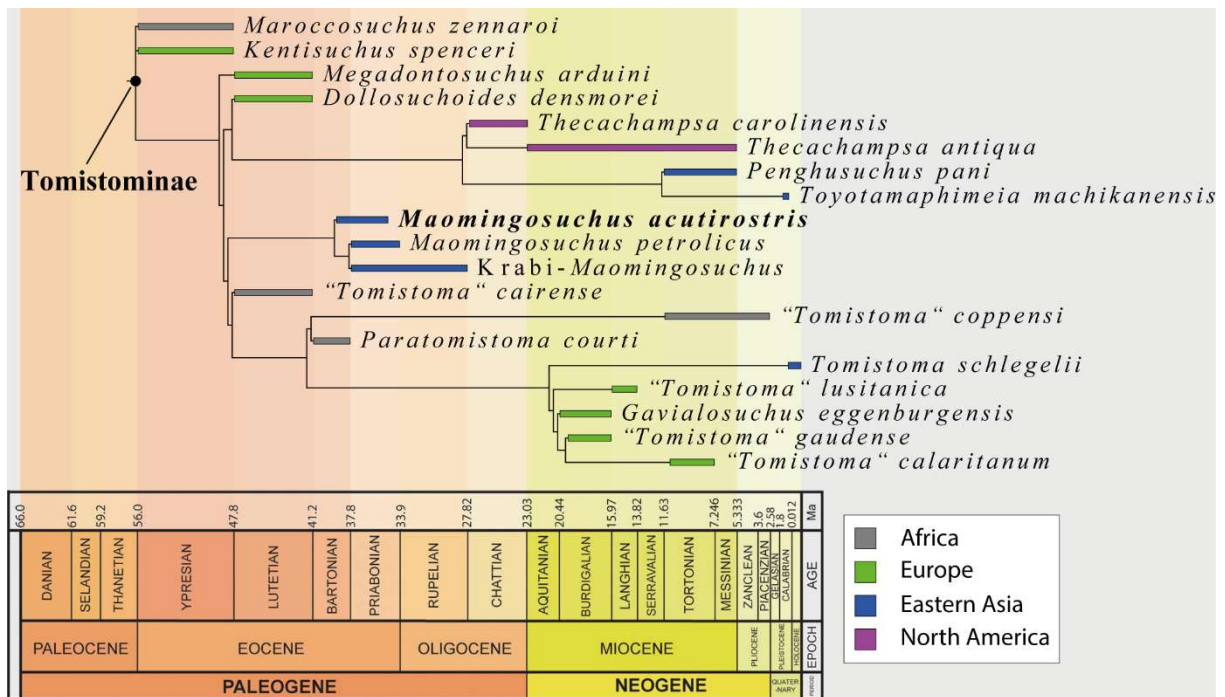


Figure 17. Time-calibrated Tomistominae phylogeny of the reduced strict consensus tree of 17,496 equally optimal trees, obtained from the maximum parsimony analysis of 72 taxa and 244 characters; length: 1017; CI: 0.317 and RI: 0.690. *Kentisuchus astrei* and *Melitosaurus champsoides* are pruned. (Massonne et al., 2021)

dispersal routes seem possible for the stem lineage of *Maomingosuchus*: an eastward route from Europe along the Neotethys coast to Southeast Asia or a westward route from Europe via North America and Beringia to Southeast Asia. However, the latter, as proposed for *Orientalosuchina* (see above), seems rather unlikely due to the lack of suitable fossils in North America at that time.

2.3 A tarsometatarsus from the Eocene of Na Duong – the first Palaeogene fossil bird from Vietnam

The third contribution to the thesis is a bird specimen (GPIT-PV-122865) (Fig. 18) from the Na Duong Basin of Vietnam. Like the other material (see above), the bone was collected during systematic surveys between 2009 and 2012 at the base of layer 80 in the Na Duong coal mine and subsequently prepared at the Geological-Paleontological Institute of the Eberhard Karls University of Tübingen (GPIT) (Böhme et al., 2012). The specimen represents the distal part of a right tarsometatarsus with a shaft covering approximately half to two-thirds of its original length. Diagenetic compression has flattened the bone dorsoplantarily, and both its plantar surface and the dorsal surface of the distal end are weathered. For a full description of the material, see Massonne et al. (2022) in the appendix.

One of the greatest challenges with fragmentary preserved material is its assignment to a particular genus or family. Another major obstacle in this case is the sparse fossil record of birds for the Palaeogene of East and Southeast Asia (see Introduction). For this reason, the comparative material was selected mainly on the basis of extant groups that evolved during the Palaeogene, with the idea that GPIT-PV-122865 might represent an identifiable stem member of one of these groups. However, the first step was to identify the higher-level clade to which the fossil probably belonged.

Extant bird species can be divided into two higher-level clades: Palaeognathae and Neognathae. GPIT-PV-122865 most likely represents a member of the latter group. The only long-legged palaeognaths that occurred in Eurasia during the Eocene are members of the Palaeotididae and Eogruidae (Mayr, 2022). In contrast to GPIT-PV-122865, they have a less robust shaft, a larger foramen vasculare distale, wider incisurae intertrochleares lateralis and medialis, and lack an equally sized trochleae metatarsorum. This combination of characters precludes an assignment to either Palaeotididae or Eogruidae, making it unlikely that the specimen from Vietnam is a palaeognath.

During the Eocene, the Na Duong Basin was a swampy ecosystem within a dense forest (see Introduction). For this reason, GPIT-PV-122865 was compared with extant aquatic and semiaquatic members of Aequornithes (e.g. loons and storks) and Gruiformes (e.g. cranes), as well as with terrestrial representatives of Galliformes (e.g. chickens) and arboreal members of Coliiformes (mouse birds), all of which share

a similar tarsometatarsal morphology (Fig. 19). However, the morphology of GPIT-PV-122865 is not identical in any of these groups and it is therefore impossible to assign it with certainty to any of them.

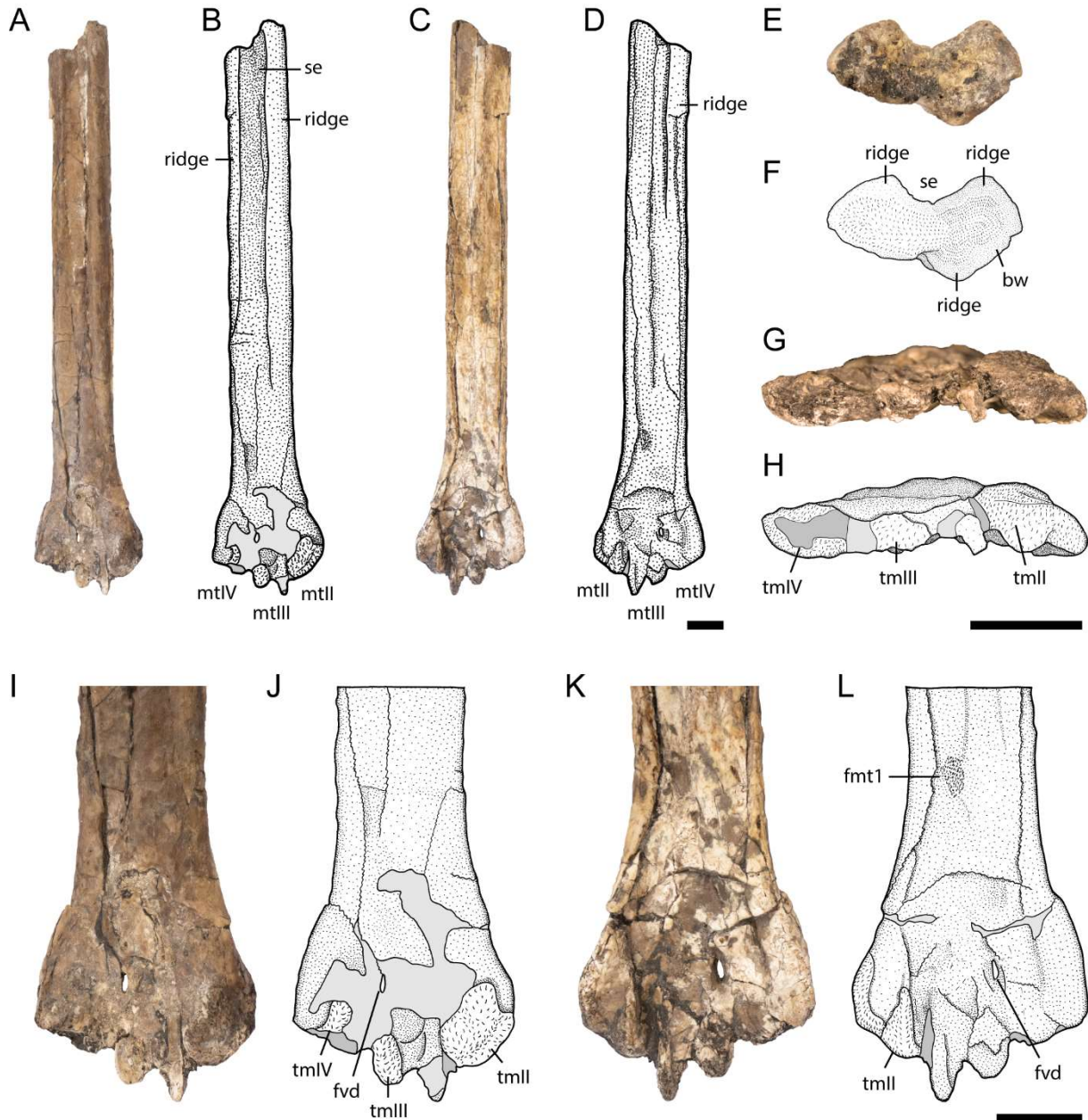


Figure 18. ?*Neognathae incertae sedis* (GPIT-PV-122865), Na Duong Formation, late Eocene, Vietnam. Tarsometatarsus in **A, B**, dorsal view; **C, D**, plantar view; **E, F**, cross-section of the proximal end of the shaft; **G, H**, distal view; **I, J**, enlargement of the distal end in dorsal view; **K, L**, enlargement of the distal end in plantar view. **Abbreviations:** **bw**, bone wall; **fmt1**, fossa metatarsi 1; **fvd**, foramen vasculare distale; **mt**, metatarsale; **se**, sulcus extensorius; **tm**, trochlea metatarsi. Scale bar = 5 mm. (Massonne et al., 2022)

Gallus gallus Linnaeus, 1758 lacks an elongated extensor sulcus along its dorsal surface, as well as a plantar ridge, and its shaft is generally shorter. Ardeidae (herons), Ciconiidae (storks and related species) and Gruidae (cranes) have an elongated shaft



Figure 19. Comparison of Tarsometatarsi of ?*Neognathae incertae sedis*, GPIT-PV-122865, Na Duong Formation, late Eocene, Vietnam in **A**, dorsal view, **G**, plantar view with *Gallus gallus* (Galliformes) (GPIT-PV-122866) in **B**, dorsal view, **H**, plantar view, *Ardea herodias* (Pelecaniformes) (NMNH 555715) in **C**, dorsal view, **I**, plantar view, *Mycteria americana* (Ciconiiformes) (NMNH 16295) in **D**, dorsal view, **J**, plantar view, *Antigone canadensis* (Gruiformes) (NMNH 432705) in **E**, dorsal view, **K**, plantar view and *Colius striatus* (Coliiformes) (SMF 8019) in **F**, dorsal view and **L**, plantar view. Pictures from NMNH 555715, NMNH 16295 and NMNH 432705 are taken from the public image database of the Smithsonian National Museum of Natural History under copyright CC0. Scale bar = 5 mm. (Massonne et al., 2022)

like GPIT-PV-122865, but they lack a marked sulcus extensorius along the dorsal surface of the shaft and a plantar ridge on the ventral surface. They also have more

slender shaft proportions and a larger foramen vasculare distale. The representative of the arboreal Coliiformes, *Colius striatus* Gmelin, 1789, has an overall similar tarsometatarsal shape, a similarly robust shaft, a small foramen vasculare distale, equally sized trochleae metatarsorum, and narrow incisurae intertrochleares lateralis and medialis. However, in contrast to GPIT-PV-122865, *C. striatus* has a less pronounced sulcus extensorius along the dorsal surface of the shaft and lacks a plantar ridge along its ventral surface, and has a trochlea metatarsi III that does not project further distally than the trochleae metatarsorum II and IV. In addition, all extant and fossil members of mouse birds are much smaller than the bird from Na Duong. Other Eocene groups with a similar habitat to GPIT-PV-122865, are members of Strigiformes (owls) and Psittacopasseres (parrots and passerines). However, the tarsometatarsus of these lineages differs significantly from GPIT-PV-122865 in proportions and morphology of the distal extremity (Mayr, 2022).

Unfortunately, due to poor preservation, GPIT-PV-122865 cannot be identified beyond ?Neognathae *incertae sedis*, but may represent an endemic neognath not known from other Palaeogene localities outside of Vietnam. Despite its incompleteness, GPIT-PV-122865 provides the first insight into the bird assemblage of the Na Duong Basin and represents a new Palaeogene avifaunal occurrence for East and Southeast Asia.

2.4 A new cryptodire from the Eocene of Vietnam sheds new light on *Pan-Trionychidae* from Southeast Asia

The fourth and final paper of the thesis is about a new species of *Pan-Trionychidae* from the Na Duong Basin of Vietnam. A total of nine individuals were collected during systematic surveys between 2009 and 2012 at the base of layer 80 in the Na Duong coal mine and subsequently prepared at the Geological-Paleontological Institute of the Eberhard Karls University of Tübingen (GPIT) (Böhme et al., 2012). The material consists of two almost complete carapaces with associated plastral elements and seven partial carapaces, some of them with associated plastral elements. In addition, a pectoral girdle and a heavily weathered skull were found, as well as several isolated plastral elements that cannot be associated with any of the carapaces. The best-preserved specimen, designated as the holotype (GPIT-PV-112860), consists of an almost complete carapace (Fig. 20), which was found associated with several plastral elements (entoplastron, both hyoplastra, the right hypoplastron and the left xiphiplastron) (Fig. 21), and additional postcranial material. For a full description of the material, see Massonne et al. (2023) in the appendix.

A single well-preserved specimen (GPIT-PV-122867) of the new pan-trionychid species was already illustrated in Böhme et al. (2011), and Böhme et al. (2012) provisionally reported a total of five to six turtle species belonging to *Pan-Trionychidae* and *Pan-Geoemydidae*. A single species of *Pan-Geoemydidae*, *Banhxeochelys trani*, was described by Garbin et al. (2019) on the basis of several individuals. After examination of all available turtle material, *B. trani* likely represents the only known species of pan-geoemydids from Na Duong, and examination of the *Pan-Trionychidae* material came to the same conclusion for this group. It is likely that all the material belongs to a single species: *Striatochelys baba* gen. et. sp. nov.

Besides *S. baba*, there is another species of the new genus named *Striatochelys impressa*. This species was originally described by Yeh (1965) as *Aspideretes impressus* from the late Eocene of the Maoming Basin. However, the species was recombined as *Trionyx impressus* by Danilov et al. (2013) and retained as '*Trionyx*' *impressus* by Georgalis & Joyce (2017), pending a redescription of the holotype. In the present work, it is assigned to *Striatochelys* based on its high similarity to *S. baba* and a comparison with other taxa.

Striatochelys is distinguished from other pan-trionychid genera by the combination of the following characters: (1) relatively small size, with an estimated maximum

carapace length of 27 cm; (2) absence of a preneural; (3) strong straight ridges on the carapace, extending from costal I to costal VIII; and (4) stronger ridges posteriorly.

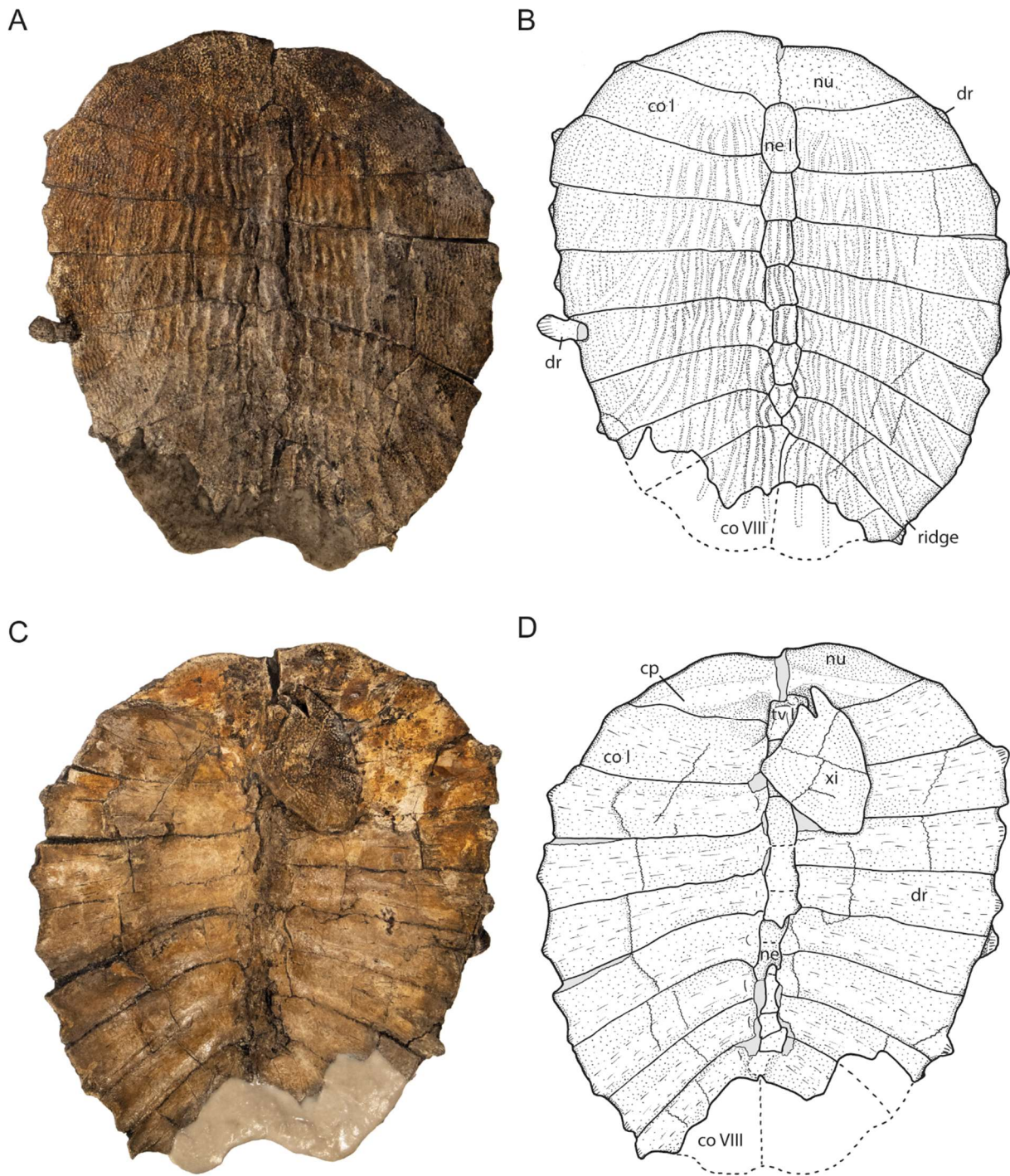


Figure 20. *Striatochelys baba*, holotype, GPIT-PV-112860-1, Na Duong Formation, late Eocene, Vietnam. Carapace in **A, B**, dorsal and **C, D**, ventral view. **Abbreviations:** **co**, costal; **cp**, costiform process; **dr**, dorsal rib; **ne**, neural; **nu**, nuchal; **tv**, thoracic vertebra; **xi**, xiphiplastron. Scale bar = 5 cm. (Massonne et al., 2023)

Within the new genus, *Striatochelys baba* can be distinguished from *S. impressa* by the combination of the following characters: (1) a larger costal VIII, forming the

posterolateral margin of the carapace; (2) presence of ridges on the neurals, which are straight anteriorly and sinusoidal posteriorly; and (3) entoplastron callosity in the shape of a bulge (unknown for *S. impressa* and possibly an autapomorphy for *S. baba* + *S. impressa*).

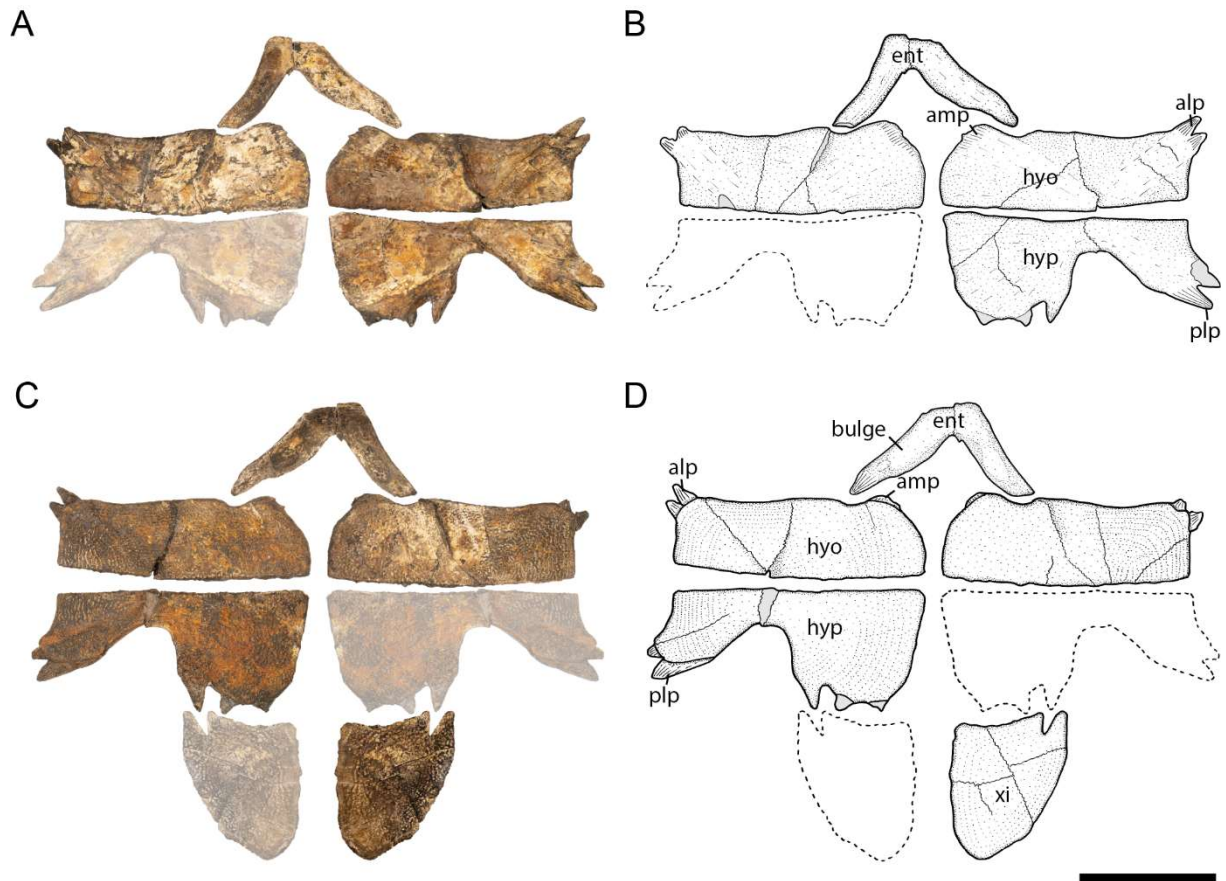


Figure 21. *Striatochelys baba*, Na Duong Formation, late Eocene, Vietnam. Plastron of holotype (GPIT-PV-112860-2, GPIT-PV-112860-3, GPIT-PV-112860-4, GPIT-PV-112860-5, GPIT-PV-112860-1) in **A, B**, dorsal and **C, D**, ventral view. Missing bones are mirrored and faded. **Abbreviations:** **alp**, anterolateral process; **amp**, anteromedial process; **ent**, entoplastron; **hyo**, hyoplastron; **hyp**, hypoplastron; **plp**, posterolateral process; **xi**, xiphiplastron. Scale bar = 5 cm. (altered after Massonne et al., 2023)

Comparison with other East and Southeast Asian *Pan-Trionychidae* is difficult. According to Georgalis and Joyce (2017), only a few named *Pan-Trionychidae* from the Palaeogene of Asia are diagnostic, and these were selected for comparison with *S. baba*. These species are *Kuhnemys palaeocenica*, *Drazinderetes tethyensis*, ‘*Trionyx*’ *linchuensis*, ‘*Trionyx*’ *gregarius*, ‘*Trionyx*’ *johnsoni*, ‘*Trionyx*’ *minusculus*, ‘*Trionyx*’ *ninae* and *Striatochelys impressa*. However, comparisons with the Palaeogene taxa from Asia highlight a general problem with *Pan-Trionychidae*. Despite many occurrences, the material in question often consists only of fragmentary shell

remains that are rarely diagnostic at the species level (see also Georgalis & Joyce [2017]). Despite these problems, the taxa that could be examined do not show a particularly high degree of similarity to the new taxon from Na Duong.

Southeast Asia, however, not only has many fossil taxa, but also the highest diversity of extant trionychids. According to molecular data, most Asian taxa belong to a single monophyletic group, including five genera, i.e. *Pelodiscus*, *Palea*, *Dogania*, *Amyda* and *Nilssonina*, which probably originated between the Eocene and Miocene (Engstrom et al., 2004; Le et al., 2014; Pereira et al., 2017; Thomson et al., 2021). Therefore, they are an ideal comparison group for the late Eocene taxa from Na Duong and Maoming.

Another interesting group of fossils are *Plastomenidae* from the Late Cretaceous of North America. With the exception of *S. impressa*, members of this group, i.e. *Gilmoremys lancensis* (Gilmore, 1916) and especially *Gilmoremys gettyspherensis* Joyce et al., 2018, are the most similar to *Striatochelys* among fossil taxa. They share with both species of *Striatochelys* prominent, anteroposteriorly extending ridges in adults and an overall very similar plastron morphology, but unlike *S. baba* they have a well-developed preneural and an anterolaterally strongly curved costal II. Furthermore, members of the *Plastomenidae* are so far only known from the Cretaceous and Palaeogene of North America (Joyce & Lyson, 2011; Joyce et al., 2018).

Anteroposteriorly projecting ridges on the carapace also occur in some individuals of extant species (e.g. *Apalone ferox* [Schneider, 1783]; *Trionyx triunguis*; *Amyda cartilaginea* [Boddaert, 1770]; *Pelodiscus sinensis* [Wiegmann, 1835]), but are much weaker and usually present only in juveniles/subadults. Although such ridges are absent in adult pan-trionychines, the presence of such ridges in juveniles of several (not particularly closely related) trionychine species indicates that some species may have retained this morphology at later ontogenetic stages. The absence of a preneural is known exclusively for basal trionychids and *Pan-Trionychinae*, with a reversal in *Nilssonina gangetica* (Cuvier, 1825) and *Nilssonina hurum* (Gray, 1831). The absence of a preneural in *S. baba* therefore strongly supports a position for *Striatochelys* within *Pan-Trionychinae*. In addition, costals I and II in *S. baba* and *S. impressa* are similar in shape to those in most Asian *Pan-Trionychidae*. This is in marked contrast to the condition present in *Gilmoremys*, in which costal II is strongly curved anterolaterally, arguing against a close relationship between *Striatochelys* and *Gilmoremys*. However, the plastron of *S. baba* is remarkably similar to that of *Gilmoremys*, whereas there are

many differences with most species of *Pan-Trionychinae*. In most species of *Pan-Trionychinae*, the plastron is much more reduced and the lateral and medial processes are longer. The exceptions to this are several species of *Nilssonina* spp. In these species, the overall plastron morphology is very similar to that of *S. baba*. Thus, the overall plastron morphology indicates a closer relationship of *Striatochelys* either with *Plastomenidae* or with extant East Asian trionychines.

From the above, it can be concluded that the carapace of *Striatochelys* shows strong affinities to *Pan-Trionychinae*. The absence of a preneural is known only in members of this group, as well as in basal trionychids, and characters indicating a close relationship with *Plastomenidae* (such as the strongly developed ridges on the carapace) can also be found in some juvenile/subadult individuals of *Pan-Trionychinae*. In addition, differences in the shape of costals I and II further support a differentiation from *Plastomenidae*. The plastron of *S. baba* is very similar to that of *Nilssonina* spp. and may indicate a close relationship of the former with members of this genus. The very similar plastron of the plastomenid *Gilmoremys*, on the other hand, probably represents a convergence.

To further clarify of the relationship of *S. baba* with other pan-trionychids, the dataset of Joyce et al. (2018) was used for the phylogenetic analysis, supplemented by taxa and rescorings from Lyson et al. (2021). Together with the new taxon, the dataset consists of 40 taxa and 95 characters. A total of 40 characters could be scored for the new taxon. A detailed description of the methods used can be found in the appendix of Massonne et al. (2023).

In the phylogenetic analysis performed here, *S. baba* is recovered within *Pan-Trionychinae* in a polytomy with *Nilssonina formosa* (Gray, 1869), *N. gangetica* and *N. hurum* (Fig. 22). Only a single autapomorphy supports *Nilssonina* spp. + *S. baba* in all trees: suprascapular fontanelles closed at hatching (20-1). Two other characters (22-2) and (50-1) are considered autapomorphies for the group only if *S. baba* and *N. gangetica* form a monophyletic sister group with *N. hurum* + *N. Formosa*, or if *N. gangetica* is the most basal taxon of the group. However, not only is the position of *S. baba* within *Nilssonina* spp. ambiguous, but also its position within *Pan-Trionychinae* in general is unstable, and a different interpretation of a single character can lead to a different position of *S. baba* in a polytomy with *Gilmoremys* at the base of *Plastomenidae*. Another problem with the current phylogeny is the position of five taxa from the Early Cretaceous (*Kuhnemys orlovi* Khosatzky, 1976, 'Aspideretes'

maortuensis Yeh, 1965, '*Trionyx*' *kyrgyzensis*, *Perochelys hengshanensis* and *Perochelys lamadongensis*) that were recovered deeply nested within *Pan-Trionychinae*. If these taxa are forced to the base of *Pan-Trionychidae* according to their age, *S. baba* is found at the base of this Early Cretaceous group, which contrasts strongly with its late Eocene age.

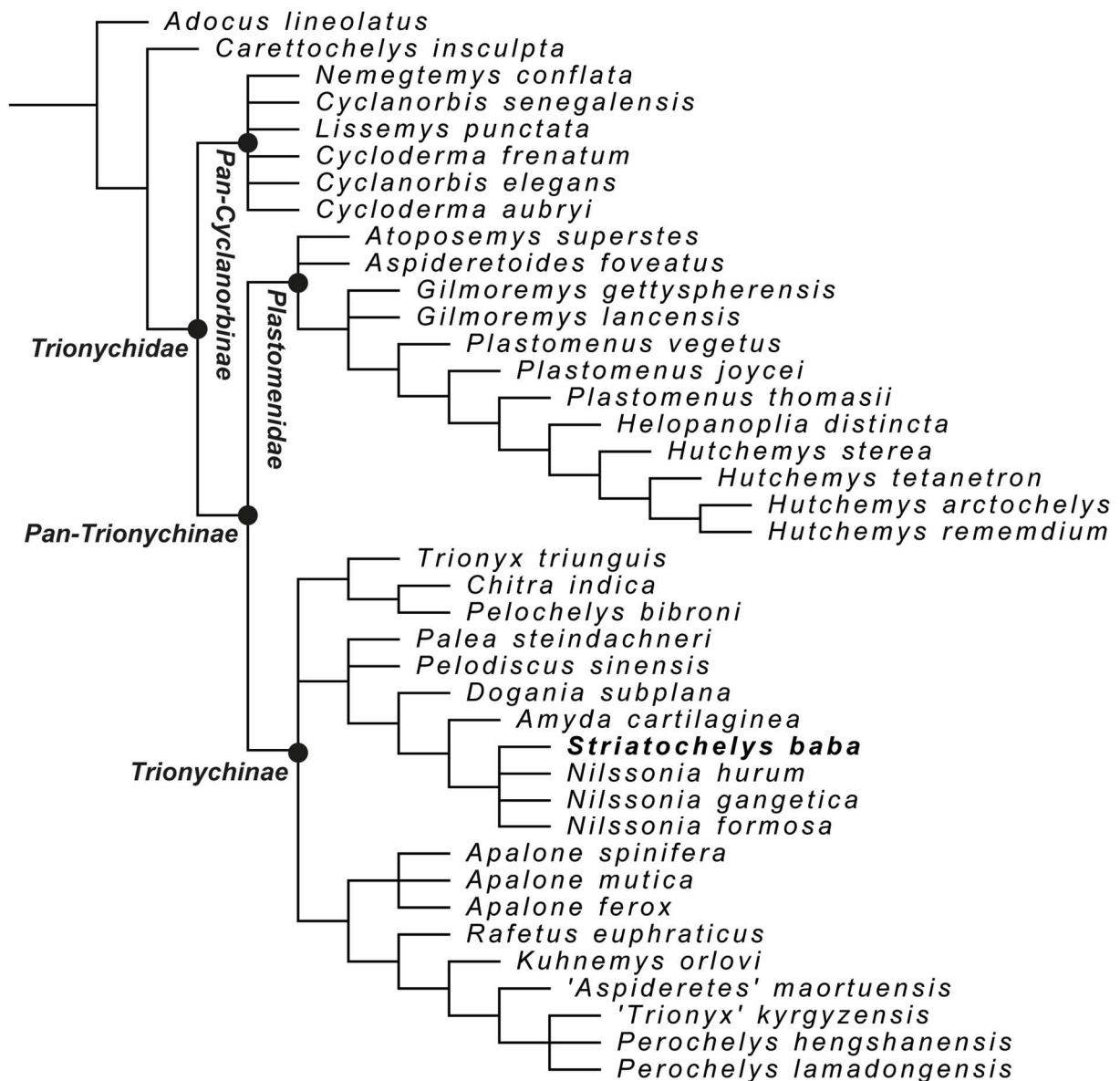


Figure 22. Strict consensus tree of 135 equally optimal trees, obtained from the maximum parsimony analysis of 40 taxa and 95 characters; tree length = 327 steps; consistency index = 0.361; and retention index = 0.605. (Massonne et al., 2023)

As highlighted above, *S. baba* can be recovered in several different positions on the tree based on only minor changes in the dataset. There are two main reasons for this uncertainty. One is related to the problematic position of Early Cretaceous taxa within the crown of *Pan-Trionychinae*, the other is the poor preservation of the skull of

S. baba, which makes cranial scoring impossible. Until these issues are resolved, the position of *S. baba* within *Nilssonina* spp. as proposed here should be treated with caution.

Although the results of the phylogenetic analyses should be treated with caution, the position of *S. baba* in a polytomy with *Nilssonina* spp. is not surprising given its age and occurrence in Southeast Asia. According to Pereira et al. (2017), the *Nilssonina* clade originated during the middle to late Oligocene in either East or Southeast Asia, and the split from *Palea steindachneri* (Siebenrock, 1906) and *A. cartilaginea* occurred sometime during the late Eocene in Southeast Asia. Based on these data, it seems possible that *S. baba* could be a basal stem member of *Nilssonina* spp. However, based on other analyses (Thomson et al., 2021; Evers et al., 2023), *Nilssonina* spp. originated much later, in the middle Miocene. These results would indicate a more basal position for *S. baba* within the extant East Asian trionychines.

3. Conclusion

The late Eocene Na Duong Basin of Vietnam is one of the richest fossil sites of Southeast Asia. Many studies focusing on its age, palaeoclimate, biostratigraphy, vegetation, vertebrates and invertebrates have been published over the past decades, but with only a single turtle species described to date, the reptile and bird fauna of the basin still remains a great mystery to science. In the present work, two crocodylians, one bird and one turtle were described and compared with fossil and extant species. Phylogenetic analyses were performed to further elucidate the relationship of the crocodylians and turtles of the Na Duong Basin with their counterparts from other late Eocene basins of East and Southeast Asia.

The first paper of the thesis is about a small alligatoroid representing a new species, *Orientalosuchus naduongensis* gen. et sp. nov., known from several well-preserved individuals. The new species is characterised by a combination of characters, such as dominant maxillary ridges along the nasal, the fifth maxillary tooth being the largest maxillary tooth, the anterior tip of the frontal being acute, a large supraoccipital exposure and a very small external mandibular fenestra. In the phylogenetic analysis performed, *O. naduongensis* was recovered as a sister taxon to *Krabisuchus siamogallicus* from the late Eocene of the Krabi Basin of Thailand. Together they form a monophyletic extinct basal East to Southeast Asian alligatoroid clade called Orientalosuchina of Late Cretaceous origin, which also includes *Jiangxisuchus nankangensis*, *Eoalligator chunyii* and *Protoalligator huiningensis*. The results imply that there were at least two distinct dispersals of alligatoroids from North America to East Asia: one during the Late Cretaceous by the stem lineage of Orientalosuchina, and a second during the Cenozoic by a stem member of the *Alligator sinensis* lineage.

The content of the second paper of the thesis covers the largest carnivore of the Na Duong Basin representing a new species of Tomistominae, *Maomingosuchus acutirostris* sp. nov., which is preserved with a skull and an almost complete skeleton. The new species is characterised by the following combination of characters: robust teeth, anterior part of the prefrontal at the same level as the anterior part of the frontal, supraoccipital visible on the skull table, atlantal rib with process on the dorsal margin and ilium with a prominent anterior process. The phylogenetic analysis recovers *M. acutirostris* as the sister taxon of a monophyletic group consisting of *Maomingosuchus petrolicus* from the late Eocene of the Maoming Basin of China and

Krabi-*Maomingosuchus* from the late Eocene of the Krabi Basin of Thailand. The basal position of *Maomingosuchus* on the tree recovered by the phylogenetic analysis is congruent with the late Eocene age of the genus. The phylogenetic analysis further supports a western Tethyan origin of tomistomines with three independent dispersal events from Europe to Southeast Asia. One for the stem lineage of *Maomingosuchus*, another for the stem lineage of *Penghusuchus* + *Toyotamaphimeia* and a third for the stem lineage of the extant *Tomistoma schlegelii*.

The third paper of the thesis refers to a bird species represented by the distal part of a right tarsometatarsus. The bone is the first bird fossil from the Palaeogene of Vietnam and one of only few species from the Palaeogene of Southeast Asia. The tarsometatarsus has been compared with extant aquatic, terrestrial and arboreal bird species from the Palaeogene. However, due to diagenetic compression and fragmentary preservation, it has not been possible to assign the fossil to any particular group and it is therefore referred to as ?*Neognathae incertae sedis*. Nevertheless, the specimen has a distinctive morphology and may represent an endemic neognath, which is not known from other Palaeogene localities outside of Vietnam.

The fourth paper of the thesis is about several well-preserved individuals of a new species of *Pan-Trionychidae*: *Striatochelys baba* gen. et sp. nov. *Striatochelys baba* is a small to medium-sized species characterised by prominent carapace ridges (on both costals and neurals) in adult specimens, a larger costal VIII, forming the posterolateral margin of the carapace, and an entoplastron callosity in the shape of a bulge. Comparison with plastomenids, other Palaeogene pan-trionychids from Asia and extant taxa from Southeast Asia revealed a close resemblance of *S. baba* to the latter group, especially to members of the genus *Nilssonina*. Some other characters of *S. baba* are otherwise unique to *Plastomenidae*. The phylogenetic analysis supports the results of these comparisons and recovers *S. baba* in a polytomy with *Nilssonina* spp. *Striatochelys baba* is morphologically very similar to a pan-trionychid from the late Eocene of the Maoming Basin of China, which has previously been referred to as '*Trionyx*' *impressus*. Accordingly, '*T.*' *impressus* is assigned to the new genus *Striatochelys* as *S. impressa*.

The combined results presented above allow for an interesting conclusion about the late Eocene world of Southeast Asia: a close connection between three basins, now located in Vietnam (Na Duong), China (Maoming) and Thailand (Krabi) (Fig. 23).

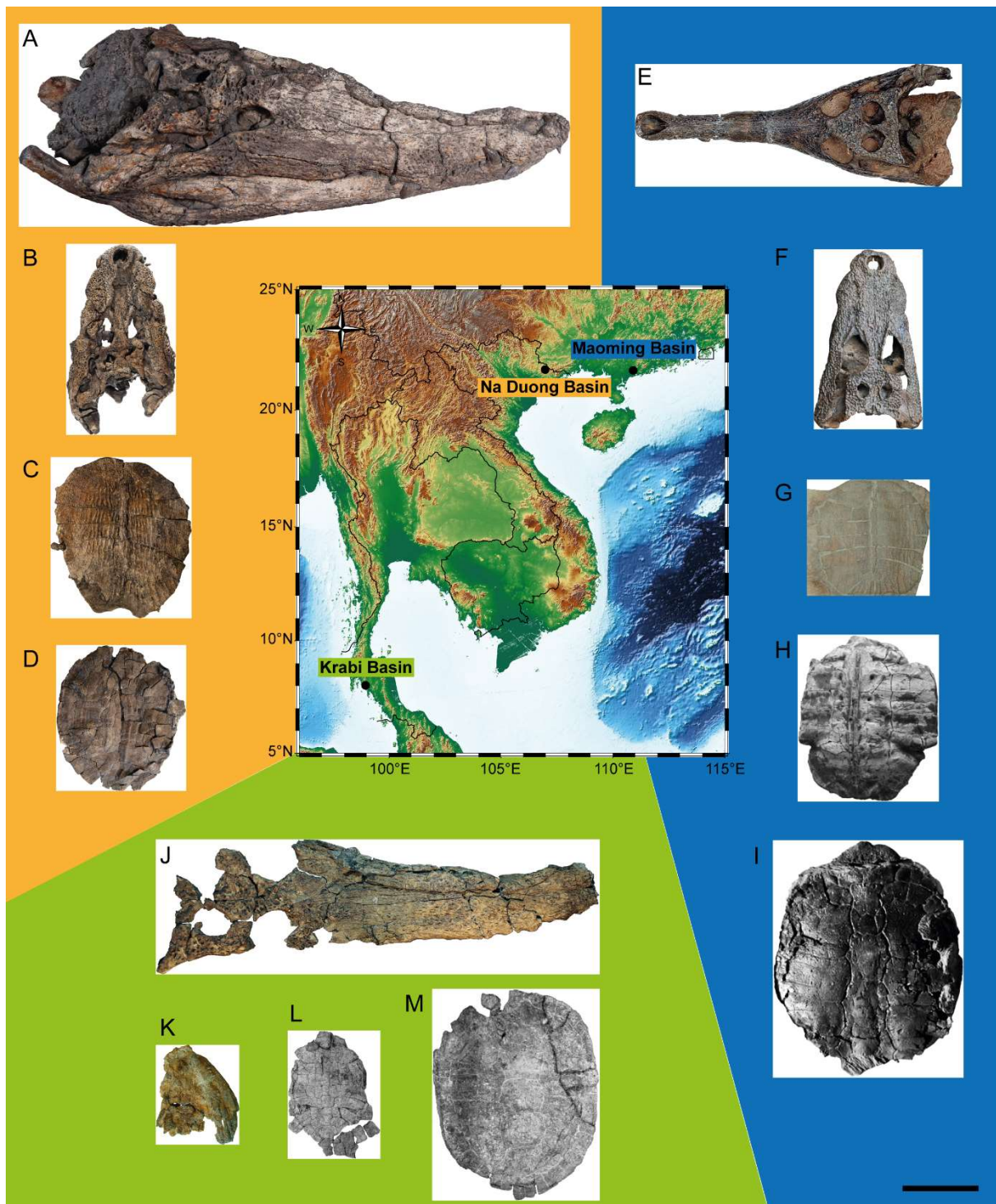


Figure 23. Map of Southeast Asia showing the Na Duong Basin in Vietnam (orange), the Maoming Basin in China (blue) and the Krabi Basin in Thailand (green) and taxa of crocodylians and turtles found in the respective location. **A**, *Maomingosuchus acutirostris* (Tomistominae); **B**, *Orientalosuchus naduongensis* (Orientalosuchina); **C**, *Striatochelys baba* (*Pan-Trionychoidea*); **D**, *Banhxeochelys trani* (*Pan-Geoemydidae*); **E**, *Maomingosuchus petrolicus* (Tomistominae) (altered after Shan et al., 2017); **F**, *Dongnanosuchus hsui* (Orientalosuchina) (altered after Shan et al., 2022); **G**, *Striatochelys impressa* (*Pan-Trionychoidea*) (© Walter G. Joyce), **H**, *Isometremys lacuna* (*Pan-Geoemydidae*) (altered after Claude et al., 2012); **I**, *Guangdongemys pingi* (*Pan-Geoemydidae*) (altered after Claude et al., 2012); **J**, *Krabi-Maomingosuchus* (Tomistominae) (altered after Martin et al., 2019a), **K**, *Krabisuchus siamogallicus* (Orientalosuchina) ((© Jeremy E. Martin); **L**, *Hardella siamensis* (*Pan-Geoemydidae*) (altered after Claude et al., 2007); **M**, *Mauremys thanhinensis* (*Pan-Geoemydidae*) (altered after Claude et al., 2007). Scale bar = 10 cm.

The results for the crocodylian fauna are quite clear: both *Orientalosuchina* and *Maomingosuchus* have one species in each of the three basins. This result is already indicated by the comparisons and is further supported by the phylogenetic analyses in the current work. Although the material of a 'Maoming-alligatoroid' originally described by Skutschas et al. (2014) and used in the analysis of Massonne et al. (2019) is poorly preserved and the taxon had to be pruned from the tree, the similarity to *O. naduongensis* was remarkable. Finally, *Dongnanosuchus hsui* was described by Shan et al. (2021) based on new material from Maoming, and the suggestion of a close relationship between the two taxa was supported by the phylogenetic analysis, which recovered *D. hsui* in a polytomy with *O. naduongensis* in a derived position within *Orientalosuchina*. For *Maomingosuchus*, the result was already clear in Massonne et al. (2022), as all three species were found as a monophyletic group within *Tomistominae*. Martin et al. (2019a) initially refrained from erecting a new species for the *Krabi-Maomingosuchus*, but after the comparison with *M. acutirostris* and *M. petrolicus* and the results of the phylogenetic analysis in the current work, it appears to be a valid but unnamed taxon.

For turtles, the results are less clear and more difficult. One of the two groups (*Pan-Geoemydidae*) was not studied for this thesis because Garbin et al. (2019) have already described the only species from Na Duong, *Banhxeochelys trani*. The authors mentioned that *B. trani* was most similar to the two Maoming species, *Guangdongemys pingi* Claude et al., 2012 and *Isometremys lacuna* Chow & Yeh, 1962, of all pan-geoemydids studied. However, their phylogenetic analysis did not recover a monophyletic East Asian group, but instead most species (except *G. pingi*) were found in a large polytomy at the base of *Pan-Geoemydidae*. Other taxa found in this polytomy included two pan-geoemydids from the Krabi Basin (*Hardella siamensis* Claude et al., 2007 and *Mauremys thanhinensis* Claude et al., 2007), among other species, which were initially referred to modern genera by Claude et al. (2007) and Claude et al. (2012), a result that was not supported by the analysis of Garbin et al. (2019). Although a high degree of similarity was found between taxa from Na Duong and Maoming, the phylogenetic results were not sufficient to infer a close relationship between these taxa, and thus did not allow the conclusion of a close connection between the localities themselves. A similar, but slightly different picture emerges for the *Pan-Trionychidae*, which were studied for this thesis. The material is much sparser than that of pan-geoemydids. There is only one poorly preserved specimen from

Maoming, which could not be analysed in a phylogenetic analysis, while no specimens are known from the Krabi Basin. However, the lack of specimens from Krabi is not surprising. Based on the minimum number of individuals (MNI) from all localities, pan-geomydids are about ten times more abundant than pan-trionychids (Na Duong: 100 to 9, Maoming: 10 to 1 and Krabi: 12 to 0). This result makes it very likely that the lack of pan-trionychids in Krabi is due to sampling bias rather than unsuitable environmental conditions, as already suggested by Massonne et al. (2023). Despite the lack of phylogenetic support, the high degree of similarity found in the comparison between *S. baba* from Na Duong and *S. impressa* from Maoming led to the decision to place them in the same genus, underlining the presumed close relationship between the two taxa.

The results of the thesis show that the three East Asian basins of Na Duong, Maoming, and Krabi had a closely related crocodylian and turtle fauna (Fig. 23). Representatives of *Orientalosuchina* and the genus *Maomingosuchus* were found in each of these basins, and the turtle genus *Striatochelys* was represented at least in Na Duong and Maoming. These findings strongly suggest a connection between the three basins during the Palaeogene, enabling faunal exchange. However, the results also indicate that either a physical barrier existed prior to the End of the Eocene, resulting in the basin separation and the distinction of the herpetofauna, or that the similar species are in fact chronospecies. This point is significant as it is difficult to ascertain the exact age of all three basins, which makes it possible that they might be separated by several million years. This would also account for the small morphological variations observed between species.

The results of the thesis also allow some limited conclusion to be drawn about the impact of the major cooling event at the end of the Eocene ('Grande Coupure') on the reptilian fauna of Southeast Asia. However, the conclusions are limited by the lack of fossils from the Oligocene of Southeast Asia. Oligocene assemblages in Asia are generally very sparse (Ni et al., 2016), and well-documented fossil sites yielding crocodylians and turtles are even rarer. One of the richest fossil localities are the Bugti Hills in Pakistan, where representatives of crocodyloids and tomistomines have been excavated (Martin, 2019; Martin et al., 2019b). *Astorgosuchus bugtinensis* Martin et al., 2019 represents a very large but poorly preserved crocodyloid, and several skull fragments from very large representatives of tomistomines could not be assigned to a specific genus (Martin, 2019). Oligocene fossils of *Pan-Trionychidae* are

known from sites in Japan and Kazakhstan (Georgalis & Joyce, 2017). Nevertheless, a few things can be said about the reptilian fauna before and after the ‘Grande Coupure’.

During the Late Cretaceous to the late Eocene, *Orientalosuchina* were widely distributed in East and Southeast Asia. From the Oligocene/Miocene onwards, however, no representatives have been found so far. Instead, the vacant niche for a small alligatoroid in Southeast Asia has been filled by the genus *Alligator* from the Miocene to the present (Li & Wang, 1987; Shan et al., 2013; Iijima et al., 2016; Darlim et al., 2023). The Oligocene falls within the molecular time estimate for the split between *Alligator mississippiensis* and *Alligator sinensis*, and for the arrival of the stem members of the latter in East Asia via Beringia (e.g. Oaks, 2011; Massonne et al., 2019; Darlim et al., 2023). The greater cold tolerance of *Alligator* may have played a key role in the cooler environment of the Oligocene and may have contributed to the extinction of *Orientalosuchina*. However, whether the cooler temperatures played the main role in the extinction of *Orientalosuchina* and *Alligator* merely occupied vacant niches, or whether direct competition occurred, is still unclear. Tomistomines have survived to the present day, but the *Maomingosuchus* lineage is no longer found in Miocene assemblages. Instead, it was replaced by much larger tomistomines (e.g. *Penghusuchus pani*), which probably arrived in East Asia from Europe in a later dispersal event (Massonne et al., 2021). As with *Orientalosuchina* and *Alligator*, it is unclear whether there was a direct competition between the two groups or whether vacant niches were occupied. For the pan-trionychid *Striatochelys baba*, however, the case is different. According to direct comparison and phylogenetic analyses, *S. baba* could represent a stem member of the extant genus *Nilssonina* (Massonne et al., 2023). If this is true, *S. baba* or one of its descendants or a closely related species survived the ‘Grande Coupure’ and subsequently radiated in Southeast Asia. Unfortunately, nothing can be said about the survival of the only known bird from the Na Duong Basin. Its preservation is too poor to allow assignment to a specific family, and the lack of well-preserved fossil birds from the Eocene and Oligocene of Southeast Asia makes any further statement difficult (Massonne et al., 2022). More data, especially from the Oligocene, are certainly needed to better assess the impact of the ‘Grande Coupure’ on the reptilian fauna of Southeast Asia. However, the Na Duong, Maoming and Krabi basins together already offer a significant initial insight into reptilian fauna of Southeast Asia during the late Eocene.

References

- Anquetin, J., Tong, H. & Claude, J.** 2017. A Jurassic stem pleurodire sheds light on the functional origin of neck retraction in turtles. *Scientific Reports*, **7**, 42376, 1–10.
- Bailey, I. W. & Sinnott, E. W.** 1916. The Climatic Distribution of Certain Types of Angiosperm Leaves. *American Journal of Botany* **3**(1), 22–39.
- Baker, A. J., Haddrath, O., McPherson, J. D. & Cloutier, A.** 2014. Genomic Support for a Moa–Tinamou Clade and Adaptive Morphological Convergence in Flightless Ratites. *Molecular Biology and Evolution*, **31**(7), 1686–1696.
- Baker-Brosh, K. F. & Peet, R. K.** 1997. The Ecological Significance of Lobed and Toothed Leaves in Temperate Forest Trees. *Ecology*, **78**(4), 1250–1255.
- Benton, M. J. & Clark, J. M.** 1988. Archosaur phylogeny and the relationships of the Crocodylia. In: Benton, M. J. (eds.) *The Phylogeny and Classification of the Tetrapods, Volume 1: Amphibians, Reptiles, Birds, Systematics Association Special Volume 35*, 295–338.
- Berg, D. E.** 1966. Die Krokodile, insbesondere *Asiatosuchus* und aff. *Sebecus?*, aus dem Eozän von Messel bei Darmstadt/Hessen. *Hessisches Landesamt für Bodenforschung*, **52**, 1–105.
- Bezuijen, M. R., Shwedick, B. M., Sommerlad, R., Stevenson, C. & Steubing, R. B.** 2010. *Tomistoma Tomistoma schlegelii*. In: Manolis, S. C. & Stevenson, C. (eds.) *Crocodyles. Status Survey and Conservation Action Plan*. Third Edition. Crocodile Specialist Group: Darwin, 133–138.
- Bezuijen, M., Simpson, B., Behler, N., Daltry, J. & Tempsiripong, Y.** 2012. *Crocodylus siamensis*, Siamese Crocodile. *The IUCN Red List of Threatened Species*. e.T5671A3048087, 1–17.
- Bezuijen, M. R., Cox, J. H., Thorbjarnarson, J. B., Phothitay, C., Hedemark, M. & Rasphone, A.** 2013. Status of Siamese Crocodile (*Crocodylus siamensis*) Schneider, 1801 (Reptilia: Crocodylia) in Laos. *Journal of Herpetology*, **47**(1), 41–65.
- Bezuijen, M.R., Shwedick, B., Simpson, B.K., Staniewicz, A. & Stuebing, R.** 2014. *Tomistoma schlegelii*, False Gharial. *The IUCN Red List of Threatened Species*. e.T21981A2780499, 1–19.
- Boddaert, P.** 1770. *Over de Kraakbeenige Schildpad*. De Testudine Cartilaginea. Kornelis van Tongerlo, Amsterdam, 1–39.
- Boerman, S. A., Perrichon, G., Yang, J., Li, C.-S., Martin, J. E., Speijer, R. P. & Smith, T.** 2023. A juvenile skull from the early Palaeocene of China extends the appearance of crocodyloids in Asia back by 15–20 million years. *Zoological Journal of the Linnean Society*, **197**(3), 787–811.
- Boev, Z.** 2022. Late Pleistocene and Early Holocene Birds of Northern Vietnam (Caves Dieu and Maxa I, Thanh Hoa Province)—Paleornithological Results of the Joint Bulgarian-Vietnamese Archaeological Expeditions, 1985–1991 (Paleoavifaunal Research). *Quaternary*, **5**(31), 1–115.
- Böhme, M.** 1995. Eine Weichschildkröte (Trionychidae) aus dem Untermiozän vom Dietrichsberg bei Vacha/Rhön. *Mauritania (Altenburg)*, **15**(3), 357–366.
- Böhme, M., Aiglstorfer, M., Antoine, P.-O., Appel, E., Havlik, P., Métais, G., Phuc, L. T., Schneider, S., Setzer, F., Tappert, R., Tran, D. N., Uhl, D. & Prieto, J.** 2013. Na Duong (northern Vietnam) – an exceptional window into Eocene ecosystems from Southeast Asia. *Zitteliana A53*, 120–167.
- Böhme, M., Prieto, J., Schneider, S., Hung, N. V., Quang, D. D. & Tran, D. N.** 2011. The Cenozoic on-shore basins of Northern Vietnam: Biostratigraphy, vertebrate and invertebrate faunas. *Journal of Asian Earth Sciences*, **40**(2), 672–687.

- Bonnaterre, P.-J.** 1789. *Tableau encyclopédique et méthodique des trois règnes de la nature. Vol. 1 Erpétologie.* Paris: Panckoucke, Hôtel de Thou. 1–71.
- Braun, E. L. & Kimball, R. T.** 2021. Data Types and the Phylogeny of Neoaves. *Birds*, **2**(1), 1–22.
- Brinkman, D., Rabi, M. & Zhao, L.** 2017. Lower Cretaceous fossils from China shed light on the ancestral body plan of crown softshell turtles (Trionychidae, Cryptodira). *Scientific Reports*, **7**, 6719, 1–11.
- Brochu, C. A.** 1997a. Morphology, Fossils, Divergence Timing, and the Phylogenetic Relationships of *Gavialis*. *Systematic Biology*, **46**(3), 479–522.
- Brochu, C. A.** 1997b. *Phylogenetic Systematics and Taxonomy of Crocodylia*. Thesis, University of Texas, Austin. 1–708.
- Brochu, C. A.** 1999. Phylogenetics, Taxonomy, and Historical Biogeography of Alligatoroidea. *Journal of Vertebrate Paleontology*, **19**(Suppl.2), 9–100.
- Brochu, C. A.** 2003. Phylogenetic Approaches Toward Crocodylian History. *Annual Review of Earth and Planetary Sciences*, **31**, 357–397.
- Brochu, C. A.** 2007. Systematics and Taxonomy of Eocene Tomistomine Crocodylians from Britain and Northern Europe: Early Tomistomine Systematics. *Palaeontology*, **50**(4), 917–928.
- Brochu, C. A.** 2012. Phylogenetic relationships of Palaeogene ziphodont eusuchians and the status of *Pristichampsus* Gervais, 1853. *Earth and Environmental Science Transactions of the Royal Society of Edinburgh*, **103**(3-4), 521–550.
- Brochu, C. A. & Gingerich, P. D.** 2000. New Tomistomine Crocodylian from the Middle Eocene (Bartonian) of Wadi Hitán, Fayum Province, Egypt. *Contributions from the Museum of Paleontology, The University of Michigan* **30**(10), 251–268.
- Brochu, C. A. & Storrs, G. W.** 2012. A giant crocodile from the Plio-Pleistocene of Kenya, the phylogenetic relationships of Neogene African crocodylines, and the antiquity of *Crocodylus* in Africa. *Journal of Vertebrate Paleontology*, **32**(3), 587–602.
- Broin, F. de** 1980. Les Tortues de Gadoufaoua (Aptien du Niger); aperçu sur la paléobiogéographie des Pelomedusidae (Pleurodira). *Mémoires de la Société géologique de France*, **139**, 39–46.
- Buckland, W.** 1836. *Geology and mineralogy considered with reference to natural theology.* W. Pickering, London, 1–618.
- Buffetaut, E.** 2013. The giant bird *Gastornis* in Asia: A revision of *Zhongyuanus xichuanensis* Hou, 1980, from the Early Eocene of China. *Paleontological Journal*, **47**, 1302–1307.
- Burnham, R. J., Pitman, N. C. A., Johnson, K. R. & Wilf, P.** 2001. Habitat-related error in estimating temperatures from leaf margins in a humid tropical forest. *American Journal of Botany*, **88**(6), 1096–1102.
- Cadena, E. & Joyce, W. G.** 2015. A Review of the Fossil Record of Turtles of the Clades *Platycheilyidae* and *Dortokidae*. *Bulletin of the Peabody Museum of Natural History*, **56**(1), 3–20.
- Chavasseau, O., Chaimanee, Y., Ducrocq, S., Lazzari, V., Pha, P. D., Rugbumrung, M., Surault, J., Tuan, D. M. & Jaeger, J.-J.** 2019. A new primate from the late Eocene of Vietnam illuminates unexpected strepsirrhine diversity and evolution in Southeast Asia. *Scientific Reports*, **9**, 19983, 1–11.
- Chkhikvadze, V. M.** 1971. [New turtles from the Oligocene of Kazakhstan and the systematic position of some species of Mongolia]. *Soobshchniya Akademii Nauk Gruzinskoi SSR*, **62**, 489–492. [In Russian].
- Chkhikvadze, V. M.** 1973. [Tertiary turtles of the Zaisan Depression]. Tbilisi, Georgia: Metsniereba, 1–100 [In Russian].

- Cho, Y. Y., & Tsai, C. H.** 2023. Crocodylian princess in Taiwan: Revising the taxonomic status of *Tomistoma taiwanicus* from the Pleistocene of Taiwan and its paleobiogeographic implications. *Journal of Paleontology*, 1–14.
- Choudhury, B. C. & de Silva, A.** 2013. *Crocodylus palustris*, Mugger. The IUCN Red List of Threatened Species. e.T5667A3046723. 1–11.
- Chow, M. C., & Yeh, H. K.** 1962. A new emydid from Eocene of Maoming, Kwangtung. *Vertebrata Palasiatica*, 6(3), 225–229.
- Claramunt, S. & Cracraft, J.** 2015. A new time tree reveals Earth history's imprint on the evolution of modern birds. *Science Advances*, 1(11), e1501005, 1–13.
- Clark, J. M.** 1986. *Phylogenetic Relationships of the crocodylomorph archosaurs*. Thesis. The University of Chicago. 1–556.
- Clarke, J. A., Norell, M. A. & Dashzeveg, D.** 2005. New Avian Remains from the Eocene of Mongolia and the Phylogenetic Position of the Eogruidae (Aves, Gruoidea). *American Museum Novitates*, 3494, 1–17.
- Claude, J., Suteethorn, V., & Tong, H.** 2007. Turtles from the late Eocene–early Oligocene of the Krabi Basin (Thailand). *Bulletin de la Société géologique de France*, 178(4), 305–316.
- Claude, J., Zhang, J. Y., Li, J. J., Mo, J. Y., Kuang, X. W., & Tong, H.** 2012. Geoemydid turtles from the Late Eocene Maoming basin, southern China. *Bulletin de la Société géologique de France*, 183(6), 641–651.
- Clift, P. D. & Sun, Z.** 2006. The sedimentary and tectonic evolution of the Yinggehai-Song Hong basin and the southern Hainan margin, South China Sea: Implications for Tibetan uplift and monsoon intensification. *Journal of Geophysical Research*, 111(B6), 1–28.
- Colbert, E. H., Cowles, R. B. & Bogert, C. M.** 1946. Temperature tolerance in the American alligator and their bearing on the habits, evolution, and the extinction of the dinosaurs. *Bulletin of the American Museum of Natural History*, 86(7), 327–374.
- Cooper, A. & Penny, D.** 1997. Mass Survival of Birds Across the Cretaceous- Tertiary Boundary: Molecular Evidence. *Science*, 275(5303), 1109–1113.
- Costa, E., Garcés, M., Sáez, A., Cabrera, L. & López-Blanco, M.** 2011. The age of the “Grande Copure” mammal turnover: New Constraints from the Eocene-Oligocene record of the Eastern Ebro Basin (NE Spain). *Palaeogeography, Palaeoclimatology, Palaeoecology*, 301(1-4), 97–107.
- Cracraft, J.** 1973. Phylogeny and evolution of the ratite birds. *Ibis*, 116(4), 494–521.
- Cuvier, F. G.** 1825. *Recherches sur les ossemens fossiles: où l'on rétablit les caractères de plusieurs animaux dont les révolutions du globe ont détruit les espèces*. G. Dufour et E. d'Ocagne, Paris, 3(5), 1–548.
- Danilov, I. G. & Vitek, N. S.** 2013. Soft-shelled turtles (Trionychidae) from the Bissekty Formation (Late Cretaceous: late Turonian) of Uzbekistan: Shell-based taxa. *Cretaceous Research*, 41, 55–64.
- Danilov, I. G., Syromyatnikova, E. V., Skutschas, P. P., Kodrul, T. M., & Jin, J.** 2013. The first ‘true’ *Adocus* (Testudines, Adocidae) from the Paleogene of Asia. *Journal of Vertebrate Paleontology*, 33(5), 1071–1080.
- Danilov, I. G., Hirayama, R., Sukhanov, V. B., Suzuki, S., Watabe, M. & Vitek, N. S.** 2014. Cretaceous soft-shelled turtles (Trionychidae) of Mongolia: new diversity, records and a revision. *Journal of Systematic Palaeontology*, 12(7), 799–832.
- Danilov, I. G., Sukhanov, V. B., Obratsova, E. M. & Vitek, N. S.** 2015. The first reliable record of trionychid turtles in the Paleocene of Asia. *Paleontological Journal*, 49, 407–412.

- Darlim, G., Lee, M. S. Y., Walter, J. & Rabi, M.** 2022. The impact of molecular data on the phylogenetic position of the putative oldest crown crocodylian and the age of the clade. *Biology Letters*, **18**(2), 20210603, 1–6.
- Darlim, G., Suraprasit, K., Chaimanee, Y., Tian, P., Yamee, C., Rugbumrung, M., Kaweera A. & Rabi, M.** 2023. An extinct deep-snouted *Alligator* species from the Quaternary of Thailand and comments on the evolution of crushing dentition in alligatorids. *Scientific Reports*, **13**(1), 10406, 1–17.
- Daudin, F. M.** 1802. *Histoire naturelle, Générale et particulière des Reptiles*. De L'Imprimerie de F. Paris: De L'Imprimerie de F. Dufart, 1–452.
- Delfino, M., Piras, P. & Smith, T.** 2005. Anatomy and phylogeny of the gavialoid crocodylian *Eosuchus lerichei* from the Paleocene of Europe. *Acta Palaeontologica Polonica* **50**(3), 565–580.
- Densmore, L. D.** 1983. Biochemical and Immunological Systematics of the Order Crocodylia. In: Hecht, M. K., Wallace, B. & Prance, G. T. (eds) *Evolutionary Biology*. Springer US, Boston, MA, 397–465.
- Densmore, L. D. & Dessauer, H. C.** 1984. Low levels of protein divergence detected between *Gavialis* and *Tomistoma*: Evidence for crocodylian monophyly? *Comparative Biochemistry and Physiology Part B: Comparative Biochemistry*, **77**(4), 715–720.
- Densmore, L. D. & Owen, R. D.** 1989. Molecular Systematics of the Order Crocodylia. *American Zoologist*, **29**(3), 831–841.
- Ducrocq, S., Benammi, M., Chavasseau, O., Chaimanee, Y., Suraprasit, K., Phadong, P., Phuong, V. le, Phach, P. van & Jaeger, J.** 2015. New anthracotheres (Cetartiodactyla, Mammalia) from the Paleogene of northeastern Vietnam: biochronological implications. *Journal of Vertebrate Paleontology*, **35**(3), e929139, 1–11.
- Dzanh, T.** 1995. Stratigraphic correlation of Neogene sequences of Vietnam and adjacent areas. *Journal of Geology* (Hanoi), Ser. B, **5-6**. 114–120.
- Dzanh, T.** 1996. Chrono-ecological vegetative assemblage and historical development of Neogene and Neogene-Quaternary floras of Vietnam. *Palaeobotanist* **45**, 430–439.
- Englhart, S., Jubanski, J. & Siegert, F.** 2013. Quantifying Dynamics in Tropical Peat Swamp Forest Biomass with Multi-Temporal LiDAR Datasets. *Remote Sensing*, **5**(5), 2368–2388.
- Engstrom, T. N., Shaffer, H. B. & McCord, W. P.** 2004. Multiple Data Sets, High Homoplasy, and the Phylogeny of Softshell Turtles (Testudines: Trionychidae). *Systematic Biology*, **53**(5), 693–710.
- Ericson, P. G. P., Anderson, C. L., Britton, T., Elzanowski, A., Johansson, U. S., Källersjö, M., Ohlson, J. I., Parsons, T. J., Zuccon, D. & Mayr, G.** 2006. Diversification of Neoaves: integration of molecular sequence data and fossils. *Biology Letters*, **2**(4), 543–547.
- Estes, R. & Howard Hutchison, J.** 1980. Eocene lower vertebrates from Ellesmere Island, Canadian Arctic Archipelago. *Palaeogeography, Palaeoclimatology, Palaeoecology*, **30**, 325–347.
- Evers, S. W. & Benson, R. B. J.** 2019. A new phylogenetic hypothesis of turtles with implications for the timing and number of evolutionary transitions to marine lifestyles in the group Smith, A. (ed.). *Palaeontology*, **62**(1), 93–134.
- Evers, S. W., Chapelle, K. E. J. & Joyce, W. G.** 2023. Cranial and mandibular anatomy of *Plastomenus thomasi* and a new time-tree of trionychid evolution. *Swiss Journal of Palaeontology*, **142**(1), 1–40.
- Farke, A. A., Henn, M. M., Woodward, S. J. & Xu, H. A.** 2014. *Leidyosuchus* (Crocodylia: Alligatoroidea) from the Upper Cretaceous Kaiparowits Formation (late Campanian) of Utah, USA. *PaleoBios*, **30**(3), 72–88.

- Ferreira, G. S., Bronzati, M., Langer, M. C. & Sterli, J.** 2018. Phylogeny, biogeography and diversification patterns of side-necked turtles (Testudines: Pleurodira). *Royal Society Open Science*, **5**(3), 171773.
- Fiorillo, A. R.** 2008. Dinosaurs of Alaska: Implications for the Cretaceous origin of Beringia. In: Blodgett, R. B. & Stanley, G. D. Jr. (eds) *The Terrane Puzzle: New Perspectives on Paleontology and Stratigraphy from the North American Cordillera*. Geological Society of America Special Paper, **442**, 313–326.
- Forskål, P.** 1775. *Descriptiones animalium, avium, amphibiorum, piscium, insectorum, vermium: quae in itinere orientali observavit*. Hauniae, Copenhagen, Möller, 1–164.
- Fuente, M. S. de la & Iturralde-Vinent, M.** 2001. A new Pleurodiran Turtle from the Jagua Formation (Oxfordian) of Western Cuba. *Journal of Paleontology*, **75**(4), 860–869.
- Fyhn, M. B. W. & Phach, P. V.** 2015. Late Neogene structural inversion around the northern Gulf of Tonkin, Vietnam: Effects from right-lateral displacement across the Red River fault zone: Inversion in the northern Gulf of Tonkin. *Tectonics*, **34**(2), 290–312.
- Fyhn, M. B. W., Cuong, T. D., Hoang, B. H., Hovikoski, J., Olivarius, M., Tuan, N. Q., Tung, N. T., Huyen, N. T., Cuong, T. X., Nytoft, H. P., Abatzis, I. & Nielsen, L. H.** 2018. Linking Paleogene Rifting and Inversion in the Northern Song Hong and Beibuwan Basins, Vietnam, With Left-Lateral Motion on the Ailao Shan-Red River Shear Zone. *Tectonics*, **37**(8), 2559–2585.
- Gaffney, E. S., Tong, H. & Meylan, P. A.** 2006. Evolution of the Side-Necked Turtles: The Families Bothremydidae, Euraxemydidae, and Araripemydidae. *Bulletin of the American Museum of Natural History*, **300**, 1–698.
- Garbin, R. C., Böhme, M. & Joyce, W. G.** 2019. A new testudinoid turtle from the middle to late Eocene of Vietnam. *PeerJ*, **7**, e6280, 1–39.
- Gatesy, J., Amato, G., Norell, M., DeSalle, R. & Hayashi, C.** 2018. Combined Support for Wholesale Taxic Atavism in Gavialine Crocodylians. *Systematic Biology*, **52**(3), 403–422.
- Gauthier, J.** 1986. Saurischian Monophyly and the Origin of Birds. In: Padian, K. (ed.) *The origin of birds and the evolution of flight*. San Francisco, California. *Memoirs of the California Academy of Sciences*, **8**, 1–55.
- Gauthier, J. & Queiroz, K. de.** 2001. Feathered dinosaurs, flying dinosaurs, crown dinosaurs, and the name “Aves”. In: Ostrom, J. H., Gauthier, J. & Gall, L. F. (eds). *New Perspectives on the Origin and Early Evolution of Birds: Proceedings of the International Symposium in Honor of John H. Ostrom*. Peabody Museum of Natural History Yale University, New Haven, Conn, 7–41.
- Geoffroy Saint-Hilaire, E.** 1809. Sur les tortues molles, nouveau genre sous le nom de *Trionyx* et sur la formation des carapaces. *Annales du Muséum national d’histoire naturelle*, Paris, **14**, 1–20.
- Georgalis, G. L.** 2021. First pan-trionychid turtle (Testudines, Pan-Trionychidae) from the Palaeogene of Africa. *Papers in Palaeontology*, **7**(4), 1919–1926.
- Georgalis, G. L. & Joyce, W. G.** 2017. A Review of the Fossil Record of Old World Turtles of the Clade *Pan-Trionychidae*. *Bulletin of the Peabody Museum of Natural History*, **58**(1), 115–208.
- Gilmore, C. W.** 1911. A New Fossil Alligator from the Hell Creek Beds of Montana. *Proceedings of the United States National Museum*, **41**(1860), 297–301.
- Gilmore, C. W.** 1916. Description of two new species of fossil turtles, from the Lance formation of Wyoming. *Proceedings of the United States National Museum*, **50**(2137), 641–646.
- Gilmore, C. W.** 1931. Fossil Turtles of Mongolia. *Bulletin of the American Museum of Natural History*, **59**, 213–257.

- Gilmore, C. W.** 1934. Fossil Turtles of Mongolia: Second Contribution. *American Museum Novitates*, **689**, 1–14.
- Gmelin, J. F.** 1789. Regnum animale. In: Caroli a Linne *Systema Naturae per regna tri naturae, secundum classes, ordines, genera, species, cum characteribus, differentilis, synonymis, locis*. Volume 1. G. E. Beer, Leipzig. 1033–1516.
- Gray, J. E.** 1831. *Synopsis Reptilium, Pt. 1, Cataphracta. Tortoises, Crocodiles, Enaliosaurians*. Treuttel, Wurtz, London, 1–85.
- Gray, J. E.** 1869. Notes on the families and genera of tortoises (Testudinata), and on the characters afforded by the study of their skulls. In *Proceedings of the Zoological Society of London*, **37**(1), 165–225.
- Greenwood, D. R.** 2005. Leaf Margin Analysis: Taphonomic Constraints. *PALAIOS*, **20**, 498–505.
- Gunawan, H., Kobayashi, S., Mizuno, K. & Kono, Y.** 2012. Peat swamp forest types and their regeneration in Giam Siak Kecil-Bukit Batu Biosphere Reserve, Riau, East Sumatra, Indonesia. *Mires and Peat*, **10**, 1–17.
- Gussekloo, S. W. S. & Zweers, G. A.** 1999. The Paleognathous Pterygoid-Palatinum Complex. A True Character?. *Netherlands Journal of Zoology*, **49**(1), 29–43.
- Haddrath, O. & Baker, A. J.** 2012. Multiple nuclear genes and retroposons support vicariance and dispersal of the palaeognaths, and an Early Cretaceous origin of modern birds. *Proceedings of the Royal Society B: Biological Sciences*, **279**(1747), 4617–4625.
- Hagan, J. M., Smithson, P. C. & Doerr, P. D.** 1983. Behavioral Response of the American Alligator to Freezing Weather. *Journal of Herpetology*, **17**(4), 402–404.
- Härlid, A. & Arnason, U.** 1999. Analyses of mitochondrial DNA nest ratite birds within the Neognathae: supporting a neotenus origin of ratite morphological characters. *Proceedings of the Royal Society of London. Series B: Biological Sciences*, **266**(1416), 305–309.
- Harshman, J., Huddleston, C. J., Bollback, J. P., Parsons, T. J. & Braun, M. J.** 2003. True and False Gharials: A Nuclear Gene Phylogeny of Crocodylia. *Systematic Biology*, **52**(3), 386–402.
- Hass, C. A., Hoffman, M. A., Densmore, L. D. & Maxson, L. R.** 1992. Crocodylian evolution: Insights from immunological data. *Molecular Phylogenetics and Evolution*, **1**(3), 193–201.
- Head, J. J., Mahmood, S. & Gingerich, P. D.** 1999. *Drazinderetes tethyensis*, a new large Trionychnid (Reptilia: Testudines) from the Marine Eocene Drazinda Formation of the Sulaiman Range, Punjab (Pakistan). *Contributions from the Museum of Paleontology*, **30**(7), 199–214.
- Hood, S. C., Torres, C. R., Norell, M. A. & Clarke, J. A.** 2019. New Fossil Birds from the Earliest Eocene of Mongolia. *American Museum Novitates*, **3934**, 1–22.
- Hou, L. H.** 1980. New form of the Gastornithidae from the Lower Eocene of the Xichuan, Honan. *Vertebrata Palasiatica*, **18**(2), 111–115.
- Hou, L. H., Chuong, C.-M., ang, A., Zeng, C. L. & Hou, J. F.** 2003. *Fossil birds of China*. Yunnan Science and Technology Press, Kunming. 1–234.
- Hu, H., Sansalone, G., Wroe, S., McDonald, P. G., O'Connor, J. K., Li, Z., Xu, X. & Zhou, Z.** 2019. Evolution of the vomer and its implications for cranial kinesis in Paraves. *Proceedings of the National Academy of Sciences*, **116**(39), 19571–19578.
- Hutchison, J. H.** 1982. Turtle, crocodylian, and champsosaur diversity changes in the Cenozoic of the north-central region of western United States. *Palaeogeography, Palaeoclimatology, Palaeoecology*, **37**(2-4), 149–164.

- Hwang, S. H., Mayr, G. & Bolortsetseg, M.** 2010. The earliest record of a galliform bird in Asia, from the late Paleocene–early Eocene of the Gobi Desert, Mongolia. *Journal of Vertebrate Paleontology*, **30**(5), 1642–1644.
- Iijima, M. & Kobayashi, Y.** 2019. Mosaic nature in the skeleton of East Asian crocodylians fills the morphological gap between “Tomistominae” and Gavialinae. *Cladistics*, **35**(6), 623–632.
- Iijima, M., Takahashi, K., & Kobayashi, Y.** 2016. The oldest record of *Alligator sinensis* from the Late Pliocene of Western Japan, and its biogeographic implication. *Journal of Asian Earth Sciences*, **124**, 94–101.
- Iijima, M., Momohara, A., Kobayashi, Y., Hayashi, S., Ikeda, T., Taruno, H., Watanabe, K., Tanimoto, M. & Furui, S.** 2018. *Toyotamaphimeia* cf. *machikanensis* (Crocodylia, Tomistominae) from the Middle Pleistocene of Osaka, Japan, and crocodylian survivorship through the Pliocene-Pleistocene climatic oscillations. *Palaeogeography, Palaeoclimatology, Palaeoecology*, **496**, 346–360.
- Iijima, M., Qiao, Y., Lin, W., Peng, Y., Yoneda, M. & Liu, J.** 2022. An intermediate crocodylian linking two extant gharials from the Bronze Age of China and its human-induced extinction. *Proceedings of the Royal Society B: Biological Sciences*, **289**(1970), 20220085, 1–9.
- Ito, A., Aoki, R., Hirayama, R., Yoshida, M., Kon, H. & Endo, H.** 2018. The Rediscovery and Taxonomical Reexamination of the Longirostrine Crocodylian from the Pleistocene of Taiwan. *Paleontological Research*, **22**(2), 150–155.
- Janke, A., Gullberg, A., Hughes, S., Aggarwal, R. K. & Arnason, U.** 2005. Mitogenomic Analyses Place the Gharial (*Gavialis gangeticus*) on the Crocodile Tree and Provide Pre-K/T Divergence Times for Most Crocodylians. *Journal of Molecular Evolution*, **61**, 620–626.
- Jasinski, S. E., Heckert, A. B., Sailer, C., Lichtig, A. J., Lucas, S. G. & Dodson, P.** 2022. A softshell turtle (Testudines: Trionychidae: Plastomeninae) from the uppermost Cretaceous (Maastrichtian) Hell Creek Formation, North Dakota, USA, with implications for the evolutionary relationships of plastomenines and other trionychids. *Cretaceous Research*, **135**, 105172, 1–17.
- Jetz, W., Thomas, G. H., Joy, J. B., Hartmann, K. & Mooers, A. O.** 2012. The global diversity of birds in space and time. *Nature*, **491**, 444–448.
- Jonet, S. & Wouters, G.** 1972. Presence d'un crocodyliens nouveau dans les phosphates Ypresiens du Maroc. *Bulletin de la Societe Belge de Geologie, de Paleontologie et d'Hydrologie*, **81**, 209–210.
- Jouve, S.** 2016. A new basal tomistomine (Crocodylia, Crocodyloidea) from Issel (Middle Eocene; France): palaeobiogeography of basal tomistomines and palaeogeographic consequences. *Zoological Journal of the Linnean Society*, **177**(1), 165–182.
- Jouve, S., Bardet, N., Jalil, N.-E., Suberbiola, X. P., Bouya, B. & Amaghaz, M.** 2008. The oldest African crocodylian: phylogeny, paleobiogeography, and differential survivorship of marine reptiles through the Cretaceous-Tertiary boundary. *Journal of Vertebrate Paleontology*, **28**(2), 409–421.
- Jouve, S., Bouya, B., Amaghaz, M. & Meslouh, S.** 2015. *Maroccosuchus zennaroi* (Crocodylia: Tomistominae) from the Eocene of Morocco: phylogenetic and palaeobiogeographical implications of the basalmost tomistomine. *Journal of Systematic Palaeontology*, **13**(5), 421–445.
- Joyce, W. G. & Lyson, T. R.** 2011. New material of *Gilmoremys lancensis* nov. comb. (Testudines: Trionychidae) from the Hell Creek Formation and the diagnosis of plastomenid turtles. *Journal of Paleontology*, **85**(3), 442–459.
- Joyce, W. G. & Lyson, T. R.** 2017. The shell morphology of the latest Cretaceous (Maastrichtian) trionychid turtle *Helopanoplia distincta*. *PeerJ*, **5**, e4169, 1–20.

- Joyce, W. G., Revan, A., Lyson, T. R. & Danilov, I. G. 2009. Two New Plastomenine Softshell Turtles from the Paleocene of Montana and Wyoming. *Bulletin of the Peabody Museum of Natural History*, **50**(2), 307–325.
- Joyce, W. G., Parham, J. F., Lyson, T. R., Warnock, R. C. M. & Donoghue, P. C. J. 2013. A divergence dating analysis of turtles using fossil calibrations: an example of best practices. *Journal of Paleontology*, **87**(4), 612–634.
- Joyce, W. G., Lyson, T. R. & Williams, S. 2016. New cranial material of *Gilmoremys lancensis* (Testudines, Trionychidae) from the Hell Creek Formation of southeastern Montana, U.S.A. *Journal of Vertebrate Paleontology*, **36**(6), e1225748, 1–10.
- Joyce, W. G., Lyson, T. R. & Sertich, J. J. W. 2018. A new species of trionychid turtle from the Upper Cretaceous (Campanian) Fruitland Formation of New Mexico, USA. *Journal of Paleontology*, **92**(6), 1107–1114.
- Joyce, W. G., Anquetin, J., Cadena, E.-A., Claude, J., Danilov, I. G., Evers, S. W., Ferreira, G. S., Gentry, A. D., Georgalis, G. L., Lyson, T. R., Pérez-García, A., Rabi, M., Sterli, J., Vitek, N. S. & Parham, J. F. 2021. A nomenclature for fossil and living turtles using phylogenetically defined clade names. *Swiss Journal of Palaeontology*, **140**(5), 1–45.
- Kamel, T. & Matsumoto, E. 1965. Discovery of crocodile fossil from the Osaka group. In: Kobatake, N., Chiji, M., Ikebe, N., Ishida, S., Kamei, T., Nakaseko, K. & Matsumoto, E. *Discovery of crocodile fossil from the Osaka Group. The Quaternary Research (Daiyonki-Kenkyu)*, **4**(2), 49–58.
- Katsura, Y. 2004. Paleopathology of *Toyotamaphimeia machikanensis* (Diapsida, Crocodylia) from the Middle Pleistocene of Central Japan. *Historical Biology*, **16**(2–4), 93–97.
- Khosatzky, L. I. 1976. A new representative of trionychids from the Late Cretaceous of Mongolia. *Gerpetologiya. Kubanskiy gosudarstvennyy universitet. Nauchnye trudy*, **218**, 3–19. [In Russian].
- Khuc, V., Thanh, T. D. & Tri, T. V. 2005. New schema of subdivision and correlation on on-shore Tertiary sediments in Vietnam. *Journal of Geology (Hanoi)*, B, **26**, 6–12.
- Kobayashi, Y., Tomida, Y., Kamei, T. & Eguchi, T. 2006. Anatomy of a Japanese tomistomine crocodylian, *Toyotamaphimeia machikanensis* (Kamei et Matsumoto, 1965), from the middle Pleistocene of Osaka Prefecture: the reassessment of its phylogenetic status within Crocodylia. *National Science Museum Monographs*, **35**, 1–121.
- Kominz, M. A., Browning, J. V., Miller, K. G., Sugarman, P. J., Mizintseva, S. & Scotese, C. R. 2008. Late Cretaceous to Miocene sea-level estimates from the New Jersey and Delaware coastal plain coreholes: an error analysis. *Basin Research*, **20**(2), 211–226.
- Kuhl, H., Frankl-Vilches, C., Bakker, A., Mayr, G., Nikolaus, G., Boerno, S. T., Klages, S., Timmermann, B. & Gahr, M. 2021. An Unbiased Molecular Approach Using 3'-UTRs Resolves the Avian Family-Level Tree of Life. *Molecular Biology and Evolution*, **38**(1), 108–127.
- Kuhn, O. 1938. Die Crocodilier aus dem mittleren Eozän des Geiseltales bei Halle. *Nova Acta Leopoldina*, **6**(39), 313–329.
- Kurochkin, E.N. 1976. A Survey of the Paleogene Birds of Asia. In: Olson, S. L. (ed.) *Collected Papers in Avian Paleontology Honoring the 90th Birthday of Alexander Wetmore. Smithsonian Contributions to Paleobiology*, **27**(1), 75–86.
- Kurochkin, E. N. & Dyke, G. J. 2011. The first fossil owls (Aves: Strigiformes) from the Paleogene of Asia and a review of the fossil record of Strigiformes. *Paleontological Journal*, **45**(4), 445–458.

- Lacépède, B. G. E. de** 1788. *Histoire Naturelle des Quadrupèdes Ovipares et des Serpens*. Tome Premier. Paris: Hôtel de Thou, 1–651.
- Lambe, L. M.** 1907. On a new crocodylian genus and species from the Judith River Formation of Alberta. *Transactions of the Royal Society of Canada*, **4**, 219–244.
- Lambrecht, K.** 1931. *Protoplotus beauforti* n.g. n.sp., ein Schlagenhalsvogel aus dem Tertiär von W. Sumatra. *Wetenschappelijke Mededeelingen Dienst van den Mijnbouw in Nederlandisch-Indie*, **17**, 15–24.
- Langston, W.** 1975. Ziphodont Crocodiles: *Pristichampsus vorax* (Troxell), New Combination, From the Eocene of North America. *Fieldiana Geology*, **33**(16), 291–314.
- Laurenti, J. N.** 1768. *Specimen medicum, exhibens synopsis reptilium emendatam cum experimentis circa venena et antidota reptilium austracorum, quod auctoritate et consensus*. J. Thomae, Vienna, 1–217.
- Le, M., Duong, H. T., Dinh, L. D., Nguyen, T. Q., Pritchard, P. C. H. & McCormack, T.** 2014. A phylogeny of softshell turtles (Testudines: Trionychidae) with reference to the taxonomic status of the critically endangered, giant softshell turtle, *Rafetus swinhoei*. *Organisms Diversity & Evolution*, **14**, 279–293.
- Lee, M. S. Y. & Yates, A. M.** 2018. Tip-dating and homoplasy: reconciling the shallow molecular divergences of modern gharials with their long fossil record. *Proceedings of the Royal Society B: Biological Sciences*, **285**(1881), 20181071, 1–10.
- Lee, M. S. Y., Cau, A., Naish, D. & Dyke, G. J.** 2014. Morphological Clocks in Paleontology, and a Mid-Cretaceous Origin of Crown Aves. *Systematic Biology*, **63**(3), 442–449.
- Leloup, P. H., Lacassin, R., Tapponnier, P., Schärer, U., Zhong, D., Liu, X., Zhang, L., Ji, S. & Trinh, P. T.** 1995. The Ailao Shan-Red River shear zone (Yunnan, China), Tertiary transform boundary of Indochina. *Tectonophysics*, **251**(1-4), 3–84.
- Leloup, P. H., Arnaud, N., Lacassin, R., Kienast, J. R., Harrison, T. M., Trong, T. T. P., Replumaz, A. & Tapponnier, P.** 2001. New constraints on the structure, thermochronology, and timing of the Ailao Shan-Red River shear zone, SE Asia. *Journal of Geophysical Research: Solid Earth*, **106**(B4), 6683–6732.
- Lesson, R. P.** 1831. Catalogue des Reptiles qui font partie d'une Collection zoologique recueillie dans l'Inde continentale ou en Afrique, et qpportée en France par M. Lamare-Piquot. *Bulletin des Sciences Naturelles et de Géologie, Paris*, **25**(2), 119–123.
- Li, C., Wu, X.-C. & Rufolo, S. J.** 2019. A new crocodyloid (Eusuchia: Crocodylia) from the Upper Cretaceous of China. *Cretaceous Research*, **94**, 25–39.
- Li, J.** 1976. Fossil of Sebecosuchia discovered from Nanxiong, Guangdong. *Vertebrata PalAsiatica*, **14**(3), 169-174.
- Li, J.** 1984. A new species of *Planocrania* from Hengdong, Hunan. *Vertebrata PalAsiatica*, **22**(2), 123-133.
- Li, J. & Wang, B.** 1987. A new species of Alligator from Shanwang, Shandong. *Vertebrata PalAsiatica*, **25**(3), 199–207.
- Li, L., Joyce, W. G. & Liu, J.** 2015. The first soft-shelled turtle from the Jehol Biota of China. *Journal of Vertebrate Paleontology*, **35**(2), e909450, 1–9.
- Linnaeus, C.** 1758. *Systema naturæ per regna tria naturæ, secundum classes, ordines, genera, species, cum characteribus, differentiis, synonymis, locis*. Tomus I. Edition decima, reformata. Stockholm: Laurentius salvius. 1–881.
- Linnaeus, C.** 1766. *Systema Naturæ*. Editio Duodecima, Reformata. Tomus, I, Paris, I, Regnum Animale. Holmia (Stockholm). Laurentius salvius. 1–532.
- Livezey, B. C. & Zusi, R. L.** 2007. Higher-order phylogeny of modern birds (Theropoda, Aves: Neornithes) based on comparative anatomy. II. Analysis and discussion. *Zoological Journal of the Linnean Society*, **149**(1), 1–95.

- Loewen, M. A., Irmis, R. B., Sertich, J. J. W., Currie, P. J. & Sampson, S. D.** 2013. Tyrant Dinosaur Evolution Tracks the Rise and Fall of Late Cretaceous Oceans. *PLoS ONE*, **8**(11), e79420, 1–14.
- Loiselle, B. A. & Blake, J. G.** 1992. Population Variation in a Tropical Bird Community. Implications for conservation. *BioScience*, **42**(11), 838–845.
- Longrich, N. R., Tokaryk, T. & Field, D. J.** 2011. Mass extinction of birds at the Cretaceous–Paleogene (K–Pg) boundary. *Proceedings of the National Academy of Sciences*, **108**(37), 15253–15257.
- Ludwig, R.** 1877. Fossile Crocodyliiden aus der Tertiärformation des Mainzer Beckens. *Paleontographica Supplement*, **3**, 1–52.
- Lyson, T. R., Petermann, H. & Miller, I. M.** 2021. A new plastronid trionychid turtle, *Plastomenus joycei*, sp. nov., from the earliest Paleocene (Danian) Denver Formation of south-central Colorado, U.S.A. *Journal of Vertebrate Paleontology*, **41**(1), e1913600, 1–11.
- MacArthur, R. H. & MacArthur, J. W.** 1961. On Bird Species Diversity. *Ecology*, **42**(3), 594–598.
- Markwick, P. J.** 1998a. Crocodylian diversity in space and time: the role of climate in paleoecology and its implication for understanding K/T extinctions. *Paleobiology*, **24**(4), 470–497.
- Markwick, P. J.** 1998b. Fossil crocodylians as indicators of Late Cretaceous and Cenozoic climates: implications for using palaeontological data in reconstructing palaeoclimate. *Palaeogeography, Palaeoclimatology, Palaeoecology*, **137**(3–4), 205–271.
- Marsh, O. C.** 1871. Notice of some new fossil reptiles from the Cretaceous and Tertiary formations. *American Journal of Science*, **3**(6), 447–459.
- Martin, J. E.** 2019. The taxonomic content of the genus *Gavialis* from the Siwalik Hills of India and Pakistan. *Papers in Palaeontology*, **5**(3), 483–497.
- Martin, J. E. & Benton, M. J.** 2008. Crown Clades in Vertebrate Nomenclature: Correcting the Definition of Crocodylia. *Systematic Biology*, **57**(1), 173–181.
- Martin, J. E. & Lauprasert, K.** 2010. A new primitive alligatorine from the Eocene of Thailand: relevance of Asiatic members to the radiation of the group. *Zoological Journal of the Linnean Society*, **158**(3), 608–628.
- Martin, J. E., Smith, T., de Lapparent de Broin, F., Escuillié, F. & Delfino, M.** 2014. Late Palaeocene eusuchian remains from Mont de Berru, France, and the origin of the alligatoroid *Diplocynodon*. *Zoological Journal of the Linnean Society*, **172**(4), 867–891.
- Martin, J. E., Lauprasert, K., Tong, H., Suteethorn, V. & Buffetaut, E.** 2019a. An Eocene tomistomine from peninsular Thailand. *Annales de Paléontologie*, **105**(3), 245–253.
- Martin, J. E., Antoine, P. O., Perrier, V., Welcomme, J. L., Metais, G., & Marivaux, L.** 2019b. A large crocodyloid from the Oligocene of the Bugti Hills, Pakistan. *Journal of Vertebrate Paleontology*, **39**(4), e1671427, 1–8.
- Massonne, T., Vasilyan, D., Rabi, M. & Böhme, M.** 2019. A new alligatoroid from the Eocene of Vietnam highlights an extinct Asian clade independent from extant *Alligator sinensis*. *PeerJ*, **7**, e7562, 1–60.
- Massonne, T., Augustin, F. J., Matzke, A. T., Weber, E. & Böhme, M.** 2021. A new species of *Maomingosuchus* from the Eocene of the Na Duong Basin (northern Vietnam) sheds new light on the phylogenetic relationship of tomistomine crocodylians and their dispersal from Europe to Asia. *Journal of Systematic Palaeontology*, **19**(22), 1551–1585.
- Massonne, T., Böhme, M. & Mayr, G.** 2022. A tarsometatarsus from the upper Eocene Na Duong Basin—the first Palaeogene fossil bird from Vietnam. *Alcheringa: An Australasian Journal of Palaeontology*, **46**(3–4), 291–296.

- Massonne, T., Augustin, F. J., Matzke, A. T. & Böhme, M.** 2023. A new cryptodire from the Eocene of the Na Duong Basin (northern Vietnam) sheds new light on *Pan-Trionychidae* from Southeast Asia. *Journal of Systematic Palaeontology*, **21**(1), 2217505, 1–25.
- Maury-Lechon, G. & Curtet, L.** 1998. Biogeography and evolutionary systematics of Dipterochrysochloridae. *In*: Appanah, S. & Turnbull, J. M. (eds.) *A Review of Dipterochrysochloridae: Taxonomy, Ecology and Silviculture*. Bogor, Indonesia, Center for International Forestry research, 5–44.
- Mayerl, C. J., Brainerd, E. L. & Blob, R. W.** 2016. Pelvic girdle mobility of cryptodire and pleurodire turtles during walking and swimming. *Journal of Experimental Biology*, **219**(17), 2650–2658.
- Mayr, G.** 2009. *Paleogene Fossil Birds, First Edition*. Springer, Heidelberg, 1–262.
- Mayr, G.** 2011. Cenozoic mystery birds - on the phylogenetic affinities of bony-toothed birds (Pelagornithidae). *Zoologica Scripta*, **40**(5), 448–467.
- Mayr, G.** 2022. *Paleogene Fossil Birds*. Springer International Publishing, Cham, Fascinating Life Sciences, 1–239.
- Mayr, G. & Clarke, J.** 2003. The deep divergences of neornithine birds: a phylogenetic analysis of morphological characters. *Cladistics*, **19**(6), 527–553.
- Mayr, G. & Zelenkov, N.** 2021. Extinct crane-like birds (Eogruidae and Ergilornithidae) from the Cenozoic of Central Asia are indeed ostrich precursors. *Ornithology*, **138**(4), 1–15.
- Mayr, G., Rana, R. S., Rose, K. D., Sahni, A., Kumar, K., Singh, L. & Smith, T.** 2010. *Quercypsitta*-like birds from the early Eocene of India (Aves, ?Psittaciformes). *Journal of Vertebrate Paleontology*, **30**(2), 467–478.
- Mayr, G., Gorobets, L. & Zvonok, E.** 2013. The tarsometatarsus of the Middle Eocene loon *Colymbiculus udovichenkoi*. *Paleornithological research 2013 – Proceedings of the 8th international Meeting of the Society of Avian Paleontology and Evolution*, 17–22. Vienna: Natural History Museum Vienna.
- Mazur, S., Green, C., Stewart, M. G., Whittaker, J. M., Williams, S. & Bouatmani, R.** 2012. Displacement along the Red River Fault constrained by extension estimates and plate reconstructions. *Tectonics*, **31**(5), 1–22.
- McAliley, L. R., Willis, R. E., Ray, D. A., White, P. S., Brochu, C. A. & Densmore, L. D.** 2006. Are crocodiles really monophyletic? – Evidence for subdivisions from sequence and morphological data. *Molecular Phylogenetics and Evolution*, **39**(1), 16–32.
- Meyer, H. von.** 1832. *Paleologica zur Geschichte der Erde und ihrer Geschöpfe*. Siegmund Schmerber, Frankfurt am Main, 1–560.
- Meylan, P. A.** 1987. The Phylogenetic Relationships of Soft-Shell Turtles (Family Trionychidae). *Bulletin of the American Museum of Natural History*, **186**, 1–101.
- Meylan, P. A. & Gaffney, E. S.** 1992. *Sinaspideretes* is not the oldest trionychid turtle. *Journal of Vertebrate Paleontology*, **12**(2), 257–259.
- Mitchell, K. J., Llamas, B., Soubrier, J., Rawlence, N. J., Worthy, T. H., Wood, J., Lee, M. S. Y. & Cooper, A.** 2014. Ancient DNA reveals elephant birds and kiwi are sister taxa and clarifies ratite bird evolution. *Science*, **344**(6186), 898–900.
- Mittermeier, R. A., Turner, W. R., Larsen, F. W., Brooks, T. M. & Gascon, C.** 2011. Global Biodiversity Conservation: The Critical Role of Hotspots. *In*: Zachos, F. E. & Habel, J. C. (eds) *Biodiversity Hotspots*. Springer Berlin Heidelberg, Berlin, Heidelberg, 3–22.
- Mittermeier, R. A., van Dijk, P. P., Rhodin, A. G. J. & Nash, S. D.** 2015. Turtle Hotspots: An Analysis of the Occurrence of Tortoises and Freshwater Turtles in Biodiversity Hotspots, High-Biodiversity Wilderness Areas, and Turtle Priority Areas. *Chelonian Conservation and Biology*, **14**(1), 2–10.

- Modesto, S. P. & Anderson, J. S.** 2004. The Phylogenetic Definition of Reptilia Lutzoni. *Systematic Biology*, **53**(5), 815–821.
- Molnar, R. E.** 1981. Pleistocene ziphodont crocodylians of Queensland. *Records of the Australian Museum*, **33**(19), 803–834.
- Mook, C. C.** 1940. A new fossil crocodylian from Mongolia. *American Museum Novitates*, **1097**, 1–3.
- Mook, C. C.** 1941. A new crocodylian from the Lance Formation. *American Museum Novitates*, **1128**, 1–5.
- Müller, L.** 1927. Ergebnisse der Forschungsreisen Prof. E. Stromers in den Wüsten Ägyptens. V. Tertiär Wirbeltiere. 1. Beiträge zur Kenntnis der Krokodilier des ägyptischen Tertiärs. *Abhandlungen der Bayerischen Akademie der Wissenschaften Mathematisch-naturwissenschaftliche Abteilung*, **31**, 1–96.
- Müller, S.** 1838. Waarnemingen over de Indische krokodillen en Beschrijving van eene nieuwe soort. *Tydschrift voor Natuurlijke Geschiedenis en Physiologie*, **5**, 67–87.
- Myers, N.** 1988. Threatened biotas: 'Hot spots' in tropical forests. *The Environmentalist*, **8**(3), 187–208.
- Myers, N.** 1990. The biodiversity challenge: Expanded hot-spots analysis. *The Environmentalist*, **10**(4), 243–256.
- Myers, N., Mittermeier, R. A., Mittermeier, C. G., da Fonseca, G. A. B. & Kent, J.** 2000. Biodiversity hotspots for conservation priorities. *Nature*, **403**, 853–858.
- Nessov, L. A.** 1992. Mesozoic and Paleogene birds of the USSR and their paleoenvironments. In: Campbell, K. E. (ed.) *Papers in avian paleontology honoring Pierce Brodkorb*. Natural History Museum of Los Angeles County, *Science Series*, **36**, 465–478.
- Nessov, L. A.** 1995. On some Mesozoic turtles of the Fergana depression (Kyrgyzstan) and Dzhungar Alatau ridge (Kazakhstan). *Russian Journal of Herpetology*, **2**(2), 134–141.
- Neubauer, T. A., Schneider, S., Böhme, M. & Prieto, J.** 2012. First records of freshwater rissooidean gastropods from the Palaeogene of Southeast Asia. *Journal of Molluscan Studies*, **78**(3), 275–282.
- Ni, X., Li, Q., Li, L., & Beard, K. C.** 2016. Oligocene primates from China reveal divergence between African and Asian primate evolution. *Science*, **352**(6286), 673–677.
- Nicholl, C. S. C., Rio, J. P., Mannion, P. D. & Delfino, M.** 2020. A re-examination of the anatomy and systematics of the tomistomine crocodylians from the Miocene of Italy and Malta. *Journal of Systematic Palaeontology*, **18**(22), 1853–1889.
- Niklas, K. J.** 1995. Size-dependent Allometry of Tree Height, Diameter and Trunk-taper. *Annals of Botany*, **75**(3), 217–227.
- Norell, M. A., Clark, I. J. M. & Hutchison, J. H.** 1994. The Late Cretaceous Alligatoroid *Brachychampsia montana* (Crocodylia): New Material and Putative Relationships. *American Museum Novitates*, **3116**, 1–26.
- Noss, R. F., Platt, W. J., Sorrie, B. A., Weakley, A. S., Means, D. B., Costanza, J. & Peet, R. K.** 2015. How global biodiversity hotspots may go unrecognized: lessons from the North American Coastal Plain. *Diversity and Distributions*, **21**(2), 236–244.
- Oaks, J. R.** 2011. A Time-Calibrated Species Tree of Crocodylia Reveals a Recent Radiation of the True Crocodiles: Recent Radiation of Crocodiles. *Evolution*, **65**(11), 3285–3297.
- Pan, T., Miao, J.-S., Zhang, H.-B., Yan, P., Lee, P.-S., Jiang, X.-Y., Ouyang, J.-H., Deng, Y.-P., Zhang, B.-W. & Wu, X.-B.** 2021. Near-complete phylogeny of extant Crocodylia (Reptilia) using mitogenome-based data. *Zoological Journal of the Linnean Society*, **191**(4), 1075–1089.

- Peppe, D. J., Royer, D. L., Cariglino, B., Oliver, S. Y., Newman, S., Leight, E., Enikolopov, G., Fernandez-Burgos, M., Herrera, F., Adams, J. M., Correa, E., Currano, E. D., Erickson, J. M., Hinojosa, L. F., Hoganson, J. W., Iglesias, A., Jaramillo, C. A., Johnson, K. R., Jordan, G. J., Kraft, N. J. B., Lovelock, E. C., Lusk, C. H., Niinemets, Ü., Peñuelas, J., Rapson, G., Wing, S. L. & Wright, I. J.** 2011. Sensitivity of leaf size and shape to climate: global patterns and paleoclimatic applications. *New Phytologist*, **190**(3), 724–739.
- Pereira, A. G., Sterli, J., Moreira, F. R. R. & Schrago, C. G.** 2017. Multilocus phylogeny and statistical biogeography clarify the evolutionary history of major lineages of turtles. *Molecular Phylogenetics and Evolution*, **113**, 59–66.
- Pérez-García, A.** 2016. A new turtle confirms the presence of Bothremydidae (Pleurodira) in the Cenozoic of Europe and expands the biostratigraphic range of Foxemydina. *The Science of Nature*, **103**(50), 1–14.
- Pickford, M.** 1994. Late Cenozoic crocodiles (Reptilia: Crocodylidae) from the Western Rift, Uganda. In: Senut, B. & Pickford, M. (eds) *Geology and Palaeobiology of the Albertine rift valley, Uganda-Zaire*, **2**, 137–155.
- Pickford, M.** 2008. The myth of the hippo-like anthracothere: The eternal problem of homology and convergence. *Spanish Journal of Palaeontology*, **23**(1), 31–90.
- Piras, P., Delfino, M., Favero, L. D. & Kotsakis, T.** 2007. Phylogenetic position of the crocodylian *Megadontosuchus arduini* and tomistomine palaeobiogeography. *Acta Palaeontologica Polonica*, **52**(2), 315–328.
- Platt, S. G. & Van Tri, N.** 2000. Status of the Siamese crocodile in Vietnam. *Oryx*, **34**(3), 217–221.
- Prieto-Márquez, A., Fondevilla, V., Sellés, A. G., Wagner, J. R. & Galobart, À.** 2019. *Adynomosaurus arcanus*, a new lambeosaurine dinosaur from the Late Cretaceous Ibero-Armorican Island of the European archipelago. *Cretaceous Research*, **96**, 19–37.
- Prum, R. O., Berv, J. S., Dornburg, A., Field, D. J., Townsend, J. P., Lemmon, E. M. & Lemmon, A. R.** 2015. A comprehensive phylogeny of birds (Aves) using targeted next-generation DNA sequencing. *Nature*, **526**, 569–573.
- Pubellier, M., Rangin, C., Phach, P. V., Que, B. C., Hung, D. T. & Sang, C. L.** 2003. The Cao Bang – Tien Yen Fault: Implications on the relationships between the Red River Fault and the South China coastal belt. *Advances in Natural Sciences*, **4**(4), 347–361.
- Ramsay, E. P.** 1886. On a new genus and species of fresh water tortoise from the Fly River, New Guinea. *Proceedings of the Linnaean Society of New South Wales*, **2**(1), 158–162.
- Rich, P. V., Hou, L. H., Ono, K. & Baird, R. F.** 1986. A review of the fossil birds of China, Japan and Southeast Asia. *Geobios*, **19**(6), 755–772.
- Rio, J. P. & Mannion, P. D.** 2021. Phylogenetic analysis of a new morphological dataset elucidates the evolutionary history of Crocodylia and resolves the long-standing gharial problem. *PeerJ*, **9**, e12094, 1–156.
- Rio, J. P., Mannion, P. D., Tschopp, E., Martin, J. E. & Delfino, M.** 2020. Reappraisal of the morphology and phylogenetic relationships of the alligatoroid crocodylian *Diplocynodon hantoniensis* from the late Eocene of the United Kingdom. *Zoological Journal of the Linnean Society*, **188**(2), 579–629.
- Ristevski, J., Yates, A. M., Price, G. J., Molnar, R. E., Weisbecker, V. & Salisbury, S. W.** 2020. Australia's prehistoric 'swamp king': revision of the Plio-Pleistocene crocodylian genus *Pallimnarchus* de Vis, 1886. *PeerJ*, **8**, e10466, 1–98.
- Ristevski, J., Weisbecker, V., Scanlon, J. D., Price, G. J. & Salisbury, S. W.** 2023a. Cranial anatomy of the mekosuchine crocodylian *Trilophosuchus rackhami* Willis, 1993. *The Anatomical Record*, **306**(2), 239–297.

- Ristevski, J., Willis, P. M. A., Yates, A. M., White, M. A., Hart, L. J., Stein, M. D., Price, G. J. & Salisbury, S. W. 2023b. Migrations, diversifications and extinctions: the evolutionary history of crocodyliforms in Australasia. *Alcheringa: An Australasian Journal of Palaeontology*, 1–46.
- Robson, C. 2008. *Birds of South-East Asia, Second Edition*. Helm Field Guides. 1–544.
- Salas-Gismondi, R., Moreno-Bernal, J. W., Scheyer, T. M., Sánchez-Villagra, M. R. & Jaramillo, C. 2019. New Miocene Caribbean gavialoids and patterns of longirostry in crocodylians. *Journal of Systematic Palaeontology*, **17**(12), 1049–1075.
- Salisbury, S. W. & Willis, P. M. A. 1996. A new crocodylian from the Early Eocene of south-eastern Queensland and a preliminary investigation of the phylogenetic relationships of crocodyloids. *Alcheringa: An Australasian Journal of Palaeontology*, **20**(3), 179–226.
- Scheyer, T. M., Aguilera, O. A., Delfino, M., Fortier, D. C., Carlini, A. A., Sánchez, R., Carrillo-Briceño, J. D., Quiroz, L. & Sánchez-Villagra, M. R. 2013. Crocodylian diversity peak and extinction in the late Cenozoic of the northern Neotropics. *Nature Communications*, **4**(1907), 1–9.
- Schneider, J. G. 1783. *Allgemeine Naturgeschichte der Schildkröten: nebst einem systematischen Verzeichnisse der einzelnen Arten und zwey Kupfern*. Leipzig. Johann Gottfried Müllersche Buchhandlung, 1–364.
- Schneider, J. G. 1801. *Historiae amphibiorum naturalis et literariae. Fasciculus secundus continens crocodilos, scincos, chamaesauras, boas, pseudoboas, elapes, angues, amphisbaenas et caecilias*. Jena. Frommani. 1–364.
- Schneider, S., Böhme, M. & Prieto, J. 2013. Unionidae (Bivalvia; Palaeoheterodonta) from the Palaeogene of northern Vietnam: exploring the origins of the modern East Asian freshwater bivalve fauna. *Journal of Systematic Palaeontology*, **11**(3), 337–357.
- Schweiger, A. F. 1812. *Prodromus monographiae cheloniorum, Pars 1. Königsberger Archiv für Naturwissenschaft und Mathematik*, 271–458.
- Searle, M. P. 2006. Role of the Red River Shear zone, Yunnan and Vietnam, in the continental extrusion of SE Asia. *Journal of the Geological Society*, **163**(6), 1025–1036.
- Sekercioglu, C. H. 2012. Bird functional diversity and ecosystem services in tropical forests, agroforests and agricultural areas. *Journal of Ornithology*, **153**(Suppl 1), 153–161.
- Shan, H.-Y., Wu, X.-C., Cheng, Y. & Sato, T. 2009. A new tomistomine (Crocodylia) from the Miocene of Taiwan. *Canadian Journal of Earth Sciences*, **46**(7), 529–555.
- Shan, H.-Y., Cheng, Y. N. & Wu, X.-C. 2013. The first fossil skull of *Alligator sinensis* from the Pleistocene, Taiwan, with a paleogeographic implication of the species. *Journal of Asian Earth Sciences*, **69**, 17–25.
- Shan, H.-Y., Wu, X.-C., Cheng, Y.-N. & Sato, T. 2017. *Maomingosuchus petrolica*, a restudy of ‘*Tomistoma*’ *petrolica* Yeh, 1958. *Palaeoworld*, **26**(4), 672–690.
- Shan, H.-Y., Wu, X.-C., Sato, T., Cheng, Y. & Rufolo, S. 2021. A new alligatoroid (Eusuchia, Crocodylia) from the Eocene of China and its implications for the relationships of Orientalosuchina. *Journal of Paleontology*, **95**(6), 1321–1339.
- Shikama, T. 1972. Fossil Crocodylia from Tsochin, southwestern Taiwan. *Science Report of Yokohama National University: Biological and Geological Sciences*, **19**, 125–132.
- Siebenrock, F. 1906. Zur Kenntnis der Schildkrötenfauna der Insel Hainan. *Zoologischer Anzeiger*, **30**, 578–586.
- Skutschas, P. P., Danilov, I. G., Kodrul, T. M. & Jin, J. 2014. The first discovery of an alligatorid (Crocodylia, Alligatoroidea, Alligatoridae) in the Eocene of China. *Journal of Vertebrate Paleontology*, **34**(2), 471–476.

- Sobbe, I. H., Price, G. J. & Knezour, R. A.** 2013. A ziphodont crocodile from the late Pleistocene King Creek catchment, Darling Downs, Queensland. *Memoirs of the Queensland Museum-Nature* **56**(2), 601–606.
- Sodhi, N. S., Koh, L. P. & Brook, B. W.** 2006. Southeast Asian birds in a peril. *The Auk*, **123**(1), 275–277.
- Sookias, R. B.** 2020. Exploring the effects of character construction and choice, outgroups and analytical method on phylogenetic inference from discrete characters in extant crocodylians. *Zoological Journal of the Linnean Society*, **189**(2), 670–699.
- Sorenson, M. D., Oneal, E., García-Moreno, J. & Mindell, D. P.** 2003. More Taxa, More Characters: The Hoatzin Problem Is Still Unresolved. *Molecular Biology and Evolution*, **20**(9), 1484–1498.
- Sterling, E. J. & Hurley, M. M.** 2005. Conserving Biodiversity in Vietnam: Applying Biogeography to Conservation Research. *Proceedings of the California Academy of Sciences* **56**(Suppl 1(9)), 98–114.
- Stevenson, C. & Whitaker, R.** 2010. Gharial *Gavialis gangeticus*. In: Manolis S. C. & Stevenson, C. (eds) *Crocodyles. Status Survey and Conservation Action Plan*. Third edition. Crocodile Specialist Group.: Darwin. 139–143.
- Stidham, T. A. & Xi-Jun, N.** 2014. Large anseriform (Aves: Anatidae: Romainvilliinae?) fossils from the Late Eocene of Xinjiang, China. *Vertebrata Palasiatica*, **52**(1), 98–111.
- Stidham, T. A., Holroyd, P. A., Gunnell, G. F., Ciochon, R. L., Tsubamoto, T., Egi, N. & Takai, M.** 2005. An Ibis-Like Bird (Aves: Cf. Threskiornithidae) from the Late Middle Eocene of Myanmar. *Contributions from the Museum of Paleontology*, **31**(7), 179–184.
- Stuart, B. L., Hayes, B., Manh, B. H. & Platt, S. G.** 2002. Status of crocodiles in the U Minh Thuong Nature Reserve, southern Vietnam. *Pacific Conservation Biology*, **8**(1), 62–65.
- Stuebing, R. B. & Bezuijen, M. R., Auliya, M. & Voris, H. K.** 2006. The Current and Historic Distribution of *Tomistoma Schlegelii* (The False Gharial) (Müller, 1838) (Crocodylia, Reptilia). *The Raffles Bulletin of Zoology*, **54**(1), 181–197.
- Sun, A., Li, J., Ye, X., Dong, Z. & Hou, L.** 1992. *The Chinese fossil reptiles and their kins*. Science Press, Beijing, China. 1–260.
- Lee, M. S. Y. & Spencer, P. S.** 1997. Crown-Clades, Key Characters and Taxonomic Stability: When is an Amniote not and Amniote?. In: Sumida, S. S. & Martin, K. L. M. (eds). *Amniote Origins: Completing the Transition to Land*. Academic Press, San Diego, 61–84.
- Taplin, L. E. & Grigg, G. C.** 1989. Historical Zoogeography of the Eusuchian Crocodylians: A Physiological Perspective. *American Zoologist*, **29**(3), 885–901.
- Tapponnier, P., Peltzer, G. & Armijo, R.** 1986. On the mechanics of the collision between India and Asia. *Geological Society, London, Special Publications*, **19**(1), 113–157.
- Tapponnier, P., Lacassin, R., Leloup, P. H., Schärer, U., Dalai, Z., Haiwei, W., Xiaohan, L., Shaocheng, J., Lianshang, Z. & Jiayou, Z.** 1990. The Ailao Shan/Red River metamorphic belt: Tertiary left-lateral shear between Indochina and South China. *Nature*, **343**, 431–437.
- Tarsitano, S. F., Frey, E. & Riess, J.** 1989. The Evolution of the Crocodylia: A Conflict Between Morphological and Biochemical Data. *American Zoologist*, **29**(3), 843–856.
- Thanh, P. T., Shakirov, R. B., & Syrbu, N. S.** 2019. Characteristics of tectonic activity phases along The Cao Bang – Tien Yen fault zone, Tien Yen – Lang Son section, Northeastern part, Vietnam. *Geosystems of Transition Zones*, **3**(4) 345–363.
- Thomson, R. C., Spinks, P. Q. & Shaffer, H. B.** 2021. A global phylogeny of turtles reveals a burst of climate-associated diversification on continental margins. *Proceedings of the National Academy of Sciences*, **118**(7), e2012215118, 1–10.

- Thorbjarnarson, J.** 1992. *Crocodiles: An Action Plan for their Conservation*. Messel, H., King, F. W. & Ross, J. P. (eds). Gland, Switzerland: IUCN – The World Conservation Union. 1–136.
- Thorbjarnarson, J., Platt, S. G. & Khaing, U. S. T.** 2000. A population survey of the estuarine crocodile in the Ayeyarwady Delta, Myanmar. *Oryx*, **34**(4), 317–324.
- Tompsett, P. B.** 1998. Seed Physiology. In: Appanah, S. & Turnbull, J. M. (eds.) *A Review of Dipterocarps: Taxonomy, Ecology and Silviculture*. Bogor, Indonesia, Center of International Forestry Research, 57–71.
- Tong, H., Li, L. & Ouyang, H.** 2014. A revision of *Sinaspideretes wimani* Young & Chow, 1953 (Testudines: Cryptodira: Trionychoidea) from the Jurassic of the Sichuan Basin, China. *Geological Magazine*, **151**(4), 600–610.
- Toula, F., & Kail, J. A.** 1885. Über einen Krokodil-Schädel aus den Tertiärablagerungen von Eggenburg in Niederösterreich: eine paläontologische Studie. *Denkschriften der Kaiserlichen Akademie der Wissenschaften von Wien, Mathematisch-naturwissenschaftliche Klasse*, **50**, 299–355.
- Traiser, C., Klotz, S., Uhl, D. & Mosbrugger, V.** 2005. Environmental signals from leaves – a physiognomic analysis of European vegetation. *New Phytologist*, **166**(2), 465–484.
- Troxell, E. L.** 1925. The Bridger crocodiles. *American Journal of Science*, **5**(9), 29–72.
- Tsubamoto, T., Naoko, E., Masanaru, T., Nobuo, S., Hisashi, S., Takeshi, N., Hiroaki, U. Maung-Maung, Chit-Sein, Tun, S. T., Soe, A. N., Aung, A. K., Thein, T., Thaug-Htike & Zin-Maung-Maung-Thein.** 2006a. A summary of the Pondaung fossil expeditions. *Asian Paleoprimatology*, **4**, 1–66.
- Tsubamoto, T., Egi, N. & Takai, M.** 2006b. Notes on fish, reptilian, and several fragmentary mammalian dental fossils from the Pondaung Formation. *Asian Paleoprimatology*, **4**, 98–110.
- Tsubamoto, T., Tsuihiji, T., Phan, D. P., Doan, D. H., Egi, N. & Komatsu, T.** 2022. A new specimen of *Anthrakoceryx naduongensis* (Mammalia, Artiodactyla, Anthracotheriidae) from the Eocene Na Duong Formation, northeastern Vietnam. *The Journal of the Geological Society of Japan*, **128**(1), 245–251.
- Turtle Taxonomy Working Group (Rhodin, A. G. J., Iverson, J. B., Bour, R., Fritz, U., Georges, A., Shaffer, H. B. & van Dijk, P. P.** 2021. Turtles of the World: Annotated Checklist and Atlas of Taxonomy, Synonymy, Distribution, and Conservation Status (9th Ed.). *Chelonia Research Monographs*, **8**, 1–472.
- Vinh, N. X., Long, V. N., Simpson, B. K., Tri, N. V., Quan, L. T., Quang, H. X. & Dung, V. V.** 2006. Status of the Freshwater Crocodile (*Crocodylus siamensis*) in Song Hinh District, Phu Yen Province, Viet Nam. *Mekong Wetlands Biodiversity Conservation and Sustainable Use Programme*, Vientiane, Lao PDR, 1–48.
- Vitek, N. S. & Danilov, I. G.** 2010. New material and a reassessment of soft-shelled turtles (Trionychidae) from the Late Cretaceous of Middle Asia and Kazakhstan. *Journal of Vertebrate Paleontology*, **30**(2), 383–393.
- Vitek, N. S. & Danilov, I. G.** 2012. New data on the soft-shelled turtles from the Upper Cretaceous Kyrkkuduk I locality of Southern Kazakhstan. *Proceedings of the Zoological Institute RAS*, **316**(1), 50–56.
- Vitek, N. S. & Danilov, I. G.** 2015. New material of *Ulutrionyx ninae* from the Oligocene of Kazakhstan, with a review of Oligocene trionychids of Asia. *Journal of Vertebrate Paleontology*, **35**(5), e973570, 1–9.
- Vitek, N. S. & Joyce, W. G.** 2015. A Review of the Fossil Record of New World Turtles of the Clade *Pan-Trionychoidea*. *Bulletin of the Peabody Museum of Natural History*, **56**(2), 185–244.
- Wagler, R.** 2011. The Anthropocene Mass Extinction: An Emerging Curriculum Theme for Science Educators. *The American Biology Teacher*, **73**(2), 78–83.

- Walter, J., Darlim, G., Massonne, T., Aase, A., Frey, E. & Rabi, M.** 2022. On the origin of Caimaninae: insights from new fossils of *Tsoabichi greenriverensis* and a review of the evidence. *Historical Biology*, **34**(4), 580–595.
- Wang, M., Mayr, G., Zhang, J. & Zhou, Z.** 2012. Two new skeletons of the enigmatic, rail-like avian taxon *Songzia* Hou, 1990 (Songziidae) from the early Eocene of China. *Alcheringa: An Australasian Journal of Palaeontology*, **36**(4), 487–499.
- Wang, Y.-y., Sullivan, C. & Liu, J.** 2016. Taxonomic revision of *Eoalligator* (Crocodylia, Brevirostres) and the paleogeographic origins of the Chinese alligatoroids. *PeerJ*, **4**, e2356, 1–43.
- Wang, Y., Li, Q., Bai, B., Jin, X., Mao, F. & Meng, J.** 2019. Paleogene integrative stratigraphy and timescale of China. *Science China Earth Sciences*, **62**(1), 287–309.
- Webb, G. J. W., Manolis, S. C. & Brien, M. L.** 2010. Saltwater Crocodile *Crocodylus porosus*. In: Manolis S. C. & Stevenson, C. (eds.). *Crocodiles. Status Survey and Conservation Action Plan*. Third Edition. Crocodile Specialist Group: Darwin. 99–113.
- Webb, G.J.W., Manolis, C., Brien, M.L., Balaguera-Reina, S.A. & Isberg, S.** 2021. *Crocodylus porosus*, Saltwater Crocodile. *The IUCN Red List of Threatened Species*. e.T5668A3047556, 1–35.
- Werneburg, I., Wilson, L. A. B., Parr, W. C. H. & Joyce, W. G.** 2015. Evolution of Neck Vertebral Shape and Neck Retraction at the Transition to Modern Turtles: an Integrated Geometric Morphometric Approach. *Systematic Biology*, **64**(2), 187–204.
- Whitaker, R.** 2007. The Gharial: Going Extinct Again. *Iguana*, **14**(1), 24–33.
- Whitaker, R., & Whitaker, N.** 2008. Who's got the biggest. *Crocodile Specialist Group Newsletter*, **27**(4), 26–30.
- Wiegmann, A. F. A.** 1835. Beitrage zur Zoologie gesammelt auf einer Reise um die Erde von Dr. F.J.F. Meyen. Siebente Abhandlung. Amphibien. *Nova Acta Physico-Medica Academia Caesarea Leopoldino-Carolina*, **17**, 185–268.
- Wilf, P.** 1997. When are leaves good thermometers? A new case for Leaf Margin Analysis. *Paleobiology*, **23**(3), 373–390.
- Willis, P. M. A.** 1997. Review of fossil crocodylians from Australasia. *Australian Zoologist*, **30**(3), 287–298.
- Willis, P. M. A. & Stilwell, J. D.** 2000. A probable piscivorous crocodile from Eocene deposits of McMurdo Sound, East Antarctica. *Antarctic Research Series*, **76**, 355–358.
- Willis, R. E.** 2009. Transthyretin gene (TTR) intron 1 elucidates crocodylian phylogenetic relationships. *Molecular Phylogenetics and Evolution*, **53**(3), 1049–1054.
- Wise, T. B. & Stayton, C. T.** 2017. Side-necked Versus Hidden-necked: A Comparison of Shell Morphology Between Pleurodiran and Cryptodiran Turtles. *Herpetologica*, **73**(1), 18–29.
- Wu, X.-C., Brinkman, D. B., & Russell, A. P.** 1996. A new alligator from the Upper Cretaceous of Canada and the relationship of early eusuchians. *Palaeontology*, **39**(2), 351–376.
- Wu, X.-C., Li, C. & Wang, Y.-Y.** 2018. Taxonomic reassessment and phylogenetic test of *Asiatosuchus nanlingensis* Young, 1964 and *Eoalligator chunyii* Young, 1964. *Vertebrata Palasiatica*, **56**(2), 137–146.
- Wu, X.-C., Wang, Y.-C., You, H.-L., Zhang, Y.-Q. & Yi, L.-P.** 2023. New brevirostrines (Crocodylia, Brevirostres) from the Upper Cretaceous of China. *Cretaceous Research*, **144**, 105450, 1–25.
- Wysocka, A.** 2009. Sedimentary environments of the Neogene basins associated with the Cao Bang – Tien Yen Fault, NE Vietnam. *Acta Geologica Polonica*, **59**(1), 45–69.

- Wysocka, A., Pha, P. D., Durska, E., Czarniecka, U., Filipek, A., Cuong, N. Q., Tuan, D. M. & Huyen, N. X.** 2018. New data on the continental deposits from the Cao Bang Basin (Cao Bang-Tien Yen Fault Zone, NE Vietnam) – biostratigraphy, provenance and facies pattern. *Acta Geologica Polonica*, **68**(4), 689–709.
- Wysocka, A., Pha, P. D., Durska, E., Czarniecka, U., Thang, D. V., Filipek, A., Cuong, N. Q., Tuan, D. M., Xuan Huyen, N., Tha, H. V. & Staniszewski, R.** 2020. The Na Duong Basin (North Vietnam): A key for understanding Paleogene basin evolution in relation to the left-lateral Cao Bang-Tien Yen Fault. *Journal of Asian Earth Sciences*, **195**, 104350, 1–20.
- Wysocka, A., van Tha, H., Czarniecka, U., Durska, E., Filipek, A., Pha, P. D., Cuong, N. Q., Zaszewski, D., Tuan, D. M., Thanh, N. T. & Baranowski, A.** 2022. The Hoanh Bo Trough—a landward keyhole to the syn-rift Late Eocene–Early Oligocene terrestrial succession of the northern Song Hong Basin (onshore north-east Vietnam). *Geological Journal*, **57**(10), 4216–4241.
- Yamakura, T., Hagihara, A., Sukardjo, S. & Ogawa, H.** 1986. Aboveground biomass of tropical rain forest stands in Indonesian Borneo. *Vegetatio*, **68**, 71–82.
- Yeh, H. K.** 1958. A new crocodile from Maoming, Kwangtung. *Vertebrata Palasiatica*, **2**(4), 237–242.
- Yeh, H. K.** 1962. Notes on two fossil trionychid turtles from Shantung and Chekiang. *Vertebrata Palasiatica*, **6**(4), 384–388.
- Yeh, H. K.** 1963. Fossil Turtles of China. *Palaeontologia Sinica*, **150**, 1–112.
- Yeh H. K.** 1965. New materials of fossil turtles of Inner Mongolia. *Vertebrata Palasiatica*, **9**, 47–69.
- Yonezawa, T., Segawa, T., Mori, H., Campos, P. F., Hongoh, Y., Endo, H., Akiyoshi, A., Kohno, N., Nishida, S., Wu, J., Jin, H., Adachi, J., Kishino, H., Kurokawa, K., Nogi, Y., Tanabe, H., Mukoyama, H., Yoshida, K., Rasoamiamanana, A., Yamagishi, S., Hayashi, Y., Yoshida, A., Koike, H., Akishinomiya, F., Willerslev, E. & Hasegawa, M.** 2017. Phylogenomics and Morphology of Extinct Paleognaths Reveal the Origin and Evolution of the Ratites. *Current Biology*, **27**(1), 68–77.
- Young, C. C.** 1964. New fossil crocodiles from China. *Vertebrata Palasiatica*, **8**(2), 189–208.
- Young, C. C.** 1982. A Cenozoic crocodile from Huaining, Anhui. *In: Young, C. C., Selected works of Yang Zhongjian. Beijing, Science Press*, 47–48.
- Young, C. C. & Chow, M. C.** 1953. New fossil reptiles from Szechuan, China. *Acta Scientia Sinica*, **2**, 216–229.
- Zelenkov, N. V.** 2021a. New Bird Taxa (Aves: Galliformes, Gruiformes) from the Early Eocene of Mongolia. *Paleontological Journal*, **55**(4), 438–446.
- Zelenkov, N. V.** 2021b. A revision of the Palaeocene–Eocene Mongolian Presbyornithidae (Aves: Anseriformes). *Paleontological Journal*, **55**(3), 323–330.
- Zelenkov, N. V. & Kurochkin, E. N.** 2015. Class Aves. *In: Kurochkin, E. N., Lopatin, A. V. & Zelenkov, N. V. (eds.) Fossil vertebrates of Russia and neighbouring countries. Fossil Reptiles and Birds. Part 2.* GEOS, Moscow, 86–290 [in Russian].
- Zhao, T., Mayr, G., Wang, M. & Wang, W.** 2015. A trogon-like arboreal bird from the early Eocene of China. *Alcheringa: An Australasian Journal of Palaeontology*, **39**(2), 287–294.

Appendix

First Paper

**A new alligatoroid from the Eocene of Vietnam highlights
an extinct Asian clade independent from extant *Alligator
sinensis***

**Massonne Tobias, Vasilyan Davit, Rabi Márton and Böhme
Madelaine**

PeerJ 7:e7562, 1–60, 2019

<http://dx.doi.org/10.7717/peerj.7562>

A new alligatoroid from the Eocene of Vietnam highlights an extinct Asian clade independent from extant *Alligator sinensis*

Tobias Massonne^{1,2}, Davit Vasilyan^{3,4}, Márton Rabi^{1,5,*} and Madelaine Böhme^{1,2,*}

¹ Department of Geosciences, Eberhard-Karls-Universität Tübingen, Tübingen, Germany

² Senckenberg Center for Human Evolution and Palaeoecology, Tuebingen, Germany

³ JURASSICA Museum, Porrentruy, Switzerland

⁴ Department of Geosciences, University of Fribourg, Fribourg, Switzerland

⁵ Central Natural Science Collections, Martin-Luther University Halle-Wittenberg, Halle (Saale), Germany

* shared last authors

ABSTRACT

During systematic paleontological surveys in the Na Duong Basin in North Vietnam between 2009 and 2012, well-preserved fossilized cranial and postcranial remains belonging to at least 29 individuals of a middle to late Eocene (late Bartonian to Priabonian age (39–35 Ma)) alligatoroid were collected. Comparative anatomical study of the material warrants the diagnosis of a new taxon, *Orientalosuchus naduongensis* gen. et sp. nov. The combined presence of an enlarged fifth maxillary tooth, prominent preorbital ridges, a large supraoccipital exposure on the skull table, a palatine-pterygoid suture anterior to the posterior end of the suborbital fenestra, and a pterygoid forming a neck surrounding the choana is unique to this species. Unlike previous phylogenies, our parsimony analysis recovers a monophyletic Late Cretaceous to Paleogene East to Southeastern Asian alligatoroid group, here named Orientalosuchina. The group includes *Orientalosuchus naduongensis*, *Krabisuchus siamogallicus*, *Eoalligator chunyii*, *Jiangxisuchus nankangensis* and *Protoalligator huiningensis*, all of them sharing a medial shifted quadrate foramen aerum. The recognition of this clade indicates at least two separate dispersal events from North America to Asia: one during the Late Cretaceous by Orientalosuchina and one by the ancestor of *Alligator sinensis* during the Paleogene or Neogene, the timing of which is poorly constrained.

Submitted 7 February 2019

Accepted 27 July 2019

Published 5 November 2019

Corresponding author

Tobias Massonne,

tobias.massonne@uni-tuebingen.de

Academic editor

Hans-Dieter Sues

Additional Information and
Declarations can be found on
page 54

DOI 10.7717/peerj.7562

© Copyright

2019 Massonne et al.

Distributed under

Creative Commons CC-BY 4.0

OPEN ACCESS

Subjects Evolutionary Studies, Paleontology, Taxonomy, Zoology

Keywords Eocene, Crocodylia, Asia, Na Duong, Phylogeny, Vietnam, *Alligator*

INTRODUCTION

Alligatoroidea is a monophyletic group of Crocodylia that includes extant North American/Asian *Alligator* spp. and Central to Middle American caimans, as well as many fossil taxa (*Brochu, 1999, 2004; Scheyer et al., 2013*) and is defined as a stem-based group including living alligators and caimans and all taxa closer to them than to *Crocodylus* or *Gavialis* (*Brochu, 1999*). The fossil record points to the Late Cretaceous of North America as the time and place of origin, with subsequent dispersals to South

America, Europe, and Asia, but the timing, mode, and the number of dispersals are poorly constrained (Brochu, 1999, 2004, 2010; Bona & Barrios, 2015). Europe may have been colonized multiple times by alligatoroids (Brochu, 2004), but the phylogeny is in a state of flux and key European taxa are in need of re-description.

Alligatoroids are now extinct in Europe, but they still survive in Asia with the Chinese alligator, *Alligator sinensis* Fauvel, 1879. Until now, no fossils from the Paleogene were placed on the stem-lineage of *Alligator sinensis*. Previous studies found the Paleogene East to Southeastern Asian alligatoroids *Krabisuchus siamogallicus* Martin & Lauprasert, 2010 from Thailand, *Protoalligator huiningensis* Young, 1982, *Eoalligator chunyii* Young, 1964 and the “Maoming alligatoroid” from China phylogenetically outside *Alligator* and mostly unresolved relative to other alligatoroids (Martin & Lauprasert, 2010; Skutschas et al., 2014; Wang, Sullivan & Liu, 2016; Wu, Li & Wang, 2018). Recently, *Eoalligator chunyii* was recovered as a basal member of Crocodylia together with *Jiangxisuchus nankangensis* (Li, Wu & Rufolo, 2019). The oldest record of the *Alligator sinensis* lineage has been reported from the Pliocene of Japan (Iijima, Takahashi & Kobayashi, 2016). The early Miocene *Alligator luicus* from China (Li & Wang, 1987; Brochu, 1999) was never included in a phylogenetic analysis and its relationships with extant *Alligator* species therefore remain uncertain. The ancestor of *Alligator sinensis* is nevertheless expected to be present in the Paleogene of Eastern Asia, since recent molecular clock analyses estimate its divergence from North American *Alligator mississippiensis* (Daudin, 1802) in the Paleocene or Eocene—during times of favorable climatic conditions for crocodylians crossing the Bering Strait (Wu et al., 2003; Roos, Aggarwal & Janke, 2007; Oaks, 2011). The arrival of *Alligator sinensis* from Europe is not supported by previous phylogenies, although European taxa are in need of revision. On the other hand, a post-Eocene dispersal via Beringia would have been problematic because of the low tolerance for cool climate of crocodylians (Markwick, 1998). *Alligator sinensis* therefore represents a biogeographic enigma, so the East and Southeastern Asian Paleogene fossil record is critical for resolving this issue. However, all previously described fossils from this continent are highly incomplete, which hinders a rigorous test of phylogenetic relationships.

Most of the Paleogene fossil record of Crocodylia comes from North America and Europe, whereas the Asian record is still insignificant in comparison: only ca. 10% of the Paleogene sampled taxa of phylogenies are Asian (Martin & Lauprasert, 2010; Brochu, 2012; Skutschas et al., 2014; Jouve, 2016; Wang, Sullivan & Liu, 2016; Shan et al., 2017). Moreover, with one exception (Shan et al., 2017), these taxa are only known from fragmentary or deformed fossils.

During systematic surveys in the Na Duong Basin in Northern Vietnam between 2009 and 2012, 29 well preserved individuals of an Eocene alligatoroid were collected and subsequently prepared by the Geological-Paleontological Institute of the Eberhard Karls University of Tübingen (GPIT) (Böhme et al., 2012).

In this study, we provide a complete description of this material, which represents the best preserved alligatoroid from the Paleogene of Asia. We demonstrate that Cretaceous-Eocene East to Southeastern Asian alligatoroids form a monophyletic group, here named

Orientalosuchina and that Asia was colonized by alligatoroids at least two times independently.

GEOLOGICAL SETTINGS

The Na Duong Basin is located in northern Vietnam near the border with China (Fig. 1). It represents one of the few areas in East and Southeastern Asia with continental sediments of Eocene to Oligocene age (Böhme *et al.*, 2012). The pull-apart basin is part of the Cao Bang—Tien Yen fault system and covers an area of around 45 square kilometers. The middle to upper Eocene (late Bartonian–Priabonian (39–35 Ma)) Na Duong Formation is 240 m thick; its upper 140 m are part of the Na Duong open cast coal mine. The alligatoroid remains in this work were found within the transition zone between the coaly shale of the main seam and the underlying dark-brown clay-stone (layer 80), together with many other vertebrate fossils (Böhme *et al.*, 2012).

The fossiliferous layer 80 was a tropic to warm-subtropical swamp ecosystem with aquatic and terrestrial environments. During sedimentation, the area was in a transitional stage from shallow ponds to an anoxic lake. Further, tomistomine and *Asiatosuchus*-like crocodiles, as well as many fish taxa and two different turtle species occurred sympatrically with the herein described alligatoroid (Böhme *et al.*, 2012; Garbin, Böhme & Joyce, 2019).

MATERIALS AND METHODS

We expanded the taxon-character dataset of Brochu & Storrs (2012) (see Appendix), which was the most recent global Crocodylia matrix available during the start of this study. The expanded dataset includes 202 characters; 189 characters are from Brochu & Storrs (2012), two characters from Wang, Sullivan & Liu (2016), one character from Cossette & Brochu (2018), one character from Jouve (2004), and nine new characters from the present study. We further modified characters (51) and (91) of Brochu & Storrs (2012), (190) of Wang, Sullivan & Liu (2016) and (174) of Jouve *et al.* (2008) (195 in this study). In total, we included 114 taxa: in addition to the 103 taxa added from Narváez *et al.* (2015), *Globidentosuchus brachyrostris* Scheyer *et al.*, 2013, *Culebrasuchus mesoamericanus* Hastings *et al.*, 2013 and *Centenariosuchus gilmorei* Hastings *et al.*, 2013 from Hastings, Reisser & Scheyer, 2016, the Maoming alligatoroid, *K. siamogallicus*, *Protoalligator huiningensis*, *Eoalligator chunyii* and *Asiatosuchus nanlingensis* Young, 1964 from Wang, Sullivan & Liu (2016), *Bottosaurus harlani* from Cossette & Brochu (2018), *J. nankangensis* from Li, Wu & Ruffolo (2019) and the herein described *Orientalosuchus naduongensis*. For *Orientalosuchus naduongensis*, we could score 118 characters (the complete data set is found in File S1). Character scorings were modified for 32 taxa in total (a complete list of changes together with the specimen list can be found in File S2). We provided the complete character list in File S3.

We conducted a maximum parsimony analysis in TNT 1.5 standard version updated on November 20, 2018 (Goloboff, Farris & Nixon, 2008). We treated the multistate characters as unordered and equally weighted; set the maximum of trees to 10,000, and the tree

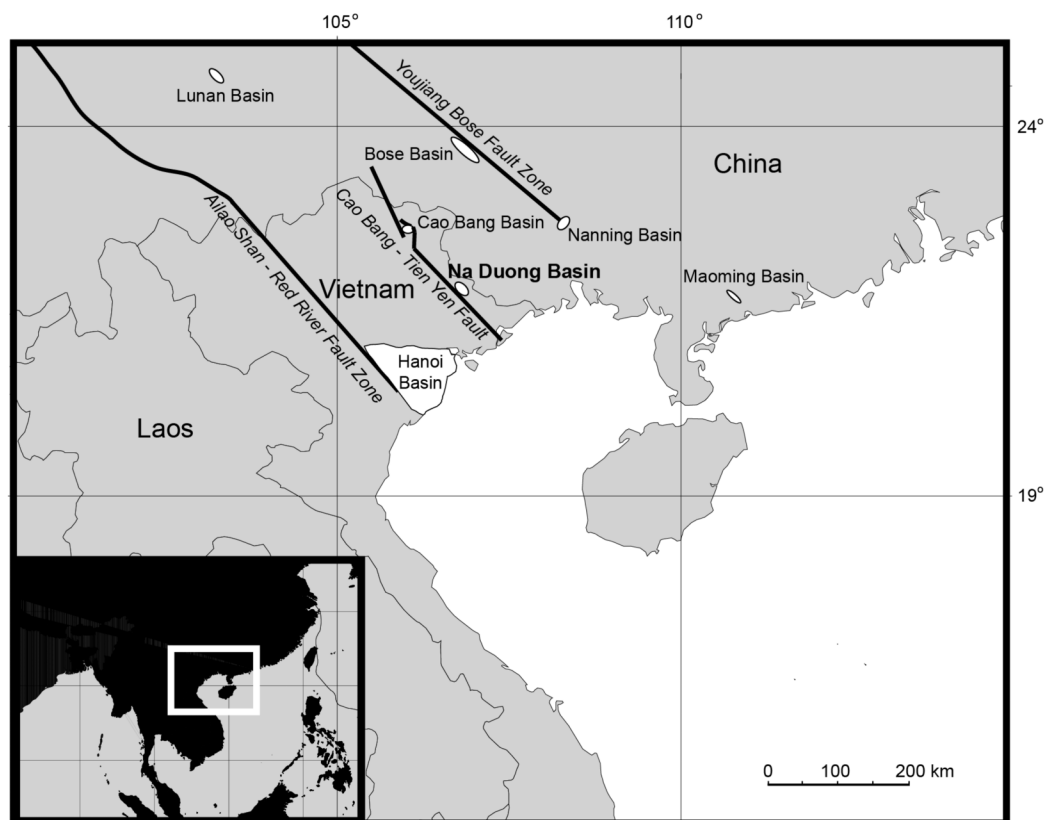


Figure 1 Map of northern southeastern Asia, showing the Na Duong Basin in northeastern Vietnam near the border with China (Böhme et al., 2012). [Full-size !\[\]\(b345a1c4255362eec3746050dd71ccac_img.jpg\) DOI: 10.7717/peerj.7562/fig-1](https://doi.org/10.7717/peerj.7562/fig-1)

replications to 1,000. For swapping algorithm, we used tree bisection reconnection with 10 trees saved per replication.

A first run of heuristic search tree-bisection-reconnection, failed to find all the most parsimonious trees (MPT) and, therefore, the heuristic search was repeated until the MPTs were found 50 times during each replicate (using the command “xmult = hits 50;”). The trees retained in the memory were exposed to a second round of tree-bisection-reconnection.

The electronic version of this article in portable document format will represent a published work according to the International Commission on Zoological Nomenclature (ICZN), and hence the new names contained in the electronic version are effectively published under that Code from the electronic edition alone. This published work and the nomenclatural acts it contains have been registered in ZooBank, the online registration system for the ICZN. The ZooBank Life Science Identifiers (LSIDs) can be resolved and the associated information viewed through any standard web browser by appending the LSID to the prefix <http://zoobank.org/>. The LSID for this publication is: urn:lsid:zoobank.org:pub:08B6F167-AAC7-4184-97BA-B7467D4F036B. The online version of this work is archived and available from the following digital repositories: PeerJ, PubMed Central and CLOCKSS.

SYSTEMATIC PALEONTOLOGY

Eusuchia Huxley, 1875 sensu Brochu, 2003

Crocodylia Gmelin, 1789 sensu Benton & Clark, 1988

Alligatoroidea Gray, 1844 sensu Brochu, 2003

Globidonta Brochu, 1999

Alligatoridae Cuvier, 1807 sensu Brochu, 2003

Orientalosuchina new clade name

***Orientalosuchus* gen. nov.**

Orientalosuchus naduongensis sp. nov.

(Fig. 2)

Orientalosuchus

Etymology: The name *Orientalosuchus* refers to the Latin word “oriens” for “east” and “suchus” the old Greek word “soukhos” for “crocodile.”

Orientalosuchus naduongensis

Etymology: The species name “*naduongensis*” refers to the Na Duong coal mine type locality in northeastern Vietnam.

Diagnosis: *Orientalosuchus naduongensis* is diagnosed by the combination of the following characters: notch between the premaxilla and maxilla; dominant maxillary ridge alongside the nasal; the fifth maxillary tooth is the largest maxillary tooth; anterior tip of frontal is acute and projects between the nasal bones; small supratemporal fenestra; large supraoccipital exposure preventing the parietal from reaching the posterior skull table in adults; quadrate foramen aerum lies on the dorsomedial angle of the quadrate; large suborbital fenestrae reaching anteriorly the level of the seventh to eighth maxillary tooth; maxilla-palatine suture forms an obtuse angle and not reaching beyond the anterior end of the suborbital fenestra; palatine-pterygoid suture lies anterior to the posterior end of the suborbital fenestra; pterygoid forms a neck surrounding the choana; dentary tooth row with only 16 teeth; laterally compressed posterior teeth; very small external mandibular fenestra; foramen aerum at the lingual margin of the retroarticular process; axis with a hypapophysis that is located near the center of the centrum; coracoid with a very large glenoid; iliac blade with a rectangular posterior outline and a dorsal indentation; dorsal osteoderms with no or only modest ridge.

Differential diagnosis: *Orientalosuchus naduongensis* differs from *Krabisuchus siamogallicus* in having dorsal osteoderms with no or only a modest ridge; an inward-pushed pterygoid around the choana and a neck surrounding the aperture, while the pterygoid surface is flush with the choanal margin in *K. siamogallicus*; and a very large supraoccipital exposure, preventing the parietal from reaching the posterior edge of the skull.

Orientalosuchus naduongensis differs from *Eoalligator chunyii* in having dorsal osteoderms with no or only a modest ridge; very prominent preorbital ridges; squamosals, that do not extend ventrolaterally to lateral extent of paroccipital process; a very large

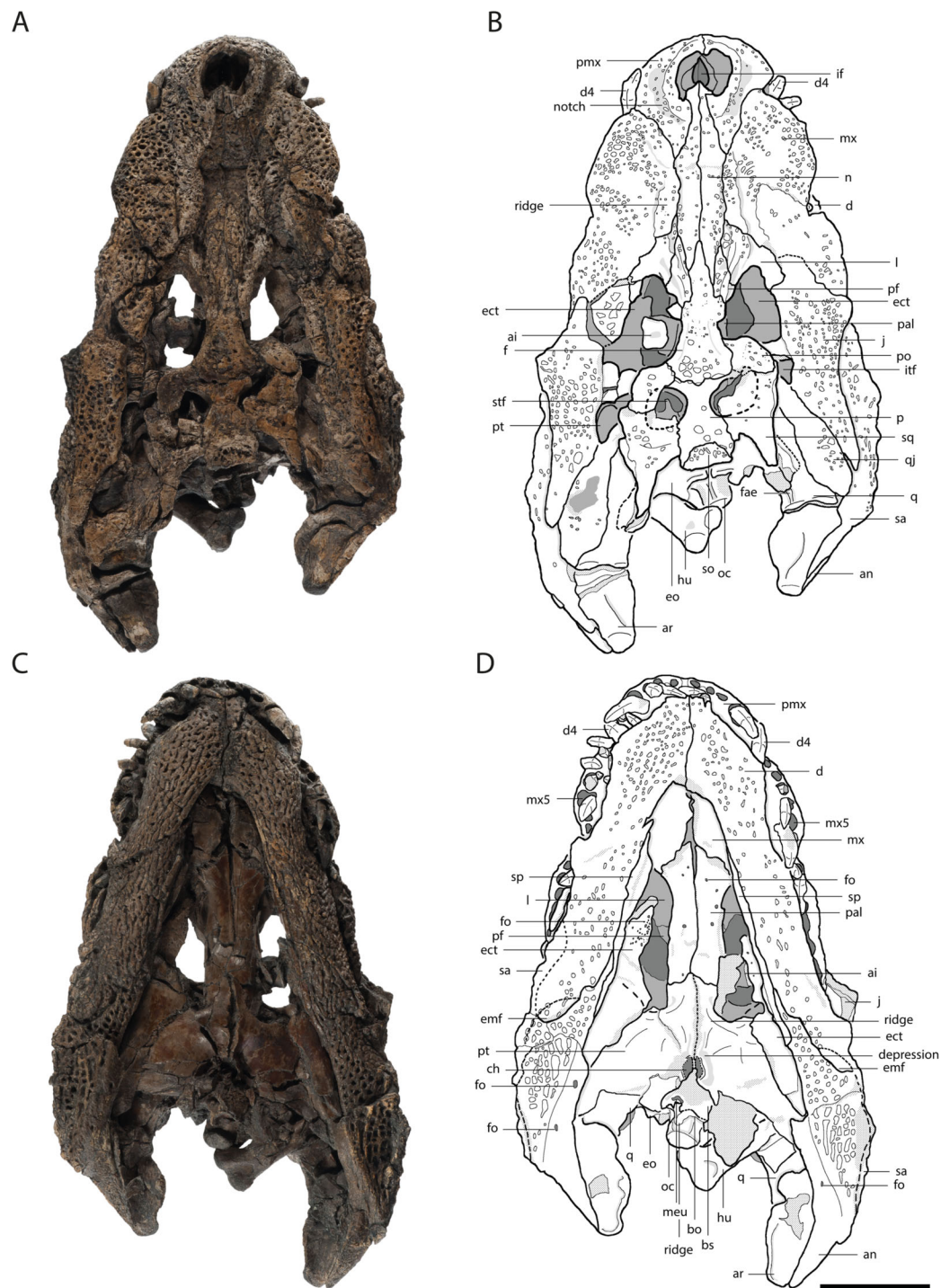


Figure 2 Skull of *Orientalosuchus naduongensis* (GPIT/RE/09761) (holotype), Na Duong Formation, upper Eocene, Vietnam. Skull in dorsal (A and B) and ventral (C and D) view. Abbreviations: ai, atlas intercentrum; an, angular; ar, articular; bo, basioccipital; bs, basisphenoid; ch, choana; d, dentary; d4, dentary tooth 4; emf, external mandibular fenestra; eo, exoccipital; ect, ectopterygoid; f, frontal; fo, foramen; fae, foramen aerum; hu, humerus; if, incisive foramen; itf, infratemporal fenestra; j, jugal; l, lacrimal; mx, maxilla; mx5, maxilla tooth 5; n, nasal; oc, occipital condylus; p, parietal; pf, prefrontal; pal, palatine; pmx, premaxilla; po, postorbital; pt, pterygoid; q, quadratum; qj, quadratojugal; sa, surangular; so, supraoccipital; sp, splenial; sq, squamosal; stf, supratemporal fenestra. Scale = 5 cm. [Full-size !\[\]\(fcc3264021d438d9732560e78099f674_img.jpg\) DOI: 10.7717/peerj.7562/fig-2](https://doi.org/10.7717/peerj.7562/fig-2)

supraoccipital exposure, preventing the parietal from reaching the posterior edge of the skull; a smooth dorsal surface of the surangular, whereas *Eoalligator chunyii* has a large sulcus next to the anterior half of the glenoid fossa; and an intersupratemporal bar similarly broad as the supratemporal fenestra, while the bar is strongly constricted in *Eoalligator chunyii*.

Orientalosuchus naduongensis differs from *Jiangxisuchus nankangensis* in having a deeply curved dentary; a small incisive foramen; prominent preorbital ridges; a palatine-pterygoid suture nearly at the posterior angle of suborbital fenestra; a frontoparietal suture entirely on the skull table (the suture modestly enters the supratemporal fenestra in *J. nankangensis*); a very large supraoccipital exposure preventing the parietal from reaching the posterior edge of the skull; anterior maxillary teeth with vertical ridges on their lateral surface; and an intersupratemporal bar that is similarly broad as the supratemporal fenestra (the bar is constricted in *J. nankangensis*).

Orientalosuchus naduongensis differs from *Protoalligator huiningensis* in having a deeply curved dentary; laterally compressed posterior teeth; a deep notch lateral to the naris; an occlusion pit between the seventh and eighth maxillary teeth with all other dentary teeth occluding lingually, while in *Protoalligator huiningensis* all dentary teeth are lingual to maxillary teeth; very prominent preorbital ridges; and maxillary teeth with vertical ridges on their lateral surface.

Holotype: GPIT/RE/09761; partial skeleton consisting of skull, lower jaws and incomplete postcranial skeleton (see [Table 1](#)).

Type locality and horizon: The fossils were recovered from layer 80 of the Na Duong coal mine in northern Vietnam (N 21°42.2', E 106°58.6'); Na Duong Formation, Eocene, late Bartonian to Priabonian age (39–35 Ma) ([Böhme et al., 2012](#)).

Referred material: A total of 29 individuals represented by incomplete skulls, skull fragments and associated postcranial material, Na Duong Formation, Na Duong coal mine, Vietnam (see a complete list of preserved specimens and their associated material is presented in [Table 1](#)).

Preservation: The material from Na Duong is mostly well preserved and nearly complete but all skulls are dorsoventrally flattened and many have deformed and crushed areas or weathered surfaces. The postcranial material is mostly disarticulated or fused together with the matrix. The majority of the bones are pyritized.

PHYLOGENETIC NOMENCLATURE

Orientalosuchina

Definition: Orientalosuchina refers to the most inclusive clade containing *Orientalosuchus naduongensis* gen. et sp. nov., *Krabisuchus siamogallicus* [Martin & Lauprasert, 2010](#), *Eoalligator chunyii* [Young, 1964](#), *Jiangxisuchus nankangensis* [Li, Wu & Ruffolo, 2019](#) and *Protoalligator huiningensis* [Young, 1982](#), but not *Brachychampsia montana* [Gilmore, 1911](#), *Stangerochampsia mccabei* [Wu, Brinkman & Russell, 1996](#), *Leidyosuchus canadensis* [Lambe, 1907](#), *Diplocynodon darwini* ([Ludwig, 1877](#)), *Bottosaurus harlani* [Von Meyer, 1832](#), or any species of recent Crocodylia.

Table 1 List of specimens of *Orientalosuchus naduongensis*, Na Duong Formation, upper Eocene, Vietnam.

Individual	Cranial material	Postcranial material
GPIT/RE/09761 (holotype) Fig. 2 and Figs. 11–20	Complete dorsoventrally flattened skull and lower jaw fused together	Atlas intercentrum; axis; seven cervical vertebrae; 10 dorsal vertebrae; one sacral vertebra; eight caudal vertebrae; two cervical ribs; four dorsal ribs; one scapula (right); one coracoid (right); two humeri; one radiale; four metacarpalia (?); seven manus phalanges (?); two ilia; one ischium (left); two femora; one tibia (left); one fibula (right); four claws; >50 osteoderms
GPIT/RE/09730 Fig. 3	Dorsoventrally flattened anterior skull part reaching slightly behind the orbita and the complete right lower jaw ramus	–
GPIT/RE/09729 Fig. 4	Well preserved dorsoventrally flattened posterior skull part reaching to the premaxilla on the right side	–
GPIT/RE/09728 Figs. 5–8	Crushed complete skull and broken but well preserved anterior lower jaw parts	–
GPIT/RE/09727 Fig. 9	Crushed complete skull and well preserved posterior lower jaw parts	Three cervical vertebrae; 11 dorsal vertebrae; six caudal vertebrae; two dorsal ribs; one scapula (left); one humerus (right); one radius (right); two ilia; two femora; two tibiae; two fibulae; >50 osteoderms
GPIT/RE/09762	Complete skull without the most anterior part, lower jaw fragments and a few further skull fragments	–
GPIT/RE/09763	Posterior skull part	–
GPIT/RE/09764	Posterior skull part	–
GPIT/RE/09765	Anterior skull part	–
GPIT/RE/09766	Posterior and lateral skull part	–
GPIT/RE/09767	Posterior and lateral skull part	One cervical vertebra
GPIT/RE/09768	Skull and lower jaw	–
GPIT/RE/09769 Fig. 6	Half skull	Vertebra + rib + osteoderms
GPIT/RE/09770	Anterolateral skull part	bone fragments
GPIT/RE/09771	Posterior and lateral skull parts	–
GPIT/RE/09772	Posterior skull part	–
GPIT/RE/09773	Posterior skull part with fused lower jaw	–
GPIT/RE/09774	Skull with fused lower jaw	–
GPIT/RE/09775	Skull and lower jaw with the anteriormost part missing	–
GPIT/RE/09776	Skull fragments and lower jaw	–
GPIT/RE/09777	Posterior skull part	–
GPIT/RE/09778	Premaxilla	One dorsal vertebra
GPIT/RE/09779	Skull fragments	–
GPIT/RE/09780	Single small skull fragment and lower jaw fragments	–
GPIT/RE/09781	Lower jaw	–
GPIT/RE/09782	Lower jaw ramus	–
GPIT/RE/09783	Lower jaw	Bone fragments
GPIT/RE/09784	Lower jaw fragment	Seven cervical vertebrae; eight dorsal vertebrae; five caudal vertebrae; one cervical rib; four dorsal ribs; one scapula (right); two ulnae; two ilia; two ischia; one pubis (left); two femora; two tibiae; two fibulae; three tarsalia; one astragalus (left); one calcaneus (left); five metatarsalia; 14 pedal phalanges; four claws; >50 osteoderms
GPIT/RE/09785	–	Fragments

Table 2 Cranial measurements of *Orientalosuchus naduongensis*, Na Duong Formation, upper Eocene, Vietnam.

	GPIT/RE/09731 (Holotype)	GPIT/RE/09728	GPIT/RE/09729	GPIT/RE/09730
Skull length (premaxilla-supraoccipital)	190.5	185.1*	?	?
Skull width (quadratojugal-quadratojugal)	127.1	135.8	82.6*	?
Preorbital length	104.5	101.8*	?	64.4
Skull table length	43.6	49.3	34.6	?
Skull table width	65.2*	65.9	46.2	49.8
External naris length	21.1	10.8*	12.8	10.1*
External naris width	22.5	24.2	10.2*	17.8*
Orbita length	41.1	42.6*	33.3	28.6
Orbita width	26.8*	27.5	17.3*	19.7
Supratemporal fenestra length	12.3*	19.4	13.6	?
Supratemporal fenestra width	13.7	15.4	8.7	?
Infratemporal fenestra length	11.4	19.2*	9.1	?
Infratemporal fenestra height	?	?	11.5*	9.0*
Suborbital fenestra length	63.7*	?	49.9	43.6
Suborbital fenestra width	?	?	17.6*	?
Width between orbits	15.8	15.9	10.3	10.3
Width between supratemporal fenestrae	12.1	11.8	11.9	?
Width between suborbital fenestrae	22.7	?	13.6*	17.4
Occipital condyle height	9.5	9.7*	?	?
Occipital condyle width	14.4	12.8*	9.3	?

Note:

All measurements in mm (*measurements on deformed sections).

DESCRIPTION

Cranial description

Measurements of the cranial material are presented in [Table 2](#). Unless otherwise stated, the description is based on the holotype (GPIT/RE/09761) ([Fig. 2](#)).

Premaxilla

The premaxilla in ventral view is best observable in GPIT/RE/09730 ([Fig. 3](#)). It has five teeth in total. Between the first and second tooth there is a large occlusion pit for the first dentary tooth. The teeth increase in size posteriorly. The first two teeth are very small with the third one nearly double their size. The fourth tooth is the largest one. The fifth tooth is again much smaller, but still larger than the first two.

The dorsal surface is best preserved in GPIT/RE/09761 ([Fig. 2](#)) and GPIT/RE/09730 ([Fig. 3](#)). It is ornamented with multiple small pits. The premaxilla surrounds the naris with a prominent anterolateral bulge, but it does not possess a crest. Lateral to this bulge, the premaxilla has a deep depression. The anterior margin of the naris has a short (roughly one third of the naris length) posteriorly reaching process formed by the premaxilla. The naris opening itself has a roughly square-shaped to round outline. The naris is dorsally oriented. The relatively small oval incisive foramen ([Fig. 3](#)) does not abut the tooth row.

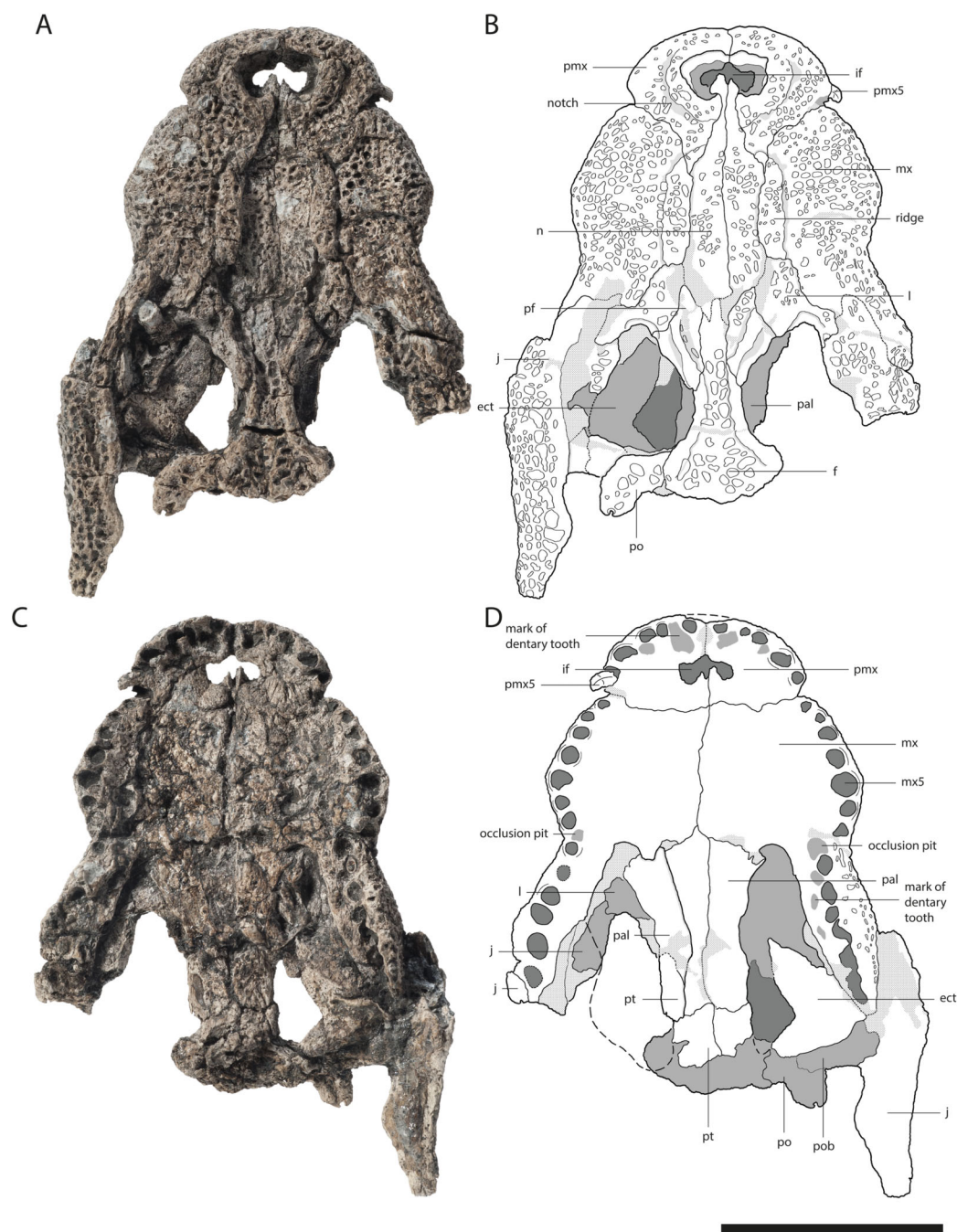


Figure 3 Skull of *Orientalosuchus naduongensis* (GPIT/RE/09730), Na Duong Formation, upper Eocene, Vietnam. Skull in dorsal (A and B) and ventral (C and D) view. Abbreviations: ect, ectopterygoid; f, frontal; if, incisive foramen; j, jugal; l, lacrimal; mx, maxilla; mx5, maxilla tooth 5; n, nasal; pal, palatine; pf, prefrontal; pmx, premaxilla; pmx5, premaxilla tooth 5; po, postorbital; pob, postorbital bar; pt, pterygoid. Scale = 5 cm. [Full-size !\[\]\(fcc3264021d438d9732560e78099f674_img.jpg\) DOI: 10.7717/peerj.7562/fig-3](https://doi.org/10.7717/peerj.7562/fig-3)

Laterally, the premaxilla-maxilla suture originates in a notch for the enlarged fourth dentary tooth and terminates in a long premaxillary process, which extends between the nasal and the maxilla up to the level of the fourth maxillary tooth. The lateral origin of

the suture lies shortly behind the level of the posterior part of the naris. The deep notch for receiving the fourth dentary tooth is present in all the large and presumably adult individuals; in the preserved juveniles, this region is damaged, making it impossible to document the condition early in ontogeny.

In ventral view, the premaxilla-maxilla suture is somewhat obscure, but seems to extend relatively straight lateromedially along the level of the notch (Fig. 3).

The premaxilla-nasal suture originates at the posterior end of the naris and flares lateromedially toward the posterior process of the dorsal plate of the premaxilla.

Maxilla

The maxillary tooth row comprises 13 teeth. The first maxillary tooth is about the same size as the fifth premaxillary tooth. They increase in size until reaching the fifth maxillary tooth, which is the largest one (Fig. 3). Between the seventh and eighth maxillary tooth there is a complete interfingering of a dentary tooth (most likely the 11th). The fourth dentary tooth fits in the notch between the premaxilla and maxilla. The posterior part of the dentary tooth row lies completely lingually to the maxillary tooth row, except for the presumably 11th dentary tooth, indicated by marks of the posterior dentary teeth lingual to the maxillary teeth, best visible in GPIT/RE/09730 (Fig. 3).

The lateral outline of the maxilla is considerably curved. In dorsal view, the bone flares laterally until reaching the level of the fifth maxillary tooth, which marks the most convex point of the snout. From there it tapers medially up to the level of the constriction between the seventh and eighth teeth and flares further posterior towards the suture with the jugal.

The dorsal surface of the maxilla is densely ornamented and has a strictly anteroposteriorly oriented prominent ridge alongside the nasal bone (best observable in GPIT/RE/09730 Fig. 3, GPIT/RE/09729 Fig. 4 and GPIT/RE/09728 Fig. 5). The dorsal surface of the ridge is rounded and becomes flatter anteriorly and terminates at the posteriormost part of the premaxillary process. Posteriorly, the ridge continues across the lacrimal and prefrontal until reaching the anteromedial part of the orbit. Laterally to the ridge, there is an elongated groove. The maxilla-premaxilla suture extends posteromedially until reaching the nasal. Slightly posteriorly to the suture, a shallow groove is present. The maxilla-nasal suture extends straight anteroposteriorly and is relatively short due to the long premaxilla process and the far anteriorly reaching lacrimal. The suture between the maxilla and lacrimal projects posterolaterally and then projects laterally in front of the orbit. The suture with the jugal is somewhat obscure, but seems to extend laterally until it becomes straight when it extends posteriorly (best observable in GPIT/RE/09729 Fig. 4).

In ventral view, the suture between the maxilla and palatine forms an obtuse angle with the anteriormost tip of the palatine situated at the level of the anterior end of the suborbital fenestra. The suture extends posterolaterally until reaching the anteromedial border of the fenestra. The small maxillary foramen for the palatine ramus of the cranial nerve V is visible in a single individual (GPIT/RE/09770) medial to the fifth tooth of the maxilla.

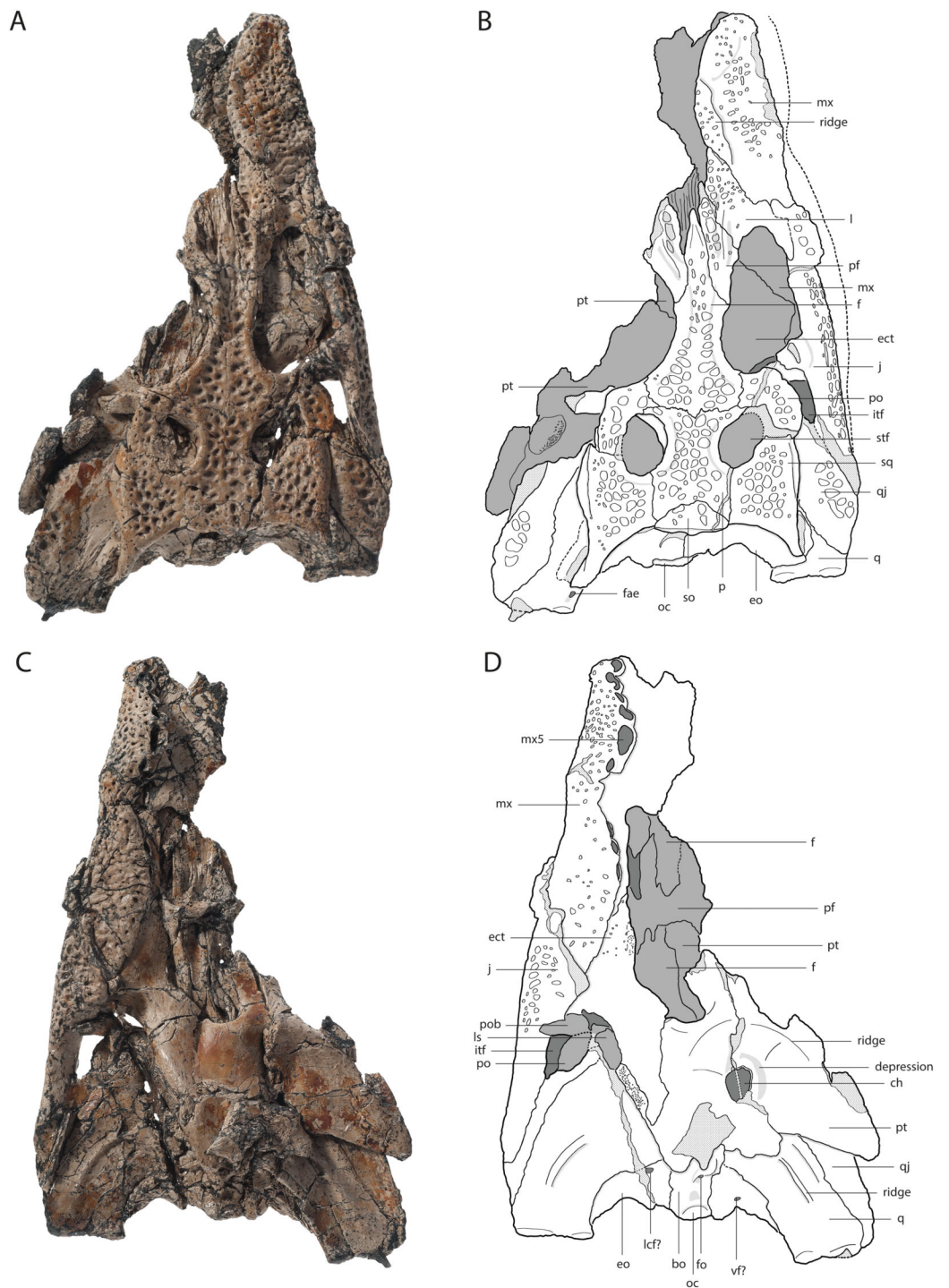


Figure 4 Skull of *Orientalosuchus naduongensis* (GPIT/RE/09729), Na Duong Formation, upper Eocene, Vietnam. Skull in dorsal (A and B) and ventral (C and D) view. Abbreviations: bo, basioccipital; ch, choana; ect, ectopterygoid; f, frontal; fae, foramen aerum; fo, foramen; itf, infratemporal fenestra; j, jugal; l, lacrimal; lcf, lateral carotid foramen; ls, laterosphenoid; mx, maxilla; mx5, maxilla tooth 5; oc, occipital condylus; p, parietal; pf, prefrontal; po, postorbital; pob, postorbital bar; pt, pterygoid; q, quadrate; qj, quadratojugal; so, supraoccipital; sq, squamosum; stf, supratemporal fenestra; vf, vagus foramen. Scale = 5 cm.

Full-size DOI: [10.7717/peerj.7562/fig-4](https://doi.org/10.7717/peerj.7562/fig-4)

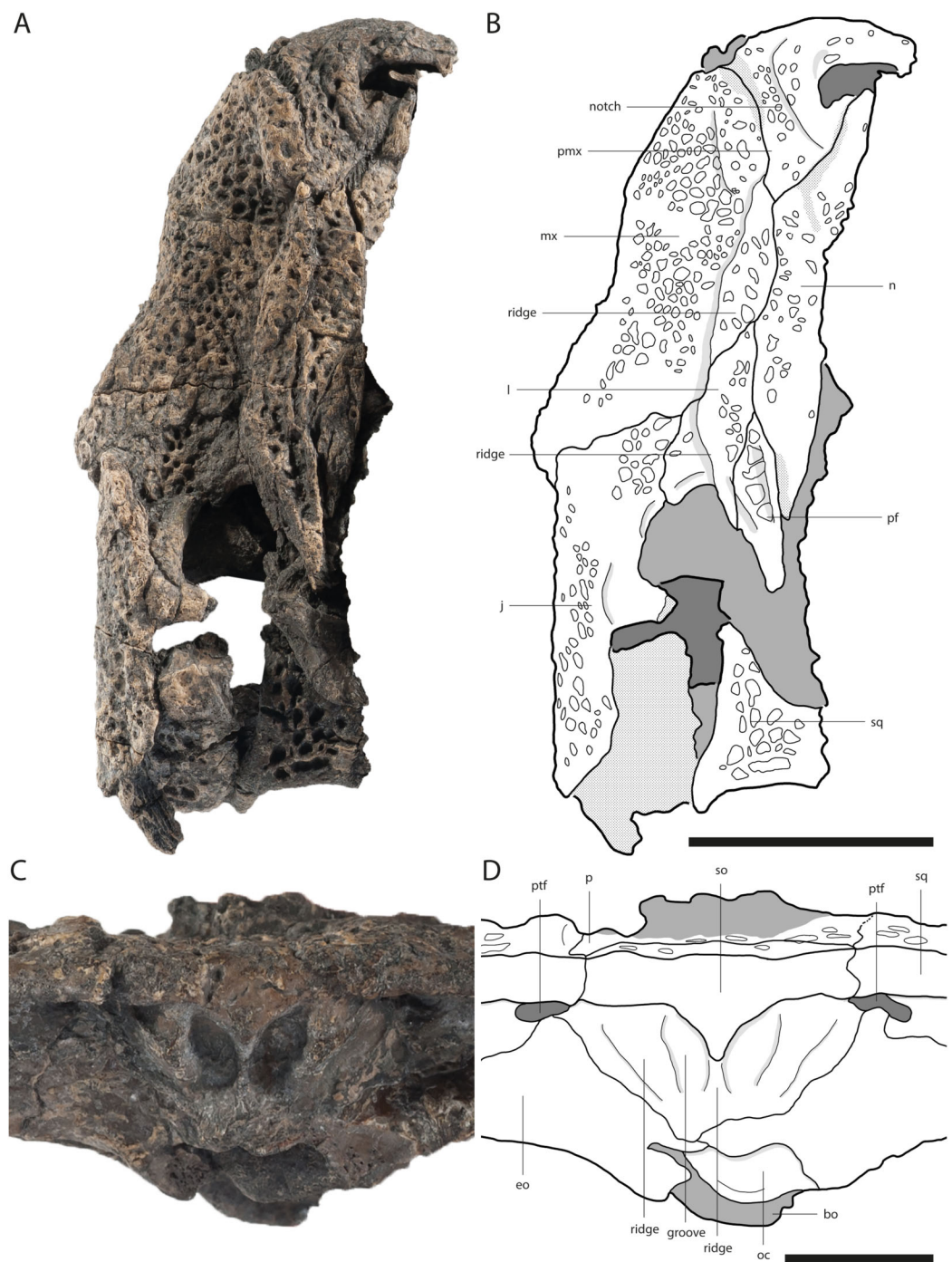


Figure 5 Skull of *Orientalosuchus naduongensis* (GPIT/RE/09728), Na Duong Formation, upper Eocene, Vietnam. Skull in dorsal (A and B) and occipital (C and D) view. Abbreviations: bo, basioccipital; eo, exoccipital; j, jugal; l, lacrimal; mx, maxilla; n, nasal; oc, occipital condylus; p, parietal; pf, prefrontal; pmx, premaxilla; ptf, posterior temporal fenestra; so, supraoccipital; sq, squamosum. Scale = 5 cm (A and B). Scale = 1 cm (C and D). [Full-size !\[\]\(1663bb69f307a960345edb0e712f8c02_img.jpg\) DOI: 10.7717/peerj.7562/fig-5](https://doi.org/10.7717/peerj.7562/fig-5)

The maxilla-ectopterygoid suture is shifted posterolaterally from the tooth row, preventing the ectopterygoid from contacting the alveoli (best seen in GPIT/RE/09730 Fig. 3).

Nasal

The elongated nasal is around four-times longer anteroposteriorly than lateromedially wide and similarly ornamented as the premaxilla and maxilla. The bone seems recessed compared to the paired maxillary ridges in GPIT/RE/09761 (Fig. 2) and GPIT/RE/09730 (Fig. 3), however, this is an artifact due to the postmortem deformation of the skull. GPIT/RE/09728 (Fig. 5) reveals, that the nasal was at the same height as the maxilla ridges, giving them a rim-like outline.

Anteriorly, the nasal projects into the naris with a short process for around one-third of the naris length, but it is unclear how complete this septum in the intact skull was. Therefore it remains unclear whether the naris was bisected. A complete or near-complete bisection would be consistent with the midline posterior process of the premaxilla but only better preserved specimens will help resolving this. The nasal-lacrimal suture is posteriorly oriented. The suture between the nasal and prefrontal slopes slightly posteromedially until reaching the frontal. Posteriorly, the nasal sends a long process between the frontal and prefrontal.

Lacrimal

The general outline of the lacrimal is roughly triangular with a concavity around the lacrimal-maxilla suture, leading to a relatively slender appearance of the bone, best visible in GPIT/RE/09730 (Fig. 3) and GPIT/RE/09729 (Fig. 4). The ornamentation is overall weak but it is pronounced near the lacrimal-nasal suture. The medial part of the lacrimal is strongly elevated as the maxilla ridge proceeds toward the orbit, which is best observable in GPIT/RE/09728 (Fig. 5).

The lacrimal-prefrontal suture originates at the anteromedial part of the orbit and extends anteromedially until reaching the nasal. Posteriorly, the lacrimal covers the anterior part of the orbit. The naso-lacrimal duct is visible on the posteromedial end of the bone near the suture with the prefrontal. The contact between the lacrimal and jugal projects nearly straight posteriorly from the anterior end of the orbit.

Prefrontal

The prefrontal is roughly wedge-shaped. Its central region is highly elevated due to the posteriorly projecting ridge, which extends roughly to the posterior part of the bone. Medially to the ridge, the prefrontal has an anteroposterior-oriented row of deep pits, especially visible in GPIT/RE/09729 (Fig. 4) and GPIT/RE/09728 (Fig. 5). The suture between the prefrontal and frontal extends anteroposteriorly and is relatively short due to the far posteriorly reaching nasal.

Frontal

The frontal is roughly wedge-shaped with an elongated anterior process projecting between the two nasal bones. It forms the dorsomedial border of the orbit. The border itself is nearly flush with the orbital margin (GPIT/RE/09729 Fig. 4) or only very slightly upturned (GPIT/RE/09730 Fig. 3). The orbit is nearly oval and slightly constricted anteromedially.

The anterior region of the frontal has nearly no ornamentation, whereas large pits are present between the orbits posteriorly. Between the orbits, the pits are roughly aligned in a pair of rows and dissolve in a field of large pits posteriorly (best observable in GPIT/RE/09729 [Fig. 4](#)).

The suture with the parietal is oriented entirely on the skull table and has a small posteriorly reaching medial process, best visible in GPIT/RE/09761 ([Fig. 2](#)) and GPIT/RE/09729 ([Fig. 4](#)). The suture with the postorbital originates near the posteromedial border of the orbit and slopes afterwards very slightly posteromedially until reaching the parietal.

Postorbital

The bone is best observable in GPIT/RE/09729 ([Fig. 4](#)). It is nearly boomerang-shaped and forms the anterolateral part of the skull table. The ornamentation is roughly arranged in a single line in the center of the bone and is composed of relatively large pits. The anterior part of the postorbital forms the posterior margin of the orbit, whereas its posterior region forms the anterolateral margin of the supratemporal fenestra. The slender postorbital bar is inset from the skull table and shapes the anterior part of the nearly triangular infratemporal fenestra.

The postorbital-parietal suture originates at the anteriormost point of the supratemporal fenestra and extends anteriorly only for a very short section until projecting straight medially and reaching the frontal. The suture between the postorbital and squamosal begins roughly at the level of the last third to the mid point of the supratemporal fenestra and projects laterally, until reaching the skull table and then it becomes obscure. The suture between the postorbital and jugal on the postorbital bar cannot be clearly followed.

Parietal

The parietal is best observable in GPIT/RE/09729 ([Fig. 4](#)). It is roughly rectangular and densely ornamented with deep pits. It forms the anteromedial and medial walls of the supratemporal fenestra. The supratemporal fenestrae are oval and open. They are relatively small and located far away from the posterior border of the skull table, leading to a very long parietal-squamosal suture, which originates at the posteromedial margin of the supratemporal fenestra and projects straight toward the posterior edge of the skull. Posteriorly, the parietal does not reach the skull table in adults because of the large trapezoid supraoccipital.

Squamosal

The squamosal forms the posterolateral margin of the skull table and the posterolateral margin of the supratemporal fenestra and is best observable in GPIT/RE/09729 ([Fig. 4](#)). Its surface is richly ornamented with deep pits. The dorsal and ventral rims of the squamosal groove for the external ear valve musculature are parallel. Due to the dorsoventral crushing of all individuals, the otic aperture is not preserved.

Posterolaterally, the squamosal has an elongated process projecting dorsally towards the paroccipital process. The most posterolateral part is not well preserved, but the squamosal does extend ventrolaterally to the lateral extent of the paroccipital process. The suture

between the squamosal and exoccipital origins ventrolaterally from the posttemporal fenestra and extends ventrolaterally. Due to the crushing, the suture between the squamosal and quadrate is obscure.

Jugal

The jugal is best observable in GPIT/RE/09761 (Fig. 2). It covers the lateral part of the skull contacting the maxilla and lacrimal anteriorly, the quadratojugal posteriorly and the postorbital on the postorbital bar dorsomedially. Its posterodorsal surface is highly ornamented with larger pits (GPIT/RE/09730 Fig. 3).

Medially, the jugal forms the ventrolateral border of the orbit and infratemporal fenestra. The border with the orbit is nearly straight, only curving slightly laterally, whereas at the border with the infratemporal fenestra, the jugal seems slightly more concave in outline. The postorbital bar is not flush with the rest of the jugal, but inserted from it medially. At the height of the postorbital bar, the posteroventral part of the jugal is strongly concave.

The jugal forms a straight suture with the quadratojugal bone, which slopes posterolaterally. The suture seems to originate from the posterolateral corner of the infratemporal fenestra (Figs. 2 and 4), but the preservation is insufficient to state this with confidence.

Quadratojugal

The quadratojugal surface is mainly smooth, but ornamented with a few large pits near the suture with the jugal.

The bone forms the posterolateral part of the skull and the posterior border of the infratemporal fenestra. The border is smooth and does not possess a spine. The quadratojugal seems to cover the whole border preventing the quadrate from reaching the postorbital, as seen in GPIT/RE/09761 (Fig. 2) and GPIT/RE/09729 (Fig. 4). Posteromedially, the bone is very broad and rounded. Posterolaterally, it nearly reaches the most posterior part of the skull, only slightly anterior to the quadrate.

Quadrate

The condyles lay on a horizontal axis, which is slightly inclined ventromedially with the lateral condyle larger than the medial one. The medial condyle bears a notch for the foramen aerum on its dorsomedial border. The relatively small foramen aerum is visible in GPIT/RE/09761 (Fig. 2) GPIT/RE/09729 (Fig. 4) and GPIT/RE/09728 and lies on the dorsomedial surface of the medial condyle. The opening of the cranioquadrate canal and the otic area are crushed. On the ventral surface of the bone, a prominent crest of the posterior mandibular abductor muscle is visible.

Palatine

The palatine shapes the most part of the interfenestral bridge between the suborbital fenestrae. Its surface is smooth, but bears many small foramina, especially in the anterolateral region (GPIT/RE/09761 Fig. 2). Anteriorly, the palatine is fan-shaped, but does not produce a shelf into the suborbital fenestra.

Anteriorly, the palatine does not reach at all, or protrudes only slightly beyond, the suborbital fenestra and contacts the maxilla with an obtuse V-shaped suture (GPIT/RE/09761 Fig. 2, GPIT/RE/09730 Fig. 3 and GPIT/RE/09769 Fig. 6). The suture with the pterygoid lies in front of the posterior end of the suborbital fenestra and is nearly straight lateromedially, except for a small midline process from the pterygoid projecting into the palatine (GPIT/RE/09761 Fig. 2).

The suborbital fenestrae are anteroposteriorly very large, reaching anteriorly the level of the inline occlusion between the seventh and eighth maxillary teeth (GPIT/RE/09730 Fig. 3). Their medial border is anteroposteriorly nearly straight, whereas the lateral border is slightly constricted due to the ectopterygoid reaching into the fenestra. The posterior border of the fenestra is smooth without a notch.

Pterygoid

The pterygoid is preserved in GPIT/RE/09761 (Fig. 2) and GPIT/RE/09729 (Fig. 4). It forms the posterior and posteromedial borders of the suborbital fenestra and contacts the palatine anterior to the posterior end of the fenestra. Dorsally, the pterygoid extends further anteriorly along the suborbital bridge and reaches the level of the prefrontal pillar (Fig. 4). Posteriorly, it is lateromedially straight, except for a very prominent pair of the posterior pterygoid processes. Laterally, it contacts the ectopterygoid with a posterolateral projecting suture. Although the anterior part of the suture is not optimally preserved, a flexure seems to be absent.

The pterygoid surface is uneven. In the medial region, posterior to the suborbital fenestra there is a prominent bulge, which transforms into a posterolaterally and a posteromedially projecting ridge. The posterolateral ridge flattens shortly after, whereas the posteromedial ridge projects caudally until reaching the choana opening. The choana itself is not entirely preserved, but its rough outline is still visible. Its orientation cannot be determined due to dorsoventral crushing, although it seems to be anteroventrally oriented in a juvenile individual (GPIT/RE/09772). A septum seems present at least anteriorly as indicated in a CT-scan of GPIT/RE/09761, but it is unclear if it projects out of the choana or remains recessed within. In adult individuals, the posterolateral margin of the choana is smooth. In the juvenile GPIT/RE/09772, the posterolateral margin seems more concave (notched), but this could be a crushing artifact.

Anterolateral to the choana, the pterygoid surface is pushed inward and forms a thin neck surrounding the choana opening in GPIT/RE/09761 (Fig. 2) and GPIT/RE/09728 (Fig. 6). Between the posterior border of the choana and the suture with the basisphenoid, the pterygoid has a shallow medial ridge (GPIT/RE/09728 Fig. 7).

Ectopterygoid

The ectopterygoid forms the posterolateral border of the suborbital fenestra. Anteromedially, the bone tapers into an acute tip and expands posteriorly, forming a small medial shelf projecting into the suborbital fenestra. Posteromedially to the suborbital fenestra, the ectopterygoid contacts the pterygoid and forms a posterolaterally projecting process that does not reach as far posteriorly as the pterygoid. The ectopterygoid

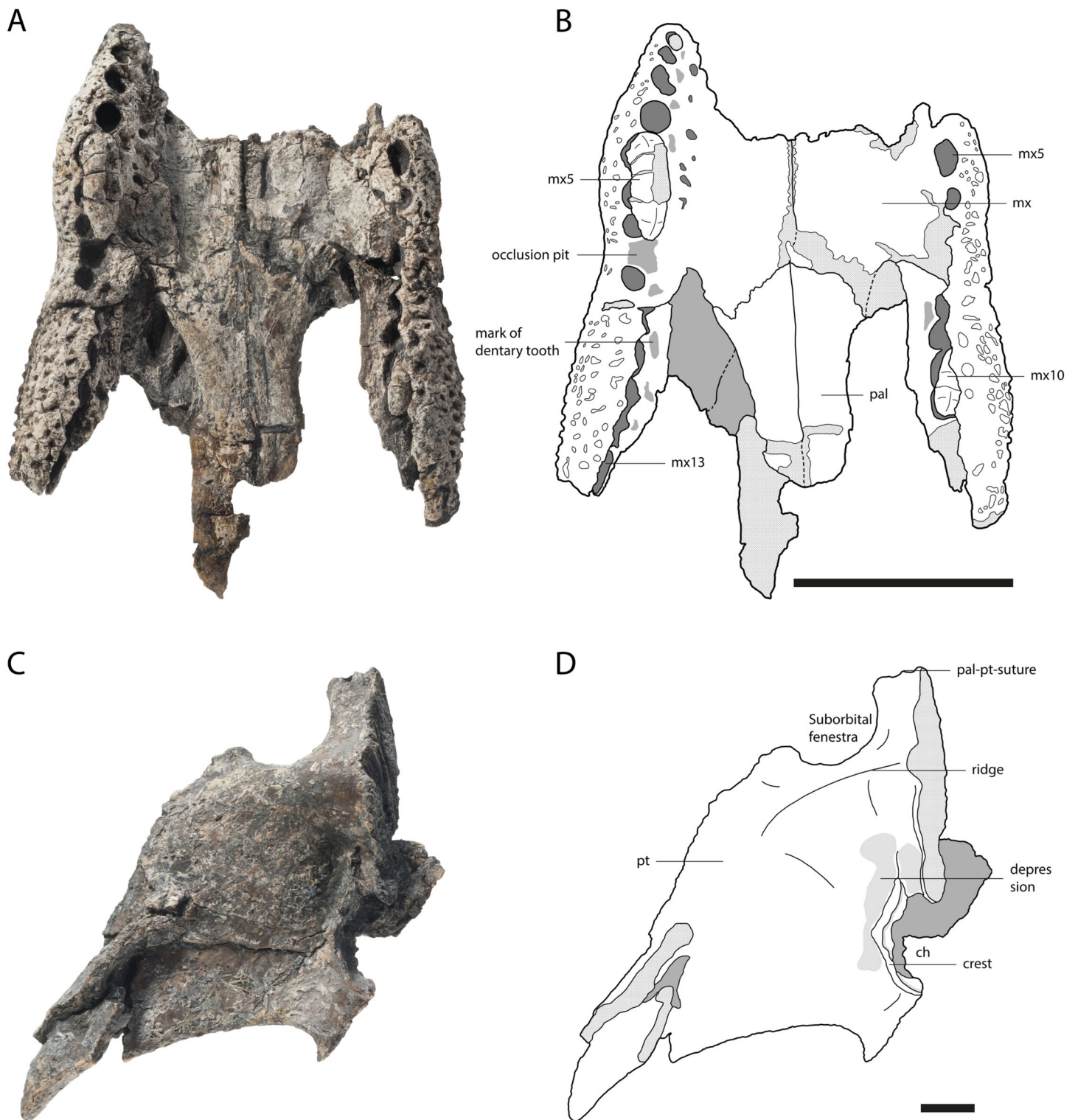


Figure 6 Partial palate (GPIT/RE/09769) and pterygoid (GPIT/RE/09728) of *Orientalosuchus naduongensi* Na Duong Formation, upper Eocene, Vietnam. Skull (A and B) and pterygoid (C and D) in ventral view. Abbreviations: ch, choana; mx, maxilla; mx5, maxilla tooth 5; mx10, maxilla tooth 10; mx13, maxilla tooth 13; pal, palatine; pt, pterygoid. Scale = 5 cm (A and B). Scale = 1 cm (C and D).

Full-size  DOI: [10.7717/peerj.7562/fig-6](https://doi.org/10.7717/peerj.7562/fig-6)

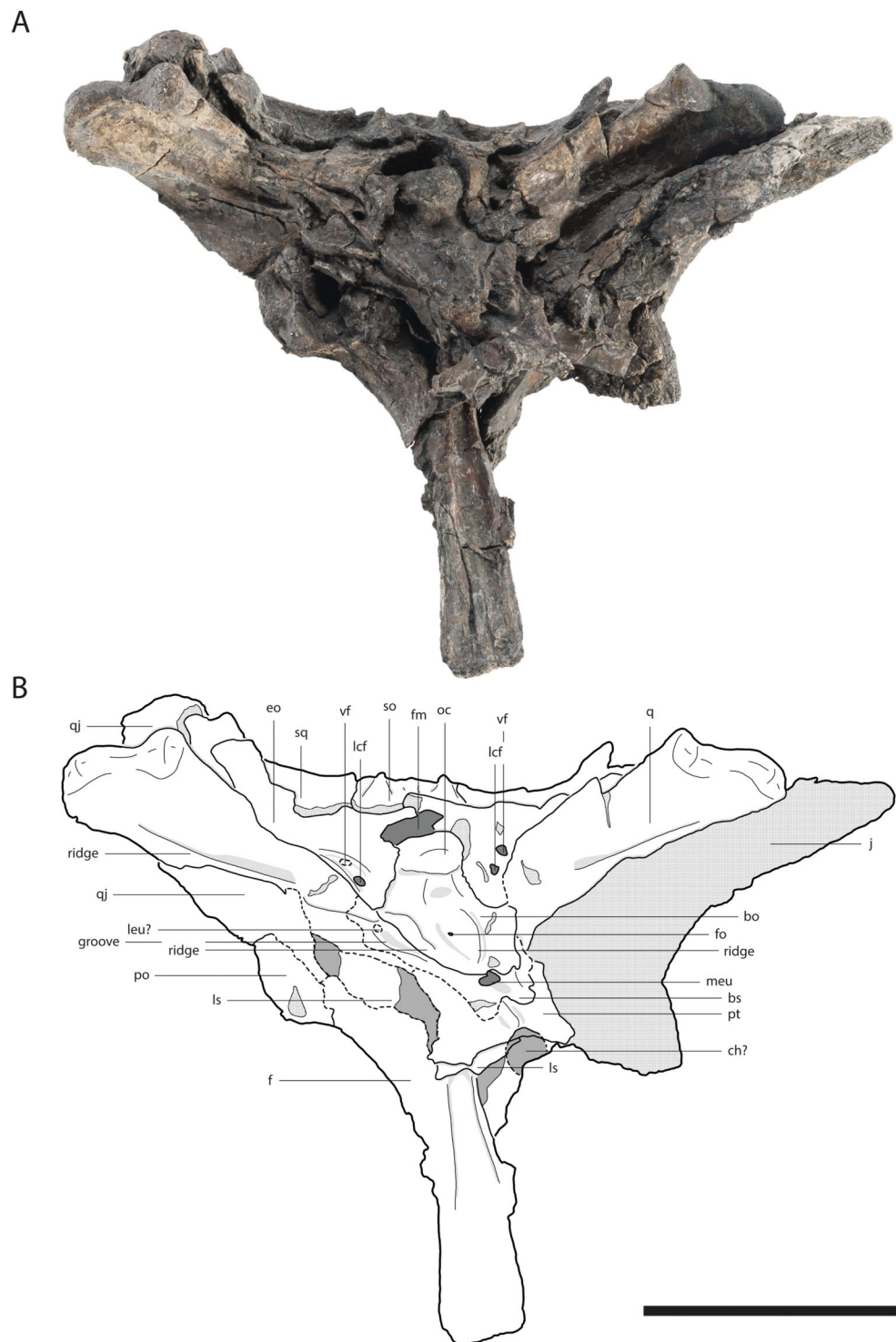


Figure 7 Skull of *Orientalosuchus naduongensis* (GPIT/RE/09729), Na Duong Formation, upper Eocene, Vietnam. Skull in occipital (A and B) view. Abbreviations: bo, basioccipital; bs, basisphenoid; ch, choana; eo, exoccipital; f, frontal; fm, foramen magnum; fo, foramen; j, jugal; lcf, lateral carotid foramen; leu?, lateral eustachian opening; ls, laterosphenoid; meu, medial eustachian opening; oc, occipital condylus; po, postorbital; pt, pterygoid; q, quadrate; qj, quadratojugal; so, supraoccipital; sq, squamosum; vf, vagus foramen. Scale = 5 cm.

Full-size  DOI: [10.7717/peerj.7562/fig-7](https://doi.org/10.7717/peerj.7562/fig-7)

does not abut the maxillary tooth row as seen in GPIT/RE/09730 (Fig. 3) and dorsally it terminates ventrally to the postorbital bar.

The surface of the anterior process bears many small foramina, whereas the posterior region is decorated with very fine anteroposteriorly oriented lines, visible in GPIT/RE/09761 (Fig. 2) and GPIT/RE/09729 (Fig. 4).

Supraoccipital

The supraoccipital is the most dorsal bone of the occipital region and has an ornamented dorsal surface. It forms a large trapezoid process on the skull table, which prevents the parietal from reaching the posterior edge of the skull table in adults. In a juvenile (GPIT/RE/09772), the supraoccipital is still large, but the parietal has a minor lateral contact with the skull table.

GPIT/RE/09728 (Fig. 5) offers the best occipital view for the supraoccipital. The bone has a dominant, strictly dorsoventrally oriented ridge, which is most prominent dorsally and becomes shallow ventrally. Laterally, there is a pair of even more dominant ridges, which extends parallel to the medial one. Between these ridges, the bone is deeply pushed inwards. The posttemporal fenestra has oval outline and slopes ventrolaterally.

The suture with the exoccipital originates ventrally to the posttemporal fenestra and projects ventromedially resulting in a roughly triangular outline of the bone.

Exoccipital

The exoccipital is best observable in GPIT/RE/09728 (Fig. 7). It shapes most of the occipital region and the paroccipital process. Further, it surrounds the foramen magnum nearly completely. Although the foramen magnum is crushed, its posterolateral margin can still be seen as well as the lateral pillars of the exoccipital, which were attached to the occipital condyle.

Alongside the ventrolaterally extending suture with the basioccipital, the exoccipital possesses a relatively short ventrally oriented process. Laterally from the occipital condyle, the caudal aperture of the carotid foramen is visible, and dorsolaterally from the occipital condyle lies the opening for the foramen vagus. The suture with the basisphenoid is not preserved.

Basioccipital

The basioccipital forms the ventral part of the occipital region and the occipital condyle. Directly ventrally to the condyle, a small foramen is visible in GPIT/RE/09729 (Fig. 4), which is not present in GPIT/RE/09728 (Fig. 7). Further ventrally, the basioccipital forms a prominent dorsoventrally projecting medial ridge leading into the median eustachian opening. On the lateral side of the ridge, a small foramen is visible in GPIT/RE/097298 (Fig. 7). At the lateral contact with the basisphenoid, the basioccipital has a bulge, whereas the ventral suture around the median eustachian opening is relatively smooth.

Basisphenoid

The basisphenoid is anteroventrally located from the basioccipital and projects relatively far ventrally. Its extension on the lateral braincase wall cannot exactly be determined in

GPIT/RE/09728 (Fig. 7), but it looks relatively narrow in GPIT/RE/09761 (Fig. 2). The lateral eustachian opening is not preserved, but a canal potentially leading into it can be seen in GPIT/RE/09728 (Fig. 7). This reconstructs the opening at the same height as the dorsal end of the medial ridge of the basioccipital. The suture between the basisphenoid and pterygoid is strongly curved with the basisphenoid sending a rounded process ventrally into the pterygoid.

Dentary

The dentary is best observable in GPIT/RE/09728 (Fig. 8) and GPIT/RE/09727 (Fig. 9). It lies nearly completely lingually to the maxilla as observable in GPIT/RE/09761 (Fig. 2). The only exception is the region around the fourth and around the 11th dentary alveoli where an inline occlusion with the maxillary tooth row occurs (indicated by occlusion pits in GPIT/RE/09730 Fig. 3 and GPIT/RE/09769 Fig. 6). The general outline of the tooth row of the dentary is strongly sigmoidal. There is a shallow curvature between the first and fourth alveoli and a much deeper one between the fourth and 11th alveoli. The level of the 11th alveolus is slightly higher than the level of the fourth one. Below the posteriormost teeth, the outline is nearly even.

In total the tooth row consists of 16 teeth (Fig. 8). The first three alveoli are nearly equal in size, whereas the fourth one is much larger, fitting in the notch between the premaxilla and maxilla. The fifth and sixth alveoli are very small, with the fifth being the smallest of the dentary. The seventh to the 10th alveoli, are as large as the third. Between the seventh and eighth alveoli, there is a small diastema for receiving the fourth maxillary tooth. A larger diastema is present between the eighth and ninth alveoli for the massive fifth maxillary tooth, which left a very prominent mark on the dentary. The 11th alveolus is slightly larger than the previous ones and the second largest alveolus in the dentary. The 11th dentary tooth is most likely the one interfingering between the seventh and eighth maxillary teeth. The 12th and 13th alveoli are again smaller. The posterior alveoli of the 14th to 16th alveoli are lateromedially flattened and anteroposteriorly elongated.

The dentary surface is ornamented with small pits anteriorly and grooves posteriorly. Anteriorly to the external mandibular fenestra, nearly no ornamentation is visible. The symphysis extends to the height of the fifth dentary tooth. The Meckelian groove is preserved as a very narrow canal, nearly closed by the surrounding dentary.

The dentary-splenic suture abuts the tooth row at the level of the 13th dentary tooth. The dentary contacts the angular posteroventrally and the surangular posterodorsally. The suture with the angular projects ventrally from the height of the most posterior dentary tooth to the ventral part of the external mandibular fenestra in a bowed line. The suture with the surangular intersects the external mandibular fenestra at its posterodorsal corner. The external mandibular fenestra itself is very small. It has nearly the same size as the foramen intermandibularis caudalis (best seen in GPIT/RE/09727 Fig. 9). Despite its size, it forms posteroventrally a clear concavity with the angular. Its anterior margin, on the other hand, is straight.

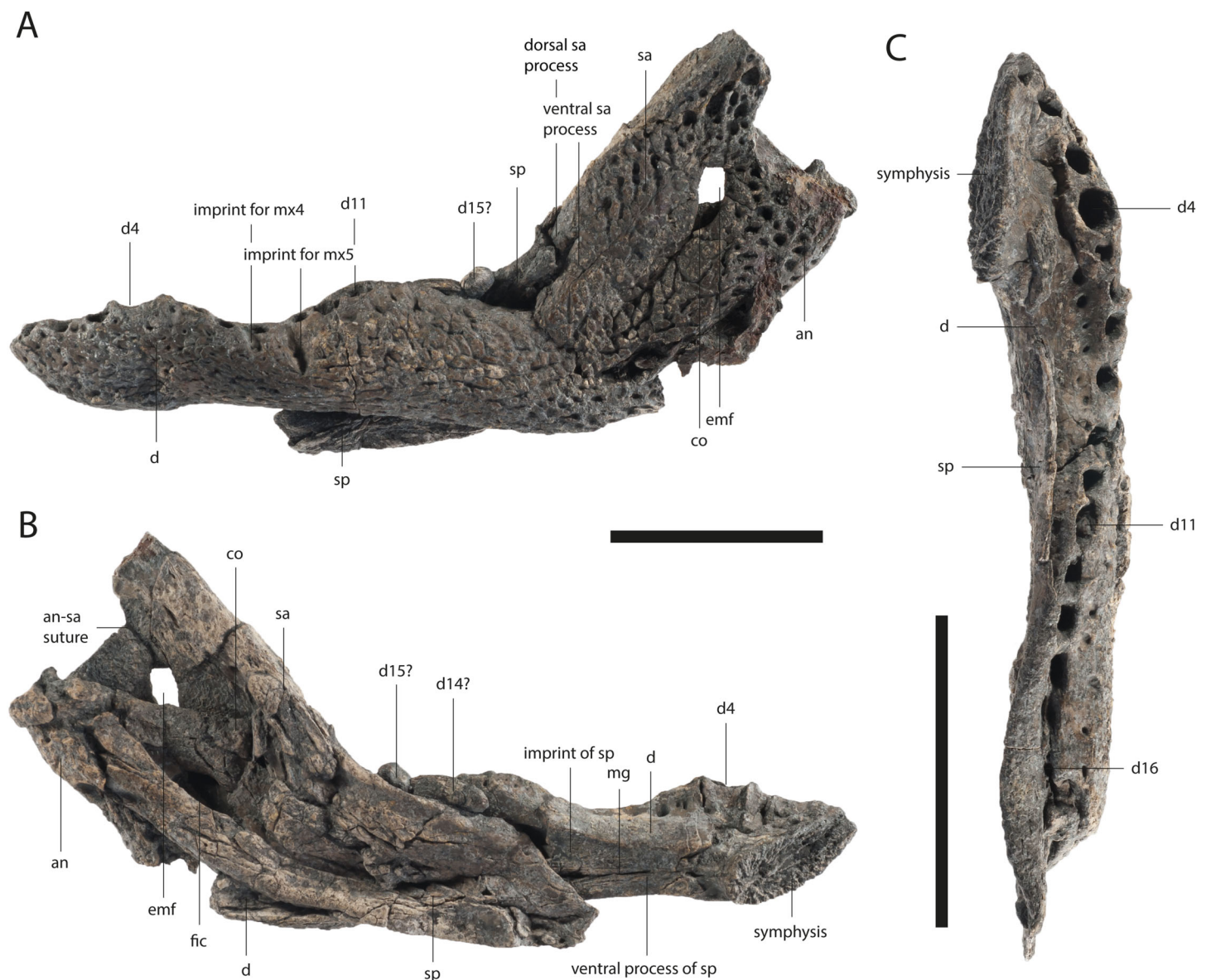


Figure 8 Lower jaw of *Orientalosuchus naduongensis* (GPIT/RE/09728), Na Duong Formation, upper Eocene, Vietnam. Lower jaw in lateral (A), medial (B) and dorsal (C) view. Abbreviations: an, angular; co, coronoid; d, dentary; d1–16, dentary tooth 1–16; emf, external mandibular fenestra; fic, foramen intermandibularis caudalis; mg, meckelian groove; mx4–5, maxilla tooth 4–5; sa, surangular; sp, splenial. Scale = 5 cm.

Full-size DOI: 10.7717/peerj.7562/fig-8

Splenial

The splenial lies lingually to the dentary and does not participate in the symphysis. Its surface is smooth. The splenial abuts the tooth row from the 13th tooth posteriorly and extends anteriorly to the level of the seventh dentary tooth. The anterior process passes ventrally to the Meckelian groove. This is visible in a single individual (GPIT/RE/09781) and in form of marks in GPIT/RE/09728 (Fig. 8). An anterior perforation for the mandibular ramus of the cranial nerve V is not present.

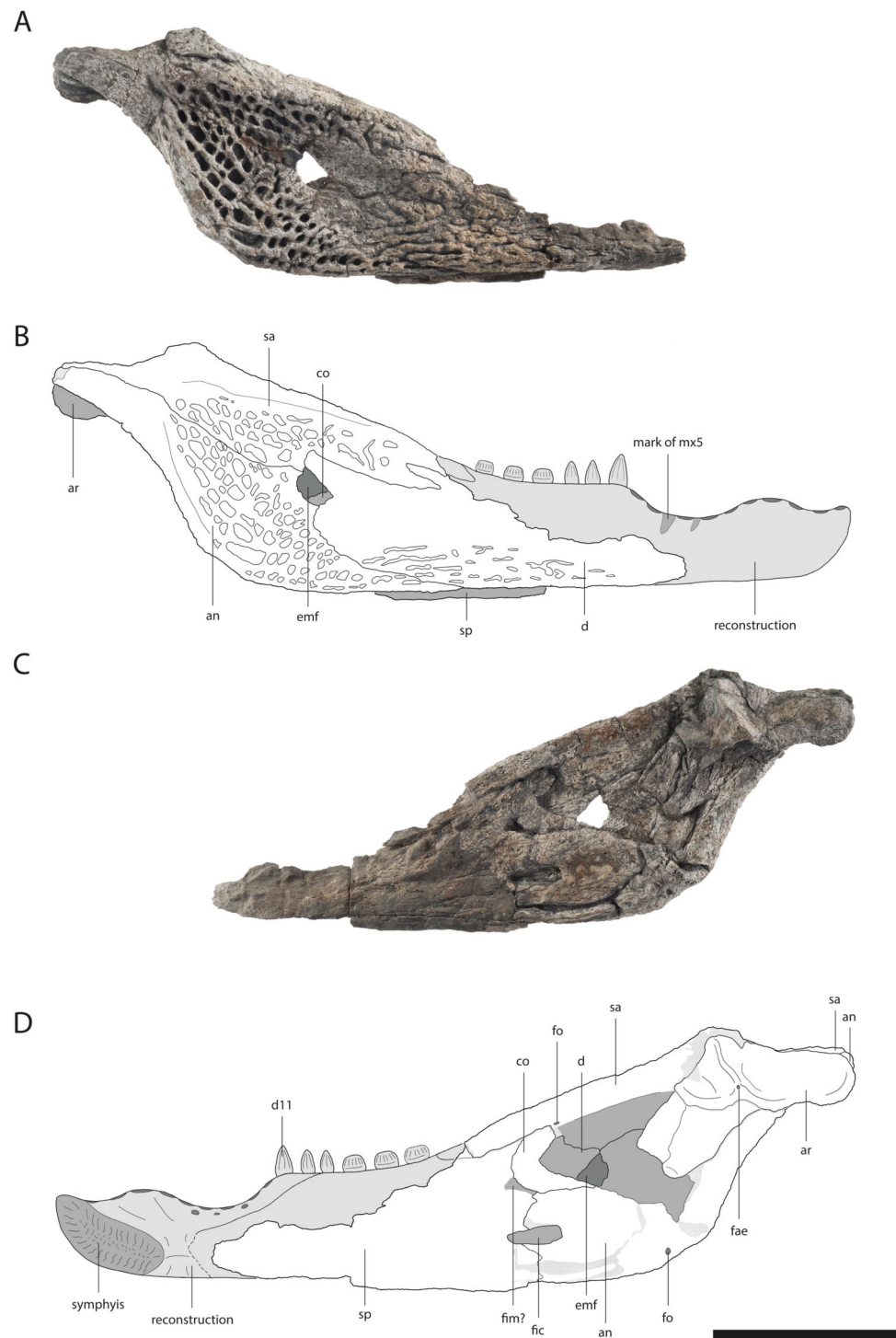


Figure 9 Lower jaw of *Orientalosuchus naduongensis* (GPIT/RE/09727), Na Duong Formation, upper Eocene, Vietnam. Lower jaw in lateral (A and B) and medial (C and D) view. Abbreviations: an, angular; ar, articular; co, coronoid; d, dentary; d11, dentary tooth 11; emf, external mandibular fenestra; fo, foramen; fic, foramen intermandibularis caudalis; fim, foramen intermandibularis medius; mx5, maxilla tooth 5; sa, surangular; sp, splenial. Scale = 5 cm.

Full-size  DOI: [10.7717/peerj.7562/fig-9](https://doi.org/10.7717/peerj.7562/fig-9)

Posteriorly, the splenial meets the surangular, coronoid and angular, as well as it forms the anterior border of the foramen intermandibularis caudalis. The suture with the surangular projects anteriorly until reaching the tooth row. The concave suture with the coronoid is only visible in the right ramus of GPIT/RE/09727 (Fig. 9). The anteroventral part of the coronoid is damaged, but it seems the foramen intermandibularis medius was located completely on the splenial or at least the coronoid only borders the most posterior border of the foramen. The suture between the splenial and angular, ventrally to the foramen intermandibularis caudalis is ambiguous, but it seems to extend slightly posteriorly, before turning ventrally. Dorsally to the foramen, the suture is visible and projects nearly straight dorsoventrally without the splenial producing a posterior process between the angular and coronoid.

Surangular

The surangular is best observable in GPIT/RE/09761 (Fig. 2) and GPIT/RE/09727 (Fig. 9) and shapes the posterodorsal portion of the lower jaw. The dorsolateral part of the bone is elevated laterally in form of a shallow bulge and densely ornamented with deep pits, whereas the anterior and the posterior parts around the retroarticular process does not possess ornamentation.

Anteriorly, the surangular has two processes. The ventral process is slightly shorter than the dorsal one, but they do not differ much in length. Posteriorly, the surangular extends to the posterior end of the retroarticular process. Dorsally, the surangular is slightly elevated, but does not seem to reach to the dorsal tip of the lateral wall of the glenoid fossa (best observable in GPIT/RE/09783). Laterally, the suture with the angular contacts the external mandibular fenestra slightly ventrally to its posterodorsal corner. Lingually, the suture between the surangular and articular cannot be clearly followed within the glenoid fossa, due to deformation. The suture ventrally to the fossa is simple, without any visible lamina. A lingual foramen is not preserved. The surangular-angular suture meets lingually the articular dorsally to the ventral tip of the articular. Posterodorsally to the surangular-coronoid suture, a small foramen is visible in GPIT/RE/09727 (Fig. 9).

Angular

The angular is best observable in GPIT/RE/09761 (Fig. 2) and GPIT/RE/09727 (Fig. 9). Its lateral surface is densely ornamented with deep posteriorly elongated pits. The retroarticular process has no ornamentation. Laterally, the angular forms the concave posterior border of the external mandibular fenestra.

The bone borders most of the foramen intermandibularis caudalis dorsally and ventrally as well as its complete posterior border. The angular-coronoid suture is nearly straight and anteroposteriorly oriented. Ventrally, anteriorly to the height of the glenoid fossa, a relatively large foramen is visible. Another posterior foramen, is only preserved in GPIT/RE/09761 (Fig. 2).

Coronoid

The coronoid is only well preserved in GPIT/RE/09727 (Fig. 9). Its outline is roughly boomerang-shaped with an incomplete posterodorsal part. The ventral process is relatively

large and projects posteriorly. The bone has a smooth surface and does not bear any foramina.

Articular

The articular possesses the glenoid fossa and the posterodorsally oriented retroarticular process in its medial part. Anteromedially, the process produces a broad shelf. The glenoid fossa is separated from the process by a mediolaterally oriented sigmoidal-shaped ridge with its lateral part being slightly more anteriorly oriented than the medial one. The foramen aerum is visible in GPIT/RE/09727 (Fig. 9) on the medial corner of the ridge.

Teeth

Most of the teeth attached to the skulls and lower jaws are poorly weathered. Only disarticulated teeth of GPIT/RE/09728 (posterior ones) and GPIT/RE/09761 (a single anterior one) (Fig. 10) are well preserved, but their original positions are not clear. Based on the size of the alveoli, the fourth and 11th dentary teeth were the largest teeth in the lower jaw, whereas in the upper jaw, the fifth maxillary tooth was by far the largest one and left deep marks on the lateral dentary wall (GPIT/RE/09728 Fig. 8).

The anterior and middle teeth are pointed. In a single well-preserved tooth several relatively dominant vertical ridges are present laterally and weaker ones lingually. This condition is not visible in poorly-preserved teeth, making it unclear if this condition is true for all pointed teeth. Laterally, the teeth are slightly convex, whereas they are concave lingually.

Posteriorly, at the 10th maxilla tooth (GPIT/RE/09769 Fig. 6) the teeth become conical and blunt.

The most posterior three teeth are relatively large, have a very blunt crown and are anteroposteriorly elongated and laterally compressed. They are smaller than in typically bulbous tooth taxa like *Hassiacosuchus haupti* Weitzel, 1935.

Both types of posterior teeth bear fine dorsoventrally oriented lines, but no clear vertical ridges are present like in the well-preserved anterior one (Fig. 10).

Postcranial Description

Most of the postcranial material is preserved in GPIT/RE/09761, GPIT/RE/09727 and GPIT/RE/09784. If not otherwise stated the description is based on the holotype GPIT/RE/09761. Measurements are deposited in the File S4.

Atlas

From the atlas, only the rectangular intercentrum is preserved dislocated into the left orbit of GPIT/RE/09761 (Fig. 2). The bone is plate-shaped in lateral view and has prominent parapophyseal processes. The slightly convex ventral part has a shallow anteroposteriorly projecting central groove.

Axis

The axis (Fig. 11) is better preserved posteriorly. The neural spine looks completely horizontal, but its surface is weathered. The base of the postzygapophysis is visible on the



Figure 10 Tooth morphology of *Orientalosuchus naluongensis*, Na Duong Formation, upper Eocene, Vietnam. Anterior tooth of GPIT/RE/09761 (holotype) in lateral (A), anterior (B) and dorso/ventral (C) view. Medial tooth of GPIT/RE/09728 in lateral (D), anterior (E) and dorso/ventral (F) view. Posterior tooth of GPIT/RE/09728 in lateral (G), anterior (H) and dorso/ventral (I) view. Scale = 0.5 cm.

Full-size [DOI: 10.7717/peerj.7562/fig-10](https://doi.org/10.7717/peerj.7562/fig-10)

left side, but also poorly preserved. The neural arch and neural canal are laterally compressed due to fossilization. The hypapophysis is posteriorly shifted.

Cervical vertebrae

A total of 18 cervical vertebrae are preserved (seven in GPIT/RE/09761 and GPIT/RE/09784, three in GPIT/RE/09727 and one in GPIT/RE/09767 (1). All of these are crushed and/or covered by a pyritized matrix except for the single vertebra of GPIT/RE/09761 (Fig. 11).

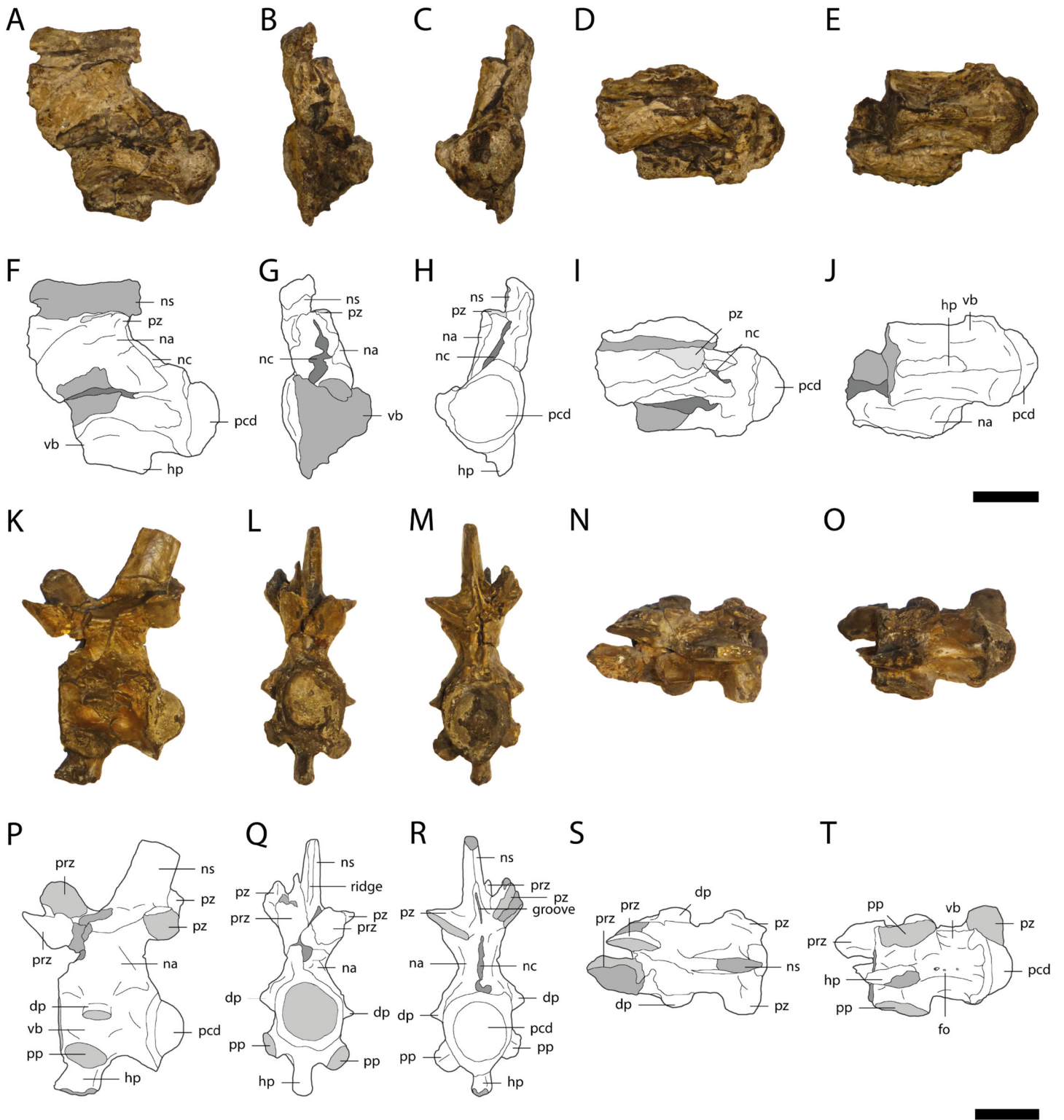


Figure 11 Cervical vertebrae of *Orientalosuchus naduongensis* (GPIT/RE/09761) (holotype), Na Duong Formation, upper Eocene, Vietnam. Cervical vertebrae in lateral left (A and F), anterior (B and G), posterior (C and H) dorsal (D and I), and ventral (E and J) view. Cervical vertebra in lateral left (K and P), anterior (L and Q), posterior (M and R) dorsal (N and S), and ventral (O and T) view. Abbreviations: dp, diapophysis; hp, hypapophysis; na, neural arch; nc, neural canal; ns, neural spine; pcd, posterior condylus; pp, parapophysis; prz, prezygapophysis; pz, postzygapophysis; vb, vertebra body. Scale = 1 cm. [Full-size !\[\]\(5f471a71b78d7676bc356df190b88ab4_img.jpg\) DOI: 10.7717/peerj.7562/fig-11](https://doi.org/10.7717/peerj.7562/fig-11)

The neural spine is slightly sloping anteriorly, but the most dorsal tip is not preserved. The spine has a dorsoventrally extending anterior ridge and a posterior groove, with the latter deepest between the postzygapophyses. The hypapophysis is located at the anterior part of the centrum and reaches posteriorly roughly its midpoint. The pre- and postzygapophyses are similarly formed and have oval articular surfaces. The diapophysis initiates above the base of the neural arch, whereas the parapophysis originates ventrally on the centrum. The centrum is concave medially, smooth and without any pits. A lateral foramen is preserved on the right side, slightly posteriorly between the diapophysis and parapophysis. A few smaller foramina are visible posterior to the hypapophysis.

Dorsal vertebrae

A total of 30 dorsal vertebrae are preserved (10 in GPIT/RE/09761, 11 in GPIT/RE/09727, one in GPIT/RE/09778 and eight in GPIT/RE/09784). They are best preserved in GPIT/RE/09761 (Fig. 12). The posterior dorsal vertebrae are anteroposteriorly elongated and lack a hypophyseal keel. The transverse processes are only preserved as small fragments. The neural spine has an anterior, dorsoventrally oriented keel and a posterior groove. In a single vertebra of GPIT/RE/09761, there is an anterior pit ventrally to the keel. The anterodorsal end of the neural spine possesses a large crest with a rounded outline, which forms a small horizontal plateau. The articular surfaces of the prezygapophyses are oval and slightly medially shifted. The articulation surfaces of the postzygapophyses are also oval, but facing straight ventrally. The vertebral centra are procoelous and differ in length. They are slightly concave and smooth without any visible foramina at the middle part of the lateral surface.

Sacral vertebra

Only the first sacral vertebra (Fig. 12) is preserved, but it is twisted and deformed. The neural spine slopes slightly anteriorly. Its dorsal tip is missing. The prezygapophyses are relatively large, whereas the only preserved left postzygapophysis in comparison is very small. The articulation facets of the prezygapophyses are oriented medially, whereas the postzygapophysis is ventrolaterally oriented. The centrum has a smooth surface with a small foramina ventrally.

Caudal vertebrae

A total of 19 caudal vertebrae are preserved (eight in GPIT/RE/09761, six in GPIT/RE/09727 and five in GPIT/RE/09784). The first caudal vertebra in GPIT/RE/09761 (Fig. 12) is by far the best preserved and can be distinguished from the others by its convex anterior and posterior condyles. The neural spine of the first caudal vertebra originates relatively anteriorly and slopes posteriorly. Its anterior part is nearly vertical and has a large dorsoventrally extending groove. The prezygapophyses are relatively large and oval. Their articulation surfaces point dorsomedially. The transverse processes are laterally oriented at their bases, but bent posterolaterally. The centrum is slightly concave medially. The condyle is slightly larger than the cotyle. The lateral surface of the centrum is smooth with

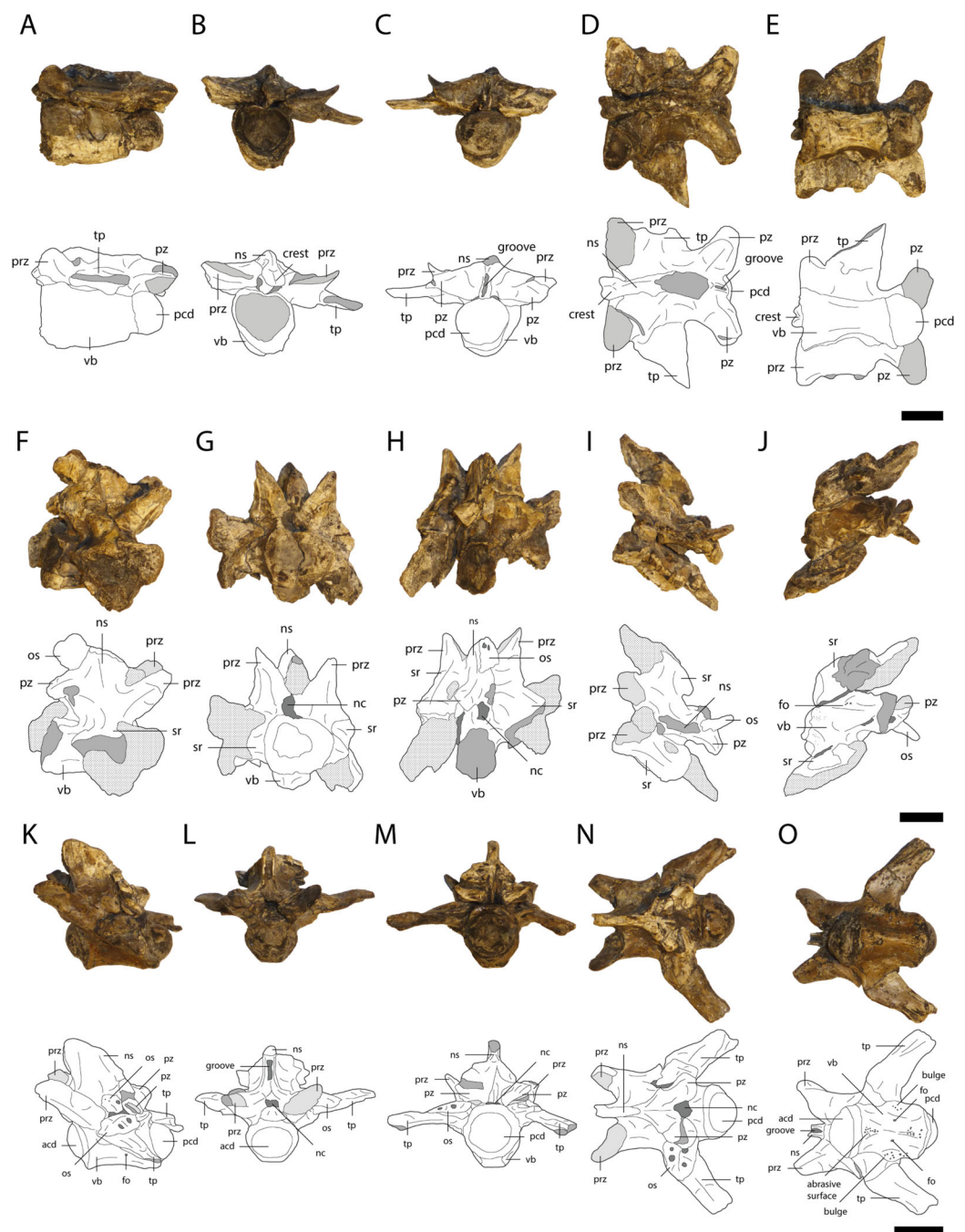


Figure 12 Vertebrae of *Orientalosuchus naduongensis* (GPIT/RE/09761) (holotype), Na Duong Formation, upper Eocene, Vietnam. Dorsal vertebra in lateral left (A), anterior (B), posterior (C), dorsal (D), and ventral (E) view. First sacral vertebra in lateral right (F), anterior (G), posterior (H), dorsal (I), and ventral (J) view. First caudal vertebra in lateral left (K), anterior (L), posterior (M), dorsal (N), and ventral (O) view. Abbreviations: acd, anterior condylus; fo, foramen; nc, neural canal; ns, neural spine; os, osteoderm; pcd, posterior condylus; prz, prezygapophysis; pzd, postzygapophysis; sr, sacral rib; tp, transverse process; vb, vertebra body. Scale = 1 cm. [Full-size !\[\]\(fcc3264021d438d9732560e78099f674_img.jpg\) DOI: 10.7717/peerj.7562/fig-12](https://doi.org/10.7717/peerj.7562/fig-12)

a lateroventrally located foramen on each side. In contrast, the antero- and posteroventral regions of the centrum have a rough surface with many small pores. A further rough surface is located posterodorsally on a small bulge of around 5 mm in length and continues from the base of the transverse process posteroventrally toward the condyle.

The rest of the caudal vertebrae are poorly preserved and their neural spines are narrower and originate more on the posterior part of the centrum. Their pre- and postzygapophyses are of similar size and relatively small. The prezygapophyses are very close to each other. Their articulation surfaces point medially. The transverse processes are fragmentarily preserved in the anterior caudal vertebrae and absent in the more posterior ones. The centra gradually elongate and flatten laterally as well as reduce in size posteriorly in the vertebral column. The centrum further has a broad, anteroposteriorly extending groove, which makes the centra even narrower and the articulation facets more oval posteriorly. The ventral side of the centra bears a deep anteroposteriorly projecting sulcus in all caudal vertebrae except for the first one.

Ribs

Three cervical and 10 dorsal ribs are preserved. The cervical ribs (Fig. 13) have a horizontally oriented shaft. The capitulum and tuberculum project at nearly 90° from this shaft near its anterior end. The capitulum is larger than the tuberculum and the articular surface of the former is nearly twice as large as the articulation surface of the latter.

The shaft of the dorsal ribs (Fig. 13) is slightly convex anteriorly and concave posteriorly. Its ventral end is broad anteroposteriorly, but flattened lateromedially.

Scapula

Two highly weathered right scapulae (GPIT/RE/09761, Fig. 14 and GPIT/RE/09784) and a well preserved, but broken left scapula (GPIT/RE/09727) were recovered. The scapular blade flares dorsally. The deltoid crest is damaged and located at the antero-ventral part of the constricted area between the base of the scapula and its blade. The crest seems to be narrow, but due to the weathering, this cannot be stated with confidence.

Coracoid

The right coracoid of GPIT/RE/09761 (Fig. 14) is well preserved. Only the posteromedial part of the scapula-coracoid suture is weathered and pushed toward the glenoid, resulting in a deep postmortem notch along the suture. The glenoid is very broad, oval and anteriorly elongated. The coracoid foramen is located anteriorly to the glenoid near the scapula-coracoid suture. The coracoid blade is relatively broad and flares anteroposteriorly. It slopes slightly anteriorly at the connection surface with the interclavicula and ends with an anterior tip in form of a small tuber.

Humerus

The humeri of GPIT/RE/09761 (Fig. 15) are partially preserved. The right humerus of GPIT/RE/09727 is complete in length (83.2 mm), but highly weathered. Its anterior part including the deltopectoral crest is missing.

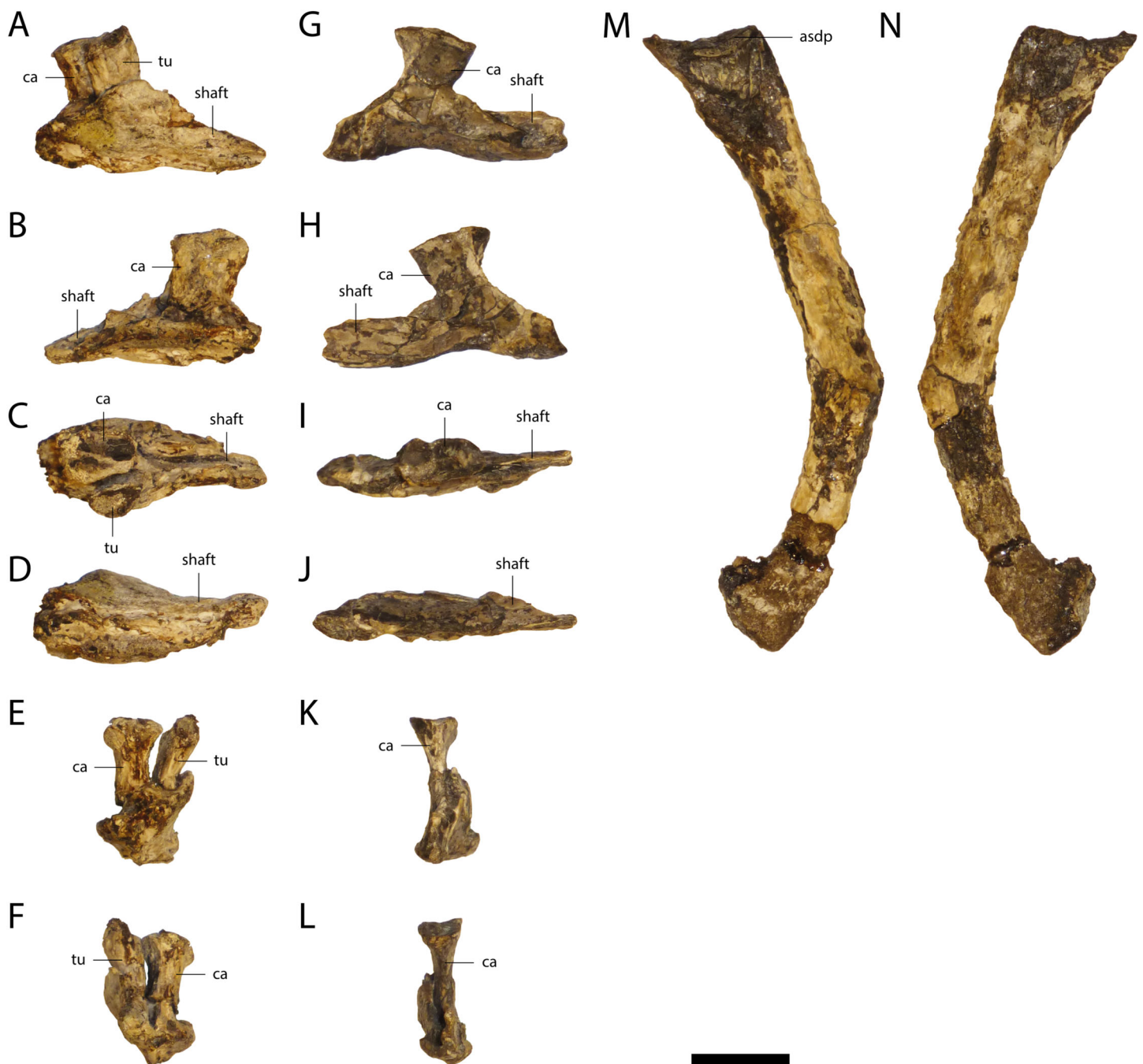


Figure 13 Ribs of *Orientalosuchus nadoungensis* (GPIT/RE/09761) (holotype), Na Duong Formation, upper Eocene, Vietnam. Cervical ribs in lateral (A and G), medial (B and H), dorsal (C and I), ventral (D and J), anterior (E and K) and posterior (F and L) views; dorsal rib in lateral (M) and medial (N) view. Abbreviations: asdp, articulation surface with diapophysis; ca, capitulum; tu, tuberculum. Scale = 1 cm.

Full-size  DOI: [10.7717/peerj.7562/fig-13](https://doi.org/10.7717/peerj.7562/fig-13)

The humeral head is only slightly elevated from the anterior tuberosity. The head and the anterior tuberosity form a nearly horizontal plateau, which bends slightly towards the latter. The posterior tuberosity lies on a small process distally from the humerus head.

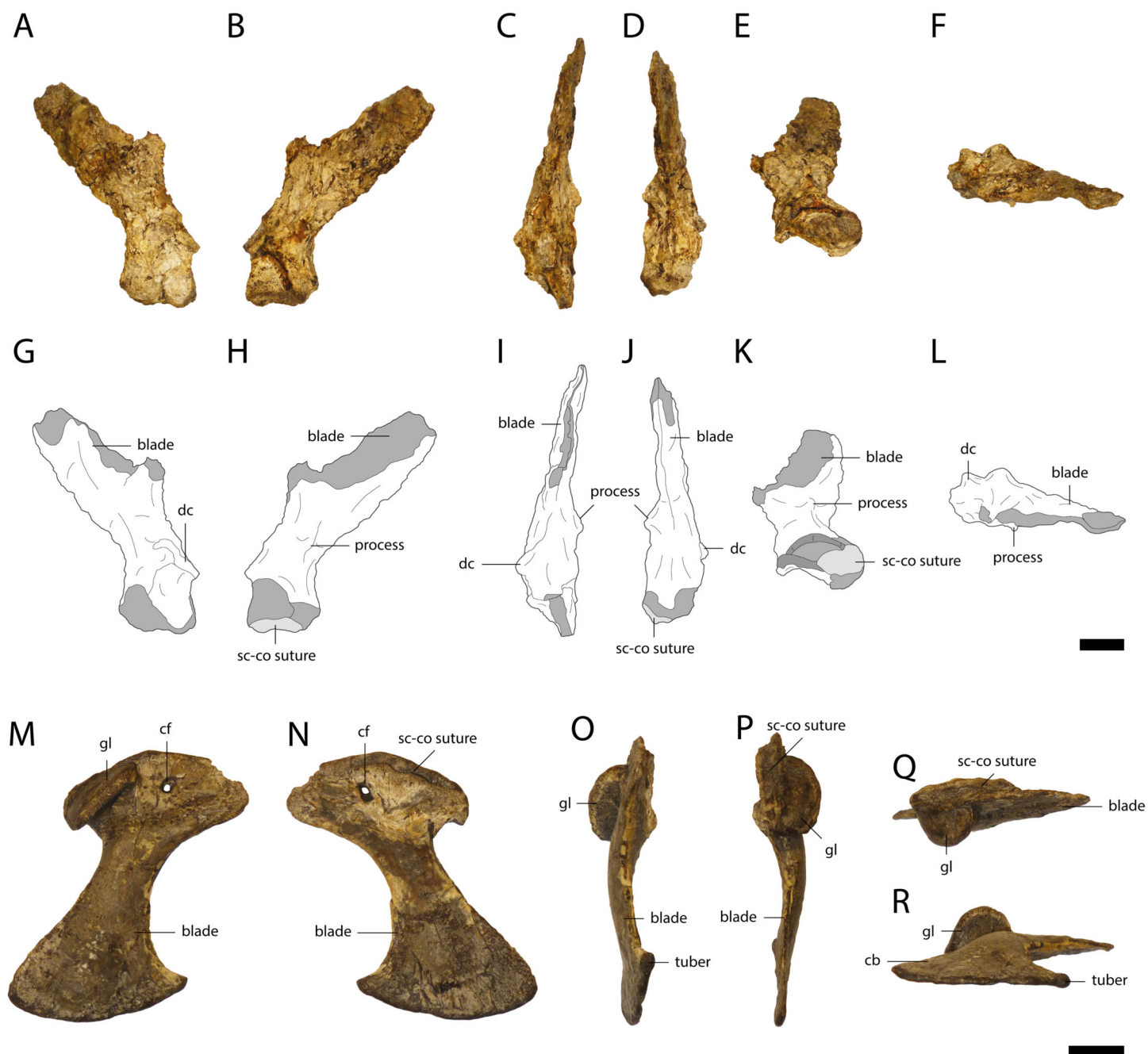


Figure 14 Pectoral girdle of *Orientalosuchus naduongensis* (GPIT/RE/09761) (holotype), Na Duong Formation, upper Eocene, Vietnam. Right scapula in lateral (A and G), medial (B and H), anterior (C and I), posterior (D and J), ventral (E and K) and dorsal (F and L) view. Right coracoid in lateral (M), medial (N), anterior (O), posterior (P), dorsal (Q), and ventral (R) view. Abbreviations: cf, coracoid foramen; dc, deltoid crest; gl, glenoid; sc-co suture, scapula-coracoid suture. Scale = 1 cm. [Full-size !\[\]\(ba1b80118482ccef74a5d718ca4d7242_img.jpg\) DOI: 10.7717/peerj.7562/fig-14](https://doi.org/10.7717/peerj.7562/fig-14)

The deltopectoral crest is damaged, but the ridge between the crest and the anterior tuberosity is partially preserved.

The lateral condyle from the distal end is larger and nearly round, whereas the medial condyle is more oval. The shaft is slightly bowed posteriorly.

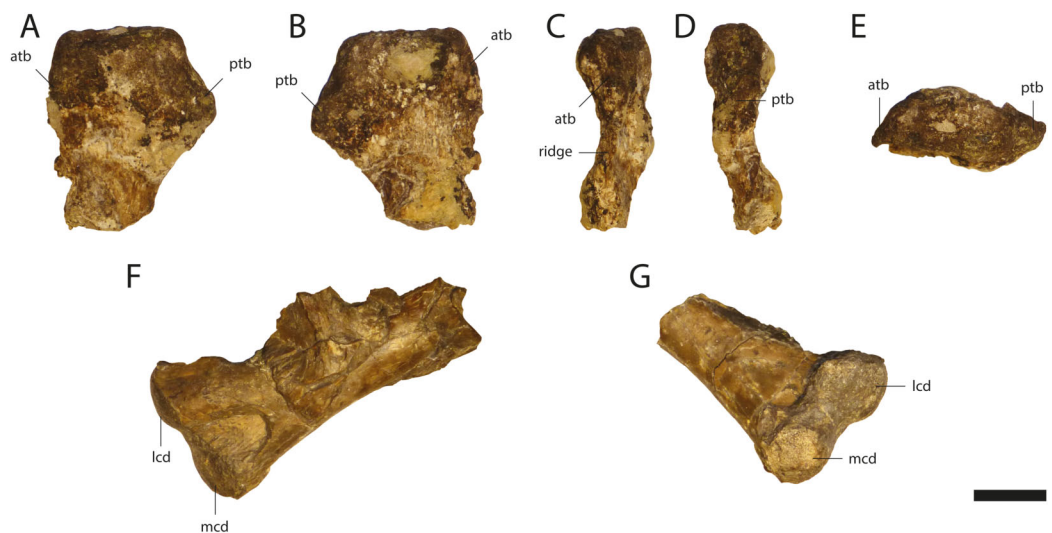


Figure 15 Humeri of *Orientalosuchus naduongensis* (GPIT/RE/09761) (holotype), Na Duong Formation, upper Eocene, Vietnam. Proximal portion of right humerus in dorsal (A), ventral (B), lateral (C), medial (D) and proximal (E) view. Distal portion of left humerus in dorsal (F) and ventro-distal (G) view. Abbreviations: atb, anterior tuberosity; lcd, lateral condylus; mcd, medial condylus; ptb, posterior tuberosity. Scale = 1 cm. [Full-size !\[\]\(5f471a71b78d7676bc356df190b88ab4_img.jpg\) DOI: 10.7717/peerj.7562/fig-15](https://doi.org/10.7717/peerj.7562/fig-15)

Ulna/Radius

Only the right radius (63.1 mm) is preserved in GPIT/RE/09727. It has a very broad proximal and a broad distal end. The shaft is slightly S-shaped, which could be an artifact of crushing. The right and left ulnae of GPIT/RE/09784 are poorly preserved.

Radiale

The left radiale (Fig. 16) is relatively well preserved, but slightly twisted and the medial part of the proximal end is eroded. The proximal end consists of the articular surface for the ulna and radius. Posteriorly the contact zone with the ulna is nearly vertical. The contact zone is very broad, giving the bone a P-shaped outline. In contrast, the contact area with the radius is kidney-shaped, nearly horizontal and slopes only slightly anterolaterally with a small lateral process. The shaft of the radiale is constricted, very thin and slightly sloping anteriorly. The distal end is oval and enlarged.

Metapodials

In GPIT/RE/09761, elongated autopodial elements (Fig. 16), either metacarpals or metatarsals are preserved, but cannot be assigned with confidence. The autopodials of GPIT/RE/09784 represent metatarsals based on their position on the excavation side and are much longer than the elements in GPIT/RE/09761 suggesting that those are metacarpals. The distal portion of the shaft of the metapodials are dorsoventrally flattened. Their proximal end is oval, whereas their distal end with two condyles is smaller and narrower.

Phalanges

There are seven disarticulated phalanges of GPIT/RE/09761 (Fig. 16), but we cannot determine whether they belong to the pes or manus. They are mostly highly weathered,

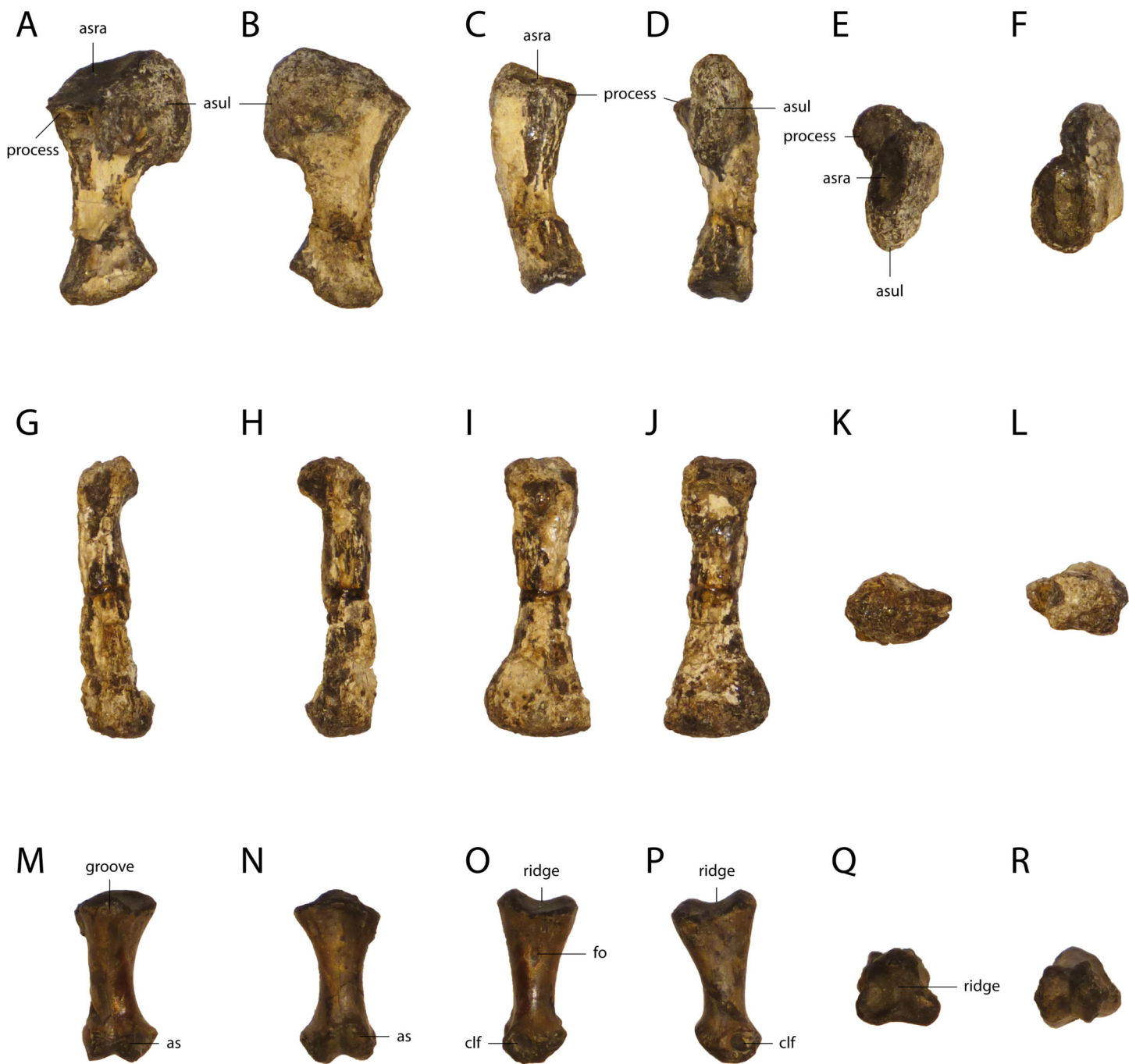


Figure 16 Left Radiale, Metapodial and Phalange of *Orientalosuchus naduongensis* (GPIT/RE/09761) (holotype), Na Duong Formation, upper Eocene, Vietnam. Left radiale in lateral (A), medial (B), anterior (C), posterior (D), proximal (E), and distal (F) view. Metapodial in lateral left or right (G and H), dorsal (I), ventral (J), proximal (K) and distal (L) view. Phalange in dorsal (M), ventral (N), lateral left or right (O and P), proximal (Q) and distal (R) view. Abbreviations: asra, articulation surface with radius; asul, articulation surface with ulna; clf, collateral ligament fossa; fo, foramen. Scale = 1 cm.

Full-size  DOI: [10.7717/peerj.7562/fig-16](https://doi.org/10.7717/peerj.7562/fig-16)

only a single one is well preserved. The 14 phalanges of GPIT/RE/09784 belong to the pes based on their recovered position.

Its proximal end is nearly triangular with three knob-like structures, which are separated by a ridge. Its distal end has two condyles. Their articulation surfaces slope dorsally and ventrally. The condyles are separated from each other by an intercondylar groove. In lateral view, relatively deep collateral ligament fossae are visible on the distal condyles. The shaft has a smooth surface, but bears a foramen on the slightly laterally bent side.

Ungual phalanges

The preserved claws of GPIT/RE/09761 differ considerably in length, but cannot be assigned to either manus or pes. They are long, only slightly curved, ventrally flattened, dorsally curved and pointed. The claws of GPIT/RE/09784 belong to the pes based on their position recorded in the field and are partly articulated with the distal phalanges. The better preserved ones are much smaller and stronger curved than the claws of GPIT/RE/09761, but it is unclear to which digit they belong.

Ilium

Both ilia are preserved in GPIT/RE/09761 (Fig. 17) and GPIT/RE/09784. The posterior part of the iliac blade is rectangular and has a modest indentation dorsally. Anteriorly, the blade slopes at approximately 30° toward a small anterior process. The sutural surface for the first sacral rib is slightly visible on the anteromedial part in the left ilium. In ventral view, the posterior sutural surface for the ischium is triangular with a larger posterior part and a narrower anterior one. The anterior sutural surface is more oval and smaller. Dorsolaterally, an articulation surface with the femur is visible. The acetabulas foramen lies between two articular surfaces. The acetabulum itself seems relatively narrow. Dorsally from the acetabulum, the supraacetabular crest is visible. It separates the acetabulum from the iliac blade. Medially, at the articular surface with the second sacral rib, a prominent ridge is present, although the surface itself is not clearly visible due to weathering.

Ischium

The best preserved ischium is the left one of GPIT/RE/09761 (Fig. 18). Its proximal region has two articulation surfaces, separated from each other by the ventral part of the acetabulas foramen. The iliac process is approximately four times larger than the pubic process. The articulation surface with the ilium is oval, broad and has a shallow posterolaterally projecting ridge. The proximal part of the pubic process is oval and lateromedially oriented. The anterior edge of the shaft is bowed and the blade projects posteriorly.

Pubis

A single left pubis is preserved in GPIT/RE/09784. Its articulation surface with the ischium is oval and anteroposteriorly elongated. The shaft is very thin and the blade flares strongly anteroposteriorly.

Femur

The femur of GPIT/RE/09761 (Fig. 19) is 112.8 mm in length, while the femora of GPIT/RE/09784 and GPIT/RE/09727 are 110.8 and 109.2 mm, respectively. The femur is slightly

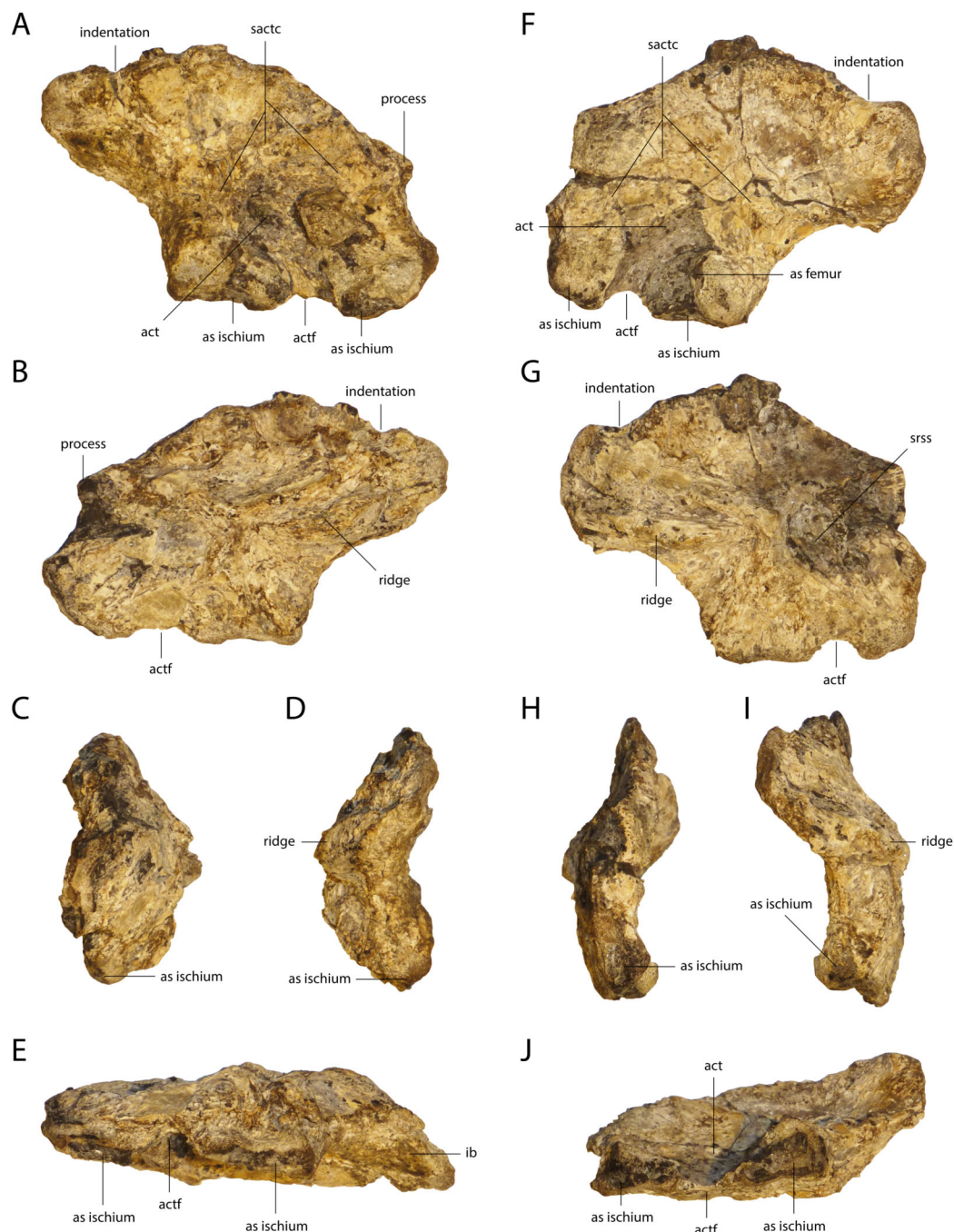


Figure 17 Ilium of *Orientalosuchus naduongensis* (GPIT/RE/09761) (holotype), Na Duong Formation, upper Eocene, Vietnam. Right ilium (left) and left ilium (right) in lateral (A and F), medial (B and G), anterior (C and H), posterior (D and I) and ventral (E and J) view. Abbreviations: as, articulation surface; act, acetabulum; actf, acetabulum foramen; sactc, supraacetabularcrest; srss, sutural surface for sacral rib. Scale = 1 cm.

Full-size DOI: [10.7717/peerj.7562/fig-17](https://doi.org/10.7717/peerj.7562/fig-17)

sigmoidal with the proximal head lateromedially flattened and anteriorly broader than posteriorly. On the convex medial region, the head forms an articular surface with the acetabulum of the ilium. The smooth shaft has a prominent fourth trochanter on its medial

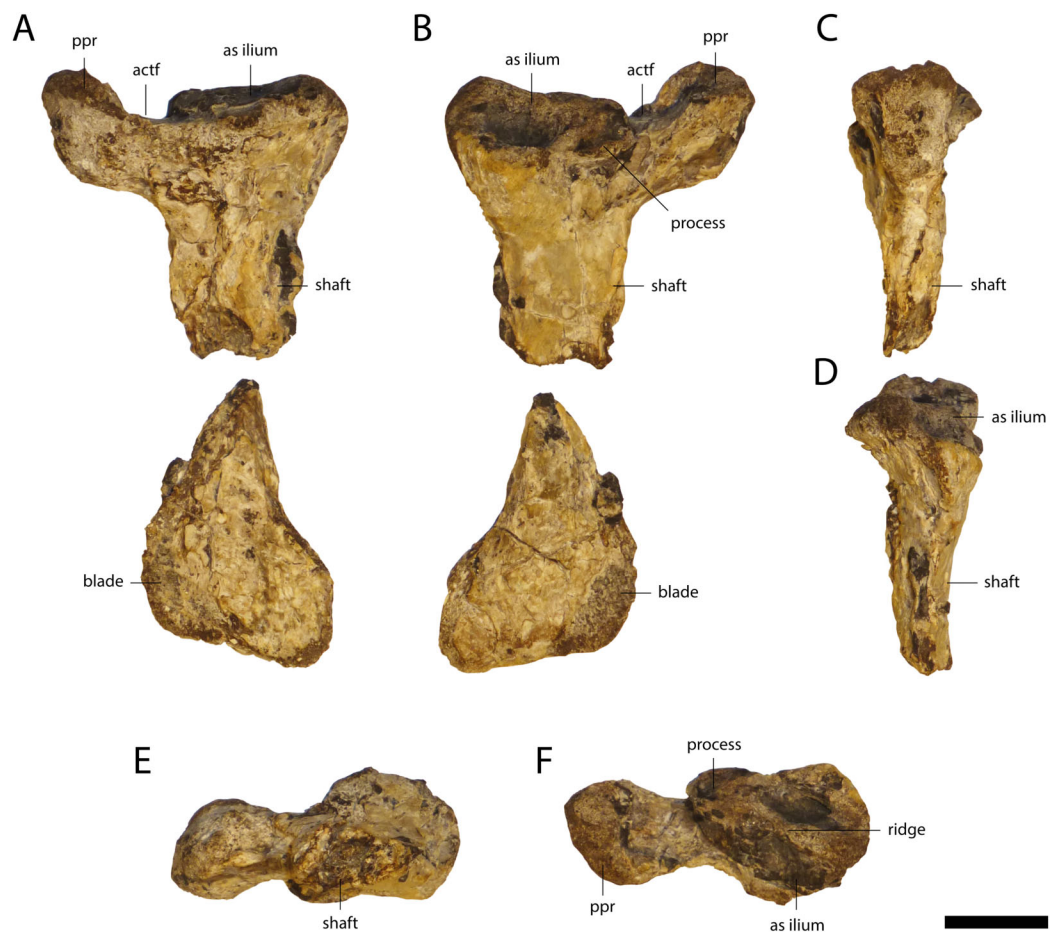


Figure 18 Ischium of *Orientalosuchus naduongensis* (GPIT/RE/09761) (holotype), Na Duong Formation, upper Eocene, Vietnam. Left ischium in lateral (A), medial (B), anterior (C), posterior (D), ventral (E) and dorsal (F) view. Abbreviations: as, articulation surface; actf, acetabulum foramen; ppr, pubic process. Scale = 1 cm. [Full-size !\[\]\(1663bb69f307a960345edb0e712f8c02_img.jpg\) DOI: 10.7717/peerj.7562/fig-18](https://doi.org/10.7717/peerj.7562/fig-18)

side. Anteriorly to the fourth trochanter, a large groove is present. The distal end of the femur consists of the larger lateral and the smaller medial condyles with an intercondylar groove between them.

Tibia/Fibula

The tibia and fibula are best preserved in GPIT/RE/09761 (Fig. 19) and GPIT/RE/09784. The tibia of GPIT/RE/09784 is 83.3 mm in length and has a slightly bowed shaft. Its proximal articulation surface is broad, whereas the distal one is narrow. Medially on the proximal epiphysis, a deep sulcus is present. The fibula of this individual is with the length of 78.1 mm, slightly smaller than the tibia and very thin.

Astragalus/Calcaneum

The left astragalus and calcaneum are preserved in GPIT/RE/09784 and show no noticeable difference from other alligatoroids.



Figure 19 Femur and fibula of *Orientalosuchus nadoungensis* (GPIT/RE/09761) (holotype), Na Duong Formation, upper Eocene, Vietnam. Right femur in lateral (A), medial (B), dorsal (C), ventral (D), proximal (E), and distal (F) view. Right fibula in lateral (G), medial (I), dorsal (J), ventral (K), proximal (L) and distal (M) view. Right tibia in medial (H) view. Abbreviations: 4th tr, fourth trochanter; acd, anterior condylus; as, articulation surface; cd, condylus; lcd, lateral condylus; mcd, medial condylus; pcd, posterior condylus. Scale = 1 cm.

Full-size  DOI: [10.7717/peerj.7562/fig-19](https://doi.org/10.7717/peerj.7562/fig-19)

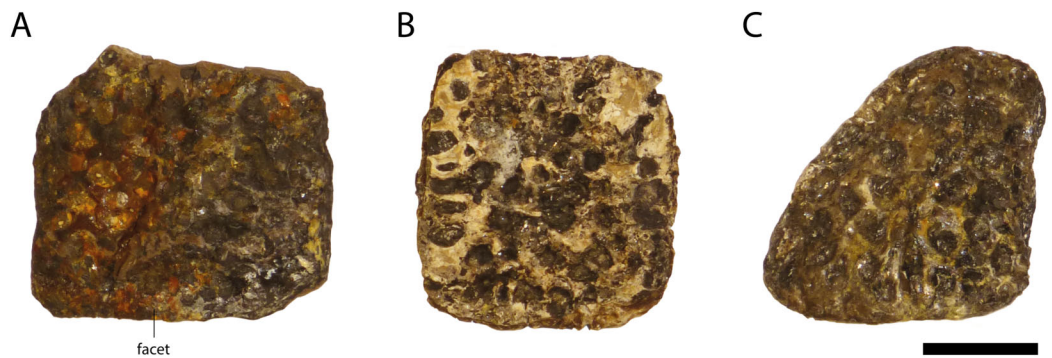


Figure 20 Osteoderms of *Orientalosuchus naduongensis* (GPIT/RE/09761) (holotype), Na Duong Formation, upper Eocene, Vietnam. Probable dorsal osteoderm (A and B) and a probable anterolateral osteoderm (C). Scale = 1 cm. [Full-size !\[\]\(fcc3264021d438d9732560e78099f674_img.jpg\) DOI: 10.7717/peerj.7562/fig-20](https://doi.org/10.7717/peerj.7562/fig-20)

Osteoderms

More than 150 osteoderms (Fig. 20) and osteoderm fragments are preserved, but most are in poor condition. All of them are ornamented with small rounded pits. Most of the osteoderms are disarticulated, but some are still in contact with the vertebra column and as such can be associated with *Orientalosuchus naduongensis*.

Most of the preserved osteoderms of GPIT/RE/09761 are dorsals. They are nearly square-shaped and possess no, or only a very shallow keel. This is also true for the posterodorsal midline osteoderms of GPIT/RE/09784.

Another osteoderm type, probably more posterolaterally located and very well preserved (GPIT/RE/09727) is relatively small and oval. These osteoderms show still weak, but slightly more pronounced keel than the dorsal osteoderms.

A single osteoderm of GPIT/RE/09761 is roughly triangular and could belong to the anterolateral region. No keel is visible, but the surface is weathered.

RESULTS OF PHYLOGENETIC ANALYSIS

A total of 20,160 equally optimal trees with a length of 927 steps were recovered, with a consistency index (CI) of 0.292 and a retention index (RI) of 0.759 (Figs. 21 and 22). Two taxa (the Maoming alligatoroid and *Asiatosuchus nanlingensis* Young, 1964) were pruned from the strict consensus tree, because of their unstable position on the tree. Due to the expansion and modification of previous matrices, the retrieved trees differ from that of previous analyses (Brochu, 2007a, 2007b; Brochu & Storrs, 2012). A list of synapomorphies can be found in the File S2.

Outside Brevirostres, the monophyletic *Arenysuchus gascabadiolorum* Puértolas, Canudo & Cruzado-Caballero, 2011 + *Allodaposuchus subjuniperus* Puértolas-Pascual, Canudo & Moreno-Azanza, 2013 + *Allodaposuchus precedens* Nopcsa, 1928 + *Lohuecosuchus mechinorum* Narváez et al., 2015 + *Lohuecosuchus megadontos* Narváez et al., 2015 group is no longer found as the sister group to Hylaeochampsidae, but as sister group to all other Crocodylia except Gavialoidea. Omitting one of the new characters (199) from the analysis results in the previous sister group relationship outside Crocodylia.

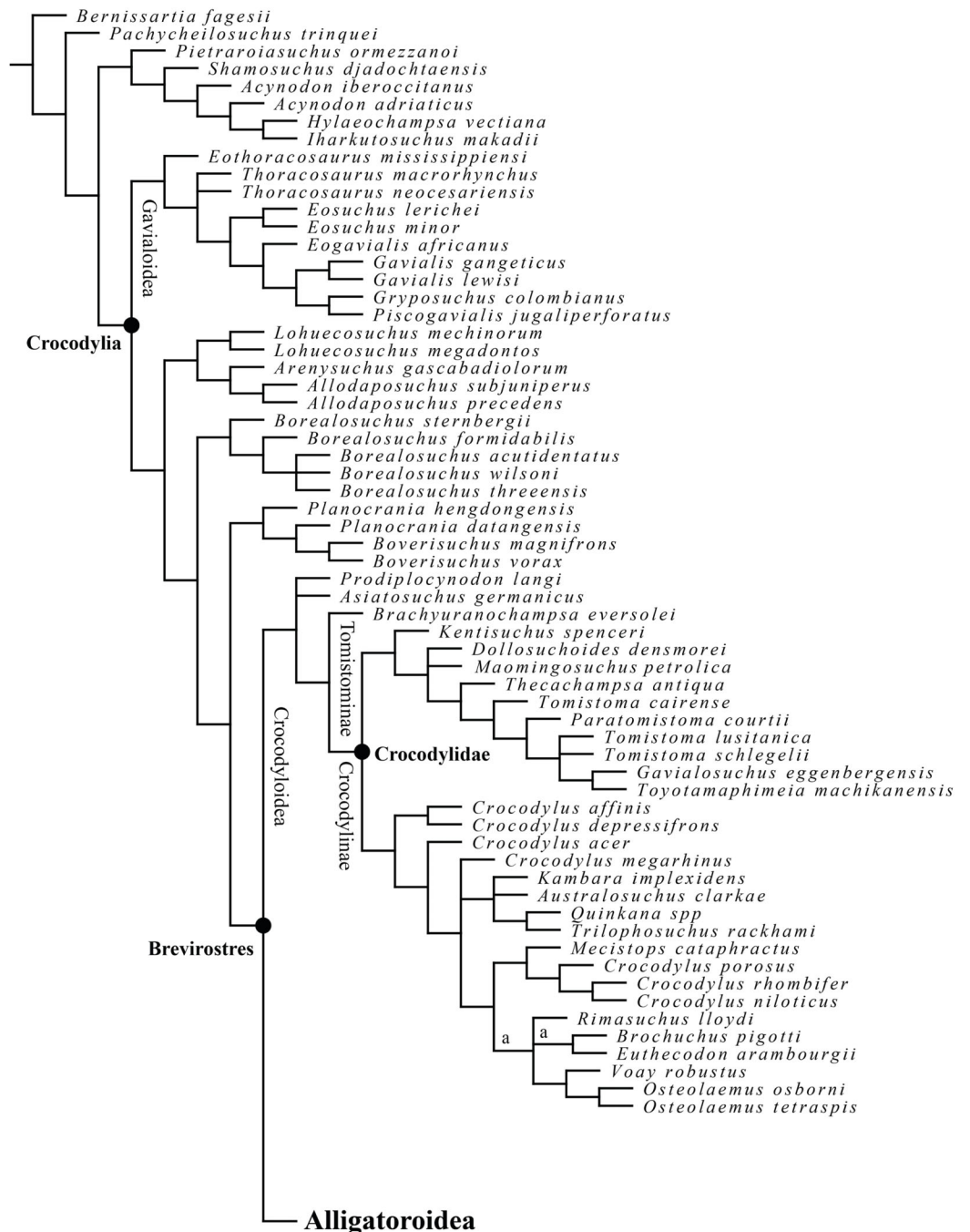


Figure 21 Reduced strict consensus tree of 20,160 equally optimal trees, obtained from the maximum parsimony analysis with 202 characters included; length: 927; CI: 0.292 and RI: 0.759. "a" indicates the alternative position of the pruned "Maoming alligatoroid".

Full-size DOI: 10.7717/peerj.7562/fig-21

The polytomy between *Pachycheilosuchus trinquei* Rogers, 2003, *Pietrarroiasuchus ormezzanoi* Buscalioni et al., 2011 and *Shamosuchus djadochtaensis* Mook, 1924a (Narváez et al., 2015), was solved in the current tree. *Pietrarroiasuchus ormezzanoi* and *Shamosuchus djadochtaensis* now form a monophyletic group with *Acynodon iberoccitanus*

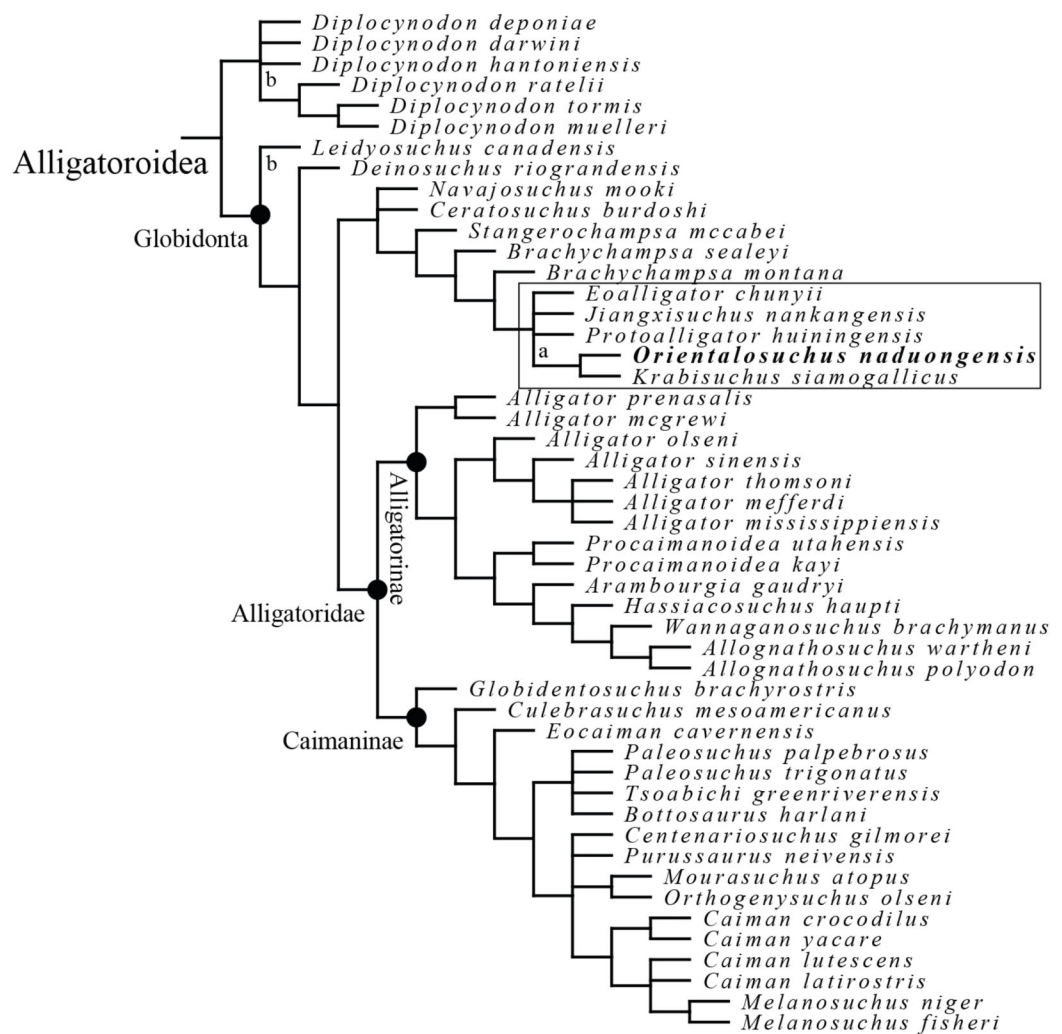


Figure 22 Alligatoroid phylogeny as inferred from the reduced strict consensus tree of 20,160 equally optimal trees, obtained from the maximum parsimony analysis with 202 characters included; length: 927; CI: 0.292 and RI: 0.759. “a” indicates the alternative position of the pruned “Maoming alligatoroid”. “b” indicates the alternative position of the pruned *Asiatosuchus nanlingensis*. The box highlights the monophyletic Orientalosuchina. [Full-size !\[\]\(ba1b80118482ccef74a5d718ca4d7242_img.jpg\) DOI: 10.7717/peerj.7562/fig-22](https://doi.org/10.7717/peerj.7562/fig-22)

Buscalioni, Ortega & Vasse, 1997, Acynodon adriaticus Delfino, Martin & Buffetaut, 2008, Hylaeochampsa vectiana Owen, 1874 and Iharkutosuchus makadii Ósi, Clark & Weishampel, 2007. The character (196) supports this monophyletic group as all of these taxa, except *Hylaeochampsa vectiana*, in which the state is unknown, lack a notch between the premaxilla and maxilla as an adult (196-1). *Pachycheilosuchus trinquei* is the sister taxon to the clade formed by these taxa and all Crocodylia.

The clade *Crocodylus depressifrons* *Blainville, 1855 + Crocodylus affinis* *Marsh, 1871*, representing basal members of Crocodyloidea in previous studies (*Delfino & Smith, 2009; Brochu & Storrs, 2012; Conrad et al., 2013*), were retrieved in a weakly supported more derived position, as a basal member of Crocodylinae. One of the characters responsible for the more derived position of *Crocodylus depressifrons + Crocodylus affinis* is their

short dentary symphysis (49-0), similar to most Crocodylidae, whereas the symphysis is long (49-1) in *Asiatosuchus germanicus* [Berg, 1966](#). The character (142; posterior angle of the infratemporal fenestra), on the contrary, points towards a close relationship with *Asiatosuchus germanicus* and a more basal position (142-0). By adding a new character (197), *Crocodylus depressifrons* and *Crocodylus affinis* are now drawn closer to Crocodylidae, but it is worth to mention that the character can be only scored for *Crocodylus depressifrons* (short sutural contact of the exoccipitals dorsal to the foramen magnum; 197-1).

In former analyses ([Brochu, 2007b](#); [Brochu & Storrs, 2012](#)), the clade *Crocodylus acer* [Cope, 1882](#) + *Brachyuranochampsa eversolei* [Zangerl, 1944](#) was found in a sister group relationship with Crocodylidae. In the current phylogeny, *Crocodylus acer* was moved to a more derived position inside Crocodylinae. The reason for this is, that the scorings for the new characters are identical in *Crocodylus acer* and *Mecistops cataphractus* ([Cuvier, 1825](#)) and similar to other Crocodylinae, while *Brachyuranochampsa eversolei* could not be scored for these new characters.

Paratomistoma courti [Brochu & Gingerich, 2000](#) was found as the sister taxon to the monophyletic group consisting of *Tomistoma lusitanica* [Antunes, 1961](#), *Tomistoma schlegelii* ([Müller, 1838](#)), *Toyotamaphimeia machikanensis* ([Kobatake et al., 1965](#)) and *Gavialosuchus eggenburgensis* [Toula & Kail, 1885](#) in the current analysis. In previous analyses ([Brochu & Storrs, 2012](#); [Conrad et al., 2013](#); [Wang, Sullivan & Liu, 2016](#)), *Paratomistoma courti* was found in a monophyletic group with *Maomingosuchus petrolica* ([Yeh, 1958](#)) and *Penghusuchus pani* [Shan et al., 2009](#). *Penghusuchus pani* was not included in the current analysis, which most likely led to the new position of *Paratomistoma courti* on the tree.

Leidyosuchus canadensis has been considered the most basal alligatoroid ([Brochu, 1999, 2004](#); [Martin & Lauprasert, 2010](#); [Wang, Sullivan & Liu, 2016](#)). In the current analysis, however, *Leidyosuchus canadensis* is positioned more crown-ward and Diplocynodontinae is found as sister group to all other Alligatoroidea. This result is due to one of the new characters: the anterior jugal process placed at the same level (195-1) or posterior (195-2) to the anterior frontal process in Diplocynodontinae (only preserved in *D. tormis* [Buscalioni, Sanz & Casanovas, 1992](#) and *D. muelleri* ([Kälin & Peyer, 1936](#))), as opposed to *Leidyosuchus canadensis*, in which the jugal processes is anterior to the frontal (195-0).

Navajosuchus mooki ([Simpson, 1930](#)) and *Ceratosuchus burdoshi* [Schmidt, 1938](#) are outside of Alligatoridae, while in previous analyses they were unresolved at the base of Alligatorinae ([Brochu, 1999, 2004](#); [Cossette & Brochu, 2018](#)). In the current analysis, they form a polytomy with a monophyletic group consisting of *Stangerochampsa mccabei*, *Brachychampsa sealeyi* [Williamson, 1996](#), *Brachychampsa montana* and *Orientalosuchina*.

Orientalosuchina is supported by one synapomorphy (see “Discussion”). Inside *Orientalosuchina*, *Orientalosuchus naduongensis* and *Krabisuchus siamogallicus* form a monophyletic group, which in turn forms a polytomy with *Eoalligator chunyii*, *Jiangxisuchus nankangensis* and *Protoalligator huiningensis*.

In the present analysis, a broad scapulacoracoid facet immediately anterior to the glenoid fossa (26-1) and nearly squared dorsal midline osteoderms (39-1) defines Alligatoridae and three characters define Alligatorinae: eight contiguous dorsal osteoderms per row at maturity (40-2), a premaxilla with a deep notch lateral to the naris (86-1) and a longer prefrontal than the lacrimal (130-1).

The Bremer support for *Orientalosuchina* is 1 and the absolute frequency Bootstrap value is 5%. The Bremer support for *Orientalosuchus naduongensis* + *K. siamogallicus* is 1 and the absolute frequency bootstrap value is 35%. If the poorly preserved *Protoalligator huiningensis* is removed from the analysis, the absolute frequency bootstrap value of *Orientalosuchina* goes up to 45% and further removing the also poorly preserved *Eoalligator chunyii* results in a bootstrap value of 54% for *Orientalosuchina* and 51% for *Orientalosuchus naduongensis* + *K. siamogallicus*.

DISCUSSION

Phylogeny of Globidonta

Globidonta is better resolved in the current analysis compared to previous studies with East and Southeastern Asian alligatoroids included (*Skutschas et al., 2014; Wang, Sullivan & Liu, 2016; Wu, Li & Wang, 2018*). Statistical support (Bremer and Bootstrap), however, remains low. The group has three synapomorphies: a lingual foramen for articular artery and alveolar nerve perforates surangular entirely (69-0), a concavo-convex frontoparietal suture (151-0) and an anterior jugal process extending anterior to the anterior process of frontal (195-0), but none is unique for this group.

Omitting the new characters **194**, **195**, **197** and **199**, results in a similar phylogeny in most non-globidontan taxa as in former analyses (*Brochu, 1999, 2007b; Brochu & Storrs, 2012; Cossette & Brochu, 2018*), but the resolution is reduced inside Tomistominae and Alligatorinae.

Orientalosuchina

Orientalosuchina, includes *Orientalosuchus naduongensis* from the middle to late Eocene of Vietnam, *Krabisuchus siamogallicus* from the late or latest Eocene of Thailand (*Benammi et al., 2001; Martin & Lauprasert, 2010*), *Protoalligator huiningensis* from the middle Paleocene of Southeast China, and *Eoalligator chunyii* and *J. nankangensis* from the Late Cretaceous-early Paleocene of Southeast China.

In all trees, the single synapomorphy of *Orientalosuchina* is a short dentary symphysis extending to the height of the fourth to fifth alveolus (49-0) as opposed to the long symphysis (49-1) of for example, *Brachychampsa* spp. and *Stangerochampsa mccabei*. A short symphysis is otherwise common for alligatoroids (most *Alligator* spp. and most Caimaninae).

Inside *Orientalosuchina*, *J. nankangensis*, *Eoalligator chunyii*, *Protoalligator huiningensis* and *Orientalosuchus naduongensis* + *K. siamogallicus* form a polytomy. In those trees in which *Protoalligator huiningensis* is ancestral, the presence of a notch between the premaxilla and maxilla (196-0) is a further synapomorphy for the group.

If *Eoalligator chunyii* is recovered as the most basal taxon, the monophyly of Orientalosuchina is further supported by seven synapomorphies:

(1) a truncated surangular around the lateral wall of the glenoid fossa (67-1); (2) the medial position of the foramen aerum on the retroarticular process (70-0) and (3) the quadrate (177-0); (4) a very short anterior palatine process, not reaching the anterior end of the suborbital fenestra (115-1); (5) the quadratosquamosal suture extends dorsally along the caudal margin of the external auditory meatus (148-1); (6) the squamosal extends ventrolaterally to lateral extent of paraoccipital process (159-1); and (7) the 11th dentary tooth is the largest one after the fourth one (200-0).

Further synapomorphies may diagnose Orientalosuchina including: (1) the posterior lateral edges of the palatines are parallel (120-0); (2) the lacrimal makes broad contact with the nasal without any sign of a maxillary process (128-0); (3) the anterior tip of the frontal is acute (131-0); (4) the postorbital does not contact the quadrate and quadratojugal at the mediodorsal angle of the infratemporal fenestra (143-0); and (5) the angular-surangular suture lingually originates near the dorsal border of the external mandibular fenestra and is straight (201-1). However, given that the corresponding anatomical regions are unknown in the basally branching and poorly preserved taxa these now define a more inclusive clade.

Consistent with their basal divergence and age, orientalosuchians retain several crocodylian plesiomorphies, which may explain their recovery inside Crocodyloidea in previous analyses (Wang, Sullivan & Liu, 2016; Wu, Li & Wang, 2018; Li, Wu & Rufolo, 2019). These characters include: (1) and (2) the medially located foramen aerum (70-0) (177-0); (3) the fifth maxillary tooth is the largest one (93-1); (4) the anterior palatine process does not extend anterior to the suborbital fenestra (115-1); (5) the lateral edges of palatines are posteriorly parallel (120-0); (6) an acute anterior frontal tip (131-0); (7) a postorbital neither contacting the quadrate nor the quadratojugal medially at the dorsal angle of the infratemporal fenestra (143-0); (8) the quadratosquamosal suture extends dorsally along the caudal margin of the external auditory meatus (148-1); (9) the squamosals extend ventrolaterally to the lateral extent of the paraoccipital process (159-1); and (10) the presence of a notch between the premaxilla and maxilla (196-0).

Relationships inside Orientalosuchina

Orientalosuchus naduongensis and *Jiangxisuchus nankangensis* share a very similar pterygoid around the choana opening (123-2), which strongly resembles the morphology of *Osteolaemus tetraspis* Cope, 1861 and *Voay robustus*. The choanal region in *Krabisuchus siamogallicus* (though not intact) looks like the pterygoid surface is flush with the choanal margin (123-0). In *Eoalligator chunyii* and *Protoalligator huiningensis* the pterygoid is not preserved. The pterygoid forming a neck around the choana is a condition unknown for any other alligatoroid and could be a further synapomorphy for Orientalosuchina with a potential reversal in *K. siamogallicus*.

A further potential synapomorphy for the group is the axial hypapophysis located towards the centrum of the axis body (15-1) in *Orientalosuchus naduongensis* and

Eoalligator chunyii. The axis is, unfortunately, not preserved in any other members of Orientalosuchina. A shifted axial hypapophysis among Crocodylia is otherwise only present in Diplocynodontinae and *Crocodylus depressifrons*.

The clade of *Orientalosuchus naduongensis* + *K. siamogallicus* has no synapomorphies in all trees, but has five in some trees including (1) the intersupratemporal bar being similarly broad as the supratemporal fenestra (199-1); (2) the dentary curves deeply between the fourth and 10th dentary alveoli (50-1); (3) a palatine-pterygoid-suture situated far from the posterior angle of the suborbital fenestra (118-1); (4) the frontoparietal suture lies entirely on the skull table (150-2); and (5) the anterior and medial teeth have dominant vertical ridges on their labial surface (198-1) and to a lesser extent on their mesial side. Such strong ridges are only present in few crocodylians (*Allodaposuchus precedens*, *Allodaposuchus subjuniperus* and *Maomingosuchus petrolica*), but not in other member of Alligatoidea.

[Martin & Lauprasert \(2010\)](#) described *K. siamogallicus* as having unusually long lacrimals, reaching the premaxilla and as a result preventing the maxilla from contacting the nasal. These sutures are more likely the preorbital ridges (97-1) also present in *Orientalosuchus naduongensis*. These ridges may be a further autapomorphy for *Orientalosuchus naduongensis* or a synapomorphy for *Orientalosuchus naduongensis* + *K. siamogallicus*. Prominent preorbital ridges are otherwise only present in *Mourasuchus atopus* [Langston, 1966](#) among alligatoroids and in some members of Crocodyloidea, like in *Osteolaemus tetraspis* and *Crocodylus porosus*, but these structures are more prominently developed in *Orientalosuchus naduongensis*.

Orientalosuchus naduongensis is characterized by a very large supraoccipital exposure on the skull table (160-3), whereas the exposure is large (160-2) in *Eoalligator chunyii* and *K. siamogallicus*, but small (160-0) in *J. nankangensis*. The state of this character for *Protoalligator huiningensis* is unknown. A very large supraoccipital exposure is otherwise found in some Caimaninae, but in most of those taxa, except for *Globidentosuchus brachyrostris*, the supraoccipital is not trapezoid-shaped but block-shaped.

Omitting *Protoalligator huiningensis* from the phylogenetic analysis results in a sister taxon relationship between *J. nankangensis* and *Eoalligator chunyii*, forming a sister group to *Orientalosuchus naduongensis* + *K. siamogallicus*. A close relationship between the two Late Cretaceous/early Paleocene species *J. nankangensis* and *Eoalligator chunyii* was also recently found in the analysis of [Li, Wu & Rufolo \(2019\)](#), although the clade was nested inside of Crocodyloidea.

***Brachychampsia* spp., *Stangerochampsia mccabei* and Orientalosuchina**

In some trees, the monophyly of *Stangerochampsia mccabei* + *Brachychampsia* spp. + Orientalosuchina is supported by: (1) a dorsally projecting naris (81-1), (2) a large incisive foramen, intersecting the premaxillary-maxillary suture (88-2), (3) a maxilla with posterior process between lacrimal and prefrontal (128-2) and (4) a frontoparietal suture making modest entry into the supratemporal fenestra (150-1).

The monophyly of *Brachychampsa* spp. + Orientalosuchina is supported by: (1) the fifth maxillary alveolus as the largest (93-1) and (2) a large supraoccipital exposure on the skull table (160-2).

In basal members of Alligatoroidea (*Diplocynodon* spp. and *Leidyosuchus canadensis*), the fourth and fifth maxillary teeth have the same size (93-3), whereas it is the fourth tooth (93-2) in members of Alligatoridae. The only exception is the Late Cretaceous/early Paleocene *Bottosaurus harlani*, although position of this taxon inside Caimaninae is questionable (*Cossette & Brochu, 2018*).

The monophyly of *Brachychampsa montana* + Orientalosuchina is supported by the anterior tip of the splenial passing ventrally to the Meckelian groove (54-1).

A closer relationship between *Brachychampsa montana* and Orientalosuchina than between *Brachychampsa montana* and *Brachychampsa sealeyi* seems unlikely and could be an artifact due to the poor preservation of the latter.

Navajosuchus mooki* and *Ceratosuchus burdoshi

The shift to a more basal position of *N. mooki* and *Ceratosuchus burdoshi* compared to Alligatoridae in this study can be explained by: (1) a straight dentary (50-0), (2) the presence of a large incisive foramen (88-1), and (3) a relatively flat skull in lateral view (193-0) unlike in the monophyletic group consisting of *Arambourgia gaudryi* (*De Stefano, 1905*) + *Hassiacosuchus haupti* + *Wannaganosuchus brachymanus* (*Erickson, 1982*) + *Allognathosuchus* spp..

***Allognathosuchus* spp.**

The monophyly of *Allognathosuchus* spp. is supported by: (1) a surangular-dentary suture intersecting the external mandibular fenestra at the posterodorsal corner (64-1) and (2) an anterior jugal process extending anterior to the frontal (195-0). In *Wannaganosuchus brachymanus*, *Arambourgia gaudryi* and *Hassiacosuchus haupti*, the anterior jugal process lies at the same height as the anterior frontal process (195-1).

***Alligator* spp.**

In the present phylogeny, *Alligator* is polyphyletic with *Alligator prenasalis* (*Loomis, 1904*) + *Alligator mcgrewi* (*Schmidt, 1941*) outside the other *Alligator* species due to a long dentary symphysis (49-1). They further differ in: (1) an anterodorsally projecting naris (81-0), (2) a lingual foramen for the articular artery and alveolar nerve perforating the surangular/angular suture (69-1) and (3) a maxilla bearing a broad shelf extending into the suborbital fenestra (112-1). The last two characters, however, can also be found in other *Alligator* species (*Alligator mississippiensis*, *Alligator mefferdi* (*Mook, 1946*) and *Alligator sinensis*).

Caimaninae

Eocaiman caverensis (*Simpson, 1933*) is found as the sister taxon to most of other caimans with the exception of the Miocene *Globidentosuchus brachyrostris* and *Culebrasuchus mesoamericanus*, which are found in an ancestral position in the current analysis, with *Globidentosuchus brachyrostris* as the most basal caiman.

This basal position of *Globidentosuchus brachyrostris* results mainly from (1) the splenial participating in the mandibular symphysis (54-0), (2) a concavoconvex frontoparietal suture (151-0) and (3) a trapezoid-shaped supraoccipital exposure on the skull table (202-0). *Globidentosuchus brachyrostris* and *Culebrasuchus mesoamericanus* both differ from most of other Caimaninae in: (1) having an angular-surangular suture contacting the external mandibular fenestra at the posterior angle (60-0) and (2) an exoccipital terminating dorsally to the basioccipital tubers (176-0) in *Culebrasuchus mesoamericanus*, whereas this is unknown for *Globidentosuchus brachyrostris*.

Considering the Miocene age of both taxa, either they have a ghost lineage reaching back to the Cretaceous, or their basal position is an artifact due to incompleteness of those taxa.

As in [Cossette & Brochu \(2018\)](#), the Late Cretaceous/early Paleocene *Bottosaurus harlani* was found in a polytomy with *Paleosuchus* spp.. In the present analysis, however, *Tsoabichi greenriverensis* [Brochu, 2010](#) was also found inside this polytomy. The reason for this is the new character (202). In *Tsoabichi greenriverensis* and *Paleosuchus* spp., the large supraoccipital exposure is triangular (202-1), while it is block-shaped (202-2) or unknown for the remaining caimans, including all recent species.

Taxonomic status of the Maoming alligatoroid

Two taxa were pruned from the consensus tree because of their unstable positions: the fragmentary *Asiatosuchus nanlingensis* and the Maoming alligatoroid. The Maoming taxon ([Skutschas et al., 2014](#)) is either the sister taxon to *Orientalosuchus naduongensis* or placed inside Crocodylinae. This is due to the poor character support, resulting in the same character combination for the Maoming alligatoroid as that of the crocodyline *Brochuchus pigotti* ([Tchernov & van Couvering, 1978](#)).

Orientalosuchus naduongensis and the Maoming alligatoroid closely resemble each other in the prominent ridges along the nasals, the triangular-shaped lacrimals and anteriorly shifted supratemporal fenestrae are marked similarities. The Maoming alligatoroid was interpreted as lacking a premaxilla-maxilla notch ([Skutschas et al., 2014](#)), but this is likely an artifact of deformation as indicated by a flattened specimen of *Orientalosuchus naduongensis* ([Fig. 5](#)) in which the notch appears absent even though better preserved specimens clearly reveal the presence of the notch in this species. The complex sutural contact between the nasal and frontal, proposed for the Maoming alligatoroid by [Skutschas et al. \(2014\)](#), differs from *Orientalosuchus naduongensis* but the area in the Maoming specimen is damaged and an anterior process of the frontal, similar to the one in *Orientalosuchus naduongensis*, could be assumed, making the taxa identical in this regard. These two taxa further share a close geographic and temporal proximity and we predict that they either represent the same taxon or are closely related to each other.

Biogeographic implications

The Chinese alligator, *Alligator sinensis*, is the only recent alligatoroid in Asia and the timing and climatic context of its dispersal from North America to Asia is still unresolved ([Brochu, 1999](#); [Snyder, 2007](#); [Oaks, 2011](#); [Shan, Cheng & Wu, 2013](#); [Wang, Sullivan & Liu, 2016](#)). [Martin & Lauprasert \(2010\)](#) were the first to include an Asian alligatoroid

(*Krabisuchus siamogallicus*), other than *Alligator sinensis* into a phylogeny, followed by [Skutschas et al. \(2014\)](#) (Maoming alligatoroid), [Wang, Sullivan & Liu \(2016\)](#) (*Eoalligator chunyii* and *Protoalligator huiningensis*) and [Li, Wu & Rufolo \(2019\)](#) (*Jiangxisuchus nankangensis*).

Our phylogenetic analysis robustly places Orientalosuchina including all the above taxa distantly from *Alligator sinensis* and their morphology as well as their Cretaceous origin (*Eoalligator chunyii* and *J. nankangensis*) strongly suggest that they represent a more basal monophyletic clade of alligatoroids. East and Southeastern Asia was, therefore, colonized by alligatoroids twice: once by Orientalosuchina during the Late Cretaceous and once by the *sinensis* lineage during the Cenozoic ([Brochu, 1999](#)). For both lineages, dispersal via Beringia is the most consistent with paleogeography, climate, phylogeny, inferred stenohalinity, the fossil record, and divergence dates ([Taplin & Grigg, 1989](#); [Brochu, 1999](#); [Fiorillo, 2008](#); [Oaks, 2011](#); [Li, Wu & Rufolo, 2019](#)). Inferred late Maastrichtian lower eustatic sea level ([Kominz et al., 2008](#)) would have favored the dispersal of Orientalosuchina, which is consistent with the probable age of *Eoalligator chunyii* and *J. nankangensis*. Evidence for Late Cretaceous vertebrate dispersal from North America to Asia is otherwise scarce and include some tyrannosauroid, hadrosaurid, and ceratopsian dinosaurs ([Loewen et al., 2013](#); [Farke et al., 2014](#); [Prieto-Márquez et al., 2019](#)). Dispersal from Asia to North America, on the other hand, has been more commonly inferred for the Late Cretaceous ([Russell, 1993](#); [Hutchison, 2000](#); [Serenó, 2000](#); [Godefroit, Bolotsky & Alifanov, 2003](#)). The relationships of the Late Cretaceous *Asiatosuchus nanlingensis* from Asia and *Prodiplocynodon langi* from North America are yet to be resolved and, therefore, alligatoroids are so far the only crocodylians showing migration from North America to Asia during this time.

Timing of the dispersal of the *sinensis* lineage remains difficult to constrain because: (1) molecular divergence date estimates and fossil dates of crown-*Alligator* are in conflict, (2) pan-*sinensis* in Asia cannot be traced back further than the Pliocene ([Iijima, Takahashi & Kobayashi, 2016](#)), and (3) the dispersal may have occurred long after a possible North American divergence between *Alligator sinensis* and *mississippiensis*. The most recent molecular divergence date estimate placed the split between *Alligator sinensis* and *mississippiensis* at ≈ 58 –31 Ma ([Oaks, 2011](#)) as opposed to 14 Ma suggested by the earliest known fossil record of crown-*Alligator* (*Alligator thomsoni* [Mook & Thomson, 1923](#), [Brochu, 1997](#), this study). The early Miocene *Alligator olseni* [White, 1942](#) is also close to crown-*Alligator* ([Brochu, 1999](#); [Snyder, 2007](#), this study) and, thus, ca. 20 Ma can be considered the maximum divergence date of the lineage based on fossils. Even though the molecular data sampling of [Oaks \(2011\)](#) is using a multilocus sequence dataset of both mtDNA and nDNA, similar analyses have been subjected to overestimate shallow nodes (<10 MY), particularly when they are dated with old external priors ([Van Tuinen & Torres, 2015](#)). Given that both calibration points of [Oaks \(2011\)](#) are deep (Alligatorinae-Caimaninae split, 71–64 Ma; Crocodylia, 90 Ma), a potential overestimation of *Alligator* divergence should be taken into account. Climate obviously constrained *Alligator* dispersal via Beringia ([Markwick, 1998](#)) but a revised molecular clock analysis using shallower

calibration points and the inclusion of the Chinese Miocene *Alligator luicus* is critical for evaluating the more precise role it played.

CONCLUSIONS

Parsimony analysis finds the new late Eocene taxon from Vietnam, *Orientalosuchus naduongensis*, as the sister taxon to *Krabisuchus siamogallicus* from the Eocene of Thailand. Together they form a monophyletic extinct basal East to Southeastern Asian alligatoroid clade of Late Cretaceous origin that also included *Jiangxisuchus nankangensis*, *Eoalligator chunyii* and *Protoalligator huiningensis*. The current phylogeny supports at least two different dispersals from North America to Eastern Asia: one during the Late Cretaceous (*Orientalosuchina*) and a second during the Cenozoic (*Alligator sinensis* lineage). Improved fossil calibrations and taxon sampling will be vital for further constraining the timing and resolving the climatic/paleogeographical context of these dispersals.

APPENDIX

Modifications and new characters added to the characterlist of *Brochu & Storrs (2012)*

See [Supplementary file 2](#) for further modifications and [Supplementary file 3](#) for a complete character list.

(51) Largest dentary alveolus immediately caudal to fourth is (0) 13 or 14, (1) between 11 and 14 and a series behind it, (2) 11 or 12, (3) no differentiation, (4) behind 14, (5) 10. (modified from *Brochu & Storrs (2012)*).

Comments: According to *Brochu (2004:867)*, “this character expresses the enlarged rear dentition of some fossil alligatorids.” and “The exact position of the largest alveolus varies within species, but it is never in front of the thirteenth in most taxa, and is never behind the twelfth in crown-group caimans. Behind these, alveoli grow progressively smaller. But in some blunt-snouted forms, there is a third region of maximum diameter behind the thirteenth or fourteenth alveolus. This is where globular teeth erupt in those taxa bearing them-teeth erupting from the large 13th or 14th alveoli are still conical.”

We rephrased character state (1) of *Brochu & Storrs (2012)* from “largest dentary alveolus immediately caudal to fourth is 13 or 14 and a series behind it” to “between 11 and 14 and a series behind it” in order to score all taxa with enlarged posterior teeth, regardless the shape of the crown, with the same state. Previously, some taxa with a lower tooth count (e.g., *Hassiacosuchus haupti*) were scored with (1) despite the fact that their largest tooth was not the 13 or 14 because they also possess enlarged posterior teeth. In addition, taxa with enlarged posterior teeth that are compressed instead of globular were furthermore excluded previously from this state. For instance, in *Orientalosuchus naduongensis*, *Bottosaurus harlani*, *Procaimanoidea utahensis* (*Gilmore, 1946*) and *Procaimanoidea kayi* (*Mook, 1941*) the rear dentition consists of enlarged but laterally compressed teeth. Previously both species of *Procaimanoidea*, as well as *B. harlani* were scored with (2) as in recent *Alligator* spp. or *Caiman* spp., but here we score them as (1).

(193) Skull in lateral view relatively flat (0) or wedge-shaped (1) (new character).

Comments: A triangular- or wedge-shaped skull in lateral view occurs in some short snouted taxa. The character is not fully correlated with the presence of an anterodorsally positioned external narial opening because some fossil taxa with an anterodorsally positioned naris have a relatively long and flat snout (e.g. *Navajosuchus mooki*). The character is somewhat problematic to score due to the often occurring dorsoventrally deformation in most crocodylian fossils. In most taxa, the skull shows a sudden increase in height between the orbits giving it a slide-like outline in lateral view. In wedge-shaped taxa, however, the snout region is nearly straight triangular from the narial opening to the skull table, clearly visible in some basal alligatorines like *Hassiacosuchus haupti*.

All specimens of *Orientalosuchus naduogensis* are dorsoventrally compressed due to deformation, making a reliable scoring for this character impossible. The snout, however, looks more elongated than that of the typical wedge-shaped short snouted alligatorines. [Martin & Lauprasert \(2010\)](#) described *Krabisuchus siamogallicus* as having a similar morphology as *H. haupti* and the head of Kr-C-007 indeed looks wedge-shaped, although the preservation is suboptimal and it could be an artifact due to the apparent postmortem deformation.

(194) Nasal bone does (0) or does not (1) reach to the level of the orbita (new character).

Comments: In *Alligator*, the nasal usually reaches the level of the orbits, but not in *Alligator sinensis* in which the nasal terminates anterior to the orbits in the herein analyzed individuals (SMNS 4915, IRSNB 13904-3487). *Hassiacosuchus haupti* and *Arambourgia gaudryi* have a far posteriorly reaching nasal bone, while it is shorter in all other basal alligatorines and *Navajosuchus mooki*. In crown-group Caimaninae, only *Melanosuchus niger* ([Spix, 1825](#)), *Orthogenysuchus olseni* [Mook, 1924b](#) and both *Paleosuchus* species have a nasal bone, reaching to the level of the orbits. In Orientalosuchina, this character can be scored for *Orientalosuchus naduogensis* and *Krabisuchus siamogallicus*, which have far posterior reaching nasal processes reaching the orbita.

(195) Anterior process of jugal extends anterior (0), lies at the same level as (1), or well posterior to the anterior process of frontal (2). (Modified from [Jouve \(2016\)](#) (174), [Jouve et al. \(2008\)](#) (174), [Jouve \(2004\)](#) (177)).

Comments: In Crocodylia, the jugal shows different anterior extensions, which can be compared to the anterior extension of the frontal. In non-Brevirostres taxa, the anterior process of the jugal commonly lies posteriorly to the anterior frontal process, which is present in some species like *Procaimanoidea utahensis*, *Alligator mcgrewi* [Schmidt, 1941](#) or *Paleosuchus palpebrosus* ([Cuvier, 1807](#)), but in most Brevirostres, the anterior jugal process either extends anterior or lies at the same level as the anterior process of the frontal. The prior version of this character from [Jouve \(2016\)](#) did not differentiate between (0) and (1), which led to the present modification of this character.

Among Globidonta, the jugal extends anteriorly to the frontal (0) in *Allognathosuchus polyodon* ([Cope, 1873](#)), *Allognathosuchus wartheni* [Case, 1925](#), *Alligator sinensis*, *Alligator*

mississippiensis and *Alligator prenasalis*, as well as in *Brachychampsa montana* and *Stangerochampsa mccabei* while it is on the same level (1) in *Hassiacosuchus haupti*, *Arambourgia gaudryi*, *Navajosuchus mooki*, *Wannaganosuchus brachymanus* and *Procaimanoidea kayi*. In crown-group Caimaninae, the process always reaches anterior to the frontal, except for *Paleosuchus palpebrosus* and *Melanosuchus niger*, in which the process lies on the same height as the frontal. For Orientalosuchina, only *Orientalosuchus naduongensis* could be reliably be scored as state (1).

(196) Notch between the premaxilla and maxilla present (0) or not present (1) in adult individuals (new character).

Comments: A few characters in the matrix are referring to an early ontogenetic state of a taxon (10, 25, 60, 87, 91, 126 and 152). The reason for this is potential changes during ontogeny like the development of a notch between the premaxilla and maxilla late in ontogeny in *Caiman crocodilus* (*Linnaeus, 1758*) (*Brochu, 1999*).

However, several fossil taxa are scored for such “ontogenetic characters” even if no juvenile specimens are known.

We added a new character that pertains to the presence of the premaxillary-maxillary notch in adult individuals in order to allow consistent scoring of fossil taxa with unknown juvenile stage. To avoid double weighting, character (91) was reviewed based on published work and if the scoring was solely based on adult individuals, they were rescored as (?) and the previous scoring was added to the new character (196).

(197) Sutural contact of the exoccipitals dorsal to the foramen magnum (0) long, at least half the height of the foramen magnum, (1) short, shorter than half the height of the foramen magnum, or (2) no sutural contact between the exoccipitals (new character).

Comments: In recent *Crocodylus* and *Alligator* species, the supraoccipital does not project far ventrally, resulting in a relatively long suture between the two exoccipitals. In for example, *Osteolaemus tetraspis* and some globidonts (*Brachychampsa montana*, *Stangerochampsa mccabei*, *Hassiacosuchus haupti*, *Arambourgia gaudryi* and *Eoalligator chunyii*) the supraoccipital projects further ventrally and the sutural contact between the exoccipitals becomes smaller, until it is only roughly half as long as the maximal height of the foramen magnum. Unfortunately, in many fossil taxa, the occipital region is too poorly preserved or not figured to reliably score this character, but it could be valuable to understand whether some basal *Alligator* species show a short suture and if there are differences between basal Alligatorinae taxa. Among recent Caimaninae, in *Paleosuchus palpebrosus* and *Melanosuchus niger* the suture is long and it is short in *Caiman crocodilus* and *Caiman latirostris* (*Daudin, 1802*). In Orientalosuchina, only *Eoalligator chunyii* could be scored (with a short suture).

In two non-Brevirostres taxa (*Allodaposuchus precedens* and *Borealosuchus sternbergii* (*Gilmore, 1911*)) the supraoccipital reaches the foramen magnum preventing the exoccipitals from contacting one another.

(198) Anterior maxillary teeth without (0) or with (1) ridges on their lateral surface (new character).

Comments: In many crocodylians, the maxillary teeth bear fine striae, but in *Orientalosuchus naduongensis* and *Krabisuchus siamogallicus* there are marked dorsoventrally running ridges present on the labial surface of the anterior teeth, (unknown for *Eoalligator chunyii*). Dominant ridges are also present in the tomistomine *Maomingosuchus petrolica* and in *Allodaposuchus precedens* and *Allodaposuchus subjuniperus*.

(199) Intersupratemporal bar (0) as or near as broad as the supratemporal fenestra, (1) at least twice as broad as the supratemporal fenestra, (2) around half the broadness of the supratemporal fenestra or (3) constricted, less than half the broadness of the supratemporal fenestra (new character).

Comments: The intersupratemporal region differs among crocodylians, but most commonly, the region is either similarly broad as the supratemporal fenestra or constricted, especially in longirostrine taxa. The level of constriction was divided in two states (2 and 3). A markedly broad state is only present in few taxa, especially in crown-group Caimaninae in which the supratemporal fenestrae are overgrown, but it is not completely correlated with (152) as a broad intersupratemporal bar is also present in *Procaimanoidea kayi*, which has open fenestrae.

Other globidonts mostly have an intersupratemporal bar as broad as the fenestra or a slender, but not constricted one. Exceptions are *Brachychampsa montana*, *Ceratosuchus burdoshi* and *Eoalligator chunyii*, which have a constricted bar.

(200) If largest dentary alveolus is between 11th and 14th and a series behind it, is it the (0) 11th, (1) 12th, or (2) 13th to 14th (new character).

Comments: This character is only applicable for taxa with (51-1).

(201) Surangular-angular suture lingually originates (0) near the ventral border of the external mandibular fenestra, (1) near the dorsal border of the external mandibular fenestra and straight, (2) near the dorsal border of the external mandibular fenestra and bowed (new character).

Comments: In most crocodylians, the surangular-angular suture lingually originates near the ventral border of the external mandibular fenestra (201-0). In *Orientalosuchina*, however, the suture originates near the dorsal border of the external mandibular fenestra and is notably straight (201-1). The state is, however, unknown for *Eoalligator chunyii*. The only other taxon showing this morphology is *Maomingosuchus petrolica*. In *Stangerochampsa mccabei* and *Voay robustus* (*Grandidier & Vaillant, 1872*), the suture also originates near the dorsal border of the fenestra, but the suture is notably bowed (201-2).

(202) Large to very large supraoccipital exposure on skull table is (0) trapezoid, (1) triangular, or (2) block-shaped (new character).

Comments: In most crocodylians, the supraoccipital exposure on the skull table is either small (160-0) or absent (160-1). In some species, however, the exposure is either large (160-2) or very large, excluding the parietal from the posterior edge of skull table (160-3). Among species with a large to very large exposure, the shape can differ markedly. In *Orientalosuchina*, except for *Jiangxisuchus nankangensis*, which only has a small exposure, the supraoccipital is trapezoid. This also true for *Stangerochampsia mccabei*, *Brachychampsia* spp., *Bottosaurus harlani* and *Globidentosuchus brachyrostris*. In most *Caimaninae*, on the other hand, the shape is either triangular, for example, in *Paleosuchus* spp. or block-shaped like in *Caiman* spp.. This character is only applicable for taxa with large to very large supraoccipital exposure on the skull roof.

INSTITUTIONAL ABBREVIATIONS

AMNH	American Museum of Natural History, New York, USA
GMH	Geiseltal Museum of Martin-Luther-University Halle-Wittenberg, Halle (Saale), Germany
GPIT	Geologisch-Paläontologisches Institut Tübingen, Tübingen, Germany
IRSNB	Institut royal des Sciences naturelles de Belgique Brussels, Belgium
IVPP	Institute of Vertebrate Paleontology and Paleoanthropology, Chinese Academy of Sciences, Beijing, China
Kr	Krabi crocodylian, Sirindhorn Museum, Kalasin Province, Thailand
SMNS	Staatliches Museum für Naturkunde Stuttgart, Stuttgart
SZ	Museum der Universität Tübingen, Zoologische Schausammlung, Tübingen, Germany
UMMP	University of Michigan, Museum of Paleontology, Ann Arbor, USA.

ACKNOWLEDGEMENTS

Christopher Brochu, an anonymous reviewer and the editor Hans-Dieter Sues are thanked for their comments that helped us improving the manuscript. We thank our Vietnamese colleagues who facilitated and participated in the Na Duong paleontological expeditions of 2009, 2011 and 2012: Nguyễn Việt Hưng, La Thế Phúc, Đặng Ngọc Trần, Đỗ Đức Quang, Phan Đồng Pha. The authors further wish to thank Erich Weber (Zoologische Schausammlung Tübingen), Massimo Delfino (University of Turin), Roland Sookias (Museum für Naturkunde Berlin), Hervé Bocherens (University of Tübingen), and Walter G. Joyce (University of Fribourg) for discussions. We are indebted to Jeremy Martin (University of Lyon) for providing us with photographs of *Krabisuchus siamogallicus*. Wolfgang Gerber is thanked for helping with photographing the cranial material in [Figs. 2–9](#); Regina Ellenbracht and Henrik Stöhr for preparation. Juliane Hinz and Adrian Tröscher (University of Tübingen) helped with manuscript proofreading. Erich Weber, Ingmar Werneburg (University of Tübingen), Alexander Kupfer (Staatliches Museum für Naturkunde Stuttgart), Oliver Wings and Michael Stache (Martin Luther University of Halle-Wittenberg), Torsten Wappler (Hessisches Landesmuseum Darmstadt), H. Dieter Schreiber (Staatliches Museum für Naturkunde Karlsruhe) are

thanked for providing access to specimens under their care. The Willi Hennig Society is thanked for providing access to the software TnT 1.5.

ADDITIONAL INFORMATION AND DECLARATIONS

Funding

This study was supported by the Volkswagen Foundation grant 90 978 (to Márton Rabi). All fieldwork was funded by Deutsche Forschungsgemeinschaft grant numbers BO 1550/11-1 & 2 and 417629144. The funders had no role in study design, data collection and analysis, decision to publish, or preparation of the manuscript.

Grant Disclosures

The following grant information was disclosed by the authors:

Volkswagen Foundation: 90 978.

Deutsche Forschungsgemeinschaft: BO 1550/11-1 & 2 and 417629144.

Competing Interests

The authors declare that they have no competing interests.

Author Contributions

- Tobias Massonne conceived and designed the experiments, performed the experiments, analyzed the data, prepared figures and/or tables, authored and reviewed drafts of the paper, approved the final draft.
- Davit Vasilyan conceived and designed the experiments, performed the experiments, reviewed drafts of the paper, approved the final draft.
- Márton Rabi conceived and designed the experiments, performed the experiments, analyzed the data, authored and reviewed drafts of the paper, approved the final draft.
- Madelaine Böhme conceived and designed the experiments, performed the experiments, reviewed drafts of the paper, approved the final draft.

Data Availability

The following information was supplied regarding data availability:

The raw data are available in the [Supplemental Files](#).

New Species Registration

The following information was supplied regarding the registration of a newly described species:

Publication LSID:

urn:lsid:zoobank.org:pub:08B6F167-AAC7-4184-97BA-B7467D4F036B.

Orientalosuchus LSID:

urn:lsid:zoobank.org:act:BAF6DB3F-0207-42E0-8220-06F9F6D89217.

Orientalosuchus naduongensis LSID:

urn:lsid:zoobank.org:act:9DEB3FC9-ED1F-4D30-96FE-236AD7B82C06.

Supplemental Information

Supplemental information for this article can be found online at <http://dx.doi.org/10.7717/peerj.7562#supplemental-information>.

REFERENCES

- Antunes MT. 1961.** *Tomistoma lisitanica*, crocodilien du Miocène du Portugal. *Revista|Faculdade de Ciências da Universidade de Lisboa* **9(Ser.2)**:5–88.
- Benammi M, Chaimanee Y, Jaeger JJ, Suteethorn V, Ducrocq S. 2001.** Eocene Krabi basin (southern Thailand): paleontology and magnetostratigraphy. *Geological Society of America Bulletin* **113(2)**:265–273.
- Benton MJ, Clark JM. 1988.** Archosaur phylogeny and the relationships of the Crocodylia. In: Benton MJ, ed. *The Phylogeny and Classification of the Tetrapods, Vol 1, Amphibians, Reptiles, Birds*. Oxford: Clarendon Press, 295–338.
- Berg DE. 1966.** Die Krokodile, insbesondere “*Asiatosuchus*” und aff. “*Sebecus?*”, aus dem Eozän von Messel bei Darmstadt/Hessen. *Hessisches Landesamt fuer Bodenforschung* **52**:1–105.
- Blainville DH. 1855.** *Ostéographie: atlas du genre Crocodilus: Explication des planches*. Paris, New York: J. B. Bailliere et fils, Bailliere brothers.
- Böhme M, Aiglstorfer M, Antoine PO, Appel E, Havlik P, Métais G, Phug LT, Schneider S, Setzer F, Tappert R, Tran DN, Uhl D, Prieto J. 2012.** Na Duong (northern Vietnam)—an exceptional window into Eocene ecosystems from Southeast Asia. *Zitteliana A* **53**:121–167.
- Bona P, Barrios F. 2015.** The Alligatoroidea of Argentina: an update of its fossil record. *Publicación Electrónica de la Asociación Paleontológica Argentina* **15(1)**:143–158.
- Brochu CA. 1997.** Fossils, morphology, divergence timing, and the phylogenetic relationships of *Gavialis*. *Systematic Biology* **46(3)**:479–522 DOI [10.1093/sysbio/46.3.479](https://doi.org/10.1093/sysbio/46.3.479).
- Brochu CA. 1999.** Phylogenetics, taxonomy, and historical biogeography of Alligatoroidea. *Journal of Vertebrate Paleontology* **19(S2)**:9–100 DOI [10.1080/02724634.1999.10011201](https://doi.org/10.1080/02724634.1999.10011201).
- Brochu CA. 2003.** Phylogenetic approaches toward crocodylian history. *Annual Review of Earth and Planetary Sciences* **31(1)**:357–397 DOI [10.1146/annurev.earth.31.100901.141308](https://doi.org/10.1146/annurev.earth.31.100901.141308).
- Brochu CA. 2004.** Alligatorine phylogeny and the status of *Allognathosuchus* Mook, 1921. *Journal of Vertebrate Paleontology* **24(4)**:857–873 DOI [10.1671/0272-4634\(2004\)024\[0857:APATSO\]2.0.CO;2](https://doi.org/10.1671/0272-4634(2004)024[0857:APATSO]2.0.CO;2).
- Brochu CA. 2007a.** Systematics and taxonomy of Eocene tomistomine crocodylians from Britain and Northern Europe. *Palaeontology* **50(4)**:917–928 DOI [10.1111/j.1475-4983.2007.00679.x](https://doi.org/10.1111/j.1475-4983.2007.00679.x).
- Brochu CA. 2007b.** Morphology, relationships, and biogeographical significance of an extinct horned crocodile (Crocodylia, Crocodylidae) from the Quaternary of Madagascar. *Zoological Journal of the Linnean Society* **150(4)**:835–863 DOI [10.1111/j.1096-3642.2007.00315.x](https://doi.org/10.1111/j.1096-3642.2007.00315.x).
- Brochu CA. 2010.** A new alligatorid from the lower Eocene Green River Formation of Wyoming and the origin of caimans. *Journal of Vertebrate Paleontology* **30(4)**:1109–1126 DOI [10.1080/02724634.2010.483569](https://doi.org/10.1080/02724634.2010.483569).
- Brochu CA. 2012.** Phylogenetic relationships of Palaeogene ziphodont eusuchians and the status of *Pristichampsus* Gervais, 1853. *Earth and Environmental Science Transactions of the Royal Society of Edinburgh* **103(3–4)**:521–550 DOI [10.1017/S1755691013000200](https://doi.org/10.1017/S1755691013000200).
- Brochu CA, Gingerich PD. 2000.** New tomistomine crocodylian from the middle Eocene (Bartonian) of Wadi Hitán, Fayum Province, Egypt. *Contributions of Museum of Paleontology of University of Michigan* **30**:251–268.
- Brochu CA, Storrs GW. 2012.** A giant crocodile from the Plio-Pleistocene of Kenya, the phylogenetic relationships of Neogene African crocodylines, and the antiquity of *Crocodylus*

- in Africa. *Journal of Vertebrate Paleontology* **32**(3):587–602
DOI [10.1080/02724634.2012.652324](https://doi.org/10.1080/02724634.2012.652324).
- Buscalioni AD, Ortega F, Vasse D. 1997.** New crocodiles (Eusuchia: Alligatoroidea) from the Upper Cretaceous of southern Europe. *Comptes Rendus de l'Académie des Sciences-Series IIA-Earth and Planetary Science* **325**(7):525–530.
- Buscalioni AD, Piras P, Vullo R, Signore M, Barbera C. 2011.** Early eusuchia crocodylomorpha from the vertebrate-rich Plattenkalk of Pietraroia (Lower Albian, southern Apennines, Italy). *Zoological Journal of the Linnean Society* **163**(suppl_1):S199–S227
DOI [10.1111/j.1096-3642.2011.00718.x](https://doi.org/10.1111/j.1096-3642.2011.00718.x).
- Buscalioni AD, Sanz JL, Casanovas ML. 1992.** A new species of the eusuchian crocodile *Diplocynodon* from the Eocene of Spain. *Neues Jahrbuch für Geologie und Paläontologie Abhandlungen* **187**:1–29.
- Case EC. 1925.** Note on a new species of the Eocene crocodylian *Allognathosuchus*, *A. wartheni*. *Contributions from the Museum of Geology, University of Michigan* **2**:93–97.
- Conrad JL, Jenkins K, Lehmann T, Manthi FK, Peppe DJ, Nightingale S, Cossette A, Dunsworth HM, Harcourt-Smith WEH, Mcnulty KP. 2013.** New specimens of ‘*Crocodylus*’ *pigotti* (Crocodylidae) from Rusinga Island, Kenya, and generic reallocation of the species. *Journal of Vertebrate Paleontology* **33**(3):629–646 DOI [10.1080/02724634.2013.743404](https://doi.org/10.1080/02724634.2013.743404).
- Cope ED. 1861.** List of the recent species of emydosaurian reptiles in the Museum of the Academy of Natural Sciences. *Proceedings of the Academy of Natural Sciences of Philadelphia* **12**:549–550.
- Cope ED. 1873.** On the extinct vertebrata of the Eocene of Wyoming: observed by the expedition of 1872, with notes on the geology. U.S. Geological Survey of Montana, Idaho, Wyoming, and Utah. Sixth Annual Report of the U.S. Geological Survey of the Territories by F. V. Hayden, 546–649.
- Cope ED. 1882.** The reptiles of the American Eocene. *American Naturalist* **16**(12):979–993
DOI [10.1086/273224](https://doi.org/10.1086/273224).
- Cossette AP, Brochu CA. 2018.** A new specimen of the alligatoroid *Bottosaurus harlani* and the early history of character evolution in alligatorids. *Journal of Vertebrate Paleontology* **38**:1–22.
- Cuvier FG. 1807.** Sur les différentes espèces de Crocodiles vivans et Sur leurs caractères distinctiss. *Annales du Museum d'Histoire Naturelle de Paris* **10**:8–66.
- Cuvier FG. 1825.** *Recherches sur les ossemens fossiles: ou l'on re' tablit les caracte`res de plusieurs animaux dont les re'volutions du globe ont de' truit les espe`ces*. Paris: G. Dufour et E. d'Ocagne.
- Daudin FM. 1802.** *Histoire naturelle, générale et particulière des Reptiles*. De L'Imprimerie de F. Paris: De L'Imprimerie de F. Dufart, 452.
- De Stefano G. 1905.** Appunti sui Batraci e rettili del Quercy appartenenti alla collezioni Rossignol. *Bolletino della Societa Geologia Italiana* **24**:17–67.
- Delfino M, Martin JE, Buffetaut E. 2008.** A new species of *Acynodon* (Crocodylia) from the upper cretaceous (Santonian–Campanian) of Villaggio del Pescatore, Italy. *Palaeontology* **51**(5):1091–1106 DOI [10.1111/j.1475-4983.2008.00800.x](https://doi.org/10.1111/j.1475-4983.2008.00800.x).
- Delfino M, Smith T. 2009.** A reassessment of the morphology and taxonomic status of ‘*Crocodylia*’ *depressifrons* (Crocodylia, Crocodyloidea) based on the Early Eocene remains from Belgium. *Zoological Journal of the Linnean Society* **156**(1):140–167
DOI [10.1111/j.1096-3642.2008.00478.x](https://doi.org/10.1111/j.1096-3642.2008.00478.x).
- Erickson BR. 1982.** *Wannaganosuchus*, a new alligator from the Paleocene of North America. *Journal of Paleontology* **56**:492–506.
- Farke AA, Maxwell WD, Cifelli RL, Wedel MJ. 2014.** A ceratopsian dinosaur from the Lower Cretaceous of Western North America, and the biogeography of Neoceratopsia. *PLOS ONE* **9**(12):e112055 DOI [10.1371/journal.pone.0112055](https://doi.org/10.1371/journal.pone.0112055).

- Fauvel AA. 1879. Alligators in China. *Journal of the North China Branch of the Royal Asiatic Society* 13:1–36.
- Fiorillo AR. 2008. Dinosaurs of Alaska: implications for the Cretaceous origin of Beringia. *Geological Society of America Special Papers* 442:313–326.
- Garbin CG, Böhme M, Joyce WG. 2019. A new testudinoid turtle from the middle to late Eocene of Vietnam. *PeerJ* 7(1):e6280 DOI 10.7717/peerj.6280.
- Gilmore CW. 1911. A new fossil alligator from the Hell Creek beds of Montana. *Proceedings of the United States National Museum* 41(1860):297–302 DOI 10.5479/si.00963801.41-1860.297.
- Gilmore CW. 1946. A new crocodylian from the Eocene of Utah. *Journal of Paleontology* 20:62–67.
- Gmelin J. 1789. *Linnei systema naturae*. Leipzig: GE Beer, 1057.
- Godefroit P, Bolotsky Y, Alifanov V. 2003. A remarkable hollow-crested hadrosaur from Russia: an Asian origin for lambeosaurines. *Comptes Rendus Palevol* 2(2):143–151 DOI 10.1016/S1631-0683(03)00017-4.
- Goloboff PA, Farris JS, Nixon KC. 2008. TNT, a free program for phylogenetic analysis. *Cladistics* 24(5):774–786 DOI 10.1111/j.1096-0031.2008.00217.x.
- Grandidier A, Vaillant L. 1872. Sur le crocodile fossile d'Amboulintsatre (Madagascar). *Comptes Rendus de l'Academie des Sciences de Paris* 75:150–151.
- Gray JE. 1844. *Catalogue of the tortoises, crocodiles, and amphisbaenians, in the collection of the British museum*. London: British Museum (Natural History).
- Hastings AK, Bloch JI, Jaramillo CA, Rincon AF, Macfadden BJ. 2013. Systematics and biogeography of crocodylians from the Miocene of Panama. *Journal of Vertebrate Paleontology* 33(2):239–263 DOI 10.1080/02724634.2012.713814.
- Hastings AK, Reisser M, Scheyer TM. 2016. Character evolution and the origin of Caimaninae (Crocodylia) in the new world tropics: new evidence from the Miocene of Panama and Venezuela. *Journal of Paleontology* 90(2):317–332 DOI 10.1017/jpa.2016.37.
- Hutchison JH. 2000. Diversity of Cretaceous turtle faunas of eastern Asia and their contribution to the turtle faunas of North America. *Paleontological Society of Korea Special Publication* 4(2):27–38.
- Huxley TH. 1875. On *Stagonolepis robertsoni*, and on the evolution of the Crocodylia. *Quarterly Journal of the Geological Society* 31(1–4):423–438 DOI 10.1144/GSL.JGS.1875.031.01-04.29.
- Iijima M, Takahashi K, Kobayashi Y. 2016. The oldest record of *Alligator sinensis* from the Late Pliocene of Western Japan, and its biogeographic implication. *Journal of Asian Earth Sciences* 124:94–101 DOI 10.1016/j.jseaes.2016.04.017.
- Jouve S. 2004. Etude des Crocodyliformes fini Crétacé-Paléogène du Bassin des Oulad Abdoun (Maroc) et comparaison avec les faunes africaines contemporaines: systématique, phylogénie et paléobiogéographie. Doctoral dissertation. Paris: Muséum national d'histoire naturelle.
- Jouve S. 2016. A new basal tomistomine (Crocodylia, Crocodyloidea) from Issel (Middle Eocene; France): palaeobiogeography of basal tomistomines and palaeogeographic consequences. *Zoological Journal of the Linnean Society* 177(1):165–182 DOI 10.1111/zoj.12357.
- Jouve S, Bardet N, Jalil N-E, Suberbiola XP, Bouya B, Amaghaz M. 2008. The oldest African crocodylian: phylogeny, paleobiogeography, and differential survivorship of marine reptiles through the Cretaceous-Tertiary boundary. *Journal of Vertebrate Paleontology* 28(2):409–421 DOI 10.1671/0272-4634(2008)28[409:TOACPP]2.0.CO;2.
- Kälin JA, Peyer B. 1936. *Hispanochampsia mülleri* nov. gen. sp., ein neuer Crocodylide aus dem unteren Oligocaen von Tárrega (Catalonien). *Abhandlungen der Schweizerische Paläontologischen Gesellschaft* 58:1–40.

- Kobatake N, Chiji M, Ikebe N, Ishida S, Kamei T, Nakaseko K, Matsumoto E. 1965.** Discovery of crocodile fossil from the Osaka Group. *Quaternary Research (Daiyonki-Kenkyu)* **4(2)**:49–58 DOI [10.4116/jaqua.4.49](https://doi.org/10.4116/jaqua.4.49).
- Kominz MA, Browning JV, Miller KG, Sugarman PJ, Mizintseva S, Scotese CR. 2008.** Late Cretaceous to Miocene sea-level estimates from the New Jersey and Delaware coastal plain coreholes: an error analysis. *Basin Research* **20(2)**:211–226 DOI [10.1111/j.1365-2117.2008.00354.x](https://doi.org/10.1111/j.1365-2117.2008.00354.x).
- Lambe LM. 1907.** On a new crocodylian genus and species from the Judith River formation of Alberta. *Transactions of the Royal Society of Canada* **4**:219–244.
- Langston W. 1966.** *Mourasuchus* price, *Nettosuchus* Langston, and the family Nettosuchidae (Reptilia: Crocodylia). *Copeia* **1966(4)**:882–885 DOI [10.2307/1441424](https://doi.org/10.2307/1441424).
- Li JL, Wang BZ. 1987.** A new species of Alligator from Shanwang, Shandong. *Vertebrata Palasiatica* **25(3)**:199.
- Li C, Wu X-C, Rufolo SJ. 2019.** A new crocodyloid (Eusuchia: Crocodylia) from the upper cretaceous of China. *Cretaceous Research* **94**:25–39 DOI [10.1016/j.cretres.2018.09.015](https://doi.org/10.1016/j.cretres.2018.09.015).
- Linnaeus C. 1758.** *Systema naturæ per regna tria naturæ, secundum classes, ordines, genera, species, cum characteribus, differentiis, synonymis, locis. Tomus I. Editio decima, reformata.* Stockholm: Laurentius Salvius.
- Loewen MA, Irmis RB, Sertich JJ, Currie PJ, Sampson SD. 2013.** Tyrant dinosaur evolution tracks the rise and fall of Late Cretaceous oceans. *PLOS ONE* **8(11)**:e79420 DOI [10.1371/journal.pone.0079420](https://doi.org/10.1371/journal.pone.0079420).
- Loomis FB. 1904.** Two new river reptiles from the titanotheres beds. *American Journal of Science* **18(108)**:427–432 DOI [10.2475/ajs.s4-18.108.427](https://doi.org/10.2475/ajs.s4-18.108.427).
- Ludwig R. 1877.** Fossile Crocodyliden aus der Tertiärformation des Mainzer Beckens. *Paleontographica Supplement* **3**:1–52.
- Markwick PJ. 1998.** Fossil crocodylians as indicators of Late Cretaceous and Cenozoic climates: implications for using palaeontological data in reconstructing palaeoclimate. *Palaeogeography, Palaeoclimatology, Palaeoecology* **137(3–4)**:205–271 DOI [10.1016/S0031-0182\(97\)00108-9](https://doi.org/10.1016/S0031-0182(97)00108-9).
- Marsh OC. 1871.** Notice of some new fossil reptiles from the Cretaceous and Tertiary formations. *American Journal of Science and Arts* **1(6)**:447–459 DOI [10.2475/ajs.s3-1.6.447](https://doi.org/10.2475/ajs.s3-1.6.447).
- Martin JE, Lauprasert K. 2010.** A new primitive alligatorine from the Eocene of Thailand: relevance of Asiatic members to the radiation of the group. *Zoological Journal of the Linnean Society* **158(3)**:608–628 DOI [10.1111/j.1096-3642.2009.00582.x](https://doi.org/10.1111/j.1096-3642.2009.00582.x).
- Mook CC. 1924a.** A new crocodylian from Mongolia. *American Museum Novitates* **117**:1–5.
- Mook CC. 1924b.** A new crocodylian from the Wasatch Beds. *American Museum Novitates* **137**:1–4.
- Mook CC. 1946.** A new Pliocene alligator from Nebraska. *American Museum Novitates* **1311**:295–304.
- Mook CC. 1941.** A new crocodylian, *Hassiacosuchus kayi*, from the Bridger Eocene beds of Wyoming. *Annals of Carnegie Museum* **28**:207–220.
- Mook CC, Thomson A. 1923.** A new species of *Alligator* from the Snake Creek beds. *American Museum Novitates* **73**:1–13.
- Müller S. 1838.** Waarnemingen over de Indische krokodillen en Beschrijving van eene nieuwe soort. *Tydschrift voor Natuurlijke Geschiedenis en Physiologie* **5**:67–87.
- Narváez I, Brochu CA, Escaso F, Pérez-García A, Ortega F. 2015.** New crocodyliforms from southwestern Europe and definition of a diverse clade of European Late Cretaceous basal eusuchians. *PLOS ONE* **10(11)**:e0140679 DOI [10.1371/journal.pone.0140679](https://doi.org/10.1371/journal.pone.0140679).

- Nopcsa F. 1928.** Paleontological notes on Reptilia. 7. Classification of the Crocodylia. *Geologica Hungarica, Series Palaeontologica* **1**:75–84.
- Oaks JR. 2011.** A time-calibrated species tree of Crocodylia reveals a recent radiation of the true crocodiles. *Evolution* **65**(11):3285–3297 DOI [10.1111/j.1558-5646.2011.01373.x](https://doi.org/10.1111/j.1558-5646.2011.01373.x).
- Ósi A, Clark JM, Weishampel DB. 2007.** First report on a new basal eusuchian crocodyliform with multicusped teeth from the Upper Cretaceous (Santonian) of Hungary. *Neues Jahrbuch für Geologie und Paläontologie-Abhandlungen* **243**(2):169–177.
- Owen R. 1874.** Monograph on the fossil Reptilia of the Wealden and Purbeck formations. Suppl. no. 6 (Hylaeochampsa). *Monograph of the Palaeontographical Society* **27**(6):7.
- Prieto-Márquez A, Fondevilla V, Sellés AG, Wagner JR, Galobart À. 2019.** *Adynomosaurus arcanus*, a new lambeosaurine dinosaur from the Late Cretaceous Ibero-Armorican Island of the European archipelago. *Cretaceous Research* **96**:19–37 DOI [10.1016/j.cretres.2018.12.002](https://doi.org/10.1016/j.cretres.2018.12.002).
- Puértolas-Pascual E, Canudo JI, Moreno-Azanza M. 2013.** The eusuchian crocodylomorph *Allodaposuchus subjuniperus* sp. nov., a new species from the latest Cretaceous (upper Maastrichtian) of Spain. *Historical Biology* **26**(1):91–109 DOI [10.1080/08912963.2012.763034](https://doi.org/10.1080/08912963.2012.763034).
- Puértolas E, Canudo JI, Cruzado-Caballero P. 2011.** A new crocodylian from the Late Maastrichtian of Spain: implications for the initial radiation of crocodyloids. *PLOS ONE* **6**(6): e20011 DOI [10.1371/journal.pone.0020011](https://doi.org/10.1371/journal.pone.0020011).
- Rogers JV II. 2003.** *Pachycheilosuchus trinquei*, a new procoelous crocodyliform from the Lower Cretaceous (Albian) Glen Rose Formation of Texas. *Journal of Vertebrate Paleontology* **23**(1):128–145 DOI [10.1671/0272-4634\(2003\)23\[128:PTANPC\]2.0.CO;2](https://doi.org/10.1671/0272-4634(2003)23[128:PTANPC]2.0.CO;2).
- Roos J, Aggarwal RK, Janke A. 2007.** Extended mitogenomic phylogenetic analyses yield new insight into crocodylian evolution and their survival of the Cretaceous-Tertiary boundary. *Molecular Phylogenetics and Evolution* **45**(2):663–673 DOI [10.1016/j.ympev.2007.06.018](https://doi.org/10.1016/j.ympev.2007.06.018).
- Russell DA. 1993.** The role of Central Asia in dinosaurian biogeography. *Canadian Journal of Earth Sciences* **30**(10):2002–2012 DOI [10.1139/e93-176](https://doi.org/10.1139/e93-176).
- Scheyer TM, Aguilera OA, Delfino M, Fortier DC, Carlini AA, Sánchez R, Carrillo-Briceno JD, Quiroz L, Sánchez-Villagra MR. 2013.** Crocodylian diversity peak and extinction in the late Cenozoic of the northern Neotropics. *Nature Communications* **4**:1907.
- Schmidt KP. 1938.** New crocodylians from the upper Paleocene of western Colorado. *Field Museum of Natural History Geological Series* **6**:315–321.
- Schmidt KP. 1941.** A new fossil alligator from Nebraska. *Fieldiana: Geology* **8**:27–32.
- Sereno PC. 2000.** The fossil record, systematics and evolution of pachycephalosaurs and ceratopsians from Asia. In: Benton MJ, Shishkin MA, Unwin DM, Kurochkin EN, eds. *The Age of Dinosaurs in Russia and Mongolia*. Cambridge: Cambridge University Press, 480–516.
- Shan H-Y, Cheng Y-N, Wu X-C. 2013.** The first fossil skull of *Alligator sinensis* from the Pleistocene, Taiwan, with a paleogeographic implication of the species. *Journal of Asian Earth Sciences* **69**:17–25 DOI [10.1016/j.jseaes.2012.05.026](https://doi.org/10.1016/j.jseaes.2012.05.026).
- Shan HY, Wu XC, Cheng YN, Sato T. 2009.** A new tomistomine (Crocodylia) from the Miocene of Taiwan. *Canadian Journal of Earth Sciences* **46**(7):529–555 DOI [10.1139/E09-036](https://doi.org/10.1139/E09-036).
- Shan HY, Wu XC, Cheng YN, Sato T. 2017.** *Maomingosuchus petrolica*, a restudy of ‘*Tomistoma*’ *petrolica* Yeh, 1958. *Palaeoworld* **26**(4):672–690 DOI [10.1016/j.palwor.2017.03.006](https://doi.org/10.1016/j.palwor.2017.03.006).
- Simpson GG. 1930.** *Allognathosuchus mooki*, a new crocodile from the Puerco Formation. *American Museum Novitates* **445**:1–16.
- Simpson GG. 1933.** A new crocodylian from the Notostylops beds of Patagonia. *American Museum Novitates* **965**:1–20.

- Skutschas PP, Danilov IG, Kodrul TM, Jin J. 2014.** The first discovery of an alligatorid (Crocodylia, Alligatoroidea, Alligatoridae) in the Eocene of China. *Journal of Vertebrate Paleontology* **34**(2):471–476 DOI [10.1080/02724634.2013.809725](https://doi.org/10.1080/02724634.2013.809725).
- Snyder D. 2007.** Morphology and systematics of two Miocene alligators from Florida, with a discussion of *Alligator* biogeography. *Journal of Paleontology* **81**(5):917–928 DOI [10.1666/pleo05-104.1](https://doi.org/10.1666/pleo05-104.1).
- Spix JB. 1825.** Animalia nova sive species novae Lacertarum, quas in itinere per Brasiliam annis MDCCCXVII-MDCCCXX jussu et auspiciis Maximiliani Josephi I. In: *Bavaria Regis suscepto collegit et descripsit D. J. B. De Pix*. Munich: Typis Franc. Seraph. Hübschamanni.
- Taplin LE, Grigg GC. 1989.** Historical zoogeography of the eusuchian crocodylians: a physiological perspective. *American Zoologist* **29**(3):885–901 DOI [10.1093/icb/29.3.885](https://doi.org/10.1093/icb/29.3.885).
- Tchernov E, van Couvering J. 1978.** New crocodiles from the early Miocene of Kenya. *Palaeontology* **21**:857–867.
- Toula F, Kail JA. 1885.** Über einen Krokodil-Schädel aus den Tertiärlagerungen von Eggenburg in Niederösterreich: eine paläontologische Studie. *Denkschriften der Kaiserlichen Akademie der Wissenschaften von Wien, Mathematisch-naturwissenschaftliche Klasse* **50**:299–355.
- Van Tuinen M, Torres CR. 2015.** Potential for bias and low precision in molecular divergence time estimation of the Canopy of Life: an example from aquatic bird families. *Frontiers in Genetics* **6**(362):203 DOI [10.3389/fgene.2015.00203](https://doi.org/10.3389/fgene.2015.00203).
- Von Meyer H. 1832.** *Paleologica zur Geschichte der Erde und ihrer Geschöpfe*. Frankfurt-am-Main: S. Schmerber, 560.
- Wang YY, Sullivan C, Liu J. 2016.** Taxonomic revision of *Eoalligator* (Crocodylia, Brevirostres) and the paleogeographic origins of the Chinese alligatoroids. *PeerJ* **4**(5562):e2356 DOI [10.7717/peerj.2356](https://doi.org/10.7717/peerj.2356).
- Weitzel K. 1935.** *Hassiacosuchus haupti* n. sp., ein durophages Krokodil aus dem Mitteleozän von Messel. *Notizblatt des Vereins für Erdkunde und der Hessischen Geologischen Landesanstalt Darmstadt* **16**:40–49.
- White TE. 1942.** A new alligator from the Miocene of Florida. *Copeia* **1942**(1):3–7 DOI [10.2307/1437933](https://doi.org/10.2307/1437933).
- Williamson TE. 1996.** *Brachychampsia sealeyi*, sp. nov., (Crocodylia, Alligatoroidea) from the Upper Cretaceous (lower Campanian) Menefee Formation, northwestern New Mexico. *Journal of Vertebrate Paleontology* **16**(3):421–431 DOI [10.1080/02724634.1996.10011331](https://doi.org/10.1080/02724634.1996.10011331).
- Wu XC, Brinkman DB, Russell AP. 1996.** A new alligator from the Upper Cretaceous of Canada and the relationship of early eusuchians. *Palaeontology* **39**:351–376.
- Wu XC, Li C, Wang YY. 2018.** Taxonomic reassessment and phylogenetic test of *Asiatosuchus nanlingensis*. Young 1964 and *Eoalligator chunyii* Young, 1964. *Vertebrata Palasiatica* **56**:137–146.
- Wu X, Wang Y, Zhou K, Zhu W, Nie J, Wang C. 2003.** Complete mitochondrial DNA sequence of Chinese alligator, *Alligator sinensis*, and phylogeny of crocodiles. *Chinese Science Bulletin* **48**(19):2050–2054.
- Yeh HK. 1958.** A new crocodile from Maoming, Kwangtung. *Vertebrata Palasiatica* **2**(4):237–242.
- Young CC. 1964.** New fossil crocodiles from China. *Vertebrata Palasiatica* **8**(2):189–208.
- Young CC. 1982.** *A Cenozoic crocodile from Huaining, Anhui. Selected works of Yang Zhongjian*. China: Academia Sinica, 47–48.
- Zangerl R. 1944.** *Brachyuranochampsia eversolei*, gen. et sp. nov., a new crocodylian from the Washakie Eocene of Wyoming. *Annals of Carnegie Museum* **30**:77–84.

Second Paper

A new species of *Maomingosuchus* from the Eocene of the Na Duong Basin (northern Vietnam) sheds new light on the phylogenetic relationships of tomistomine crocodylians and their dispersal from Europe to Asia



Massonne Tobias, Augustin Felix J., Matzke Andreas T., Weber Erich and Böhme Madelaine

Journal of Systematic Palaeontology, 19(22), 1551–1585, 2021

<https://doi.org/10.1080/14772019.2022.2054372>



A new species of *Maomingosuchus* from the Eocene of the Na Duong Basin (northern Vietnam) sheds new light on the phylogenetic relationship of tomistomine crocodylians and their dispersal from Europe to Asia

Tobias Massonne^{a,b,*} , Felix J. Augustin^b , Andreas T. Matzke^b, Erich Weber^c and Madelaine Böhme^{a,b}

^aSenckenberg Center of Human Evolution and Palaeoecology, Tübingen, Germany; ^bDepartment of Geosciences, Eberhard-Karls-Universität Tübingen, Tübingen, Germany; ^cInstitute for Evolution and Ecology, Eberhard-Karls-Universität Tübingen, Tübingen, Germany

(Received 28 September 2021; accepted 14 March 2022)

Maomingosuchus acutirostris sp. nov. is a new tomistomine crocodile from the middle–upper Eocene deposits (late Bartonian–Priabonian age, 39–35 Ma) of the Na Duong Basin in northern Vietnam. *M. acutirostris* can be differentiated from the type species *Maomingosuchus petrolicus* by having an acute anterior tip of the premaxilla. Both species differ from another *Maomingosuchus* from Krabi (Thailand) by differences in the surangular–dentary suture and maxillary alveoli. According to our phylogenetic results, *M. acutirostris* seems to be the sister species to the group *M. petrolicus* + Krabi-*Maomingosuchus*. The close relationship between those three tomistomines is supported in the present phylogenetic analysis by three synapomorphies. In our phylogenetic analysis, *Maomingosuchus* was retrieved in a basal position forming the sister group to *Paratomistoma* + *Gavialosuchus* + *Melitosaurus* + *Tomistoma*, including the extant *Tomistoma schlegelii*. This phylogeny indicates three different dispersal events of Tomistominae from Europe towards eastern Asia: 1) for the stem lineage of *Maomingosuchus*, no later than the late Eocene; 2) for the stem lineage of *Penghusuchus pani* + *Toyotamaphimeia machikanensis*, no later than the early–middle Miocene; and (3) for the stem lineage of *T. schlegelii*, during the Neogene.

<http://zoobank.org/urn:lsid:zoobank.org:pub:19B27C1E-0A3F-4425-AA8C-F904277DF327>

Keywords: Eocene; Crocodylia; Asia; phylogeny; biogeography

Introduction

The subfamily Tomistominae is commonly regarded as a monophyletic clade of crocodiles (e.g. Brochu 2007; Jouve 2016; Shan *et al.* 2017; Nicholl *et al.* 2020; but see Lee & Yates 2018; Iijima & Kobayashi 2019; Rio & Mannion 2021; Darlim *et al.* 2022) with only one living representative, the false gharial *Tomistoma schlegelii* (Müller, 1838) from the Malaysian Peninsula, Borneo, Sumatra and Java (Bezuijen *et al.* 2010). Their fossil record is much more diverse, with representatives found in Europe, Africa, America, Asia and Australia (Jouve *et al.* 2015; Jouve 2016; Kuzmin & Zvonok 2021; Ristevski *et al.* 2021). Previous studies suggested that Tomistominae originated in the upper Paleocene to lower Eocene in the region around western Tethys (e.g. Brochu 2007; Piras *et al.* 2007; Jouve *et al.* 2015; Jouve 2016; Shan *et al.* 2017; Martin *et al.* 2019), but the position of basal species differs between studies. *Marccosuchus zennaroi* Jonet & Wouters, 1977 was retrieved as the most basal taxon by several recent studies (Jouve *et al.* 2015; Jouve 2016; Shan *et al.* 2017;

Nicholl *et al.* 2020), whereas a polytomy between *Marccosuchus*, *Kentisuchus* and, if included, *Xaymacachampsia kugleri* (Berg, 1969) was recovered by others (Jouve *et al.* 2015; Iijima *et al.* 2018; Iijima & Kobayashi 2019; Martin *et al.* 2019; Nicholl *et al.* 2020).

During the early and middle Eocene, the tomistomine crocodiles lived in central and southern Europe (*Dollosuchoides densmorei* Brochu, 2007 and *Megadontosuchus arduini* [de Zigno, 1880]), northern Africa (*Tomistoma cairensis* Müller, 1927 and *Paratomistoma courti* Brochu & Gingerich, 2000) and even Central America (*Xaymacachampsia sensu* Jouve *et al.* 2015 and Jouve 2016). Slightly younger, during the middle–upper Eocene, the first undisputed tomistomines are known from Asia (Shan *et al.* 2017; Iijima *et al.* 2018; Martin *et al.* 2019; Nicholl *et al.* 2020). All other tomistomines from eastern Asia are Miocene and Pleistocene in age (*Toyotamaphimeia machikanensis* [Kobatake, ChiJi, Ikebe, Ishida, Kamei, Nakaseko & Matsumoto, 1965]) and *Penghusuchus pani* Shan, Wu,

*Corresponding author. Email: tobias.massonne@uni-tuebingen.de

Cheng & Sato, 2009) (Kobayashi *et al.* 2006; Shan *et al.* 2009; Iijima *et al.* 2018).

Maomingosuchus petrolicus (Yeh, 1958) was described based on a fragmentary skull. Later, a partially preserved individual was described by Li (1975), based on new material from the Youganwo Formation of the Maoming Basin; Shan *et al.* (2017) later provided a re-description of this material. Recently, another *Maomingosuchus* from Wai-Lek, Krabi Province, Thailand was described by Martin *et al.* (2019). Unfortunately, this specimen is poorly preserved and was provisionally referred to as *Krabi-Maomingosuchus* sp., but it might represent a distinct species.

In this study, we describe a new almost complete species of *Maomingosuchus*, which was excavated in the Na Duong Basin in northern Vietnam in 2011 (Böhme *et al.* 2013) and prepared at the laboratory of the

Geological-Palaeontological Institute of the Eberhard Karls University of Tübingen (GPIT). The new species allows novel insights into the anatomy of *Maomingosuchus*. We incorporated these new data in an expanded phylogenetic analysis of Tomistominae, retrieving a more basal position for *Maomingosuchus* than previously suggested (Shan *et al.* 2017; Iijima *et al.* 2018; Martin *et al.* 2019; Nicholl *et al.* 2020).

Geological setting

The Na Duong Basin is located in northern Vietnam near the Chinese border (Fig. 1). It represents one of the few areas in eastern and south-eastern Asia with a complete sequence of continental sediments from the middle Eocene–lower Oligocene (Böhme *et al.* 2013). The basin is part of the Cao Bang-Tien Yen fault system and

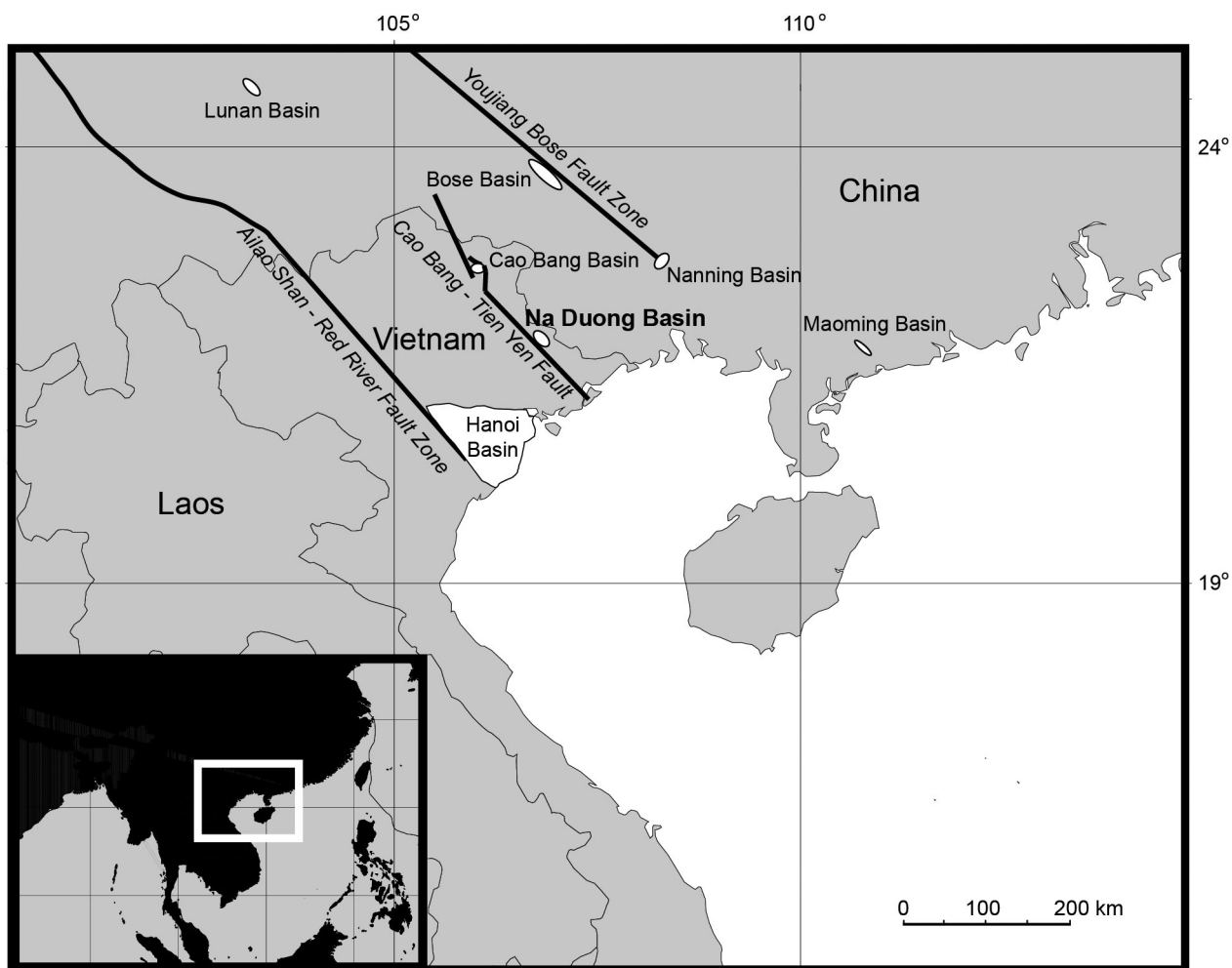


Figure 1. Map of the northern part of south-eastern Asia, showing the Na Duong Basin in north-eastern Vietnam close to the border with China (Böhme *et al.* 2013).

covers an area of 45 km². The middle–upper Eocene (late Bartonian–Priabonian, 39–35 Ma) Na Duong Formation is 240 m thick with the upper 140 m of the section being exposed in the Na Duong open cast coal mine.

The tomistomine remains described in this study were found within the transition zone between the coaly shale of the main seam and the underlying dark-brown claystone (layer 80).

The sediments of layer 80 are lacustrine lignitic shales and were deposited during a time of tropical to warm sub-tropical climate. During this time, this region was in a transitional stage from an environment characterized by shallow ponds to a large anoxic lake environment (Böhme *et al.* 2013; Garbin *et al.* 2019). The ecosystem yielded both aquatic and terrestrial faunal elements. The new tomistomine *Maomingosuchus acutirostris* occurred sympatrically with *Orientalosuchus naduongensis* Massonne, Vasilyan, Rabi & Böhme, 2019, members of Cetartiodactyla and Perissodactyla, many fish and two turtle species (Böhme *et al.* 2013; Garbin *et al.* 2019). While the majority of aquatic specimens were found articulated, the terrestrial mammals were preserved disarticulated (Garbin *et al.* 2019).

Materials and methods

All of the herein described material belongs to one individual GPIT-PV-31657, which was found at the base of layer 80 (*sensu* Böhme *et al.* 2011) in the Na Duong coal mine. The bones were disarticulated and dispersed over a small area of around 4 m². Since all of the bones were found in close proximity, and are of the same general size with no duplication of elements, it is clear that GPIT-PV-31657 represents a single individual. The material consists of a skull with articulated mandibles as well as the almost complete disarticulated postcranial material. The skull is dorsolaterally compressed, so the ventral and occipital regions are poorly preserved. The disarticulated vertebral column consists of the proatlas, seven cervical, 12 dorsal, two sacral and 15 caudal vertebrae, as well as multiple chevrons. Of the ribs, a single atlantal rib, seven cervical ribs and nine dorsal ribs are preserved. Both scapulae and coracoids are also preserved as well as both humeri and a single ulna, while the radius, the metacarpals and the manual phalanges are missing. Also preserved are both ilia, ischia and pubes, both femora, a single tibia and fibula, as well as four metatarsals, whereas all pedal phalanges are missing. Osteoderms from the dorsal and lateral body sections were found in large numbers.

For our phylogenetic analysis we used the dataset of Nicholl *et al.* (2020) (see [Supplemental material S1](#)), which was the most recent dataset focusing mainly on the relationships of tomistomines. Their dataset is mainly based on Jouve (2016), which is derived from multiple previous datasets including Brochu (1999) and Jouve *et al.* (2015). The focus of our updated phylogeny is to clarify the relationships of *Maomingosuchus* within the family Tomistominae. The species *Maomingosuchus acutirostris* sp. nov. as well as the Krabi-*Maomingosuchus* (Martin *et al.* 2019) were added to the dataset that now consists of 72 taxa and 244 characters. *Bernissartia fagesii* Dollo, 1883 was used as the out-group taxon. For the analysis, we followed Nicholl *et al.* (2020) and retained the 31 ordered characters from that analysis (characters 7, 30, 37, 62, 64, 75, 78, 81, 87, 91, 95, 103, 124, 131, 145, 151, 152, 153, 156, 161, 169, 171, 173, 174, 176, 177, 179, 194, 195, 206, 238). For *M. acutirostris* we scored 111 characters (see dataset in [Supplemental material S1](#)). Character scorings were modified for *Maomingosuchus petrolicus* and the Krabi-*Maomingosuchus* (a complete list of changes and the list of specimens are in [Supplemental material S2](#), while the list of characters is in [Supplemental material S3](#)).

We conducted a maximum parsimony analysis as a ‘traditional’ search in TNT v. 1.5 standard version updated on 31 March 2021 (Goloboff & Catalano 2016). We treated the multistate characters as ordered (see above) and equally weighted; set the maximum of trees to 99,999 and the tree replications to 1000. For the branch swapping algorithm, we used tree bisection reconnection with 10 trees saved per replication. A first run of heuristic search tree-bisection-reconnection failed to find all the most parsimonious trees (MPT) and, therefore, the heuristic search was repeated until the MPTs were found 50 times during each replicate (using the command ‘xmult = hits 50;’), as in Massonne *et al.* (2019). The trees retained in the memory were exposed to a second round of tree-bisection-reconnection.

We also conducted a ‘New Technology’ search due to the large dataset (Goloboff *et al.* 2008). The random addition sequence was set to 1000. For the search algorithm, sectorial search, ratchet and tree fusing were used. For sectorial search in the RSS settings, the maximal sector size was set to 36, representing half of the taxa in the dataset, in the CSS settings the rounds were set to 100 and the minimal sector size to five, and for the XSS settings the number of rounds was set to 10. In the ratchet settings the total number of iterations was set to 100, for tree fusing the rounds were set to 100. All other options were left as default. After the first round, we conducted a second round of new technology search with the trees saved from ram. Sectorial search was

disabled, and we changed the number of iterations in the ratchet settings to 1000 and the tree fusing to 1000 rounds. The result was filtered for sub-optimal trees and the analysis was run again until the number of found trees did not change further.

Institutional abbreviations

DM, Darwin Fossil Museum, Keelung, Taiwan; **GPIT** Geologisch-Paläontologisches Institut Tübingen, Tübingen, Germany; **NMNS** National Museum of Natural Science, Taichung, Taiwan.

Systematic palaeontology

Eusuchia Huxley, 1875 *sensu* Brochu 2003

Crocodylia Gmelin, 1789 *sensu* Benton & Clark 1988

Crocodyloidea Fitzinger, 1826 *sensu* Brochu 2003

Tomistominae Kälin, 1955 *sensu* Brochu 2003

Maomingosuchus Shan *et al.*, 2017

Emended genus diagnosis. *Maomingosuchus* is diagnosed by the unique combination of the following characters: 1) distinct dorsoventrally extending ridges on the lateral and mesial surfaces of the anterior teeth (shared with an indeterminate tomistomine from the Ikovo locality and some non-tomistomine taxa); 2) presence of a frontal fossa between the orbits, close to the posterior end of the prefrontals (shared with ‘*Crocodylus*’ *affinis* Marsh, 1871 and *Prodiplocynodon langi* Mook, 1941); 3) a flat frontal margin between the orbits (shared with *Dollosuchoides*). Only preserved in *Maomingosuchus acutirostris* and *Maomingosuchus petrolicus* are: 4) perforations for the first dentary tooth anterior to the external naris (shared with *Kentisuchus spenceri* [Buckland, 1836]); 5) 15 maxillary teeth in total (shared with *Dollosuchoides*); and (6) exoccipital with ventrally projecting lamina hiding the entrance to the cranio-quadrate passage (shared with gharials and basal eusuchians).

Maomingosuchus acutirostris sp. nov.

(Figs 2–14)

Diagnosis. *M. acutirostris* is a medium-sized tomistomine with a skull length (premaxilla–supraoccipital) of 546 mm and an estimated total length of around 3.5 m based on the skull to body length ratio of extant *Tomistoma schlegelii* (1:6.4 according to Whitaker & Whitaker 2008), which presumably has similar body proportions. It can be diagnosed by the combination of

the following characters: 1) relatively robust teeth, especially the 5th maxillary tooth and the 11th or 12th dentary teeth (similar to *Marccosuchus*); 2) anterior part of the prefrontal on the same level as anterior part of the frontal (shared with the Krabi-*Maomingosuchus*, some individuals of *Maomingosuchus petrolicus* and *Gavialosuchus eggenburgensis* [Toula & Kail, 1885]); 3) supraoccipital visible on dorsal skull table (shared with ‘*Tomistoma*’ *cairensis*, ‘*Tomistoma*’ *coppense*, *Paratomistoma* and *M. petrolicus*); 4) atlantal rib with process on dorsal margin (shared with *Toyotamaphimeia* and some non-tomistomines); and 5) ilium with a prominent anterior process (shared with *Penghusuchus* and *Toyotamaphimeia*).

Beside the characters mentioned above, *M. acutirostris* can be further differentiated from *M. petrolicus* by: having an elongated premaxilla, anterior to the external naris; a ratio of the mediolateral width of the supratemporal fenestral bar to the width of the skull table at the same level of 0.100–0.175, and a ratio of the anteroposterior length of supratemporal fenestra to the anteroposterior length of the orbit >0.75.

Both *M. acutirostris* and *M. petrolicus* can be differentiated from the Krabi-*Maomingosuchus* by: having the first five maxillary teeth getting continuously larger posteriorly; the 7th and 8th maxillary teeth more widely spaced than other teeth; a ratio of the anteroposterior length of the supratemporal fenestra to the anteroposterior length of the orbit >0.75 and a surangular–dentary suture intersecting the external mandibular fenestra anterior to its posterior corner.

Etymology. The species name derives from the Latin word *acutus* for ‘acute’ and *rostrum* for ‘snout’ and refers to the elongated acute premaxilla anterior to the external naris, which stands in a marked contrast to the short and rounded premaxilla of *M. petrolicus*.

Holotype. GPIT-PV-31657, partial skeleton consisting of the complete skull, lower jaw and incomplete postcranial material (see [Supplemental material S4](#) for a complete list of the material).

Type locality and horizon. The fossil was recovered from layer 80 of the Na Duong coal mine (Böhme *et al.* 2013) in northern Vietnam (21°42.2’N, 106°58.6’E); Na Duong Formation, Eocene, late Bartonian–Priabonian age (39–35 Ma).

Remarks. Martin *et al.* (2019) described a *Maomingosuchus* sp. from the upper Eocene–lower Oligocene Wai-Lek Formation from Krabi Province, Thailand based on a partly preserved skull and lower jaw. The authors refrained from erecting a new species for the Krabi-*Maomingosuchus* due to its fragmentary preservation and the overall similarity with *Maomingosuchus petrolicus*. In our analysis, the Krabi-*Maomingosuchus* was found to be

closely related to *M. petrolicus*, but with three autapomorphies distinguishing it from the other maomingosuchids: 1) a surangular–dentary suture that intersects the external mandibular fenestra at its posterior corner (character [ch.] 65-1); 2) from the 1st to the 10th maxillary alveolus only one tooth larger, the others being of nearly same size (ch. 203-1); and 3) maxillary teeth widely spaced and the 7th and 8th teeth not more widely spaced than other teeth (ch. 235-1). We therefore treat the Krabi-*Maomingosuchus* as a provisionally valid

but unnamed species of *Maomingosuchus* (see Discussion, below).

Description

Overall, the material is well preserved and represents nearly a complete individual. The skull is articulated

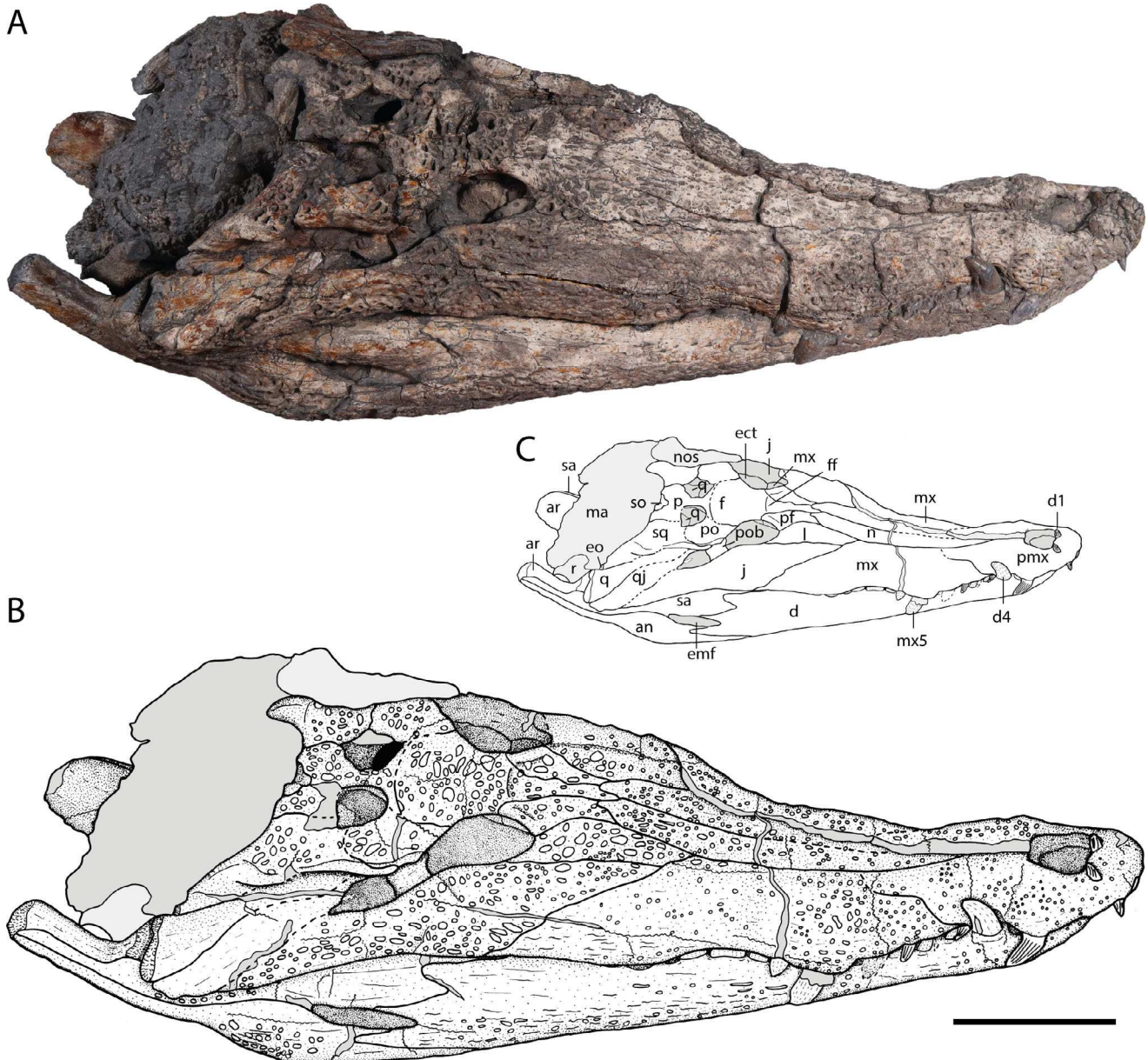


Figure 2. *Maomingosuchus acutirostris*, holotype, GPIT-PV-31657, Na Duong Formation, middle to upper Eocene, Vietnam. Skull in **A**, **B**, dorsolateral view and **C**, a sketch with the visible bones and characteristics. **Abbreviations:** an, angular; ar, articular; d, dentary; d1, dentary tooth 1; d4, dentary tooth 4; ect, ectopterygoid; emf, external mandibular fenestra; eo, exoccipital; f, frontal; ff, frontal fossa; j, jugal; l, lacrimal; ma, matrix; mx, maxilla; mx5, maxillary tooth 5; n, nasal; nos, nuchal osteoderm; p, parietal; pf, prefrontal; pmx, premaxilla; po, postorbital; pob, postorbital bar; q, quadrate; qj, quadratojugal; r, rib; sa, surangular; so, supraoccipital; sq, squamosal. Scale bar = 10 cm.

with the lower jaw and dorsolaterally flattened. The posterior part of the skull is still covered in matrix. The postcranial material is disarticulated and preserved three dimensionally with only minor compression artefacts. Most of the bones are pyritized.

For measurements of the cranial and postcranial material see [Supplemental material S4](#).

Cranial bones

General shape and taphonomic remarks. The skull is relatively robust, with the snout (measured from the snout tip to the anterior margin of orbit) making up around 72% of total skull length. The snout is overall

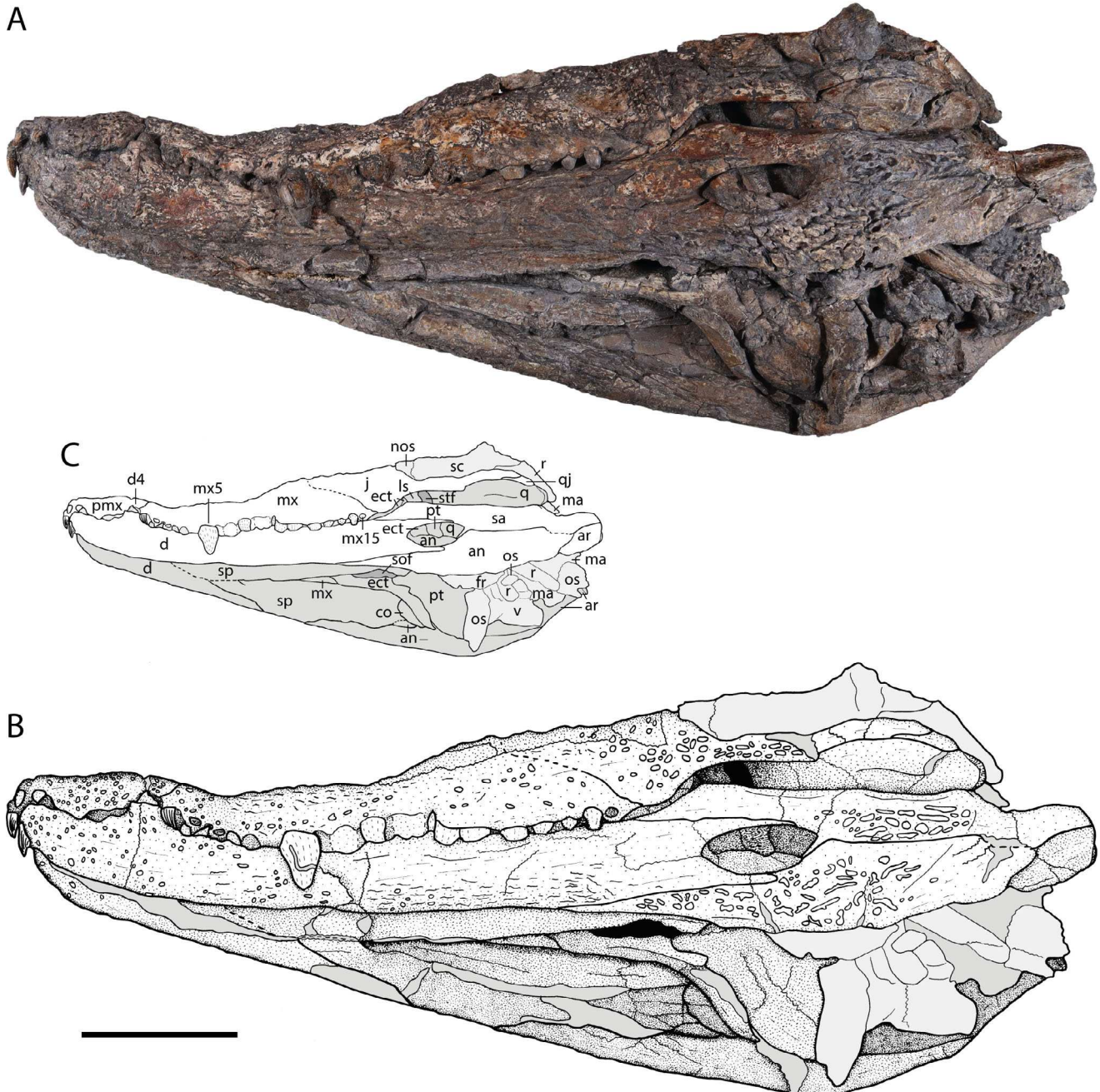


Figure 3. *Maomingosuchus acutirostris*, holotype GPIT-PV-31657, Na Duong Formation, middle to upper Eocene, Vietnam. Skull in **A**, **B**, ventrolateral view and **C**, a sketch with the visible bones and characteristics. **Abbreviations:** an, angular; ar, articular; co, coronoid; d, dentary; d4, dentary tooth 4; ect, ectopterygoid; fr, fragment; j, jugal; ls, laterosphenoid; ma, matrix; mx, maxilla; mx5, maxillary tooth 5; mx15, maxillary tooth 15; nos, nuchal osteoderm; os, osteoderm; pmx, premaxilla, pt, pterygoid; q, quadrate; qj, quadratojugal; r, rib; sa, surangular; sc, scapula; sof, suborbital fenestra; sp, splenial; stf, supratemporal fenestra; v, vertebra. Scale bar = 10 cm.

narrow but widens at the level of the 5th maxillary tooth. The skull table is solid with relatively small supratemporal fenestrae and a wide frontal region between the orbits. The postorbital bar is very robust. The skull is highly pyritized and cracked in multiple regions; for example, posterior to the external naris, the region of the skull table and the otic region. The skull is articulated with the lower jaw and dorsolaterally compressed, so that most of its ventral surface is obscured. The occiput is partly embedded in matrix together with some postcranial elements. Most cranial features described below can be seen in [Figures 2 and 3](#).

Cranial openings. The external naris ([Fig. 2](#)) is a large singular opening in the anterior region of the snout and formed exclusively by the premaxillae. Due to mediolateral compression of the skull the exact shape of the external naris is difficult to assess, but it seems to be trapezoidal and broader anteriorly than posteriorly. Both orbits ([Fig. 2](#)) are preserved, but only the right one is well exposed and is oriented dorsolateral and almost oval, but slightly lateromedially compressed. Its margins are formed by the lacrimal, prefrontal, frontal, post-orbital and jugal. Both supratemporal fenestrae ([Fig. 2](#)) are visible, lie on the skull table, and are small for a tomistomine. The outlines of the fenestrae are difficult to determine due to some broken areas and compression but they seem to be rounded and slightly longer than broad. Their medial walls are smooth without any visible foramina, and their margins are formed by the post-orbitals, squamosals and parietals. Only the right infratemporal fenestra ([Fig. 2](#)) is visible posterior to the orbits. It is triangular in shape and enclosed by the post-orbital, jugal and quadratojugal. Only the left suborbital fenestra ([Fig. 3](#)) is exposed in ventral view, bordered by the ectopterygoid and pterygoid so far as visible. Both external mandibular fenestrae ([Figs 2, 3](#)) are preserved and lie in the posterolateral region of the lower jaw. They are oval and anteroposteriorly elongated. Their margins are formed by the dentaries, angulars and sur-angulars. The incisive foramen, posttemporal foramen, foramen magnum, eustachian opening, choana and the foramen intermandibularis caudalis are not exposed.

Premaxilla. The right premaxilla is better preserved than the left. The premaxillae form the anterior part of the snout and entirely surround the external naris. Their surface is weakly ornamented. Close to the tooth row, small, rounded foramina for the receptor canals are exposed. The premaxilla projects anterior to the external naris for around half of narial length and forms the acute tip of the snout. In front of the external naris a perforation for the first dentary tooth is visible. The premaxilla extends posterior to the level of the 3rd

maxillary tooth, presumably reaching the level of the posterior border of the 4th maxillary tooth parasagittally. Both premaxillae meet each other anterior to as well as posterior to the external naris. The premaxillary-maxillary suture extends as a sinusoidal line from the notch for the 4th dentary tooth posteromedially. The premaxilla contacts the nasal behind the external naris. Only one large tooth is visible, which can be identified as the 4th premaxillary tooth, based on comparisons with other tomistomines. Taking the length of the premaxilla into account a total of five premaxillary teeth is estimated.

Maxilla. The maxilla forms the posterolateral part of the snout, most of the tooth row and terminates about 15 mm posterior to the last tooth. It is weakly ornamented with a higher density of pits and grooves on the level between the 3rd and 5th maxillary tooth. Along the tooth row, openings for the receptor canals can be observed. These foramina are rounded anteriorly and get more elongated posteriorly. In dorsal view, the maxilla broadens slightly from the notch for the 4th dentary tooth towards the level of the 5th maxillary tooth, narrowing again at level of the 7th to 8th maxillary tooth, before bending posterolaterally. The maxilla sutures with the nasal medially, the lacrimal posteromedially, the jugal posteriorly and the ectopterygoid posteroventrally. The maxilla has a total of 15 alveoli. The 1st maxillary alveolus is the smallest. The teeth then increase in diameter until the 5th maxillary tooth, which is the largest in the series. The teeth become slightly smaller posteriorly, but stay relatively large, except for the last four which are significantly smaller than the previous ones. The alveoli are widely spaced ([Fig. 2](#)), especially among the smaller anterior teeth, whereas the larger posterior teeth are closer together. Between the 7th and 8th maxillary teeth there is a wider gap.

Nasal. The nasals are thin, elongate bones forming the medial part of the snout. Their anterior-most part is not clearly visible but it is definitely excluded from the external naris. The nasal surface is only weakly ornamented anteriorly, but more strongly so posteriorly with rounded and elongated pits. The nasal contacts the premaxilla anteriorly, the maxilla laterally and the lacrimal posterolaterally. Posteriorly, the nasal sutures with the prefrontal for a short distance (only 20 mm), whereas posteromedially they are separated by a 15 mm long anterior process of the frontal.

Lacrimal. Only the right lacrimal is well preserved. The bone is elongated anteroposteriorly, slightly bowed medially and forms the anterolateral margin of the orbit. The bone is almost double the size of the prefrontal and projects far anteriorly between the nasal and maxilla. Its surface is heavily ornamented with large rounded pits. The opening for the ductus nasolacrimalis is not

exposed. The lacrimal contacts the maxilla anterolaterally, the jugal laterally, the prefrontal medially and the nasal anteromedially.

Prefrontal. The prefrontal forms the anteromedial margin of the orbit. The bone is almost rectangular and does not project further anteriorly than the anterior end of the frontal and is approximately as broad as the lacrimal. The orbital margin has a small bulge extending medially onto the frontal fossa. The surface of the prefrontal is weakly ornamented with a few deeper pits posteriorly. Due to crushing of the skull, neither prefrontal pillars is preserved. The prefrontal contacts the nasal anteriorly, the lacrimal laterally and the frontal medially.

Frontal. The frontals are fused and form the anterior part of the skull table. The bone is almost square-shaped with an elongate anterior wedge-shaped process, which projects with its anterior-most extension between the nasals. The whole process has nearly the same length as the broad part between the orbits and the skull table. The frontal does not reach the supratemporal fenestra posteriorly. The region between the orbits is flat, not upturned, very broad and around three times wider than the supratemporal bridge. The region between the broader part of the frontal and the narrow region of the anterior process is marked by a lateromedially oriented frontal fossa forming a ledge between the skull table and the snout. This fossa extends anterolaterally onto the prefrontal. The frontal is weakly ornamented anteriorly, but heavily ornamented with deep rounded pits posterior to the ledge. Anteromedially, the frontal contacts the nasal and anterolaterally, the prefrontal. On the skull table, the frontal contacts the postorbital laterally and the parietal posteriorly. The suture with the latter seems to project relatively straight lateromedially, but a slight posteromedial convexity is visible.

Postorbital. The right postorbital is the better preserved and forms the anterolateral part of the skull table, the posterolateral margin of the orbit, the anterolateral margin of the supratemporal fenestra and the anterior margin of the infratemporal fenestra. The skull table is damaged and therefore the postorbital is somewhat distorted with its surface partially broken off. The preserved part is ornamented with large rounded pits, especially posteriorly. In dorsal view, the postorbital contacts the frontal anteromedially, the parietal posteromedially and the squamosal posteriorly. In lateral view, the postorbital is indented by an anterior process of the squamosal. The postorbital bar is slightly inset from the margin of the skull table, very robust and is at least 50% the size of the infratemporal fenestra. The sutural contact with the jugal is not visible.

Parietal. The flat, dumbbell-shaped parietals are fused at midline and form most of the posteromedial part of the skull table as well as the medial margin of the supratemporal fenestra. The region posterior to the supratemporal fenestra is very broad. The supratemporal bar is narrow, but quite broad for a tomistomine. The parietal surface is ornamented with deep rounded pits. The parietal contacts the frontal anteriorly, the postorbital anterolaterally and the squamosal posterolaterally. The parietal encompasses the supraoccipital in the posterior part of the skull table, so that the parietal does not form the entire skull table. Inside the supratemporal fenestra, the parietal contacts the quadrate along its posterior wall, but the suture is difficult to see.

Squamosal. The squamosal is better preserved on the right side, and forms the posterolateral part of the skull table and the posterolateral margin of the supratemporal fenestra. The squamosal prongs extend posterolaterally, away from the skull table. The dorsal and ventral rims of the squamosal groove for the external ear valve musculature are parallel. The squamosal surface is ornamented with rounded pits only in the skull table region. Due to compression, the squamosal completely covers the auditory meatus. On the skull table, the squamosal contacts the postorbital anteriorly, the parietal posterolaterally and the quadrate on the lateral wall of the supratemporal fenestra. In lateral view, the squamosal projects anteriorly into the postorbital and contacts the quadrate posterolaterally on the squamosal prongs. The suture with the exoccipital is poorly preserved, but it is clear that the squamosal does not cover the paroccipital process.

Jugal. The right jugal is better preserved than the left and forms the lateral part of the skull as well as the ventrolateral margins of the orbit and the infratemporal fenestra. Anteriorly, a process extends far anteriorly to the level of the anterior extension of the frontal. The jugal is narrowest at level of the postorbital bar. The postorbital bar is set inwards from the lateral part of the skull and separated from it by a deep groove. The entire surface of the jugal is heavily ornamented. The jugal contacts the maxilla anteriorly, the lacrimal medially and the ectopterygoid ventrally. The jugal–quadratojugal suture is somewhat damaged posteriorly and its interaction with the posterior margin of the infratemporal fenestra is unclear. The jugal–postorbital suture on the postorbital bar is not visible.

Quadratojugal. The right quadratojugal is the best preserved. The bone is small, situated at the posterolateral part of the skull and forms the posterior margin of the infratemporal fenestra. The quadratojugal extends to the posterior end of the skull, surpassed only by the

quadrate condyles. No surface ornamentation is observable. The quadratojugal contacts the jugal anteriorly and the quadrate posteromedially. A potential contact with the postorbital and squamosal at the superior margin of the infratemporal fenestra is not exposed.

Quadrate. The right quadrate is visible in dorsal and posterior views, while the left quadrate is exposed in ventral view only. It forms the posterior-most part of the skull, the inner posterior part of the supratemporal fenestra as well as the articulation with the articular of the lower jaw and most of the margin of the auditory meatus, which is not exposed. The articular surface of the quadrate is formed by two condyles, of which the lateral one is more expanded lateromedially than the medial one. The surface of the bone is unornamented. The quadrate foramen aerum is located in the dorsomedial corner of the bone. The quadrate is broad at the level of the condyles and narrows anteriorly close to the quadratojugal. The ventral surface of the quadrate is generally smooth with a moderate ridge for the insertion of the posterior mandibular adductor muscle. In dorsolateral view, the quadrate contacts the quadratojugal anteriorly, the squamosal medially and the exoccipital posteromedially. Inside the supratemporal fenestra, the quadrate contacts the parietal posteromedially and the squamosal posterolaterally, but this region is poorly preserved. In occipital view, the quadrate contacts the exoccipital dorsally.

Pterygoid. The pterygoid is only visible in ventral view where it forms the posterior part of the palate and the posterior margin of the suborbital fenestra. Due to dorsolateral compression, it is poorly preserved and only the left wing of the pterygoid is exposed (Fig. 3). The region around the choana is damaged. The pterygoid contacts the ectopterygoid anterolaterally. Unfortunately, no other sutural contacts are visible.

Ectopterygoid. Only the left ectopterygoid is exposed in ventral view. It forms the posterolateral part of the palate and forms the posterolateral margin of the suborbital fenestra. The ectopterygoid is poorly preserved and distorted, but its posterior extension contacts the pterygoid and ends anterior to the posterior tip of the latter. It further contacts the maxilla anteriorly and the jugal dorsally.

Supraoccipital. The supraoccipital is an unpaired bone and forms a small part of the skull roof and the central dorsal part of the occiput. On the skull table, it is a small triangular element that is pinched between the parietals. Its surface is somewhat weathered but no surface ornamentation is visible. The occipital part of the bone is damaged due to dorsolateral compression.

Exoccipital. The right exoccipital is exposed in occipital view but only its posterolateral-most parts are preserved. It forms most of the posterolateral region of the skull and the paroccipital process is visible in lateral view. The opening for the cranioquadrate passage is not directly visible, but the exoccipital shows a ventrally projecting convexity at the level of the foramen. The exoccipital contacts the squamosal dorsal and the quadrate ventrally. No other sutural contacts are visible.

Laterosphenoid. Only the left laterosphenoid is partly exposed and situated on the anteroventral part of the skull table, posteromedial to the orbit. It forms the anterolateral braincase wall and the inner anteromedial wall of the supratemporal fenestra. Sutural contacts with other bones are not discernible.

Dentary. Both dentaries are well-preserved in lateral view. The bone covers the anterolateral part of the lower jaw and reaches the anterodorsal and anteroventral part of the external mandibular fenestra. The dentary symphysis is relatively short for a tomistomine and seems to extend back to the level of the 6th to 8th dentary alveolus, although its exact length is difficult to determine due to poor preservation. The surface of the dentary is slightly ornamented with rounded pits anteriorly and elongated grooves ventrally, while its posterodorsal part is almost smooth. The tooth row is almost straight and, close to it, openings for receptor canals are visible. The slight curvature of the dentary, observable on the right side in lateral view (Fig. 2) is most likely a compressional artefact, as it is not present on the left side (Fig. 3). The dentary contacts the surangular posterodorsally, the angular posteroventrally and the splenial posteromedially. The total tooth number is unclear. The 1st dentary tooth perforates the premaxilla immediately anterior to the external naris. The 4th dentary tooth is the largest tooth in the anterior half of the lower jaw and its alveolus is slightly elevated. Posteriorly, the teeth are smaller but the 11th or 12th tooth (estimated based on the distance between the anterior teeth) is very broad and slightly larger than the 4th. Posteriorly, the tooth row is not exposed.

Splenial. The left splenial is the best preserved but is somewhat distorted. It forms the posteromedial part of the mandibular symphysis with a length that is less than the distance between five alveoli. An anterior foramen for cranial nerve V is not visible, but this could be a preservational artefact. There is no surface ornamentation. The splenial contacts the dentary laterally, the coronoid posterodorsally and the angular posteroventrally.

Coronoid. The left coronoid is exposed medially but is poorly preserved, and only its crescent-shaped anterior

part is visible. Its surface is smooth, with no visible foramina, but this could be an artefact. The coronoid contacts the splenial anteriorly and the angular ventrally. The contact with the surangular is not exposed.

Surangular. Both surangulars are preserved in lateral view only. The surangular forms the posterodorsal part of the lower jaw, the posterodorsal margin of the external mandibular fenestra, contributes laterally to the posterior-most end of the retroarticular process, and reaches the dorsal tip of the lateral wall of the glenoid fossa. Anteriorly, the bone has two processes, a longer dorsal one, presumably reaching the tooth row, and a shorter ventral one, extending anteriorly to the external mandibular fenestra for around half of the fenestral length. The surangular is strongly ornamented with deep elongated pits posterior to the external mandibular fenestra. It contacts the dentary anteriorly, the angular ventrally and the articular dorsomedially.

Angular. Both angulars are preserved in lateral view and the right one is partially visible in medial view. The angular forms the posteroventral part of the mandible and the posteroventral margin of the external mandibular fenestra. Anteroventrally, the bone forms a process projecting between the dentary and splenial while extending posteriorly alongside the surangular on the lateral wall of the retroarticular process until its posterior-most end. The angular is strongly ornamented on its lateral part with deep and elongated pits, as well as with a few rounded pits posteroventral to the external mandibular fenestra. On its posteroventral part, a small nutritional foramen is visible in ventral view. In lateral view, the angular contacts the dentary anteriorly and the surangular dorsally. In medial view, the angular contacts the splenial anteriorly, the coracoid anterodorsally and the articular posterodorsally. A contact with the surangular in medial view is not exposed.

Articular. Both articulars are preserved in dorsolateral view and the right one is partially visible in medial view. The articular forms the posteromedial part of the mandible, the articulation surface with the quadrate, most of the retroarticular process and is slightly visible in lateral view. The retroarticular process projects posterodorsally. The glenoid fossa and the foramen aerum are not exposed. In lateral view, the articular contacts the surangular ventrolaterally and, in medial view, the angular ventrally.

Hyoid. Both hyoids (Fig. 4) are preserved and have a recumbent 'L'-shaped outline with a longer ventral than dorsal branch of the cornu. The dorsal branch is flattened and the ventral one is broadened anteriorly. The lateral part of the ventral branch of the cornu is slightly

bowed medially, whereas its medial part is nearly straight and dorsoventrally oriented. The anterior-most extension is rounded and has a rough surface. Posterior to this surface there are multiple shallow pits of different sizes. The dorsal surface of the ventral cornual branch has a shallow anteroposteriorly oriented groove. The dorsal branch of the cornu is lateromedially flattened with parallel sides. Its dorsal-most part is slightly posteriorly shifted and has a rugose surface.

Dentition. The teeth of *M. acutirostris* are circular in cross-section and differ in size. The premaxillary, anterior maxillary (to the 5th tooth position) and anterior dentary teeth (to the 4th tooth position) have multiple dorsoventrally oriented ridges on their lateral and medial surfaces, and sharp but unserrated edges. In the premaxilla, the 4th tooth is the largest one. In the maxilla, the 1st tooth is small and the following teeth are gradually larger until the 5th maxillary tooth, the largest tooth in the tooth row. Posteriorly, the teeth become gradually smaller, but are still much larger overall than the first four maxillary teeth. The posterior-most four teeth are reduced in size and the smallest in the series. In the mandible, the 4th dentary tooth is the largest one in the anterior half of the lower jaw and projects into a notch between the premaxilla and maxilla. The other anterior dentary teeth are small until reaching the presumably 11th or 12th tooth, which is very broad and even slightly larger than the 4th one. Further posteriorly, the teeth seem to get smaller, but due to the occlusion of the jaws this region is not exposed. The dentary teeth are in line with the maxillary tooth row and the teeth are more widely spaced anteriorly, but closer together posteriorly due to their larger size. An enlarged gap can be found between the 7th and 8th maxillary teeth for the enlarged 11th or 12th tooth.

Postcranial bones

Axial skeleton. The vertebral column (Figs 5–8) is nearly complete and in total, the proatlas, seven cervical, 12 dorsal, two sacral and 15 caudal vertebrae are preserved.

Proatlas. The proatlas (Fig. 5A–D) is boomerang-shaped with a posterolateral process on each side. The anterior part is slightly offset from the main body without forming a distinct process. The ventral tubercle is not clearly discernible, but based on the general morphology it is relatively large and at least half the width of the dorsal crest. Sagittally, a well-developed median keel is present that has a slightly rounded dorsal surface and slopes strongly posteriorly.

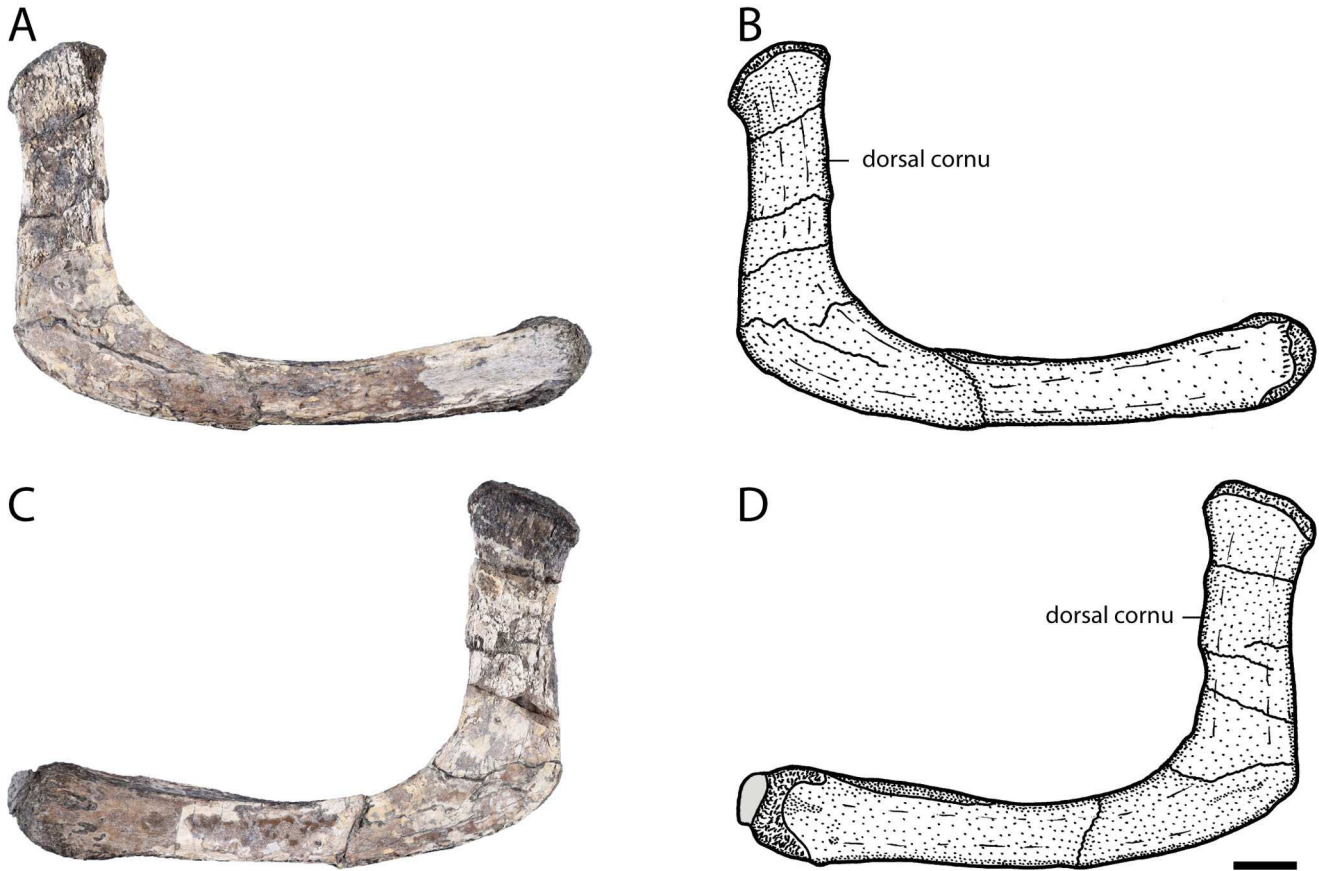
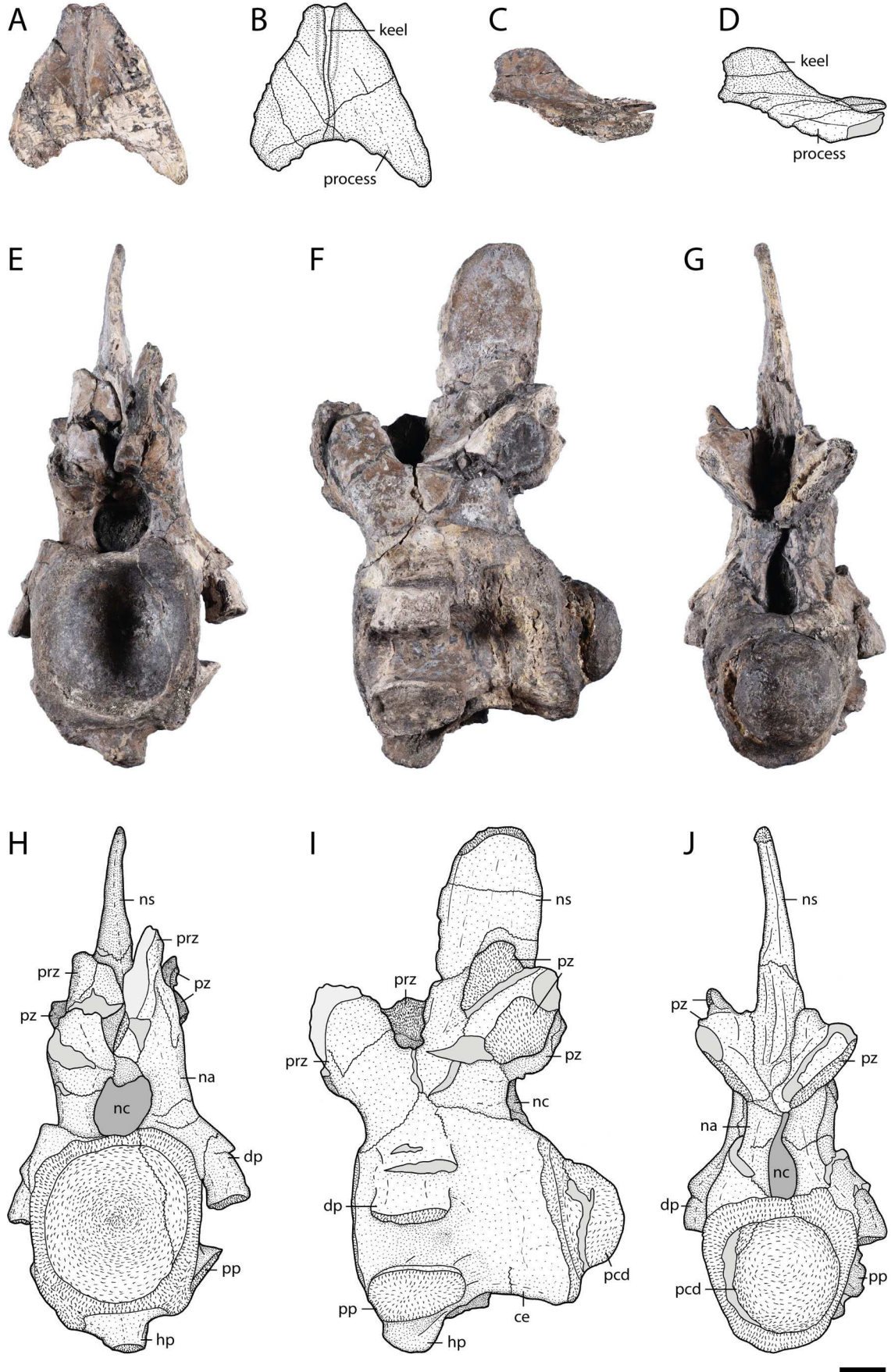


Figure 4. *Maomingosuchus acutirostris*, holotype, GPIT-PV-31657, Na Duong Formation, middle to upper Eocene, Vietnam. Right hyoid in **A, B**, lateral and **C, D**, medial views. Scale bar = 1 cm.

Cervical vertebrae. The best-preserved cervical vertebra (Fig. 5E–J) is from the anterior region, but its exact position is unknown. Because the cervical vertebrae are rather uniform in morphology, we only describe the best-preserved in detail. The centrum is longer than wide but its height and width are similar. The centrum is constricted between the parapophysis and diapophysis and is ventrally convex in lateral view. The surface is smooth but bears small nutritional foramina below the diapophysis. The anterior articular surface is rounded and slightly more expanded dorsoventrally than the centrum. The posterior condylus is rounded. The hypapophysis is short and does not reach the middle of the centrum. Posteroventrally, a short shallow ridge is discernible. The articular surface of the parapophysis is oval and projects mostly laterally. The slightly damaged diapophysis is lateroventrally oriented and its articular surface is oval and smaller than the articular surface of the parapophysis. The prezygapophysis is oval-shaped and larger than the postzygapophysis. It projects dorsally, whereas the oval-shaped postzygapophysis turns ventrally, both at a 45° angle. The neural spine is nearly

as high as the ventral part of the vertebra, is anteroposteriorly broad and slightly rounded dorsally.

Dorsal vertebrae. The best-preserved dorsal vertebra (Fig. 6) is from the anterior region, but its exact position is unknown. Because the dorsal vertebrae, like the cervical vertebrae (see above), are rather uniform in morphology, we only describe the best-preserved dorsal vertebra in detail. The centrum is nearly as long as wide but damaged by deep cracks. The anterior articular surface is round and wider than the centrum, while the posterior condylus seems to be nearly equal in size to the centrum. Ventrally, the centrum is slightly convex in lateral view. Its surface is smooth without visible foramina. The hypapophysis is narrow and anteriorly oriented, and does not reach the central part of the centrum. The transverse process is relatively slender and projects horizontally at an angle of 90° from the centrum. The parapophysis is located anteroventrally at mid-length and the diapophysis is positioned on the distal end of the transverse process. The prezygapophysis projects dorsally and seems to be larger than the



postzygapophysis. The latter faces ventrally with an oval articular surface. A deep groove is present between the postzygapophyses. The neural spine is long and relatively low. Its dorsal tip is generally wide but broader anteriorly than posteriorly.

Sacral vertebra. Both sacral vertebrae (Fig. 7) are preserved. In the first sacral vertebra, the lateral extensions of the sacral ribs are covered by osteoderm fragments, the neural spine is broken into two pieces and the neural canal is damaged due to dorsoventral compression. The second sacral vertebra is also covered by osteoderms and its neural spine is broken but the neural canal is intact.

The centrum of the first sacral vertebra (Fig. 7A–F) is nearly as broad as long, and anteriorly and posteriorly slightly ventrally curved and posteriorly sloped. The surface of the centrum is smooth without discernible foramina. On the ventral part of the centrum there is a sulcus reaching from near its posterior end to the middle of the centrum. The anterior articular surface is concave, lateromedially expanded and deep, whereas the posterior articular surface is also expanded but nearly flat with only a very slight concavity. The sacral rib is dorsoventrally compressed. The anterior extension of the articular surface for the ilium reaches further laterally than the posterior one. The prezygapophysis is one-quarter larger than the postzygapophysis and its articular surface is rectangular. The prezygapophysis projects dorsally, whereas the postzygapophysis turns ventrally. The neural spine is long and reaches two-thirds of the dorsoventral length of the centrum. Its dorsal-most extension is damaged but seems to be slightly broader anteriorly than posteriorly.

The second sacral vertebra (Fig. 7G–L) has a similar morphology to the first, but the sacral ribs are anteroposteriorly compressed. The centrum has small nutritional foramina anterolaterally and the sulcus on the ventral surface is less pronounced than in the first sacral. The centrum is nearly straight in lateral view with only a slight ventral projection at its anterior and posterior ends. The anterior articular surface with the first sacral vertebra is wide and flat with a slight concavity. The posterior articular surface is also wide but with a deep concavity for the anterior condylus of the first caudal vertebra. The lateral articular surface of the sacral rib with the ilium is boomerang-shaped with a posterodorsal extension contacting the posterior part of

the iliac blade. The prezygapophysis is larger than the postzygapophysis and projects dorsally, whereas the postzygapophysis turns ventrally, and both have a lateromedially shifted angle of 45°. The neural spine is broken but its height is around two-thirds of the dorsoventral length of the centrum.

Caudal vertebrae. The first caudal vertebra (Fig. 8A–F) differs significantly from the more posterior caudal vertebrae and is described separately. The first caudal vertebra is biconvex and its centrum is similar to the centrum of the sacral vertebra in being as wide as it is long. The surface of the centrum is mostly smooth and no sulcus is present, but the ventral part slightly posterior to the anterior condylus has a rugose surface. In lateral view, the centrum is concave with a strong ventral shift posteriorly. Both condyles are similarly sized with the anterior condylus being slightly broader, whereas the posterior condylus is more rounded. The transverse process is incomplete but its lateral-most part shifts slightly posteriorly. The prezygapophysis is larger than the postzygapophysis and its articular surface is oval. The neural spine is elongated but narrower than the neural spines of the sacral vertebrae.

More posteriorly positioned caudal vertebrae (Fig. 8G–L) have a slenderer morphology than the first caudal vertebra and the centrum is elongated, mediolaterally narrow and slightly convex in lateral view. The centrum tapers towards its middle part and a deep sulcus extends over the whole length of the centrum on its ventral surface. The anterior articular surface is rounded and concave, whereas the posterior articular surface has a round condylus. The transverse process is incomplete and projects straight from the centrum at almost 90°. The articular surface of the prezygapophysis is oval and projects dorsally, whereas the articular surface of the postzygapophysis turns ventrally. The neural spine is posteriorly shifted. In the anterior caudal vertebrae, the spine is elongated and flares towards the postzygapophyses. In the posterior caudal vertebrae, the spine tapers into a rod-like morphology and is shifted even more posteriorly and transverse processes are lost.

Chevron. The articular surface of the chevron (Fig. 8M–P) for the caudal vertebra is dumbbell-shaped and the haemal canal is rectangular and slightly ventrally tapered. The haemal arch is narrow in anteroposterior view but expanded in lateral view. The haemal spine

←
Figure 5. *Maomingosuchus acutirostris*, holotype, GPIT-PV-31657, Na Duong Formation, middle to upper Eocene, Vietnam. Proatlas in **A, B**, dorsal and **C, D**, lateral left views. Cervical vertebra in **E, H**, anterior, **F, I**, lateral left and **G, J**, posterior views. **Abbreviations:** **ce**, centrum; **dp**, diapophysis; **hp**, hypapophysis; **na**, neural arch; **nc**, neural canal; **ns**, neural spine; **pcd**, posterior condylus; **pp**, parapophysis; **prz**, prezygapophysis; **pz**, postzygapophysis. Scale bar = 1 cm.

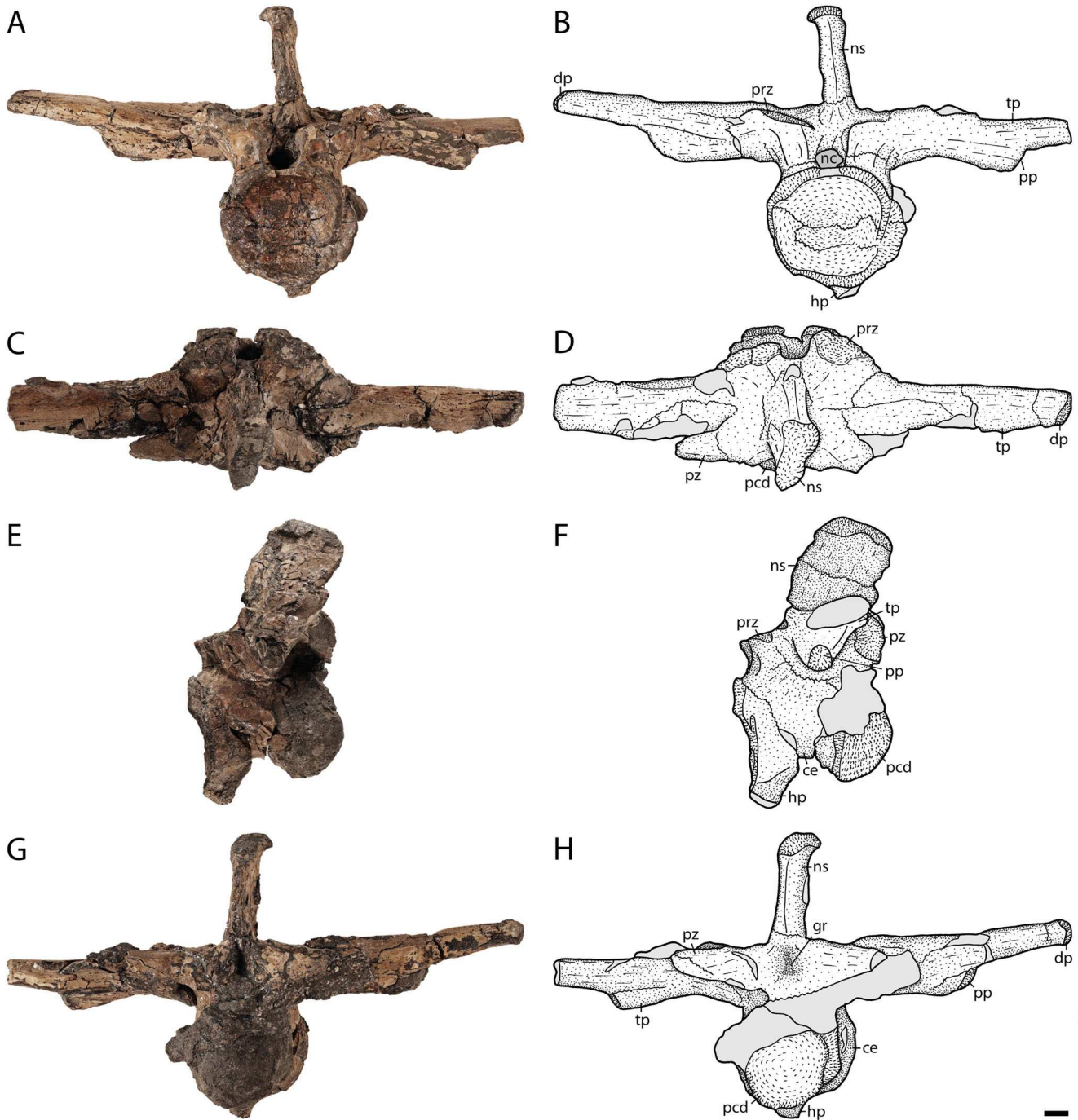


Figure 6. *Maomingosuchus acutirostris*, holotype, GPIT-PV-31657, Na Duong Formation, middle to upper Eocene, Vietnam. Dorsal vertebra in **A, B**, anterior, **C, D**, dorsal, **E, F**, lateral and **G, H**, posterior views. **Abbreviations:** **ce**, centrum; **dp**, diapophysis; **gr**, groove; **hp**, hypapophysis; **nc**, neural canal; **ns**, neural spine; **pcd**, posterior condylus; **pp**, parapophysis; **prz**, prezygapophysis; **pz**, postzygapophysis; **tp**, transverse process. Scale bar = 1 cm.

comprises around two-thirds of the total chevron length and is slightly thickened at its ventral-most part.

Atlantal rib. The atlantal rib (Fig. 9A–D) is elongated and flat. The articular surface with the atlas is kidney-

shaped and the anterior part of the rib has parallel sides. Neither a large articular facet for the other atlantal rib nor a thin medial lamina are present. The medial part is slightly concave, whereas the lateral part is slightly convex. From the middle part onwards, the rib expands and

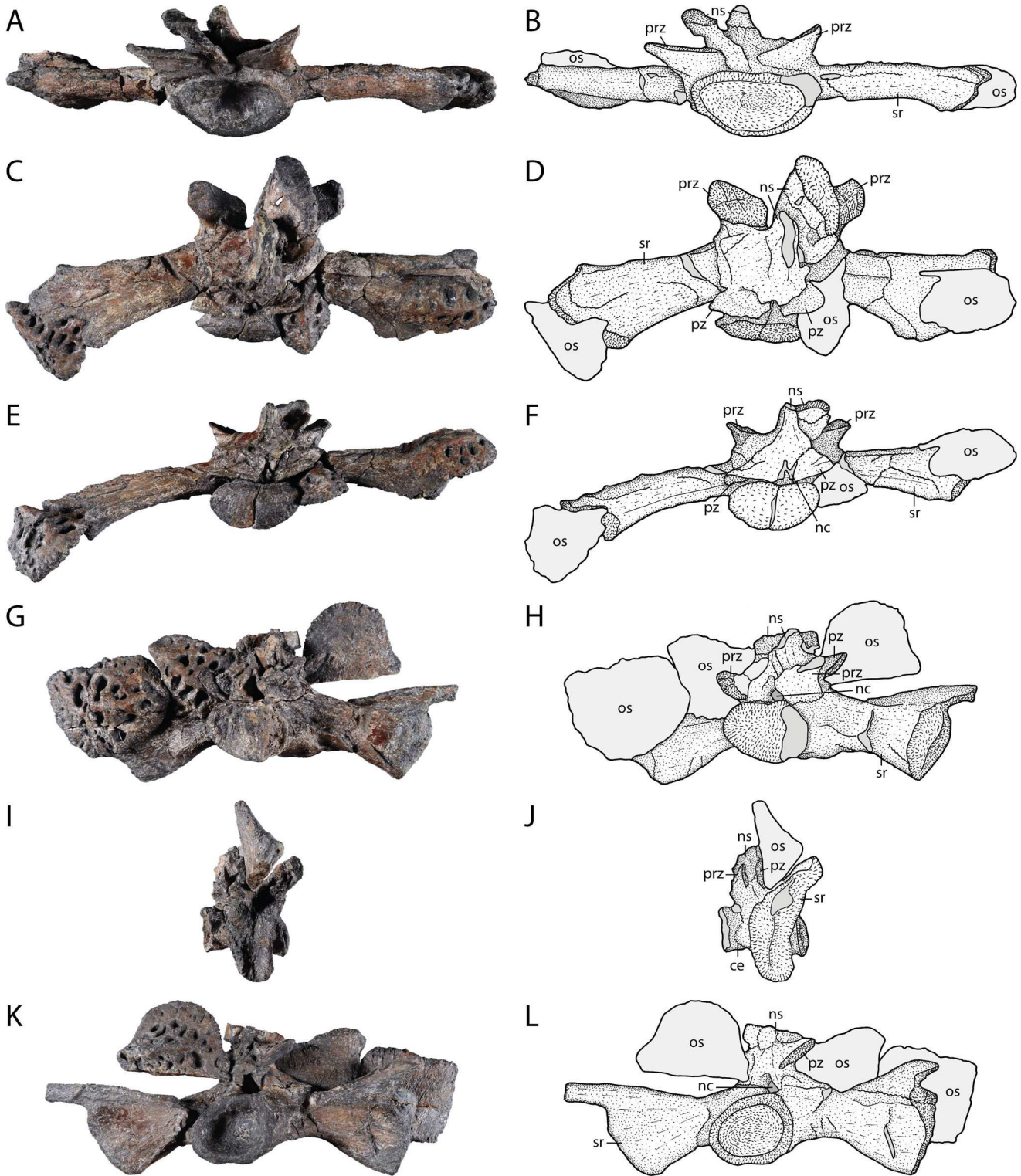


Figure 7. *Maomingosuchus acutirostris*, holotype, GPIT-PV-31657, Na Duong Formation, middle to upper Eocene, Vietnam. First sacral vertebra in **A, B**, anterior, **C, D**, dorsal and **E, F**, posterior views. Second sacral vertebra in **G, H**, anterior, **I, J**, lateral left and **K, L**, posterior views. **Abbreviations:** ce, centrum; nc, neural canal; ns, neural spine; os, osteoderm; prz, prezygapophysis; pz, postzygapophysis; sr, sacral rib. Scale bar = 1 cm.

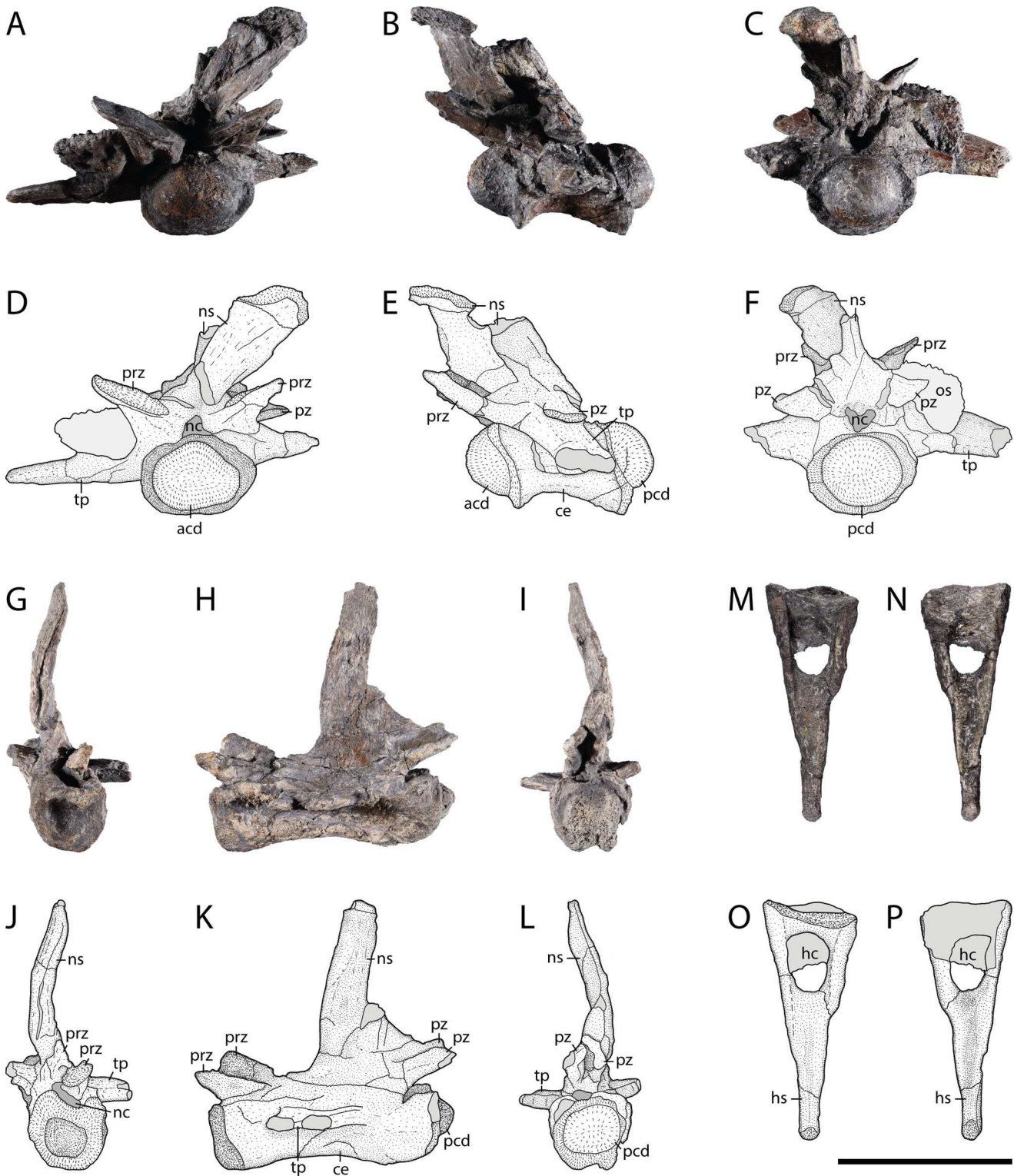


Figure 8. *Maomingosuchus acutirostris*, holotype, GPIT-PV-31657, Na Duong Formation, middle to upper Eocene, Vietnam. First caudal vertebra in **A, D**, anterior, **B, E**, lateral and **C, F**, posterior views. Middle caudal vertebra in **G, J**, anterior, **H, K**, lateral left and **I, L**, posterior views. Chevron in **M, O**, anterior and **N, P**, posterior views. **Abbreviations:** **acd**, anterior condylus; **ce**, centrum; **hc**: haemal canal; **hs**, haemal spine; **nc**, neural canal; **ns**, neural spine; **os**, osteoderm; **pcd**, posterior condylus; **prz**, prezygapophysis; **pz**, postzygapophysis; **tp**, transverse process. Scale bar = 1 cm.

forms a dorsal process, which tapers rapidly posteriorly. The ventral part expands only slightly before projecting straight posteriorly.

Cervical ribs. The best-preserved cervical rib is from the anterior region (Fig. 9E–J), but its exact position is unclear. The dorsal part consists of two columnar processes, the medial capitulum and the lateral tuberculum. The capitulum contacts the parapophysis of the cervical vertebra, whereas the tuberculum contacts the diapophysis. The capitulum is shorter than the tuberculum, but its articular surface is broader and rounded, while that of the tuberculum is more elongate. The anterior region of the ventral part of the bone is shorter than the posterior extension and steep, whereas the posterior part is flat with a deep medial concavity.

A posterior left cervical rib (Fig. 9K–N) is preserved and likely contacted the 6th cervical vertebra. The capitulum is elongated and much longer than the tuberculum. The articular surface of the capitulum is small and rounded, while that of the tuberculum is nearly double the size and broad. A lateral projecting lamina was folded due to compression, but would normally project perpendicular to the shaft. The posteroventrally projecting shaft tapers slightly distally and has a lateral ridge contacting the lamina and reaches the posterior third of the bone. The medial part of the shaft is flat.

Dorsal rib. The dorsal ribs are incomplete, but their general morphology does not seem to differ from other tomistomines.

Scapula. Both scapulae (Fig. 10A, B, E, F) are present, but only the right one is well preserved. The scapular blade expands dorsally, with a relatively straight anterior edge. The deltoid crest is partially covered by a dorsal rib, but the bulge of the crest is relatively narrow. The articular surface for the coracoid is elongate, but lateromedially flattened due to compression. Anterior to the deltoid crest and anterodorsal to the articulation surface, the scapula is elongated and rectangular. The glenoid fossa is ventrolaterally oriented and oval.

Coracoid. The left coracoid (Fig. 10C, D, G, H) is better-preserved, but lateromedially compressed. The shaft is slightly bowed and the coracoid blade expands ventrally, but is narrow compared to the scapular blade. Anteroventrally, the blade has a small process projecting anteriorly. The articular surface for the scapula is elongate, but lateromedially flattened due to compression. Anterior to the articular surface with the scapula, the coracoid is elongated and rectangular. The glenoid fossa has an oval outline and the coracoid foramen is small and situated well anterior to the glenoid fossa.

Humerus. The right humerus (Fig. 11A–H) is better preserved than the left. The bone is relatively slender and its surface is mostly smooth with rugose areas ventral to the proximal and dorsal to the distal articulation surfaces. The humeral head is divided in an anterior and a posterior tubercle. The anterior tubercle forms the proximal-most point of the humerus, whereas the posterior tubercle is posterodistally shifted. The deltopectoral crest has a concave surface and projects nearly perpendicular to the shaft. Close to its distal end, the humerus has a visible central concavity on its dorsal and ventral part. Distally, the medial and lateral condyles form the articular surfaces for the radius and ulna. Both condyles are rounded with the lateral condylus being slightly larger. Scars for the musculature are not visible.

Ulna. Only the left ulna (Fig. 11I–L) is preserved. It is sigmoidal and proximally expanded. The articular surfaces are compressed. The small olecranon process forms its proximal-most point and the proximal articular surface slopes anteriorly. The distal articular surface is kidney-shaped.

Ilium. The right ilium (Fig. 12A–D) is better preserved, but deformed with its posterodorsal end shifted, whereas the left ilium is less deformed but fused to the left ischium. The dorsal part of the bone has a rugose surface, is slightly sigmoidal with a shallow indentation posteriorly and a small anterior process. The iliac blade in general is narrow but posteroventrally slightly broadened. In medial view, the bone has two prominent scars for articulation with the first and second sacral ribs. The anterior scar is oval, whereas the posterior scar is elongated and reaches the ventral part of the iliac blade. In lateral view, the supraacetabular crest is narrow with a rounded outline and the acetabulum forms a broadly rounded depression. The ventral part of the ilium forms the articular surfaces for the ischium. The posterior articular surface is boomerang-shaped, whereas the anterior one is elongate and kidney-shaped. The acetabulum foramen is visible between the two surfaces.

Ischium. The right ischium (Fig. 12E–H) is better preserved, but has a deformed posteroventral part, whereas the left ischium is less deformed but fused to the left ilium. The ventral part is formed by the ventromedially bowed ischium blade and the anteroventral part of the blade is nearly rectangular, whereas the posterior part extends far posteriorly. The dorsal part of the bone can be divided into two processes. The posterior process forms the articular surface with the posterior part of the ilium. This surface is triangular with a small elongate anterior process. The anterior process is slenderer and has two separated articular surfaces. The dorsal one contacts the anterior articular surface of the ilium, whereas

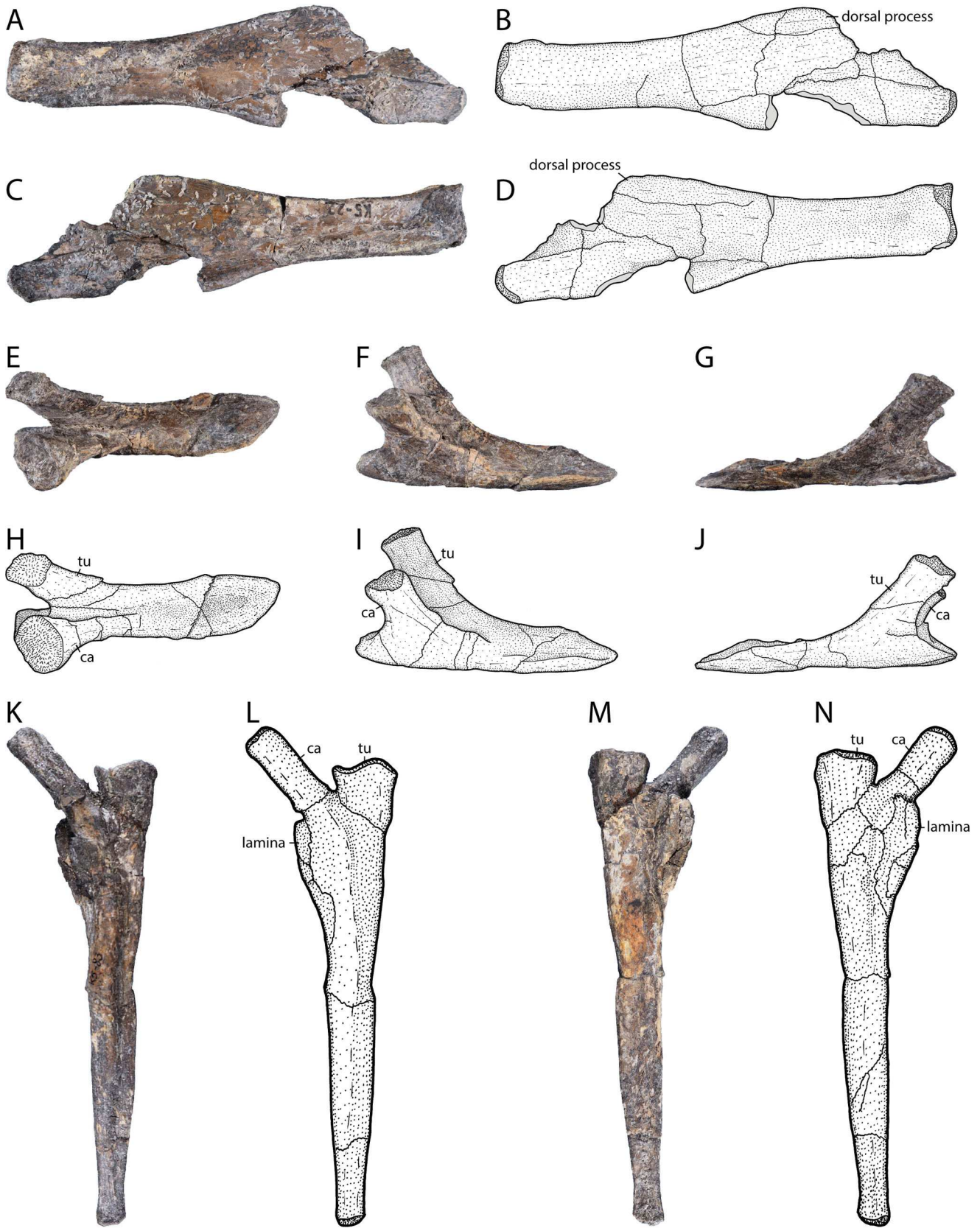


Figure 9. *Maomingosuchus acutirostris*, holotype, GPIT-PV-31657, Na Duong Formation, middle to upper Eocene, Vietnam. Left atlantal rib in **A, B**, lateral and **C, D**, medial views. Right anterior cervical rib in **E, H**, dorsal, **F, I**, medial and **G, J**, lateral views. Left posterior cervical rib in **K, L**, lateral and **M, N**, medial views. **Abbreviations:** ca, capitulum; tu, tuberculum. Scale bar = 1 cm.

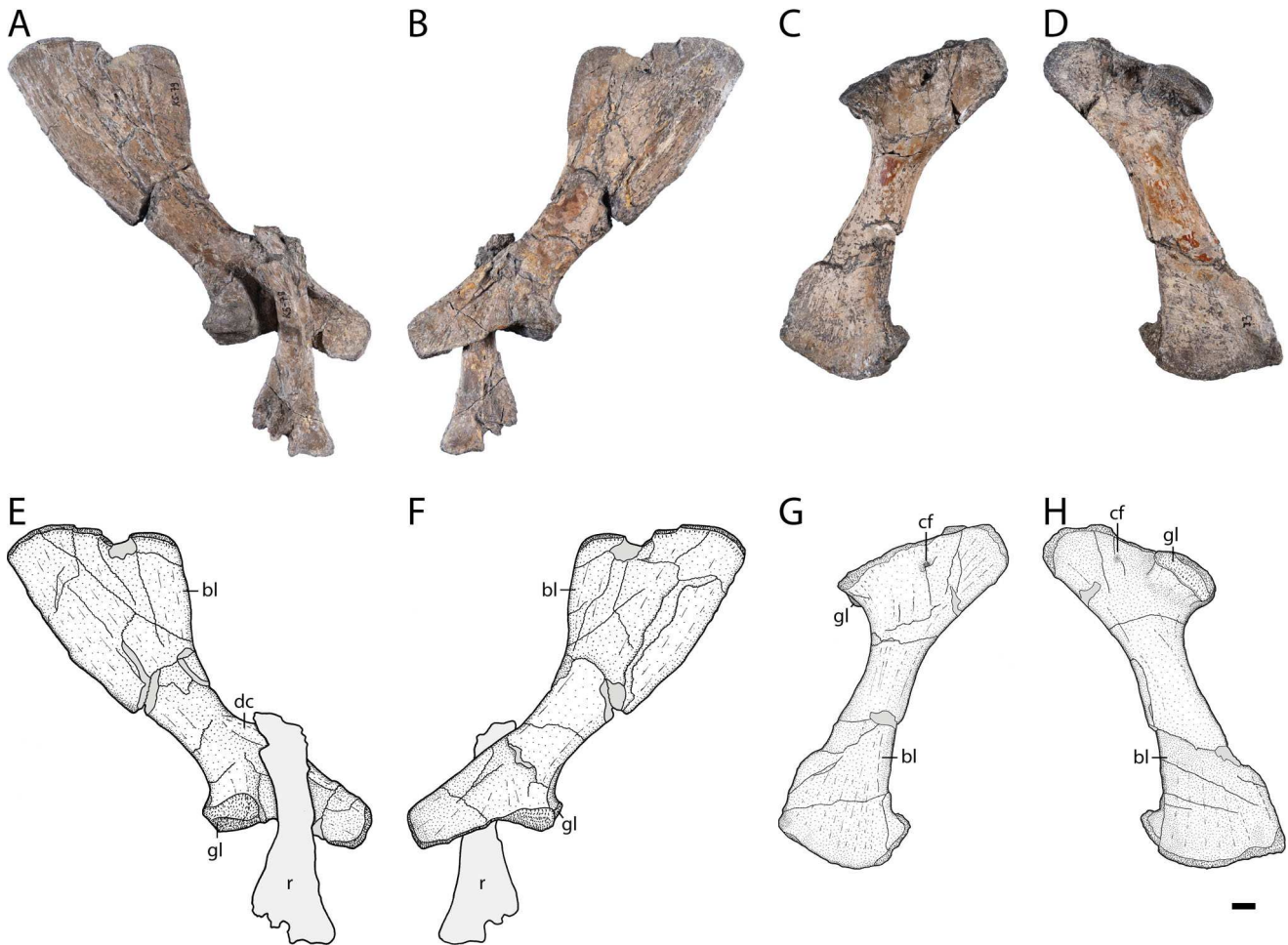


Figure 10. *Maomingosuchus acutirostris*, holotype, GPIT-PV-31657, Na Duong Formation, middle to upper Eocene, Vietnam. Right scapula in **A**, **E**, lateral and **B**, **F**, medial views. Right coracoid in **C**, **G**, lateral and **D**, **H**, medial views. **Abbreviations:** **bl**, blade; **cf**, coracoid foramen; **dc**, deltoid crest; **gl**, glenoid, **r**, rib. Scale bar = 1 cm.

the anteroventrally projecting one contacts the pubis. The articular surface with the ilium is lateromedially elongate and the articular surface with the pubis is oval. Between the anterior and posterior process, the acetabulum foramen is present.

Pubis. The left pubis (Fig. 12I–L) is well-preserved. Its ventral blade flares nearly symmetrically with a rounded ventral edge. The posteroventral part of this edge is vertical for a short distance. The blade is lateromedially flattened and the shaft is oval in cross-section. The dorsal articular surface is oval and slightly shifted posteriorly. It contacts the anteroventral articular surface of the anterior process of the ischium.

Femur. The left femur (Fig. 13A–H) is better preserved, relatively slender, larger than the humerus and has a sigmoidal outline with a slight torsion. The femoral head is compressed and therefore appears to be oval. Directly ventral to the femoral head, the bone surface is rugose,

with small openings, most likely representing nutritional foramina. Proximocaudally, the insertion scar for the *M. puboischiofemoralis externus* is visible. The 4th trochanter is prominent and positioned on the proximal one-third of the bone. The distal end of the femur is divided into two condyles: a lateral condylus and a slightly smaller medial condylus. In dorsal view, a small groove between the two condyles is present, whereas a deeper depression can be seen in ventral view.

Tibia. The left tibia (Fig. 13I–L) is poorly preserved and its shaft is damaged. The proximal part is divided into a medial and lateral condylus. The medial condylus is oval and separated from the larger lateral one by a groove. The distal articular surface is crescent-shaped with an anterior and a posterior condylus, which are separated from each other by a shallow groove.

Fibula. The left fibula (Fig. 13M–P) is poorly preserved, with a proximal articular surface that has been



Figure 11. *Maomingosuchus acutirostris*, holotype, GPIT-PV-31657, Na Duong Formation, middle to upper Eocene, Vietnam. Left humerus in **A, B**, dorsal, **C, D**, ventral, **E, G**, proximal and **F, H**, distal views. Left ulna in **I, J**, lateral and **K, L**, medial views. **Abbreviations:** **acd**, anterior condylus; **atb**, anterior tubercle; **dpc**, deltopectoral crest; **hh**, humeral head; **lcd**, lateral condylus; **mcd**, medial condylus; **op**, olecranon process; **pcd**, posterior condylus; **ptb**; posterior tubercle. Scale bar = 5 cm.

nearly completely lost. The shaft is oval in cross-section. The distal articular surface is bean-shaped and slightly shifted posteriorly.

Metatarsals. The left metatarsal II (Fig. 13Q–T) is the best preserved and its proximal articular surface is flat and elongate. The shaft is flattened proximally, but is slightly oval in cross-section distally. The distal articular surface is broad with a nearly rectangular outline. The two condyles

are very low with only a very shallow groove separating them. In ventral view, a deep depression is visible directly proximal to the distal articular surface.

Osteoderms. Several dorsal osteoderms (Fig. 14A, B), some putative lateral osteoderms (Fig. 14C, D) and many osteoderm fragments are preserved – most of them occurring isolated. The osteoderm central surface is strongly ornamented with a pattern of deep oval and

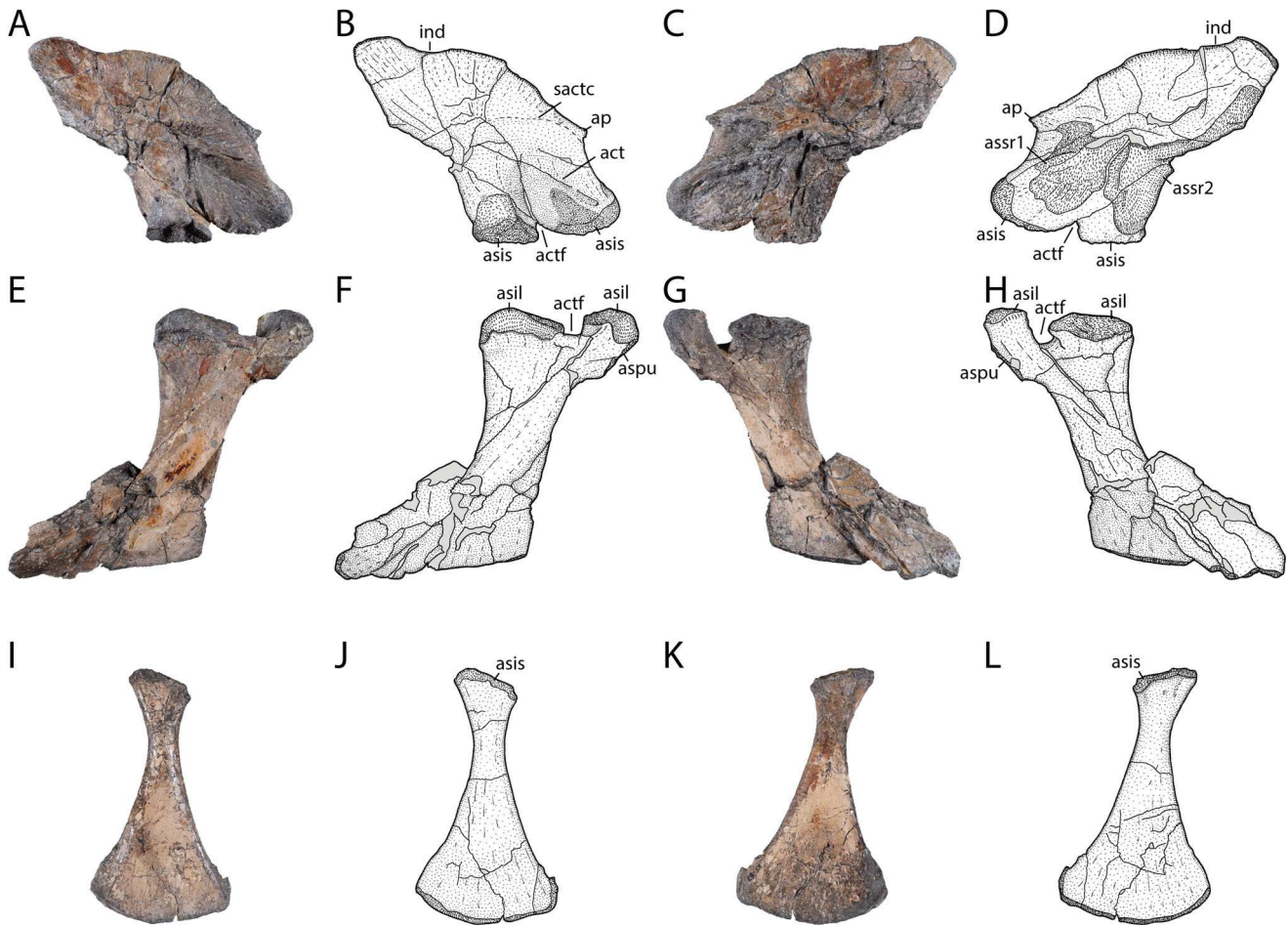


Figure 12. *Maomingosuchus acutirostris*, holotype, GPIT-PV-31657, Na Duong Formation, middle to upper Eocene, Vietnam. Right ilium in **A, B**, lateral and **C, D**, medial views. Right ischium in **E, F**, lateral and **G, H**, medial views. Left pubis in **I, J**, lateral and **K, L**, medial views. **Abbreviations:** **act**, acetabulum; **actf**, acetabulum foramen; **ap**, anterior process; **asil**, articulation surface with ilium; **asis**, articulation surface with ischium; **aspu**, articulation surface with pubis; **assr1**, articulation surface with sacral rib 1; **assr2**, articulation surface with sacral rib 2; **ind**, indentation; **sactc**, supraacetabular crest. Scale bar = 1 cm.

round pits. Towards the edges, the surface is smooth. The dorsal osteoderms are rectangular with a broad facet to contact the anteriorly positioned osteoderm. A well-developed dorsal keel is present, projecting from slightly posterior of the anterior facet to the posterior end of the osteoderm. The putative lateral osteoderms have a more oval outline and are slightly curved, but show a well-developed dorsal keel also. A contact surface is not visible but the edges seem to be damaged.

Comparisons

Comparisons with other *Maomingosuchus* specimens

Skulls. *Maomingosuchus acutirostris*, *Maomingosuchus petrolicus* and the Krabi-*Maomingosuchus* are all

medium-sized tomistomines with skull lengths of slightly over 500 mm (*M. acutirostris*, 546 mm; *M. petrolicus*, 280–503 mm, with NMNS005825-F044383 slightly larger based on the incomplete skull table [see Shan *et al.* 2017]; Krabi-*Maomingosuchus*, >500 mm, anterior part missing [see Martin *et al.* 2019]). The snout length is also very similar within *Maomingosuchus* with a snout-to-skull length ratio ranging between 0.71 and 0.72, but the snout shape differs slightly: in *M. petrolicus* and Krabi-*Maomingosuchus* it is narrow, with only a slight broadening at the level of the 5th maxillary tooth, while the snout of *M. acutirostris* is much broader at this level with a strongly enlarged 5th maxillary tooth.

Cranial openings. The general skull shape, as well as the cranial openings, are very similar in all *Maomingosuchus* specimens. The external nares of both



M. acutirostris and *M. petrolicus* are large and broader anteriorly than posteriorly (unknown in the Krabi specimen), but the premaxillary process reaching into the external naris described for *M. petrolicus* (Shan *et al.* 2017, p. 675), is not visible in *M. acutirostris*. The orbit of *M. acutirostris* is more elongated than the rounded one of *M. petrolicus* whereas the supratemporal fenestra is smaller than in the latter, resulting in a different ratio of the supratemporal fenestral length to orbit length (0.57 in *M. acutirostris*; 0.83 in *M. petrolicus*; and 0.76 for Krabi-*Maomingosuchus*).

The supratemporal bar in *M. petrolicus* is thin compared to skull table width (Shan *et al.* 2017, fig. 2). Its ratio is only around 0.07, while it is 0.11 in *M. acutirostris*. In Krabi-*Maomingosuchus* this ratio is difficult to determine, but the bar seems to be relatively broad (Martin *et al.* 2019, fig. 1), and the ratio appears to be closer to the ratio seen in *M. acutirostris*.

Skull bones. In general, the shapes of the individual skull bones and their sutures are similar in all *Maomingosuchus* specimens.

The premaxilla is only known for *M. acutirostris* and *M. petrolicus*, but in both species the anterior-most part differs, with a short and rounded anterior snout in *M. petrolicus* (Shan *et al.* 2017, figs 2, 4) and an elongated and acute one in *M. acutirostris*.

The anterior part of the prefrontal lies at the same level as the anterior part of the frontal in *M. acutirostris* and Krabi-*Maomingosuchus*. According to Shan *et al.* (2017), this condition is variable in *M. petrolicus*, as in some specimen (e.g. NMNS005146-F041793) the frontal is shorter than the prefrontal.

In *M. petrolicus* and Krabi-*Maomingosuchus* the prefrontal slightly overhangs the orbital margin (Martin *et al.* 2019). This is not the case in *M. acutirostris* but this could be a compressional artefact.

The supraoccipital is largely exposed on the skull table in *M. acutirostris* and *M. petrolicus*. In *M. petrolicus*, the exposure and shape of the supraoccipital is variable and either more rectangular, as in DM-F0001, or more triangular, as in NMNS002060-F027511 (Shan *et al.* 2017, fig. 3). In *M. acutirostris*, it is more triangular, whereas in Krabi-*Maomingosuchus* the condition is unknown.

Krabi-*Maomingosuchus* differs from *M. acutirostris* and *M. petrolicus* in the position of the

surangular–dentary suture in the external mandibular fenestra. Only in Krabi-*Maomingosuchus* does the suture reach the posterior-most corner (Martin *et al.* 2019, fig. 2), whereas the suture intersects the fenestra anterior to its posterior margin in *M. acutirostris* and *M. petrolicus*.

Teeth. In general, the tooth rows and teeth of *Maomingosuchus* specimens are similar but there are some noteworthy differences. In total, there are 15 maxillary teeth in *M. acutirostris* and *M. petrolicus*. In Krabi-*Maomingosuchus* the tooth number is difficult to assess, but at least 14 maxillary alveoli are visible (Martin *et al.* 2019, fig. 1). The 1st dentary tooth perforates the premaxilla anterior to the external naris in *M. acutirostris* and *M. petrolicus*, which is a rare character among tomistomines (see below). Due to the missing tip of the snout this condition is unknown in Krabi-*Maomingosuchus*. In *Maomingosuchus*, the premaxillary, anterior maxillary and anterior dentary teeth have clearly visible dorsoventrally projecting ridges on their lateral and mesial surfaces and the teeth have sharp outer edges (Shan *et al.* 2017, fig. 4; Martin *et al.* 2019, fig. 3).

Differences between the *Maomingosuchus* specimens occur in tooth size. In *M. acutirostris*, the 5th maxillary tooth and the 11th or 12th dentary tooth are enlarged, whereas in *M. petrolicus* (Shan *et al.* 2017, fig. 2) and Krabi-*Maomingosuchus* (Martin *et al.* 2019, fig. 1), the 5th maxillary tooth is also enlarged but smaller overall. In *M. acutirostris* and *M. petrolicus* the anterior alveoli increase in size towards the 5th maxillary tooth, whereas there is no size difference in Krabi-*Maomingosuchus*, with the 5th maxillary tooth being only slightly larger (Martin *et al.* 2019, fig. 1).

The spacing of the teeth posterior to the 5th maxillary alveolus also differs within *Maomingosuchus*. A wider distance between the 7th and 8th maxillary alveoli for the enlarged 11th or 12th dentary tooth is only present in *M. acutirostris* and to a smaller degree in *M. petrolicus* (Shan *et al.* 2017, fig. 4c, e). In Krabi-*Maomingosuchus* there are no enlarged dentary teeth and therefore no enlarged maxillary distance is present (Martin *et al.* 2019, fig. 2).

Postcranial skeleton. Two differences between *M. acutirostris* and *M. petrolicus* are present in the postcranial skeleton but not preserved for Krabi-*Maomingosuchus*. On the atlantal rib, there is a process on the dorsal

←
Figure 13. *Maomingosuchus acutirostris*, holotype, GPIT-PV-31657, Na Duong Formation, middle to upper Eocene, Vietnam. Left femur in **A, B**, dorsal, **C, D**, ventral, **E, G**, proximal and **F, H**, distal views. Left tibia in **I, J**, anterior and **K, L**, posterior views. Left fibula in **M, N**, lateral and **O, P**, medial views. Left metatarsal two in **Q, R**, dorsal and **S, T**, ventral views. **Abbreviations:** **4th tr**, fourth trochanter; **acd**, anterior condylus; **fh**, femur head; **lcd**, lateral condylus; **mcd**, medial condylus; **mpe**, insertion scar for the *M. puboischiofemoralis externus*; **pcd**, posterior condylus. Scale bar = 5 cm.

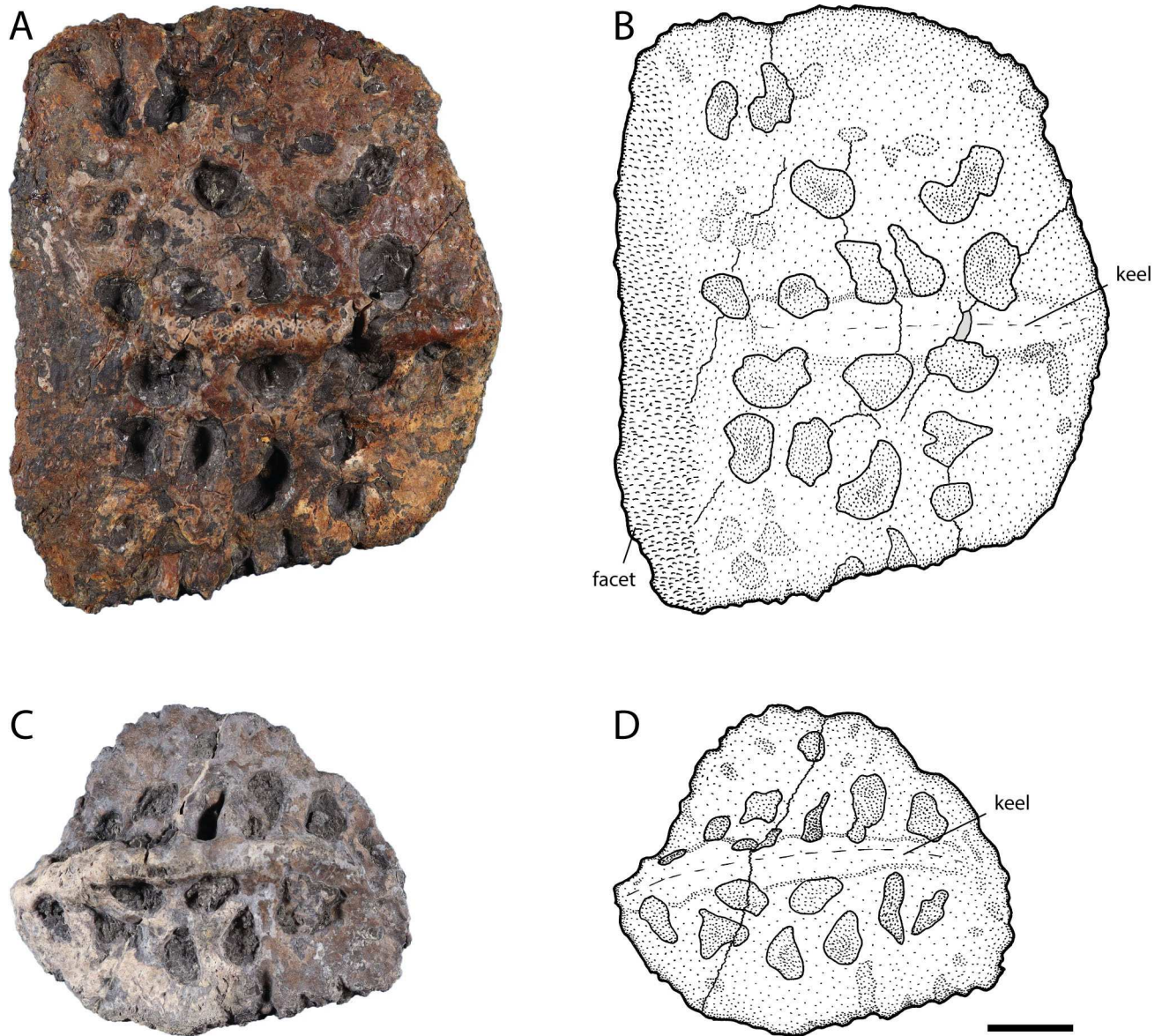


Figure 14. *Maomingosuchus acutirostris*, holotype, GPIT-PV-31657, Na Duong Formation, middle to upper Eocene, Vietnam. Dorsal midline osteoderm in **A, B**, dorsal view. Presumably lateral osteoderm in **C, D**, dorsal view. Scale bar = 1 cm.

margin in *M. acutirostris*, while this region seems to be smooth in *M. petolicus* (described as similar to *T. schlegelii* by Shan *et al.* [2017]). The ilium of *M. acutirostris* has a prominent anterior process. This region is poorly preserved in *M. petolicus* (Shan *et al.* 2017, fig. 10), but the anterior iliac border does not seem to lead into a process comparable to the one in *M. acutirostris*.

Comparisons with other taxa

Skulls. *Maomingosuchus* is a medium-sized tomistomine genus with a skull reaching slightly more than 500 mm

(see above). Tomistomines in general have a broad size range, from around 430 mm in *Kentisuchus spenceri* and *Dollosuchooides* to over 1 m in the giant species *Toyotamaphimeia*. The extant *Tomistoma schlegelii* exhibits remarkable size variation with a typical skull length of around 500 mm to a maximum of over 800 mm (Whitaker & Whitaker 2008). By contrast, the skull to snout ratio in Tomistominae remains relatively constant and ranges from around 0.7 to 0.8. With a skull to snout ratio between 0.71 and 0.72, *Maomingosuchus* is one of the shortest-snouted taxa, comparable to *Maroccosuchus* and *K. spenceri*. This is shorter than

extant *T. schlegelii* (with a ratio of 0.74) and much shorter than long snouted Miocene taxa like *Gavialosuchus* (with a ratio of 0.79).

Snout shape differs among tomistomines. In *Maroccosuchus*, the snout is laterally broadened at the level of the 5th maxillary tooth (Jouve *et al.* 2015, figs 3, 8), which is also the case in *Megadontosuchus* (Piras *et al.* 2007, fig. 1) and *M. acutirostris*, but to a slightly lesser degree. On the other hand, almost no expansion is present in *T. schlegelii*, ‘*Tomistoma*’ *calaritanum* Capellini, 1890 (Nicholl *et al.* 2020, fig. 10), *Dollosuchoides* (Brochu 2007, fig. 3) and *Gavialosuchus* (Toula & Kali 1885, table 1). Most other tomistomines have a slight expansion of the snout at the level of their largest maxillary tooth.

Cranial openings. The external naris in all known *Maomingosuchus* specimens with a preserved snout is large and anteriorly wider than posteriorly, with a nearly straight lateromedially projecting anterior margin, which is unique among tomistomines. In species like *T. schlegelii* or *Melitosaurus champsoides* Owen, 1849 (Nicholl *et al.* 2020, fig. 2) the external naris is smaller and oval. In species like *K. spenceri* (Brochu 2007, fig. 2), the external naris is relatively large and oval. A more rectangular shape with a straighter anterior margin similar to *Maomingosuchus* can be seen in *Maroccosuchus* (Jouve *et al.* 2015, figs 3, 7) and *Dollosuchoides* (Brochu 2007, fig. 3).

While the difference in orbit size seems to be small among tomistomines, the differences in supratemporal fenestra size are significant. For a longirostrine taxon, *Maomingosuchus* has relatively small fenestrae with broad posterior and lateral margins. Similar small fenestrae are present only in *Paratomistoma* (Brochu & Gingerich 2000, fig. 2). In *T. schlegelii*, *Maroccosuchus*, *Megadontosuchus*, *K. spenceri*, *Thecachampsa carolinensis* (Erickson & Sawyer, 1996), ‘*Tomistoma*’ *cairensis*, ‘*Tomistoma*’ *gaudense* (Hulke, 1871) and ‘*Tomistoma*’ *lusitanica* Antunes, 1961, the supratemporal fenestrae are medium-sized to large, while they are very enlarged in *Dollosuchoides*, *Thecachampsa antiqua* (Leidy, 1852), *Toyotamaphimeia* and *Gavialosuchus*.

The size of the supratemporal fenestrae also affects the shape of the interfenestral bar, which is usually wider in taxa with smaller fenestrae. The broadest bar is found in *Paratomistoma* (Brochu & Gingerich 2000, fig. 2) which also has the smallest fenestrae. The interfenestral bar is relatively broad in *Maroccosuchus* despite its medium-sized fenestrae (Jouve *et al.* 2015, figs 3, 8, 11).

The external mandibular fenestra of *Maomingosuchus* is medium- to large-sized for a tomistomine. In *T.*

schlegelii the fenestra is slightly larger, while it is smaller in *Toyotamaphimeia* (Kobayashi *et al.* 2006, figs 11, 12) and *Paratomistoma* (Brochu & Gingerich 2000, fig. 4).

Skull bones. In many tomistomines, the anterior-most part of the snout is more elongated, often including a lateral notch for the 1st dentary tooth (e.g. *Melitosaurus*, Nicholl *et al.* 2020, fig. 2; *Dollosuchoides*, Brochu 2007, fig. 3; most *T. schlegelii*). In other taxa, the snout is more rounded (e.g. *Toyotamaphimeia*, Kobayashi *et al.* 2006, fig. 7; *Maroccosuchus*, Jouve *et al.* 2015, figs 3, 7, 8; and *K. spenceri*, Brochu 2007, fig. 2). In *Maomingosuchus petrolicus*, the anterior region is especially short, shorter than in other tomistomines. In some more round-snouted taxa, a perforation of the premaxilla by the first dentary tooth occurs (*Toyotamaphimeia*, Kobayashi *et al.* 2006, figs 7, 15; *K. spenceri*, Brochu 2007, fig. 2; and *M. petrolicus* see above), but for taxa with a more elongated anterior snout this is only the case in *M. acutirostris*.

In *M. petrolicus* and *Krabi-Maomingosuchus*, the prefrontal slightly overhangs the orbit (see above). This is also known for *Maroccosuchus* (Jouve *et al.* 2015, fig. 9), *Penghusuchus* (Shan *et al.* 2009, fig. 2) and *T. schlegelii*. A frontal fossa is only present in *Maomingosuchus*. A similar structure is found in the crocodyloid ‘*Crocodylus*’ *affinis* (Mook 1921, pl. XVI) and *Prodiplacynodon langi* Mook (1941, fig. 2), a narrow ‘U’-shaped structure in the alligatoroid *Bottosaurus harlani* Meyer, 1832 (Cossette & Brochu 2018, figs 4, 5) and a broad ‘U’-shaped structure further anteriorly in the basal eusuchian *Acynodon iberoccitanus* Buscalioni, Ortega & Vasse, 1997 (Martin 2007, fig. 1).

The frontal in *Maomingosuchus* is wide and flat between the orbits, and the edges are not upturned, which is otherwise only known for *Dollosuchoides*. The postorbital bar in *Maomingosuchus* is anteroposteriorly expanded, whereas in most tomistomines the bar is massive but slenderer (e.g. *T. schlegelii*). Otherwise, a broad bar is only found in some basal eusuchians and gharials. The supraoccipital is only slightly exposed on the skull table and barely visible in most tomistomines, but this is pronounced in *Maomingosuchus*, ‘*T.*’ *cairensis* and ‘*Tomistoma*’ *coppensi* Pickford, 1994.

In *Maomingosuchus*, there is a ventrally projecting lamina on the exoccipital covering the entrance to the cranio-quadrangle passage. The character is otherwise only known for basal eusuchians like *Allodaposuchus precedens* Nopcsa, 1928 (Delfino *et al.* 2008, fig. 3) or *Hylaeochampsa vectiana* Owen, 1874 (Clark & Norell 1992, fig. 8) and among crocodylians only for gharials and thoracosaurus. A similar structure is present in

Penghusuchus, but here the lamina is more medially oriented.

In *Maomingosuchus acutirostris* and *M. petrolicus*, the surangular–dentary suture intersects the external mandibular fenestra anterior to its posterior border, whereas in *Krabi-Maomingosuchus*, the suture reaches the posterior-most corner of the fenestra (see above). The condition in *Krabi-Maomingosuchus* is unknown in any other tomistomine, but present in some alligatoroids like *Stangerochampsia mccabei* Wu, Brinkman & Russell, 1996, fig. 2, *Navajosuchus mooki* (Simpson, 1930) (Lucas & Estep 2000, fig. 4) or *Orientalosuchus naduogensis* (Massonne *et al.* 2019, fig. 9).

Teeth. The total tooth count in tomistomines is variable between species. *Marccosuchus*, *Thecachampsia carolinensis* and ‘*T.*’ *gaudense* have 14 teeth in the maxilla, *Dollosuchoides* and *Maomingosuchus* have a maximum of 15 teeth, *T. schlegelii* and *Toyotamaphimeia* have 16 and *Penghusuchus* 17 teeth.

In *Maomingosuchus*, the 1st dentary tooth perforates the premaxilla anterior to the external naris. In tomistomines, this is only known for *K. spenceri* (Brochu 2007, fig. 2) and some specimens of *T. schlegelii* (C. Brochu, pers. comm.). In *Toyotamaphimeia*, the premaxilla is also perforated by the 1st dentary tooth, but the openings are situated inside the external naris (Kobayashi *et al.* 2006, figs 7, 15). In other taxa, such as *Dollosuchoides* (Brochu 2007, fig. 3) or most *T. schlegelii*, the 1st dentary tooth projects into an anterolateral notch of the premaxilla. In *Marccosuchus*, there is no lateral notch or perforation for the 1st dentary tooth visible in dorsal view (Jouve *et al.* 2015, figs 7, 8), implying that the 1st dentary tooth is small. A perforated premaxilla is rare among tomistomines, but frequently present in members of Crocodylinae, such as *Crocodylus niloticus* Laurenti, 1768, in which the perforations are positioned further anteriorly.

Only the premaxillary, anterior maxillary and anterior dentary teeth of *Maomingosuchus* show dorsoventrally running ridges on their lateral and mesial surface, with sharp outer edges. Strong ridges are found in a tomistomine from the middle Eocene Ikovo locality (Kuzmin & Zvonok 2021, fig. 3) and in non-tomistomines such as *Allodaposuchus precedens* (Martin *et al.* 2016, fig. 11), *Krabisuchus siamogallicus* Martin & Lauprasert, 2010, fig. 5 and *Orientalosuchus naduogensis* (Massonne *et al.* 2019, fig. 10). Fine ridges are known for other tomistomines (such as *T. schlegelii* and *Melitosaurus*). Sharp outer edges on the teeth are present in *Thecachampsia antiqua* (Myrick 2001, fig. 5) and *Marccosuchus* (Jouve *et al.* 2015, p. 15), whereas in other species like *T. schlegelii* and *Melitosaurus*

(Nicholl *et al.* 2020 fig. 3) the teeth are more rounded with shallower edges.

In *M. acutirostris*, the difference in tooth sizes resembles the condition found in *Marccosuchus*, but the gaps between the teeth are distinctly smaller and the dentary is only slightly bent in lateral view, but more curved in *Marccosuchus* (Jouve *et al.* 2015, figs 2, 4, 15). The teeth of *Megadontosuchus* are all enlarged and represent an apomorphic morphology for a tomistomine (Piras *et al.* 2007, fig. 2). The dentition of *T. schlegelii* is homodont with only the 5th maxillary tooth being larger, and almost constant spacing along the tooth row. Similar morphology is also found in *Gavialosuchus* (Toula & Kail 1885, pl. 2), ‘*T.*’ *calaritanum* (Nicholl *et al.* 2020, fig. 14) and ‘*T.*’ *gaudense* (Nicholl *et al.* 2020, fig. 8).

Postcranial skeleton. The postcranial region is missing or poorly preserved in many tomistomines, making detailed comparisons difficult. Therefore, only species with well-known postcranial material are used here, including *Maomingosuchus*, *Penghusuchus* (Shan *et al.* 2009, figs 6–14), *Toyotamaphimeia* (Kobayashi *et al.* 2006, figs 31–68), *Thecachampsia carolinensis* (Erickson & Sawyer 1996, figs 7–21) and *T. schlegelii*.

The proatlas of *M. acutirostris* is boomerang-shaped and resembles that of *Penghusuchus* and *Toyotamaphimeia*, but it has a more elongated posterior process and a much higher medial keel. In the other species, like *T. schlegelii*, the proatlas is more block-like. An atlantal rib with a dorsal projection is known only in *Maomingosuchus* and *Toyotamaphimeia*.

In *M. acutirostris*, *Thecachampsia carolinensis* and *T. schlegelii*, the scapular blade is broad, whereas it is narrower in *Toyotamaphimeia* and even wider in *Penghusuchus*. The coracoid foramen in *M. acutirostris* is much smaller than that of *Toyotamaphimeia*, *Thecachampsia carolinensis* and *T. schlegelii*. The iliac blade of *M. acutirostris* is slightly distorted, but relatively broad with a shallow dorsal indentation, similar to *T. schlegelii*. *Toyotamaphimeia* has a narrower iliac blade and a shallower dorsal indentation. In *Penghusuchus* the dorsal indentation is very small, and in *Thecachampsia carolinensis* the posterior part of the blade seems to be sloped. Anteriorly, a prominent process is visible on the ilium of *M. acutirostris*. The process is visible, but smaller than in *Toyotamaphimeia* and *Penghusuchus*. No such process is visible in *T. schlegelii* or *Thecachampsia carolinensis*. Besides *M. acutirostris*, *Toyotamaphimeia* and *Penghusuchus*, such a process is known in gharials.

The dorsal osteoderms of *M. acutirostris*, *T. schlegelii* and *Toyotamaphimeia* have a prominent dorsal keel,

whereas no keel is present in *Penghusuchus* or *Thecachampsia carolinensis*.

Comparative discussion

Maomingosuchus differs from other tomistomines in general snout shape, but the sizes and snout-to-skull ratios are almost similar. Only in *Maomingosuchus acutirostris* is the snout much broader at the level of the 5th maxillary tooth and similar to *Marccosuchus*. Both of these species also have large teeth (see below) that could indicate a more generalist lifestyle.

The size ratio between the supratemporal fenestra and the orbit differs between *M. acutirostris* and other *Maomingosuchus* specimens. However, the size difference in the supratemporal fenestrae between *Maomingosuchus* specimens is not large, but represents the only synapomorphy in the phylogenetic analysis that unites *Maomingosuchus petrolicus* + Krabi-*Maomingosuchus*. This ratio seems to be variable between other tomistomine taxa. For ch. 244 (ratio of the anteroposterior length of the supratemporal fenestra to the anteroposterior length of the orbit: <0.5 [0], 0.5–0.75 [1] or >0.75 [2]); half of the tomistomine taxa were scored with state (1) whereas the other half were scored with state (2). The variability of this character within Tomistominae challenges the synapomorphy of *M. petrolicus* + Krabi-*Maomingosuchus*.

In most tomistomines, the intersupratemporal bar is very narrow in comparison with the width of the skull table. In *M. acutirostris* the ratio is slightly different and the bar is broader compared to other *Maomingosuchus* specimens, but the difference is not that large (for more information see [Supplemental material S2](#)).

In *M. acutirostris* and *M. petrolicus* the 1st dentary tooth perforates the premaxilla anterior to the external naris (unknown for Krabi-*Maomingosuchus*) and this could either be autapomorphic for *Maomingosuchus* or synapomorphic for *M. acutirostris* + *M. petrolicus*.

In *M. petrolicus* and Krabi-*Maomingosuchus* overall tooth size is uniform and the teeth are slender and pointed, as in most tomistomines, but some teeth are more robust and blunter in *M. acutirostris* similar to *Marccosuchus*. This may indicate a somewhat different lifestyle for *M. acutirostris* with a less exclusive piscivorous diet.

M. acutirostris and *M. petrolicus* have a thin lamina of the exoccipital projecting ventrally to cover the entrance of the cranio-quadrate passage on the exoccipital, similar to *Gavialis gangeticus* (Gmelin, 1789). This lamina could either be a synapomorphy uniting *M.*

acutirostris with *M. petrolicus* or it could be an autapomorphy for the whole genus, depending on the condition in Krabi-*Maomingosuchus*. Determination of the condition in *Penghusuchus* is needed to check if the structure present there is homologous to the condition in *Maomingosuchus*.

Phylogenetic analysis

Results

For the maximum parsimony analysis of the traditional search, a total of 17,496 equally optimal trees with lengths of 1017 steps, a consistency index (CI) of 0.317 and a retention index (RI) of 0.690 were recovered ([Figs 15, 16](#)). For the New Technology search analysis, a total of 864 equally optimal trees with the same lengths and same consistency and retention indices were found, and there are no differences in the tree topologies between the results of the traditional and the New Technology search approaches.

Two taxa (*Kentisuchus astrei* Jouve, 2016 and *Melitosaurus*) were pruned from the strict consensus tree after the analysis, because of their unstable positions in the tree. Their potential positions are indicated by the letters 'a' or '> a' for *K. astrei* and '> b' for *Melitosaurus* ([Fig. 16](#)): 'a' indicates that the taxa, if included on the tree, would be sister taxon to a single other taxon, whereas '> a' and '> b' mean that those taxa would be in a polytomy. If *K. astrei* is not pruned from the tree, the resolution is reduced at the base of Tomistominae, whereas the inclusion of *Melitosaurus* leads to a significant loss of resolution among more derived taxa. A complete tree with all of the taxa included can be found in [Supplemental material S2](#).

Overall, the consensus tree is consistent with previous analyses (e.g. Brochu 1999, 2011; Jouve *et al.* 2015; Shan *et al.* 2017; Martin *et al.* 2019; Massonne *et al.* 2019; Nicholl *et al.* 2020), but compared to the analyses of Jouve *et al.* (2015), Shan *et al.* (2017) and Iijima *et al.* (2018), our tree resolution is lower within some groups (Gavialoidea, *Borealosuchus* spp. and Crocodyloidea).

Maomingosuchus is monophyletic with *M. petrolicus* from Maoming and Krabi-*Maomingosuchus* forming the sister group to *M. acutirostris*. *Maomingosuchus* was recovered in a basal position within Tomistominae as the sister clade to *Tomistoma* + *Paratomistoma* + *Gavialosuchus* + *Melitosaurus*. A list of synapomorphies can be found in [Supplemental material S2](#).

Bremer support and bootstrap values on the tree are generally low. The Bremer support for Tomistominae is 1. This is also the case for *Maomingosuchus* and *M.*

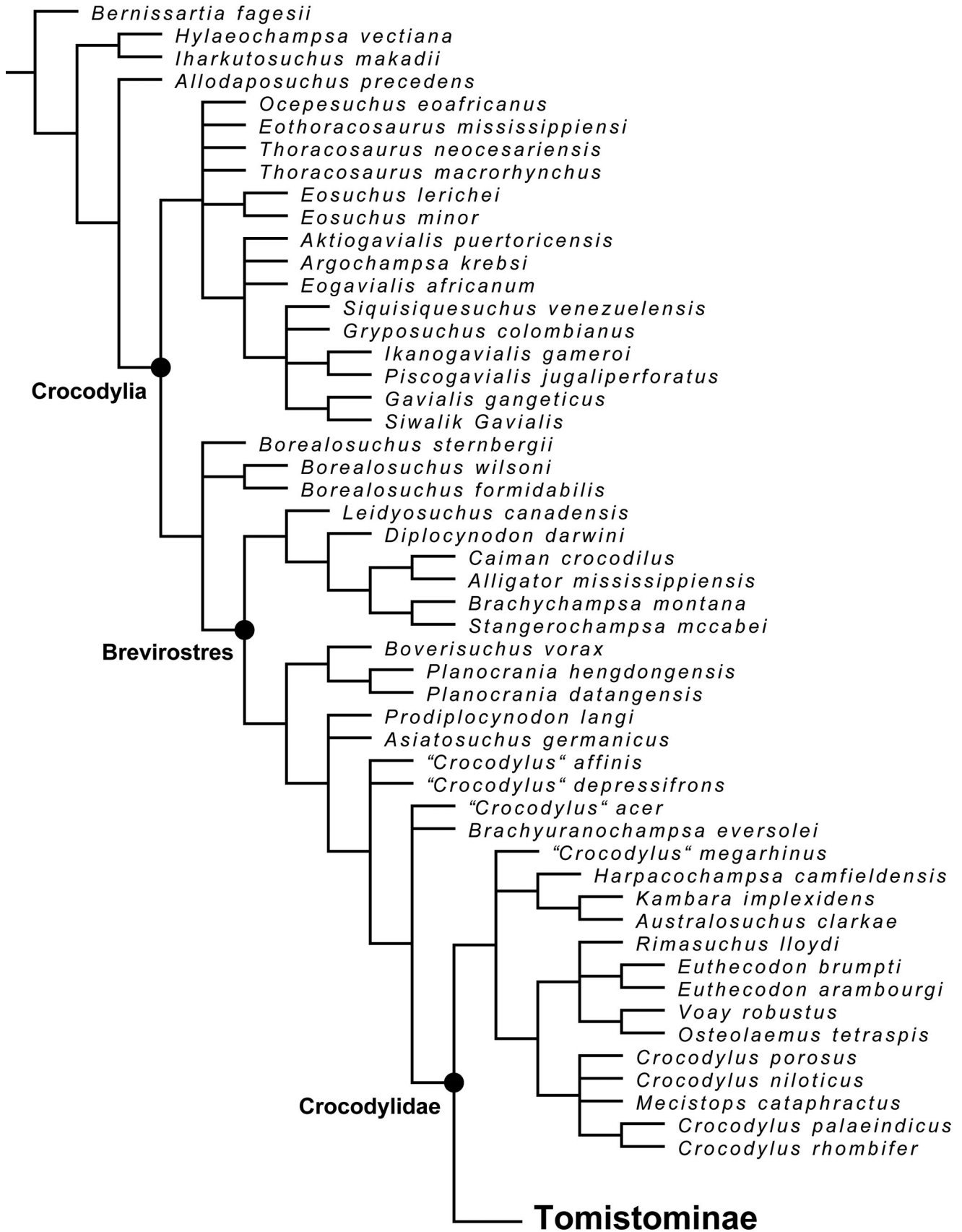


Figure 15. Reduced strict consensus tree of 17,496 equally optimal trees, obtained from the maximum parsimony analysis of 72 taxa and 244 characters; tree length = 1017 steps; consistency index = 0.317; and retention index = 0.690.

petrolicus + Krabi-*Maomingosuchus* (all Bremer support values can be found in Supplemental material S2). In Tomistominae the frequency differences (GC) standard bootstrap values are 15 for Tomistominae and 18 for *Maomingosuchus*. *M. petrolicus* + Krabi-*Maomingosuchus* have a support of 2.

Phylogenetic discussion

Outside Tomistominae, the tree is mostly consistent with previous analyses based on morphological data alone (e.g. Brochu 1999, 2011; Jouve *et al.* 2015; Shan *et al.* 2017; Martin *et al.* 2019; Massonne *et al.* 2019; Nicholl *et al.* 2020), but lacks resolution at some nodes (Gavialoidea, *Borealosuchus* spp. and Crocodyloidea) as is also the case in Nicholl *et al.* (2020). This is different in Shan *et al.* (2017) and Iijima *et al.* (2018), most likely due to our ordering of characters (see Materials and methods, above). This ordering also affects tomistomines, in that *Dollosuchoides* is considered to be the sister taxon to *Thecachampsia antiqua* + *Thecachampsia carolinensis* + *Penghusuchus* + *Toyotamaphimeia* instead of being placed in a more basal position on the tree.

Our analysis yields a polytomy at the base of Tomistominae including *Marccosuchus*, *Kentisuchus astrei*, *Kentisuchus spenceri* and *Megadontosuchus* or a polytomy between *Marccosuchus* and *K. spenceri* if *K. astrei* is pruned from the tree.

Maomingosuchus consists of *Maomingosuchus acutirostris*, *Maomingosuchus petrolicus* and the Krabi-*Maomingosuchus* and is supported by three

autapomorphies, a flush margin of the orbit with the skull surface (103–0), a ventral border of the exoccipital convex and ventrally projected (166–0) and a frontal ending at the same level as the anterior extension of the prefrontal (171–1).

The monophyly of *Maomingosuchus* is the most parsimonious hypothesis and found in all trees, despite the weak Bremer support.

In previous analyses (Shan *et al.* 2017; Iijima *et al.* 2018; Nicholl *et al.* 2020), *M. petrolicus* was found in varying positions among tomistomines, but usually in a more derived position than in our current analysis. Only Piras *et al.* (2007) obtained similar results. Only the analysis by Martin *et al.* (2019) included *M. petrolicus* as well as Krabi-*Maomingosuchus* and found *Maomingosuchus* as the sister clade to the extant *T. schlegelii*.

Our rescoring of some characters for *M. petrolicus* and Krabi-*Maomingosuchus* (Supplemental material S2), as well as the incorporation of *M. acutirostris*, results in a more basal position of *Maomingosuchus* that is more congruent with its upper Eocene–lower Oligocene age.

It is noteworthy that the position of *Maomingosuchus* is generally stable on the tree. The genus always forms the sister clade to a group consisting of ‘*Tomistoma*’ *cairensis* + ‘*Tomistoma*’ *coppensi* + *Paratomistoma* + *Tomistoma schlegelii* + ‘*Tomistoma*’ *lusitanica* + *Gavialosuchus* + ‘*Tomistoma*’ *gaudense* + ‘*Tomistoma*’ *calaritanum* + *Melitosaurus*, regardless of whether *K. astrei* or *Melitosaurus* are pruned from the tree or not.

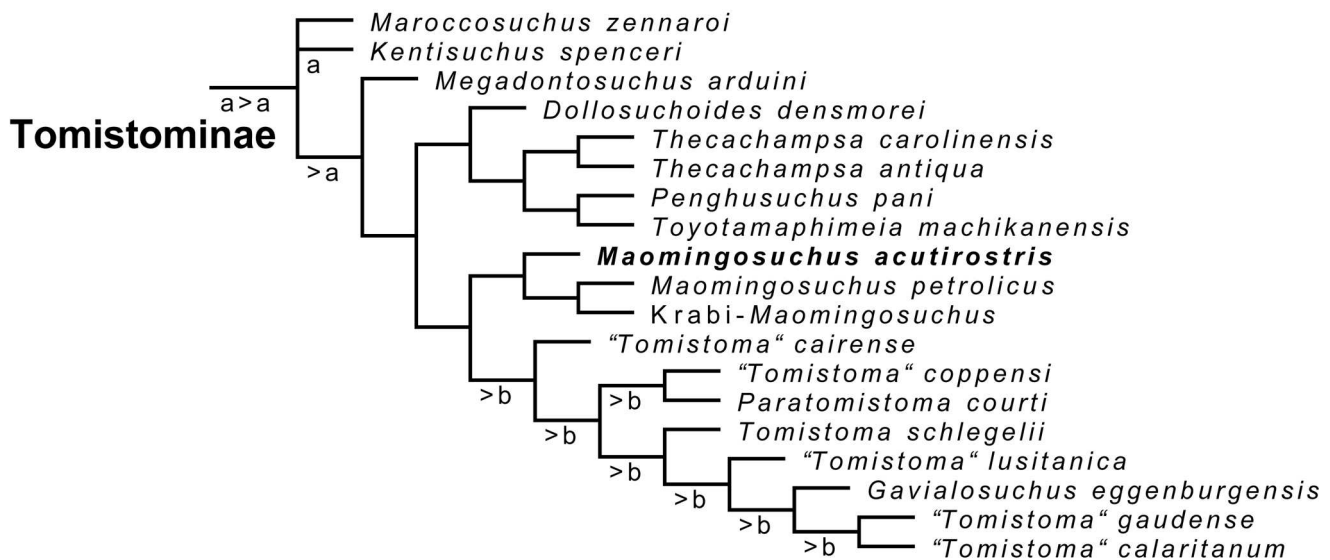


Figure 16. Tomistominae phylogeny as inferred from the reduced strict consensus tree of 17,496 equally optimal trees, obtained from the maximum parsimony analysis of 72 taxa and 244 characters; tree length = 1017 steps; consistency index = 0.317; and retention index = 0.690. ‘a’ indicates the alternative position of the pruned *Kentisuchus astrei*. ‘b’ indicates the alternative position of the pruned *Melitosaurus champsoides*.

A new phylogenetic analysis by Rio & Mannion (2021) recovered *Gavialis* as more closely related to *Tomistoma* than to other extant crocodylians, based solely on morphological data. This further suggests paraphyly of the classical subfamily Tomistominae. However, the more basal position of *M. petrolicus* is also supported in this analysis, indicating that *Maomingosuchus* belongs to a stem group leading to recent *Tomistoma* and *Gavialis*. Further analyses that include *M. acutirostris* and *Krabi-Maomingosuchus* are necessary to get better insights into the relationships between *Maomingosuchus* and other gavialoids.

Palaeobiogeographical implications

Based on our analysis and previous phylogenies most basal tomistomine taxa are from the western Tethyan region. It is therefore most parsimonious to assume that they originated in that area before the early Eocene (as already proposed by Jouve *et al.* 2015; Jouve 2016; Shan *et al.* 2017; Iijima *et al.* 2018; Nicholl *et al.* 2020). Moreover, based on our analysis, we conclude that dispersals towards eastern Asia must have happened multiple times independently. Accordingly, the first dispersal occurred no later than the late Eocene for the

stem lineage of *Maomingosuchus*, while a second dispersal occurred no later than the early–middle Miocene for the stem lineage of *Penghusuchus* + *Toyotamaphimeia*, and a third one took place for the stem lineage of the extant *Tomistoma schlegelii* during the Neogene. For better clarification, we mapped the ages of the respective fossils based on available data from the literature onto our phylogenetic tree (Fig. 17).

Based on palaeogeographical reconstructions, two different dispersal routes for the stem lineage of *Maomingosuchus* seem possible: an eastern route from Europe via coastal dispersal along the Neotethys to south-eastern Asia (consistent with Jouve *et al.* 2015, fig. 18) and a western route from Europe via North America and Beringia to south-eastern Asia. The latter one as suggested for Orientalosuchina (Massonne *et al.* 2019) seems rather unlikely, due to the absence of suitable fossils in North America at that time.

A potential key to solve this problem are the tomistomine species from the middle Eocene of central and south Asia, but their tomistomine affinities have been questioned (Jouve 2004; Jouve *et al.* 2015). ‘*Tomistoma*’ *borisovi* Efimov, 1988 and *Dollosuchus zajsanicus* (Efimov, 1982) are only fragmentary and difficult to diagnose (Piras *et al.* 2007; Jouve *et al.* 2015; Kuzmin & Zvonok 2021). ‘*Tomistoma*’ *tandoni* Sahni & Mishra, 1975 is known only from a mandible and

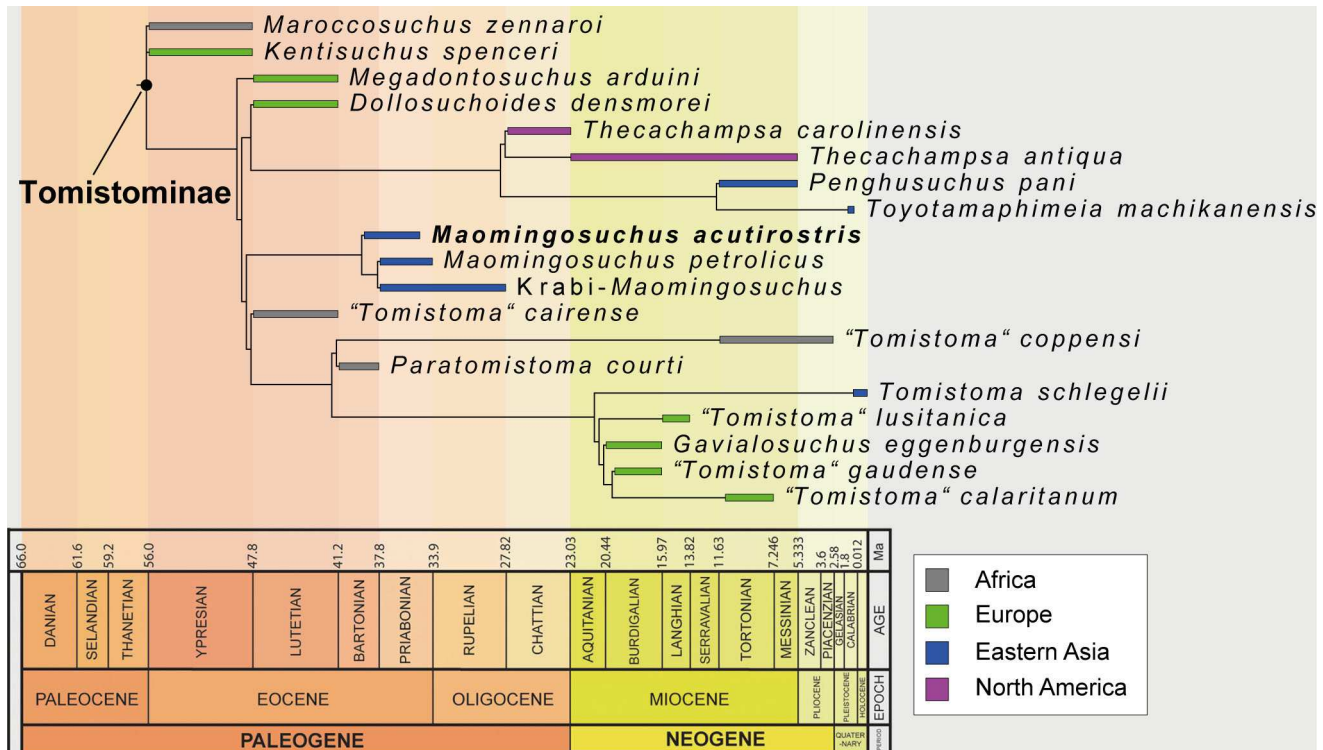


Figure 17. Time-scaled reduced strict consensus tree of Tomistominae, based on available data from the literature. *Kentisuchus astrei* and *Melitosaurus champsoides* pruned (modified after Nicholl *et al.* 2020).

Ferganosuchus planus Efimov, 1982 from a skull table and some postcranial material. Further crocodylian remains are known from the middle Eocene Pondaung Formation of central Myanmar (Tsubamoto *et al.* 2006a, b), including two different crocodylian teeth figured by Tsubamoto *et al.* (2006b, fig. 12) of which the larger one resembles the larger teeth of *Maomingosuchus acutirostris* in exhibiting a well-developed lateral edge. According to Tsubamoto *et al.* (2006a), there are more teeth and bone fragments from the same locality, but they remain unpublished.

The results of the current phylogenetic analysis, together with previous analyses (Martin & Lauprasert 2010; Skutschas *et al.* 2014; Shan *et al.* 2017, 2021; Martin *et al.* 2019; Massonne *et al.* 2019) demonstrate a close connection between the crocodylian faunas of three east Asian fossil sites: the Na Duong Basin in Vietnam (e.g. Böhme *et al.* 2011, 2013; Wysocka *et al.* 2020), the Maoming Basin in China (e.g. Jin 2008; Averianov *et al.* 2016) and the Wai-Lek from Krabi Province, Thailand (e.g. Benammi *et al.* 2001; Claude *et al.* 2007). In all three localities, similar crocodylians of two unrelated groups are found that, based on their morphology, occupied different niches, with the longirostrine *Maomingosuchus* more piscivorous (Shan *et al.* 2017; Martin *et al.* 2019), and the brevirostrine *Orientalosuchina* with a more generalist diet (Martin & Lauprasert 2010; Skutschas *et al.* 2014; Wang *et al.* 2016; Li *et al.* 2019; Massonne *et al.* 2019; Shan *et al.* 2021).

Dispersal towards eastern Asia, however, probably differed for both groups. While *Orientalosuchina* were already present in the region during the Late Cretaceous (Li *et al.* 2019) and most likely originated in North America (Massonne *et al.* 2019), the stem lineage of *Maomingosuchus* probably arrived in eastern Asia from Europe sometime before the upper Eocene (e.g. Jouve *et al.* 2015; Shan *et al.* 2017; Martin *et al.* 2019).

The crocodylian faunas of the three localities (Na Duong, Maoming and Krabi) are very similar, but show distinct species, which could be explained by either climatic and/or geographical barriers. Climatic barriers between the Na Duong and Maoming basins seem unlikely, since both basins are close to each other (~400 km apart) and at the same latitude (Fig. 1). This distribution recalls a similar case in the turtle fauna with *Banhxeochelys trani* Garbin, Böhme & Joyce, 2019 from Na Duong being closely related to *Isometremys lacuna* Chow & Yeh, 1962 and *Guangdongemys pingi* Claude, Zhang, Li, Mo, Kuang & Tong, 2012 from Maoming (Garbin *et al.* 2019). Based on the presence of closely related crocodile and turtle faunas in Na Duong, Maoming and Krabi, it seems likely that other

middle–upper Eocene deposits in eastern and south-eastern Asia (e.g. the Pondaung Formation in Myanmar) will yield species of *Maomingosuchus* and *Orientalosuchina*. Further investigations on those fossil sites are needed to obtain more information of the faunas and palaeobiogeography of eastern and south-eastern Asia during the upper Eocene–lower Oligocene.

Conclusions

Maomingosuchus acutirostris sp. nov. is a new tomistomine species from the middle–upper Eocene deposits (late Bartonian–Priabonian age, 39–35 Ma) of the Na Duong Basin in Vietnam. *M. acutirostris* is a medium-sized tomistomine with a relatively robust snout and multiple enlarged teeth, similar to *Maroccosuchus*, potentially indicating a less piscivorous diet than the extant *Tomistoma schlegelii*.

Our phylogenetic analysis recovers *M. acutirostris* as the sister taxon to a monophyletic group consisting of *M. petrolicus* from the upper Eocene of the Maoming Basin of south-eastern China and Krabi-*Maomingosuchus* from the upper Eocene–lower Oligocene of Wai-Lek from Krabi Province, Thailand. The basal position of *Maomingosuchus* is generally stable on the tree, being congruent with the upper Eocene–lower Oligocene age of *Maomingosuchus*.

The phylogenetic analysis supports a western Tethyan origin for tomistomines with three independent dispersal events from Europe to eastern Asia. One for the stem lineage of *Maomingosuchus*, another for the stem lineage of *Pengusuchus* + *Toyotamaphimeia* and a third for the stem lineage of the extant *T. schlegelii*.

The similarities between the crocodile faunas of Na Duong, Maoming and Krabi are noteworthy. More material from other upper Eocene–lower Oligocene sites in eastern Asia could show if representatives of *Maomingosuchus* and *Orientalosuchina* were more widely spread across east Asia than currently known and could shed new light on the palaeobiogeographical and faunal connections between these different Eocene–Oligocene localities in eastern Asia.

Acknowledgements

We want to thank the editor Jonah Choiniere and two anonymous reviewers for their comments, which helped us improve the manuscript. We thank our Vietnamese colleagues who facilitated and participated in the Na Duong palaeontological expeditions of 2009, 2011 and 2012: Nguyễn Việt Hưng, La Thế Phúc, Đặng Ngọc

Trần, Đỗ Đức Quang, Phan Đồng Pha. The authors further wish to thank Ivan Kuzmin (University of Saint Petersburg), Gustavo Darlim, Josephina Hartung, Panagiotis Kampouridis, Thomas Lechner, Márton Rabi, Adrian Tröscher and Jules Walter (all University of Tübingen) for discussions. Agnes Fatz and Wolfgang Gerber are thanked for helping with photographing the material in Figures 2, 3 and 6; Regina Ellenbracht and Henrik Stöhr (both University of Tübingen) are thanked for preparation. Christopher A. Brochu (University of Iowa) is thanked for stimulating discussion during his visit to Tübingen and for photographs of the *Maomingosuchus petrolicus* holotype and Krabi-*Maomingosuchus*. Sonja Scheiben and Adrian Tröscher (University of Tübingen) kindly provided us with photographs of extant crocodile material for comparisons. Ingmar Werneburg (University of Tübingen) and Alexander Kupfer (Staatliches Museum für Naturkunde Stuttgart) are thanked for granting access to specimens under their care. The Willi Hennig Society is thanked for providing access to the software TNT v. 1.5.

Supplemental material

Supplemental material for this article can be accessed here: <https://doi.org/10.1080/14772019.2022.2054372>.

ORCID

Tobias Massonne  <http://orcid.org/0000-0002-6782-5280>

Felix J. Augustin  <http://orcid.org/0000-0002-7787-5601>

References

- Antunes, M. T.** 1961. *Tomistoma lisitanica*, crocodilien du Miocène du Portugal. *Revista Faculdade de Ciências da Universidade de Lisboa (Series 2)*, **9**, 5–88.
- Averianov, A., Obratzsova, E., Danilov, I., Skutschas, P. & Jin, J.** 2016. First nimravid skull from Asia. *Scientific Reports*, **6**(1), 25812. doi:10.1038/srep25812
- Benammi, M., Chaimanee, Y., Jaeger, J. J., Suteethorn, V. & Ducrocq, S.** 2001. Eocene Krabi Basin (southern Thailand): paleontology and magnetostratigraphy. *Geological Society of America Bulletin*, **113**(2), 265–273.
- Benton, M. J. & Clark, J. M.** 1988. Archosaur phylogeny and the relationships of the Crocodylia. Pp. 295–338 in M. J. Benton (ed.) *The phylogeny and classification of the tetrapods, volume 1, amphibians, reptiles, birds*. Clarendon Press, Oxford.
- Berg, D. E.** 1969. *Charactosuchus kugleri*, eine neue Krokodilart aus dem Eozän von Jamaica. *Eclogae Geologicae Helvetiae*, **62**, 731–735.
- Bezuijen, M. R., Shwedick, B. M., Sommerlad, R., Stevenson, C. & Steubing, R. B.** 2010. *Tomistoma Tomistoma schlegelii*. Pp. 133–138 in Crocodile Specialist Group (eds) *Crocodile: status survey and conservation action plan*. IUCN, Darwin.
- Böhme, M., Prieto, J., Schneider, S., Hung, N. V. & Tran, D. N.** 2011. The Cenozoic on-shore basins of northern Vietnam: biostratigraphy, vertebrate and invertebrate faunas. *Journal of Asian Earth Sciences*, **40**(2), 672–687.
- Böhme, M., Aiglstorfer, M., Antoine, P. O., Appel, E., Havlik, P., Métails, G., Phug, L. T., Schneider, S., Setzer, F., Tappert, R., Tran, D. N., Uhl, D. & Prieto, J.** 2013. Na Duong (northern Vietnam) – an exceptional window into Eocene ecosystems from southeast Asia. *Zitteliana A*, **53**, 121–167.
- Brochu, C. A.** 1999. Phylogenetics, taxonomy, and historical biogeography of Alligatoroidea. *Memoirs of the Society of Vertebrate Paleontology*, **6**, 9–100.
- Brochu, C. A.** 2003. Phylogenetic approaches toward crocodylian history. *Annual Review of Earth and Planetary Sciences*, **31**(1), 357–397.
- Brochu, C. A.** 2007. Systematics and taxonomy of Eocene tomistomine crocodylians from Britain and Northern Europe. *Palaeontology*, **50**(4), 917–928.
- Brochu, C. A.** 2011. Phylogenetic relationships of *Necrosuchus ionensis* Simpson, 1937 and the early history of caimanines. *Zoological Journal of the Linnean Society*, **163**(supplement 1), S228–S256.
- Brochu, C. A. & Gingerich, P. D.** 2000. New tomistomine crocodylian from the middle Eocene (Bartonian) of Wadi Hitan, Fayum Province, Egypt. *Contributions from the Museum of Paleontology, University of Michigan* **30**, 251–268.
- Buckland, W.** 1836. *Geology and mineralogy considered with reference to natural theology*. W. Pickering, London, 618 pp.
- Buscalioni, A. D., Ortega, F. & Vasse, D.** 1997. New crocodiles (Eusuchia: Alligatoroidea) from the Upper Cretaceous of southern Europe. *Comptes Rendus de l'Académie des Sciences, Series IIA, Earth and Planetary Science*, **325**(7), 525–530.
- Capellini, G.** 1890. Sul coccodrilliano grialoide (*Tomistoma calaritanus*) scoperto nella collina di Cagliari nel 1868. *Atti della Reale Accademia Lincei, Memorie della Classe di Scienze Fisiche, Matematiche e Naturali, serie 4*, **6**, 507–533.
- Chow, M. C. & Yeh, H. K.** 1962. A new emydid from Eocene of Maoming Kwangtung. *Vertebrata Palasiatica*, **6**(3), 225–229.
- Clark, J. M. & Norell, M.** 1992. The Early Cretaceous crocodylomorph *Hylaeochampsia vectiana* from the Wealden of the Isle of Wight. *American Museum Novitates*, **3032**, 1–19.
- Claude, J., Suteethorn, V. & Tong, H.** 2007. Turtles from the late Eocene–early Oligocene of the Krabi Basin (Thailand). *Bulletin de la Société géologique de France*, **178**(4), 305–316.
- Claude, J., Zhang, J. Y., Li, J. J., Mo, J. Y., Kuang, X. W. & Tong, H.** 2012. Geoemydid turtles from the Late Eocene Maoming basin, southern China. *Bulletin de la Société géologique de France*, **183**(6), 641–651.

- Cossette, A. P. & Brochu, C. A.** 2018. A new specimen of the alligatoroid *Bottosaurus harlani* and the early history of character evolution in alligatorids. *Journal of Vertebrate Paleontology*, **38**(4), 1–22.
- Darlim, G., Lee, M. S. Y., Walter, J. & Rabi, M.** 2022. The impact of molecular data on the phylogenetic position of the putative oldest crown crocodylian and the age of the clade. *Biology Letters*, **18**, 20210603. doi:10.1098/rsbl.2021.0603
- Delfino, M., Codrea, V., Folie, A., Dica, P., Godefroit, P. & Smith, T.** 2008. A complete skull of *Allodaposuchus precedens* Nopcsa, 1928 (Eusuchia) and a reassessment of the morphology of the taxon based on the Romanian remains. *Journal of Vertebrate Paleontology*, **28**(1), 111–122.
- de Zigno, A.** 1880. Sopra un cranio di coccodrillo scoperto nel terreno eoceno del Veronese. *Atti della Reale Accademia Nazionale dei Lincei: Memorie della Classe di Scienze fisiche, Matematiche e Naturale, Serie 3*(5), 65–72.
- Dollo, L.** 1883. Première note sur les crocodyliens de Bernissart. *Bulletin du Musée royal d'Histoire naturelle de Belgique*, **2**, 309–338.
- Efimov, M. B.** 1982. New fossil crocodiles from the USSR. *Paleontologičeskij žurnal*, **2**, 146–150.
- Efimov, M. B.** 1988. Fossil crocodiles and champsosaurs of Mongolia and the USSR. *Trudy Sovmestnoi Sovetskogo-Mongol'skoi Paleontologičeskoi Ekspeditsii*, **36**, 1–108.
- Erickson, B. R. & Sawyer, G. T.** 1996. The estuarine crocodile *Gavialosuchus carolinensis* n. sp. (Crocodylia: Eusuchia) from the late Oligocene of South Carolina, North America. *Science Museum of Minnesota Monographs (Paleontology)*, **3**, 1–49.
- Fitzinger, L. J.** 1826. *Neue Classification der Reptilien nach ihren natürlichen Verwandtschaften. Nebst einer Verwandtschaftstafel und einem Verzeichnisse der Reptiliensammlung des K.K. zoologischen Museum's zu Wien.* J. G. Heubner, Vienna, 66 pp.
- Garbin, C. G., Böhme, M. & Joyce, W. G.** 2019. A new testudinoid turtle from the Middle to late Eocene of Vietnam. *PeerJ*, **7**(1), e6280. doi:10.7717/peerj.6280
- Gmelin, J. F.** 1789. Regnum animale. Pp. 1033–1516 in *Caroli a Linne Systema Naturae per regna tri naturae, secundum classes, ordines, genera, species, cum characteribus, differentiis, synonymis, locis. volume 1.* G. E. Beer, Leipzig.
- Goloboff, P. A., Farris, J. S. & Nixon, K. C.** 2008. TNT, a free program for phylogenetic analysis. *Cladistics*, **24**(5), 774–786.
- Goloboff, P. A. & Catalano, S. A.** 2016. TNT version 1.5, including a full implementation of phylogenetic morphometrics. *Cladistics*, **32**(3), 221–238.
- Hulke, J. W.** 1871. Note on some reptilian fossils from Gozo. *Quarterly Journal of the Geological Society of London*, **27**(1–2), 29–33.
- Huxley, T. H.** 1875. On *Stagonolepis robertsoni*, and on the evolution of the Crocodylia. *Quarterly Journal of the Geological Society of London*, **31**(1–4), 423–438.
- Iijima, M., Momohara, A., Kobayashi, Y., Hayashi, S., Ikeda, T., Taruno, H., Watanabe, K., Tanimoto, M. & Furui, S.** 2018. *Toyotamaphimeia* cf. *machikanensis* (Crocodylia, Tomistominae) from the middle Pleistocene of Osaka, Japan, and crocodylian survivorship through the Pliocene-Pleistocene climatic oscillations. *Palaeogeography, Palaeoclimatology, Palaeoecology*, **496**, 346–360.
- Iijima, M. & Kobayashi, Y.** 2019. Mosaic nature in the skeleton of East Asian crocodylians fills the morphological gap between “Tomistominae” and Gavialinae. *Cladistics*, **35**(6), 623–632.
- Jin, J. H.** 2008. On the age of the Youganwo Formation in the Maoming basin, Guangdong Province. *Journal of Stratigraphy*, **32**(1), 47–50.
- Jonet, S. & Wouters, G.** 1972. Présence d'un crocodyliens nouveau dans les phosphates Yprésiens du Maroc. *Bulletin de la Société Belge de Géologie, de Paléontologie et d'Hydrologie*, **81**, 209–210.
- Jonet, S. & Wouters, G.** 1977. *Marccosuchus zennaroi*, crocodylian Eusuchien nouveau des Phosphates du Maroc. Notes et Mémoires du Service Géologique du Maroc, **38**, 177–202.
- Jouve, S.** 2004. *Etude des Crocodyloformes fini Crétacé-Paléogène du Bassin des Oulad Abdoun (Maroc) et comparaison avec les faunes africaines contemporaines: systématique, phylogénie et paléobiogéographie.* Unpublished PhD thesis, Muséum National d'Histoire Naturelle, Paris, 651 pp.
- Jouve, S.** 2016. A new basal tomistomine (Crocodylia, Crocodyloidea) from Issel (Middle Eocene; France): palaeobiogeography of basal tomistomines and palaeogeographic consequences. *Zoological Journal of the Linnean Society*, **177**(1), 165–182.
- Jouve, S., Bouya, B., Amaghazaz, M. & Meslouh, S.** 2015. *Marccosuchus zennaroi* (Crocodylia: Tomistominae) from the Eocene of Morocco: phylogenetic and palaeobiogeographical implications of the basalmost tomistomine. *Journal of Systematic Palaeontology*, **13**(5), 421–445.
- Kälin, J. A.** 1955. Zur Stammesgeschichte der Crocodylia. *Revue Suisse de Zoologie*, **62**, 347–356.
- Kobatake, N., ChiJi, M., Ikebe, N., Ishida, S., Kamei, T., Nakaseko, K. & Matsumoto, E.** 1965. Discovery of crocodile fossil from the Osaka Group. *The Quaternary Research (Daiyonki-Kenkyu)*, **4**(2), 49–58.
- Kobayashi, Y., Tomida, Y., Kamei, T. & Eguchi, T.** 2006. Anatomy of a Japanese tomistomine crocodylian, *Toyotamaphimeia machikanensis* (Kamei et Matsumoto, 1965), from the middle Pleistocene of Osaka Prefecture: the reassessment of its phylogenetic status within Crocodylia. *National Science Museum Monographs*, **35**, 1–121.
- Kuzmin, I. T. & Zvonok, E. A.** 2021. Crocodylian assemblage from the middle Eocene Ikovo locality (Lugansk Province, Ukraine), with a discussion of the fossil record and geographic origins of crocodyliform fauna in the Paleogene of Europe. *Geobios*, **65**, 7–27. doi: 10.1016/j.geobios.2021.02.002
- Laurenti, J. N.** 1768. *Specimen medicum, exhibens synopsis reptilium emendatam cum experimentis circa venena et antidota reptilium austracorum, quod auctoritate et consensu.* J. Thomae, Vienna, 217 pp.
- Lee, M. S. Y. & Yates, A. M.** 2018. Tip-dating and homoplasy: reconciling the shallow molecular divergences of modern gharials with their long fossil record. *Proceedings of the Royal Society B*, **285**, 20181071. doi: 10.1098/rspb.2018.1071

- Leidy, J.** 1852. Description of a new species of crocodile from the Miocene of Virginia. *Journal of the Academy of Natural Sciences of Philadelphia*, **2**, 135–138.
- Li, C., Wu, X. C. & Rufolo, S. J.** 2019. A new crocodyloid (Eusuchia: Crocodylia) from the Upper Cretaceous of China. *Cretaceous Research*, **94**, 25–39.
- Li, J. L.** 1975. New material on *Tomistoma petrolicus* of Maoming, Guangdong. *Vertebrata Palasiatica*, **13**(3), 190–194.
- Lucas, S. G., & Estep, J. W.** 2000. Osteology of *Allognathosuchus mooki* Simpson, a Paleocene crocodylian from the San Juan Basin, New Mexico, and the monophyly of *Allognathosuchus*. *New Mexico Museum of Natural History and Science Bulletin*, **16**, 155–168.
- Marsh, O. C.** 1871. Notice of some new fossil reptiles from the Cretaceous and Tertiary formations. *American Journal of Science (Series 3)*, **1**(6), 447–459.
- Martin, J. E.** 2007. New material of the Late Cretaceous globidontan *Acynodon iberoccitanus* (Crocodylia) from southern France. *Journal of Vertebrate Paleontology*, **27**(2), 362–372.
- Martin, J. E., & Lauprasert, K.** 2010. A new primitive alligatorine from the Eocene of Thailand: relevance of Asiatic members to the radiation of the group. *Zoological Journal of the Linnean Society*, **158**(3), 608–628.
- Martin, J. E., Delfino, M., Garcia, G., Godefroit, P., Berton, S. & Valentin, X.** 2016. New specimens of *Allodaposuchus precedens* from France: intraspecific variability and the diversity of European Late Cretaceous eusuchians. *Zoological Journal of the Linnean Society*, **176**(3), 607–631.
- Martin, J. E., Lauprasert, K., Tong, H., Suteethorn, V. & Buffetaut, E.** 2019. An Eocene tomistomine from peninsular Thailand. *Annales de Paléontologie*, **105**(3), 245–253.
- Massonne, T., Vasilyan, D., Rabi, M. & Böhme, M.** 2019. A new alligatoroid from the Eocene of Vietnam highlights an extinct Asian clade independent from extant *Alligator sinensis*. *PeerJ*, **7**, e7562. doi:10.7717/peerj.7562
- Meyer, H. von.** 1832. *Paleologica zur Geschichte der Erde und ihrer Geschöpfe*. S. Schmerber, Frankfurt am Main, 560 pp.
- Mook, C. C.** 1921. Description of a skull of a Bridger Crocodylian. *Bulletin of the American Museum of Natural History*, **44**, 111–116.
- Mook, C. C.** 1941. A new crocodylian from the Lance Formation. *American Museum Novitates*, **1128**, 1–5.
- Müller, L.** 1927. Ergebnisse der Forschungsreisen Prof. E. Stromers in den Wüsten Ägyptens. V. Tertiär Wirbeltiere. 1. Beiträge zur Kenntnis der Krokodilier des ägyptischen Tertiärs. *Abhandlungen der Bayerischen Akademie der Wissenschaften Mathematisch-naturwissenschaftliche Abteilung*, **31**, 1–96.
- Müller, S.** 1838. Waarnemingen over de Indische krokodillen en Beschrijving van eene nieuwe soort. *Tydschrift voor Natuurlijke Geschiedenis en Physiologie*, **5**, 67–87.
- Myrick, A. C.** 2001. *Thecachampsia antiqua* (Leidy, 1852) (Crocodylidae, Thoracosaurinae) from fossil marine deposits at Lee Creek Mine, Aurora, North Carolina, USA. *Smithsonian Contributions to Paleobiology*, **90**, 219–225.
- Nicholl, C. S., Rio, J. P., Mannion, P. D. & Delfino, M.** 2020. A re-examination of the anatomy and systematics of the tomistomine crocodylians from the Miocene of Italy and Malta. *Journal of Systematic Palaeontology*, **18**(22), 1853–1889.
- Nopcsa, F.** 1928. Paleontological notes on Reptilia. 7. Classification of the Crocodylia. *Geologica Hungarica, Series Palaeontologica*, **1**, 75–84.
- Owen, R.** 1849. *A history of British fossil reptiles. Volume 1*. Cassell, London, 657 pp.
- Owen, R.** 1874. Monograph on the fossil Reptilia of the Wealden and Purbeck formations. Supplement 6 (*Hylaeochampsia*). *Monographs of the Palaeontographical Society*, **27**(6), 1–7.
- Pickford, M.** 1994. Late Cenozoic crocodiles (Reptilia: Crocodylidae) from the Western Rift, Uganda. *Geology and Palaeobiology of the Albertine Rift Valley, Uganda-Zaire*, **2**, 137–155.
- Piras, P., Delfino, M., Del Favero, L. & Kotsakis, T.** 2007. Phylogenetic position of the crocodylian *Megadontosuchus arduini* and tomistomine palaeobiogeography. *Acta Palaeontologica Polonica*, **52**(2), 315–328.
- Rio, J. P. & Mannion, P. D.** 2021. Phylogenetic analysis of a new morphological dataset elucidates the evolutionary history of Crocodylia and resolves the long-standing gharial problem. *PeerJ*, **9**, e12094. doi:10.7717/peerj.12094
- Risteovski, J., Price, G. J., Weisbecker, V., & Salisbury, S. W.** 2021. First record of a tomistomine crocodylian from Australia. *Scientific Reports*, **11**(1), 12158. doi:10.1038/s41598-021-91717-y
- Sahni, A. & Mishra, V. P.** 1975. Lower Tertiary vertebrates from western India. *Monographs of the Palaeontological Society of India*, **3**, 1–48.
- Shan, H. Y., Wu, X. C., Cheng, Y. N. & Sato, T.** 2009. A new tomistomine (Crocodylia) from the Miocene of Taiwan. *Canadian Journal of Earth Sciences*, **46**(7), 529–555.
- Shan, H. Y., Wu, X. C., Cheng, Y. N. & Sato, T.** 2017. *Maomingosuchus petrolica*, a restudy of ‘*Tomistoma petrolica*’ Yeh, 1958. *Palaeoworld*, **26**(4), 672–690.
- Shan, H. Y., Wu, X. C., Sato, T., Cheng, Y. N. & Rufolo, S.** 2021. A new alligatoroid (Eusuchia, Crocodylia) from the Eocene of China and its implications for the relationships of Orientalosuchina. *Journal of Paleontology*, **95**(6), 1321–1339.
- Simpson, G. G.** 1930. *Allognathosuchus mooki*, a new crocodile from the Puerco Formation. *American Museum Novitates*, **445**, 1–16.
- Skutschas, P. P., Danilov, I. G., Kodrul, T. M. & Jin, J.** 2014. The first discovery of an alligatorid (Crocodylia, Alligatoroidea, Alligatoridae) in the Eocene of China. *Journal of Vertebrate Paleontology*, **34**(2), 471–476.
- Toula, F. & Kail, J. A.** 1885. Über einen Krokodil-Schädel aus den Tertiärlagerungen von Eggenburg in Niederösterreich: eine paläontologische Studie. *Denkschriften der Kaiserlichen Akademie der Wissenschaften von Wien, Mathematisch-naturwissenschaftliche Klasse*, **50**, 299–355.
- Tsubamoto, T., Egi, N., Takai, M., Shigehara, N., Suzuki, H., Nishimura, T., Ugai, H., Maung, M., Sein, C., Tun, S. T., Soe, A. N., Aung, A. K., Thein, T., Htike, T. & Thein, Z. M. M.** 2006a. A summary of the Pondaung fossil expeditions. *Asian Paleoprimateology*, **4**, 1–66.
- Tsubamoto, T., Egi, N. & Takai, M.** 2006b. Notes on fish, reptilian, and several fragmentary mammalian dental

- fossils from the Pondaung Formation. *Asian Paleoprimatology*, **4**, 98–110.
- Wang, Y. Y., Sullivan, C. & Liu, J.** 2016. Taxonomic revision of *Eoalligator* (Crocodylia, Brevirostres) and the paleogeographic origins of the Chinese alligatoroids. *PeerJ*, **4**, e2356. doi:10.7717/peerj.2356
- Whitaker, R. & Whitaker, N.** 2008. Who's got the biggest? *Crocodile Specialist Group Newsletter*, **27**(4), 26–30.
- Wu, X. C., Brinkman, D. B. & Russell, A. P.** 1996. A new alligator from the Upper Cretaceous of Canada and the relationship of early eusuchians. *Palaeontology*, **39**, 351–376.
- Wysocka, A., Pha, P. D., Durska, E., Czarniecka, U., Thang, D. V., Filipek, A., Cuong, N. Q., Tuan, D. M., Huyen, N. X., Tha, H. V. & Staniszewski, R.** 2020. The Na Duong Basin (North Vietnam): a key for understanding Paleogene basin evolution in relation to the left-lateral Cao Bang-Tien Yen Fault. *Journal of Asian Earth Sciences*, **195**, 104350. doi:10.1016/j.jseas.2020.104350
- Yeh, H. K.** 1958. A new crocodile from Maoming, Kwangtung. *Vertebrata Palasiatica*, **2**(4), 237–242.

Associate Editors: Jonah Choiniere/Paul Barrett

Third Paper

A tarsometatarsus from the upper Eocene Na Duong Basin – the first Palaeogene fossil bird from Vietnam

Massonne Tobias, Böhme Madelaine and Mayr Gerald

Alcheringa: An Australasian Journal of Palaeontology, 46(3-4), 291–296, 2022

<https://doi.org/10.1080/03115518.2022.2126010>

A tarsometatarsus from the upper Eocene Na Duong Basin—the first Palaeogene fossil bird from Vietnam

Tobias Massonne , Madelaine Böhme, and Gerald Mayr 

ABSTRACT

Knowledge of the Palaeogene avifauna of East Asia is scarce, and only a few fossils have been described thus far. A tarsometatarsus from the upper Eocene Na Duong Basin represents the first Palaeogene fossil bird from Vietnam. The fossiliferous sediments in the Na Duong Basin originated from an aquatic ecosystem but also yielded terrestrial animal and plant remains suggesting a dense forest habitat surrounding an ancient lake. In accordance, the Na Duong Basin tarsometatarsus is compared with extant aquatic, terrestrial and arboreal bird species, but because of diagenetic compression and fragmentary preservation, it is difficult to classify the bone. Nevertheless, the specimen exhibits a distinctive morphology and is potentially referable to an endemic neognath unknown from other Palaeogene localities outside of Vietnam.

ARTICLE HISTORY

Received 18 July 2022
Revised 14 September 2022
Accepted 14 September 2022

KEYWORDS

Aves; Cenozoic; East Asia

Tobias Massonne [tobias.massonne@uni-tuebingen.de], Senckenberg Center of Human Evolution and Palaeoecology, Tübingen, Germany; Department of Geosciences, Eberhard-Karls-Universität Tübingen, Tübingen, Germany; Madelaine Böhme [m.boehme@ifg.uni-tuebingen.de], Senckenberg Center of Human Evolution and Palaeoecology, Tübingen, Germany; Department of Geosciences, Eberhard-Karls-Universität Tübingen, Tübingen, Germany; Gerald Mayr [gerald.mayr@senckenberg.de], Senckenberg Research Institute and Natural History Museum Frankfurt, Ornithological Section, Frankfurt am Main, Germany.

WHILE there is a rich fossil record of birds from the Cretaceous of East Asia, current knowledge of Palaeocene and Eocene avifaunas from southern and eastern Asia is scarce (Kurochkin 1976, Rich *et al.* 1986, Nessov 1992, Hood 2003, Mayr 2009, 2022, Zelenkov & Kurochkin 2015, Hood *et al.* 2019). More substantial fossils are mainly documented from the Palaeocene and Eocene of India, Mongolia and China and include, among others, species that were assigned to the Anseriformes, Galliformes, Mirandornithes, Gruiformes, and Strigiformes (e.g., Hwang *et al.* 2010, Mayr *et al.* 2010, Kurochkin & Dyke 2011, Wang *et al.* 2012, Mayr *et al.* 2013, Stidham & Ni 2014, Zhao *et al.* 2015, Hood *et al.* 2019, Zelenkov 2021a, 2021b). Fossil remains referred to Gastornithiformes are known from the early Eocene of China (Buffetaut 2013), and there is a specimen of the suliform clade Protoplotidae from Sumatra (Lambrecht 1931), and a putative record of Threskiornithidae from the upper Eocene Pondaung Formation of Myanmar (Stidham *et al.* 2005). In addition, late Eocene and early Oligocene fossils attributed to Eogruidae and Ergilornithidae have been reported from Mongolian localities (Clarke *et al.* 2005, Hood *et al.* 2019, Mayr & Zelenkov 2021, Mayr 2022).


In this study, we describe an avian tarsometatarsus from the Na Duong Basin in Northern Vietnam, that was

excavated in 2011 (Böhme *et al.* 2013). The bone represents the first record of fossil birds from the Na Duong Basin, and it is also the first evidence of bird remains from the Eocene of Vietnam. As such, it improves our knowledge of the east Asian avifaunas as a whole and Vietnam in particular. Furthermore, the specimen adds to the significance of the Na Duong Basin as a Lagerstätte from the Eocene of East Asia.

Palaeogene bird fossils from Vietnam have not been previously described, but a comprehensive Pleistocene avifauna has been recently published (Boev 2022). This latter study reported various species that no longer occur in Vietnam, but all represent modern taxa, and in most cases, the identification of fragmentary remains requires corroboration with more material.

Geological setting

The Na Duong Basin is located in northern Vietnam near the Chinese border (Fig. 1). It represents one of only a few areas in East and Southeast Asia with a complete sequence of continental sediments from the middle Eocene to lower Oligocene (Böhme *et al.* 2013). The basin is part of the Cao Bang-Tien Yen fault system and covers an area of 45 km². The middle to upper Eocene (late Bartonian–Priabonian) Na Duong Formation is 240 m thick with the upper 140 m section being exposed in the Na Duong open cast coal mine. Böhme *et al.* (2013) biochronologically correlated the fossil mammals from Na Duong (layer 80) with the Chinese Naduan land mammal age (= Ulangochuan stage: Wang *et al.* 2019), and provided an 39–34 Ma age estimate.

 Supplemental data for this article is available online at <https://doi.org/10.1080/03115518.2022.2126010>.

© 2022 The Author(s). Published by Informa UK Limited, trading as Taylor & Francis Group.

This is an Open Access article distributed under the terms of the Creative Commons Attribution License (<http://creativecommons.org/licenses/by/4.0/>), which permits unrestricted use, distribution, and reproduction in any medium, provided the original work is properly cited.

Published online 12 Oct 2022

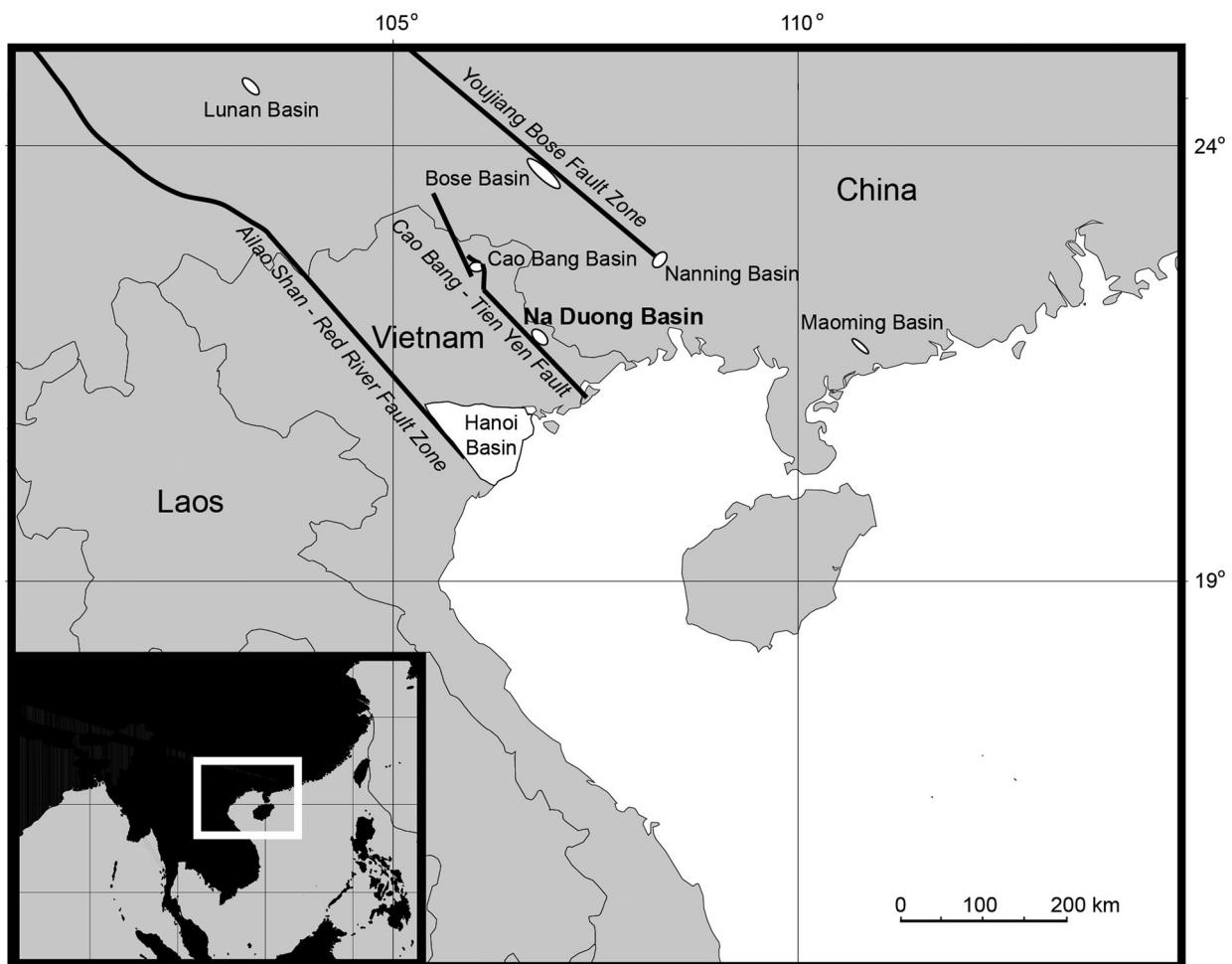


Figure 1. Map of northern Southeast Asia showing the Na Duong Basin in northeast Vietnam (after Böhme *et al.* 2013).

Palaeomagnetic data calibrate the Ulangochuian at between 40 and 37 Ma (Wang *et al.* 2019).

The tarsometatarsus described herein was excavated within the transition zone between the coaly shale of the main seam and the underlying dark-brown claystone (layer 80).

The layer 80 sediments are lacustrine lignitic shales that were deposited at a time of tropical to warm-subtropical climate. The region was also undergoing a transition from shallow pond systems to a large anoxic lake (Böhme *et al.* 2013, Garbin *et al.* 2019). This fossil ecosystem has yielded both aquatic and terrestrial faunal elements. The bird specimen occurred sympatrically with two species of crocodile (*Orientalosuchus naduongensis* Massonne, Vasilyan, Rabi & Böhme, 2019 and *Maomingosuchus acutirostris* Massonne, Augustin, Matzke, Weber & Böhme, 2021), the anthracothere *Bakalovia orientalis* Böhme, Aiglstorfer, Antoine, Appel, Halvik, Métais, Phug, Schneider, Setzer, Tappert, Tran, Uhl & Prieto, 2013, the rhinocerotine *Epiaceratherium naduongense* Böhme, Aiglstorfer, Antoine, Appel, Havlik, Métais, Phug, Schneider, Setzer, Tappert, Tran, Uhl & Prieto, 2013, a strepsirrhine (Chavasseau *et al.* 2019), fishes representing the families Amiidae and Cyprinidae, and at least two species of turtle (Böhme *et al.* 2013, Garbin *et al.* 2019).

Materials and methods

Osteological terminology is based on Baumel & Witmer (1993). Micro-CT (μ CT) scanning was undertaken on a Nikon (Minato, Tokyo, Japan) XTH 320 μ CT scanner in the 3D Imaging Lab of the Senckenberg Centre for Human Evolution and Palaeoenvironment (SHEP) and University of Tübingen (UT), Germany. This used an X-ray tube containing a multi metal reflection target with a maximum acceleration voltage of 225 kV. Scan parameters included 210 kV and 90 μ A with a voxel size of 27.31305 mm, and utilization of a 0.1 mm thick copper filter. Segmentation used threshold and brush tools in Amira v.2021.1 (Thermo Fisher, Waltham, Massachusetts, USA), with the surface mesh exported as a STL file. The 3D-Model is provided in [Supplementary Data 1](#).

Institutional abbreviations

GPIT, Geologisch-Paläontologisches Institut Tübingen, Tübingen, Germany. NMNH, National Museum of Natural History, Washington, DC, USA; SMF, Senckenberg Museum, Frankfurt am Main, Germany.

Systematic palaeontology

Aves Linnaeus, 1758

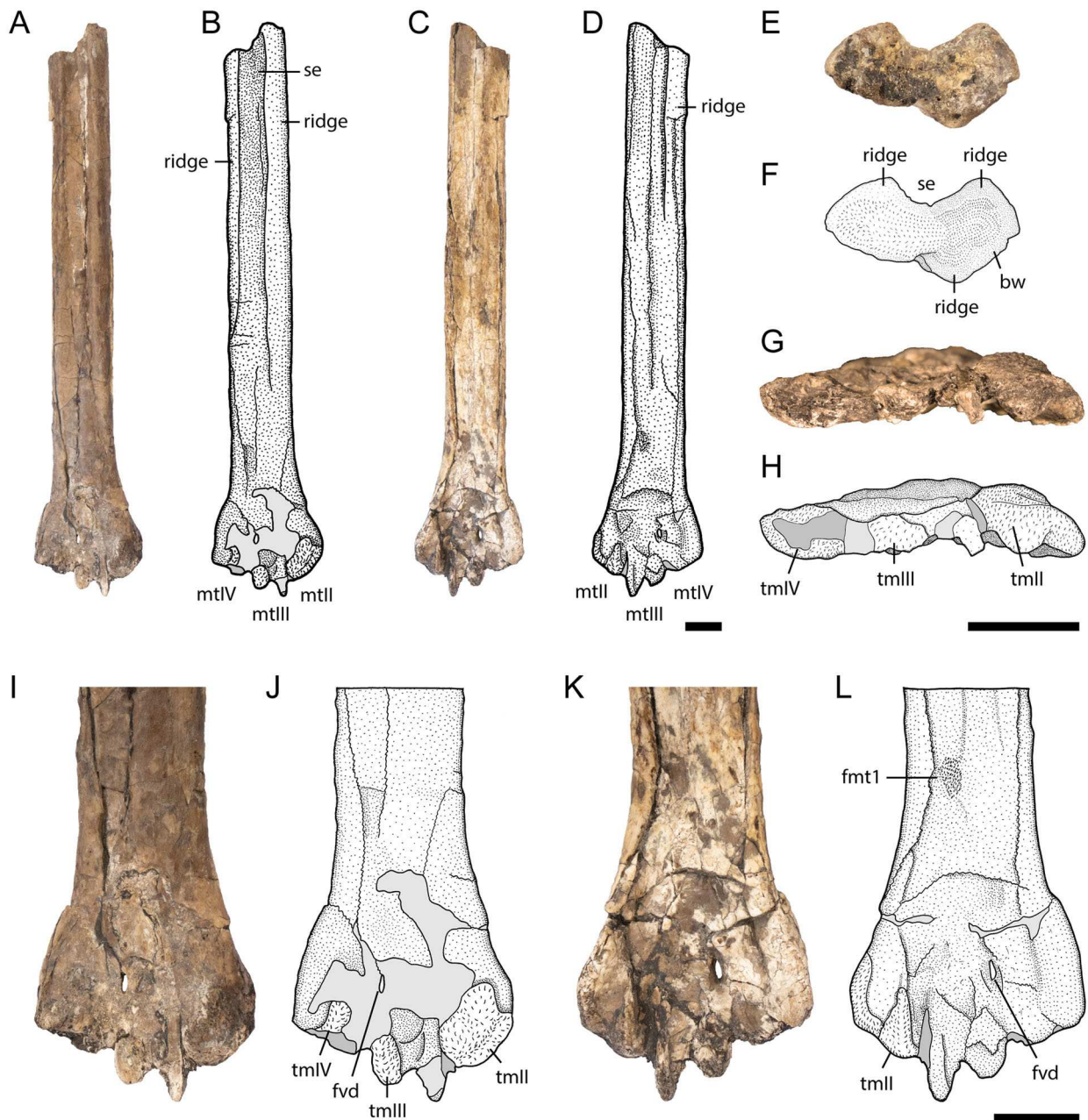


Figure 2. *Neognathae incertae sedis* (GPIT-PV-122865). Tarsometatarsus in A, B, dorsal view; C, D, plantar view; E, F, cross-section of the proximal end of the shaft; G, H, distal view; I, J, enlargement of the distal end in dorsal view; K, L, enlargement of the distal end in plantar view. Abbreviations: bw, bone wall; fvt1, fossa metatarsi 1; fvd, foramen vasculare distale; mt, metatarsale; se, sulcus extensorius; tm, trochlea metatarsi. Scale bar = 5 mm.

Neognathae incertae sedis
(Fig. 2)

Referred material. GPIT-PV-122865, a partial right tarsometatarsus.

Locality, unit and age. Layer 80 of the Na Duong coal mine in northern Vietnam (21°42.2'N, 106°58.6'E); Na Duong Formation (Na Duong Basin), late Bartonian to Priabonian (late Eocene), 39–35 Ma (Böhme *et al.* 2013).

Description. GPIT-PV-122865 represents the distal part of a right tarsometatarsus with a shaft approximately covering

half to two-third of its original length (Fig. 2). Distal width = 15.2 mm; trochlea metatarsi III width = 5.0 mm; shaft width = 8.3 mm; foramen vasculare distale length = 1.5 mm. Diagenetic compression has flattened the bone dorso-plantar, and both its plantar surface and the dorsal surface of the distal end are weathered.

The shaft is elongate with an equal width over the preserved length, but it is much wider than the trochlea metatarsi III. In dorsal view (Fig. 2A, B), GPIT-PV-122865 has a deep sulcus extensorius that is proximally bordered by prominent ridges; the shaft becomes flat and smooth towards the distal one-third of the bone (see Supplementary Data 1). On the plantar surface (Fig. 2C, D), a sulcus is bordered by a prominent latera ridge. The fossa metatarsi I is

situated on the plantar surface medial to the midline of the bone, and appears to be oval in outline but is poorly preserved (Fig. 2K, L).

The foramen vasculare distale is very small and oval-shaped. The canalis interosseus distalis cannot be discerned. The incisurae intertrochleares lateralis and medialis are not evident due to mediolateral flattening, as well as the dorso-plantar compression (Fig. 2G–L, S1).

The trochlea metatarsi II is shorter than the trochlea metatarsi III and has a medially slanting distal margin; although it does not form a plantarly directed projection. A broad sulcus on the plantar surface is bounded by two proximodistally oriented large ridges. The distal portion of the trochlea metatarsi III is damaged with ~50% being lost. The narrow plantar rims are widely separated by a large furrow, which is likely to be a taphonomic artefact. The trochlea metatarsi IV is mediolaterally broad, but its distal portion is damaged. It also lacks a distinct trochlear furrow on the preserved surface and appears to be slightly larger than the other trochleae (Fig. 2G–L, S1). The bone wall is thick in cross-section (Fig. 2E, F).

Discussion

Extant bird species can be separated into two higher-level clades: Palaeognathae and Neognathae. GPIT-PV-122865 is most likely a representative of the latter group. The only long-legged palaeognaths present during the Eocene in Eurasia are members of the Palaeotididae and Eogruidae (Mayr 2022). Although GPIT-PV-122865 shares with the latter taxa a long shaft, and the presence of a trochlea metatarsi III that reaches further distally than the trochleae metatarsorum II and IV, it differs in many other characteristics. For example, GPIT-PV-122865 has a more robust shaft, smaller foramen vasculare distale, narrower incisurae intertrochleares lateralis and medialis, and equally-sized trochleae metatarsorum. This character combination precludes referral to either Palaeotididae or Eogruidae.

The Na Duong Basin late Eocene palaeoenvironment was characterized by a transition from shallow ponds to a large anoxic lake supporting rich aquatic and terrestrial faunas (Böhme *et al.* 2013, Garbin *et al.* 2019). We therefore compared GPIT-PV-122865 with extant aquatic and semi-aquatic members of Aequornithes and Gruiformes, together with terrestrial representatives of Galliformes, and arboreal members of Coliiformes, which have similar tarsometatarsal morphologies (Fig. 3). The distal width of GPIT-PV-122865 is comparable to *Gallus gallus* Linnaeus, 1758 (Fig. 3B, H), which exhibits a trochlea metatarsi III reaching further distal than the trochleae metatarsorum II and IV, and trochleae that are subequal in size. The common presence of a small rectangular process on the medial flank of the trochlea metatarsi II is also visible in ventral view. By contrast, the shaft in GPIT-PV-122865 is longer than that of *G. gallus* and has an elongate extensor sulcus along its dorsal surface as well as a plantar ridge (absent in *G. gallus*). In addition, the foramen vasculare distale is much smaller in GPIT-PV-122865, and the incisura intertrochlearis lateralis

is nearly closed (otherwise much wider in *G. gallus*). Finally, the trochleae metatarsorum II and IV reach an equal distal distance in GPIT-PV-122865, whereas the trochlea metatarsi II is further proximally oriented in *G. gallus*.

Birds with elongate tarsometatarsi that may have occurred in the Na Duong Basin palaeoenvironment include members of the Ardeidae (herons), Ciconiidae (storks and allies), and Gruidae (cranes). We therefore used *Ardea herodias* Linnaeus, 1758 (Ardeidae; Fig. 3C, I), *Mycteria americana* Linnaeus, 1758 (Ciconiidae; Fig. 3D, J) and *Antigone canadensis* (Linnaeus, 1758; Gruidae; Fig. 3E, K) for comparisons. These taxa share an elongate tarsometatarsal shaft, although GPIT-PV-122865 has a more marked sulcus extensorius along the dorsal surface of the shaft and a plantar ridge on the ventral surface, and broader shaft proportions, as well as a smaller foramen vasculare distale. GPIT-PV-122865 specifically shares equally-sized trochleae metatarsorum and relatively narrow incisurae intertrochleares lateralis and medialis, together with a small plantar opening of the foramen vasculare distale with *A. herodias*. GPIT-PV-122865 otherwise differs in its much smaller dorsal opening for the foramen vasculare distale, and a more distally projected trochlea metatarsi III.

Similarities with *M. americana* include a relatively narrow incisurae intertrochleares lateralis and medialis, and a trochlea metatarsi III that is more distally projected than the trochlea metatarsorum II and IV. Conversely, GPIT-PV-122865 lacks a proximally positioned canal leading into the foramen vasculare distale, and the trochlea metatarsi III is subequal to the size of the trochleae metatarsorum II and IV.

GPIT-PV-122865 shares the possession of a trochlea metatarsi III that reaches further distally than the trochleae metatarsorum II and IV with *A. canadensis*. However, GPIT-PV-122865 differs in having narrower incisurae intertrochleares lateralis and medialis, the trochlea metatarsi II having the same distal extent as the trochlea metatarsi IV, and the trochleae metatarsorum being of equal size.

Amongst arboreal birds, GPIT-PV-122865 is comparable to *Colius striatus* Gmelin, 1789 (Fig. 3F, L) in overall tarsometatarsus shape, the robust shaft, small foramen vasculare distale, equally sized trochleae metatarsorum, and narrow incisurae intertrochleares lateralis and medialis. By contrast, GPIT-PV-122865 has a more marked sulcus extensorius along the dorsal surface of the shaft and a plantar ridge along its ventral surface, as well as the trochlea metatarsi III that projects further distally than the trochleae metatarsorum II and IV. In addition, the general size difference is substantial.

Well-studied Palaeogene avian fossil assemblages from the Palearctic region also include stem group representatives of Strigiformes (owls) and Psittacopasseres (parrots and passerines); however, the tarsometatarsus of these lineages differs significantly in proportions and morphology of the distal extremity compared to GPIT-PV-122865 (Mayr 2022).

The lacustrine palaeohabitat of the Na Duong Basin was surrounded by a dense dipterocarpacean swamp forest, as indicated by preserved leaves, woods and resin (Böhme



Figure 3. Tarsometatarsi comparisons. *Neognathae incertae sedis* (GPIT-PV-122865) in **A**, dorsal and **G**, plantar views; *Gallus gallus* (Galliformes) (GPIT-PV-122866) in **B**, dorsal and **H**, plantar views; *Ardea herodias* (Pelecaniformes) (NMNH 555715) in **C**, dorsal and **I**, plantar views; *Mycteria americana* (Ciconiiformes) (NMNH 16295) in **D**, dorsal and **J**, plantar views; *Antigone canadensis* (Gruiformes) (NMNH 432705) in **E**, dorsal and **K**, plantar views; *Colius striatus* (Coliiformes) (SMF 8019) in **F**, dorsal and **L**, plantar views. Images of NMNH 555715, NMNH 16295 and NMNH 432705 obtained from the open-access database of the Smithsonian Institution, Washington DC, USA: <https://collections.nmnh.si.edu/search/birds/>. Scale bar = 5 mm.

et al. 2013). Estimates of tree density and canopy height suggest ~600 individual trees/ha and a maximum canopy height of around 35 m, which is compatible with swamp forests found in Southeast Asia today (Böhme *et al.* 2013). Like these modern settings, we expect that the avian fauna was diverse and incorporated a range of arboreal, ground-dwelling, aquatic or semi-aquatic species. Unfortunately, because of the poor preservation, GPIT-PV-122865 cannot be identified beyond *Neognathae incertae sedis*. Nonetheless, GPIT-PV-122865 does provide the first insight into the Na Duong

Basin bird assemblage and offers a novel Palaeogene avifaunal occurrence for East Asia.

Acknowledgements

The Editorial Board of *Alcheringa* and two anonymous reviewers provided constructive comments and editing. Nguyễn Việt Hưng, La Thế Phúc, Đặng Ngọc Trần, Đồ Đức Quang, Phan Đông Pha assisted with our field expeditions. Felix J. Augustin, Panagiotis Kampouridis, Thomas Lechner and Andreas T. Matzke (UT) contributed to discussions. Regina Ellenbracht and Henrik Stöhr (UT) prepared the fossil,

and Sven Tränkner (SMF) provided photography. Christina Kyriakouli and Gabriel Ferreira (SHEP) conducted the CT scan. Erich Weber and Ingmar Werneburg (UT) facilitated collections access.

Disclosure statement

No potential conflict of interest was reported by the author(s).

ORCID

Tobias Massonne  <http://orcid.org/0000-0002-6782-5280>

Gerald Mayr  <http://orcid.org/0000-0001-9808-748X>

References

- BAUMEL, J.J. & WITMER, L.M., 1993. Osteologia. In *Handbook of avian anatomy: Nomina anatomica avium*. BAUMEL, J.J., KING, A.S., BREAZILE, J.E., EVANS, H.E., & VANDEN BERGE, J.C., eds. Publications of the Nuttall Ornithological Club 23, Boston, Massachusetts, 45–132.
- BÖHME, M., AIGLSTORFER, M., ANTOINE, P.O., APPEL, E., HAVLIK, P., MÉTAIS, G., PHUG, L.T., SCHNEIDER, S., SETZER, F., TAPPERT, R., TRAN, D.N., UHL, D. & PRIETO, J., 2013. Na Duong (northern Vietnam)—an exceptional window into Eocene ecosystems from Southeast Asia. *Zitteliana A* 53, 121–167.
- BÖHME, M., PRIETO, J., SCHNEIDER, S., HUNG, N.V., QUANG, D.D. & TRAN, D.N., 2011. The Cenozoic on-shore basins of Northern Vietnam: biostratigraphy, vertebrate and invertebrate faunas. *Journal of Asian Earth Sciences* 40, 672–687.
- BOEV, Z., 2022. Late Pleistocene and Early Holocene Birds of Northern Vietnam (Caves Dieu and Maxa I, Thanh Hoa Province)—Paleornithological Results of the Joint Bulgarian-Vietnamese Archaeological Expeditions, 1985–1991 (Paleoavifaunal Research). *Quaternary* 5, 31–115.
- BUFFETAUT, E., 2013. The giant bird *Gastornis* in Asia: a revision of *Zhongyuanus xichuanensis* Hou, 1980, from the Early Eocene of China. *Paleontological Journal* 47, 1302–1307.
- CHAVASSEAU, O., CHAIMANEE, Y., DUCROCQ, S., LAZZARI, V., PHA, P.D., RUGBUMRUNG, M., SURAULT, J., TUAN, D.M. & JAEGER, J.J., 2019. A new primate from the late Eocene of Vietnam illuminates unexpected strepsirrhine diversity and evolution in Southeast Asia. *Scientific Reports* 9, 1–11.
- CLARKE, J.A., NORELL, M.A. & DASHZEVEG, D., 2005. New avian remains from the Eocene of Mongolia and the phylogenetic position of the Eogruidae (Aves, Gruoidea). *American Museum Novitates* 2005, 1–17.2.0.CO;2]
- GARBIN, C.G., BÖHME, M. & JOYCE, W.G., 2019. A new testudinoid turtle from the Middle to Late Eocene of Vietnam. *PeerJ*. 7, e6280.
- GELIN, J., 1789. *Linnei Systema Naturae*. Leipzig, 1057 pp.
- HOOD, S.C., TORRES, C.R., NORELL, M.A. & CLARKE, J.A., 2019. New fossil birds from the earliest Eocene of Mongolia. *American Museum Novitates* 2019, 1–24.
- HOU, L.-H., 2003. *Fossil Birds of China*. Yunnan Science and Technology Press, Kunming. ISBN-10: 7541617245, 234 pp.
- HWANG, S.H., MAYR, G. & MINJIN, B., 2010. The earliest record of a galiform bird in Asia, from the late Paleocene/early Eocene of the Gobi Desert. *Journal of Vertebrate Palaeontology* 30, 1642–1644.
- KUROCHKIN, E.N., 1976. A survey of the Paleogene birds of Asia. *Smithsonian Contributions to Paleobiology* 27, 5–86.
- KUROCHKIN, E.N. & DYKE, G.J., 2011. The first fossil owls (Aves: Strigiformes) from the Paleogene of Asia and a review of the fossil record of Strigiformes. *Paleontological Journal* 45, 445–458.
- LAMBRECHT, K., 1931. *Protoplotus beauforti* n.g. n.sp., ein Schlangenhalsvogel aus dem Tertiär von W. Sumatra. *Wetenschappelijke Mededeelingen Dienst van den Mijnbouw in Nederlandisch-Indie* 17, 15–24.
- LINNAEUS, C., 1758. *Systema naturae per regna tria naturae, secundum classes, ordines, genera, species, cum characteribus, differentiis, synonymis, locis*. Vol. 1: *Regnum animale*. Editio decima, reformata, Laurentii Salvii, Stockholm, 824 pp.
- MASSONNE, T., VASILYAN, D., RABI, M. & BÖHME, M., 2019. A new alligatoroid from the Eocene of Vietnam highlights an extinct Asian clade independent from extant *Alligator sinensis*. *PeerJ*. 7, e7562.
- MASSONNE, T., AUGUSTIN, F.J., MATZKE, T.M., WEBER, E. & BÖHME, M., 2021. A new species of *Maomingosuchus* from the Eocene of the Na Duong Basin (northern Vietnam) sheds new light on the phylogenetic relationship of tomistomine crocodylians and their dispersal from Europe to Asia. *Journal of Systematic Palaeontology* 19, 1551–1585.
- MAYR, G., 2009. *Paleogene fossil birds*, first edition. Springer, Heidelberg, 262 pp.
- MAYR, G., 2022. *Paleogene Fossil Birds*, second edition. Springer, Cham. ISBN 978-3-030-87644-9 https://doi.org/10.1007/978-3-030-87645-6_3, 239 pp.
- MAYR, G. & ZELENKOV, N., 2021. Extinct crane-like birds (Eogruidae and Ergilornithidae) from the Cenozoic of Central Asia are ostrich precursors. *Ornithology* 138, 1–15.
- MAYR, G., RANA, R.S., ROSE, K.D., SAHNI, A., KUMAR, K., SINGH, L. & SMITH, T., 2010. Quercypsitta-like birds from the early Eocene of India (Aves, Psittaciformes). *Journal of Vertebrate Paleontology* 30, 467–478.
- MAYR, G., RANA, R.S., ROSE, K.D., SAHNI, A., KUMAR, K., & SMITH, T., 2013. New specimens of the early Eocene bird *Vastanavis* and the interrelationships of stem group Psittaciformes. *Paleontological Journal* 47, 1308–1314.
- NESSOV, L.A., 1992. Mesozoic and Paleogene birds of the USSR and their paleoenvironments. In *Papers in avian paleontology honoring Pierce Brodkorb*. CAMPBELL, K.E. ed, Natural History Museum of Los Angeles County, Science Series 36, Los Angeles, 465–478.
- RICH, P.V., HOU, L.-H., ONO, K. & BAIRD, R.F., 1986. A review of the fossil birds of China, Japan and Southeast Asia. *Geobios* 19, 755–772.
- STIDHAM, T.A. & NI, X.-J., 2014. Large anseriform (Aves: Anatidae: *Romainvillinae*?) fossils from the late Eocene of Xinjiang. *China. Vertebra Palaeontologica* 52, 98–111.
- STIDHAM, T.A., HOLROYD, P.A., GUNNELL, G.F., CIOCHON, R.L., TSUBAMOTO, T., EGI, N., & TAKAI, M., 2005. An ibis-like bird (Aves: cf. Threskiornithidae) from the Late Middle Eocene of Myanmar. *Contributions from the Museum of Paleontology University of Michigan* 31, 179–184.
- WANG, M., MAYR, G., ZHANG, J. & ZHOU, Z., 2012. Two new skeletons of the enigmatic, rail-like avian taxon *Songzia* Hou, 1990 (*Songziidae*) from the early Eocene of China. *Alcheringa* 36, 487–499.
- WANG, Y., LI, Q., BAI, B., JIN, X., MAO, F. & MENG, J., 2019. Paleogene integrative stratigraphy and timescale of China. *Science China Earth Sciences* 62, 287–309.
- ZELENKOV, N.V., 2021a. New bird taxa (Aves: Galliformes, Gruiformes) from the early Eocene of Mongolia. *Paleontological Journal* 55, 438–446.
- ZELENKOV, N.V., 2021b. A revision of the Palaeocene-Eocene Mongolian *Presbyornithidae* (Aves: Anseriformes). *Paleontological Journal* 55, 323–330.
- ZELENKOV, N.V. & KUROCHKIN, E.N., 2015. Class Aves. In *Fossil vertebrates of Russia and neighbouring countries. Fossil Reptiles and Birds. Part 2*. KUROCHKIN, E.N., LOPATIN, A.V., & ZELENKOV, N.V., eds, Geos, Moscow, 86–290. [in Russian].
- ZHAO, T., MAYR, G., WANG, M. & WANG, W., 2015. A trogon-like arboreal bird from the early Eocene of China. *Alcheringa* 39, 287–294.

Fourth Paper

**A new cryptodire from the Eocene of the Na Duong Basin
(northern Vietnam) sheds new light on *Pan-Trionychidae*
from Southeast Asia**

**Massonne Tobias, Augustin Felix J., Matzke Andreas T. and Böhme
Madelaine**

Journal of Systematic Palaeontology, 21(1), 2217505, 1–25, 2023

<https://doi.org/10.1080/14772019.2023.2217505>



A new cryptodire from the Eocene of the Na Duong Basin (northern Vietnam) sheds new light on *Pan-Trionychidae* from Southeast Asia

Tobias Massonne^{a,b*} , Felix J. Augustin^b , Andreas T. Matzke^b and Madelaine Böhme^{a,b} 

^aSenckenberg Centre for Human Evolution and Palaeoenvironment, Tübingen, Germany; ^bDepartment of Geosciences, Eberhard-Karls-Universität Tübingen, Tübingen, Germany

(Received 21 December 2022; accepted 21 May 2023)

Striatochelys baba gen. et sp. nov. is a new pan-trionychid from the middle–upper Eocene (late Bartonian–Priabonian, 39–35 Ma) of the Na Duong Basin in northern Vietnam. It represents one of the best documented and most completely known Palaeogene pan-trionychid species from Asia. *Striatochelys baba* can be diagnosed by: (1) its relatively small size; (2) the absence of a preneural; (3) the presence of well-developed straight ridges on the costals and neurals in adults; (4) ridges more strongly developed posteriorly than anteriorly; and (5) entoplastron callosity in the shape of a bulge. A phylogenetic analysis recovers *S. baba* within *Pan-Trionychinae* in an unresolved polytomy with species of the genus *Nilssonina*. In addition, comparisons of the new taxon with plastomenids, pan-trionychids from the Palaeogene and extant trionychids from Asia demonstrate a particularly close resemblance to *Nilssonina* spp. Based on the close resemblance between *S. baba* and ‘*Trionyx*’ *impressus* (a pan-trionychid from the Maoming Basin of southern China), we here assign the latter species to the new genus *Striatochelys*. The close relationship between *S. baba* gen. et sp. nov. from the Na Duong Basin and *S. impressa* comb. nov. from the Maoming Basin further supports the hypothesis that a close connection between both localities existed, as already exemplified by other faunal elements such as pan-goeemydids and crocodylians.

<http://zoobank.org/urn:lsid:zoobank.org:pub:E8E5C4DE-E52A-43FB-B9C1-CE3ED2ED66C1>

Keywords: Eocene; turtle; *Pan-Trionychinae*; *Nilssonina*; Asia

Introduction

Pan-Trionychidae (softshell turtles) represents one of the most diverse aquatic radiations of cryptodiran turtles, with more than 107 fossil and extant species and a fossil record dating back to the late Early Cretaceous (Georgalis & Joyce, 2017; Joyce et al., 2004; Turtle Taxonomy Working Group, 2021; Vitek & Joyce, 2015). The group is characterized by having a reduced carapace lacking peripherals and pygals (Joyce & Lyson, 2017; Meylan, 1987). Softshell turtles range in size from less than 10–15 cm bony disc length (BDL) (e.g. ‘*Trionyx*’ *gobiensis* Danilov, Hirayama, Sukhanov, Suzuki, Watabe & Vitek, 2014 from the Late Cretaceous of Mongolia; extant *Pelodiscus huangshannensis* Y. A. Gong, Peng, Huang, Lin, Huang, Xu, Yang & Nie, 2021; extant *Pelodiscus shipian* S. Gong, Fritz, Vamberger, Gao & Farkas, 2022 from China) to a BDL of 97 cm (completely preserved carapace of an indeterminate taxon described by Gaffney [1979] from the Eocene Bridger Formation of North America), or even larger (estimated based on a fragmentary specimen

described by Head et al. [1999] from the middle Eocene of Pakistan). The largest extant trionychids are slightly smaller than this and have a maximum BDL of 74.5 cm (Pritchard, 2001). Whereas extant trionychids are known from Asia, Africa, North America and Australasia, fossil representatives were more widespread and have also been found in Australia, Europe and South America (Böhme, 1995; Ernst & Barbour, 1989; Georgalis, 2021; Georgalis & Joyce, 2017; Joyce & Lyson, 2017; Vitek & Joyce, 2015). Recently, the in-group relationships between extant species were clarified with the use of molecular data (Le et al., 2014), but comparatively long ghost lineages are currently still reconstructed for several taxa (Danilov et al., 2014; Vitek & Joyce, 2015).

Pan-Trionychidae can be divided into three clades: *Pan-Cyclanorbinae*, *Plastomenidae* and *Pan-Trionychinae* (Joyce et al., 2018, 2021; Lyson et al., 2021). *Plastomenidae* went extinct during the Eocene (Jasinski et al., 2022; Joyce et al., 2009, 2016, 2018; Lyson et al., 2021), whereas the latter two groups still have extant representatives.

*Corresponding author. Email: tobias.massonne@uni-tuebingen.de

The oldest known pan-trionychids originated in Asia during the Early Cretaceous (*Trionyx* *kyrgyzensis* Nessov, 1995, *Perochelys lamadongensis* Li, Joyce & Liu, 2015, *Perochelys hengshanensis* Brinkman, Rabi & Zhao, 2017) (see Brinkman *et al.*, 2017; Danilov & Vitek, 2013). However, the phylogenetic positions of these early members are poorly understood, and they are either recovered as basal pan-trionychids (in accordance with their old geological age) or nested inside Trionychinae, due to their derived set of characters (Brinkman *et al.*, 2017; Georgalis & Joyce, 2017; Joyce *et al.*, 2021). Upper Cretaceous sites in central and east Asia (China, Kazakhstan, Kyrgyzstan and Mongolia) have yielded abundant remains of pan-trionychids (e.g. Brinkman *et al.*, 2017; Danilov *et al.*, 2014; Danilov & Vitek, 2013; Georgalis & Joyce, 2017; Vitek & Danilov, 2010; 2012), but taxa from the Palaeogene are far less common. *Kuhnemys palaeocenica* (Danilov, Sukhanov, Obraztsova & Vitek, 2015) from the Thanetian (late Paleocene) of Mongolia and *Drazinderetes tethyensis* Head, Raza & Gingerich, 1999 from the Bartonian (late Eocene) of Pakistan are the only taxa that have not been assigned to the ‘waste-basket’ genus *Trionyx* (Georgalis & Joyce, 2017). Among the latter, *Trionyx linchuensis* (Yeh, 1962), *Trionyx gregarius* (Gilmore, 1934), *Trionyx johnsoni* (Gilmore, 1931) and *Trionyx impressus* (Yeh, 1963) from the Eocene of China and *Trionyx minusculus* (Chkhikvadze, 1973) from the Eocene and *Trionyx ninae* Chkhikvadze, 1971 from the Eocene and Oligocene of Kazakhstan are known. None of these taxa, however, has been included in a phylogenetic analysis, and their relationships are unresolved (Georgalis & Joyce, 2017).

Trionyx impressus from the Maoming locality of South China represents the only taxon of Bartonian–Priabonian age (late Eocene) from east Asia. Other named species and all other specimens from the late middle Eocene of Myanmar, east China (Zhejiang Province), or east-central China (Henan Province) can only be identified as *Pan-Trionychidae* indet. (Georgalis & Joyce, 2017).

Recent excavations in the middle–late Eocene deposits of the Na Duong Basin (northern Vietnam) have recovered a diverse vertebrate fauna that includes – besides fishes, pan-geoemydid turtles, crocodylians, birds and mammals – several well-preserved specimens of a pan-trionychid turtle, which has not been studied so far. Here, we describe the pan-trionychid turtle remains from Na Duong, and, based on a set of unique characters, assign it to a new genus and species. Interestingly, the new taxon shows several morphological similarities to *Trionyx impressus* from the late Eocene of southern

China, originally described as *Aspideretes impressus* by Yeh (1963) and subsequently revised by Danilov *et al.* (2013) and Georgalis & Joyce (2017). Due to the close resemblance of *T. impressus*, we herein assign it to the new genus as well.

Geological setting

The Na Duong Basin is located in northern Vietnam close to the Chinese border (Fig. 1). It represents one of the few areas in East and Southeast Asia with a complete sequence of continental sediments from the middle Eocene to lower Oligocene (Böhme *et al.*, 2013). The basin is part of the Cao Bang-Tien Yen fault system and covers an area of 45 km². The middle–upper Eocene (late Bartonian–Priabonian) Na Duong Formation is 240 m thick with the upper 140 m section being exposed in the Na Duong open cast coal mine. Böhme *et al.* (2013) biochronologically correlated the fossil mammals from Na Duong (layer 80) with the Chinese Naduan land mammal age (= Ulangochuian stage: Wang *et al.*, 2019), and provided an age estimate of 39–35 Ma. Palaeomagnetic data calibrates the Ulangochuian at 40–37 Ma (Wang *et al.*, 2019).

The new taxon, together with most of the other vertebrates, was excavated within the transition zone between the coaly shale of the main seam and the underlying dark-brown claystone (layer 80). The layer 80 sediments represent lacustrine lignitic shales that were deposited at a time of tropical to warm-subtropical climate. The area was also undergoing a transition from shallow pond systems to a large anoxic lake (Böhme *et al.*, 2013; Garbin *et al.*, 2019). This fossil ecosystem has yielded both aquatic and terrestrial faunal elements. The new taxon occurred together with the *pan-geoemydid* *Banhxeochelys trani* Garbin, Böhme & Joyce, 2019, two species of crocodyles (*Orientalosuchus naduongensis* Massonne, Vasilyan, Rabi & Böhme, 2019 and *Maomingosuchus acutirostris* Massonne, Augustin, Matzke, Weber & Böhme, 2021), a bird (Massonne *et al.*, 2022), anthracotheriids and rhinocerotids (Böhme *et al.*, 2013), a strepsirrhine primate (Chavasseau *et al.*, 2019), and fishes representing the families Amiidae and Cyprinidae (Böhme *et al.*, 2013).

Materials and methods

All of the specimens of the new taxon described herein were found at the base of layer 80 (*sensu* Böhme *et al.*, 2011) in the Na Duong coal mine. The material consists

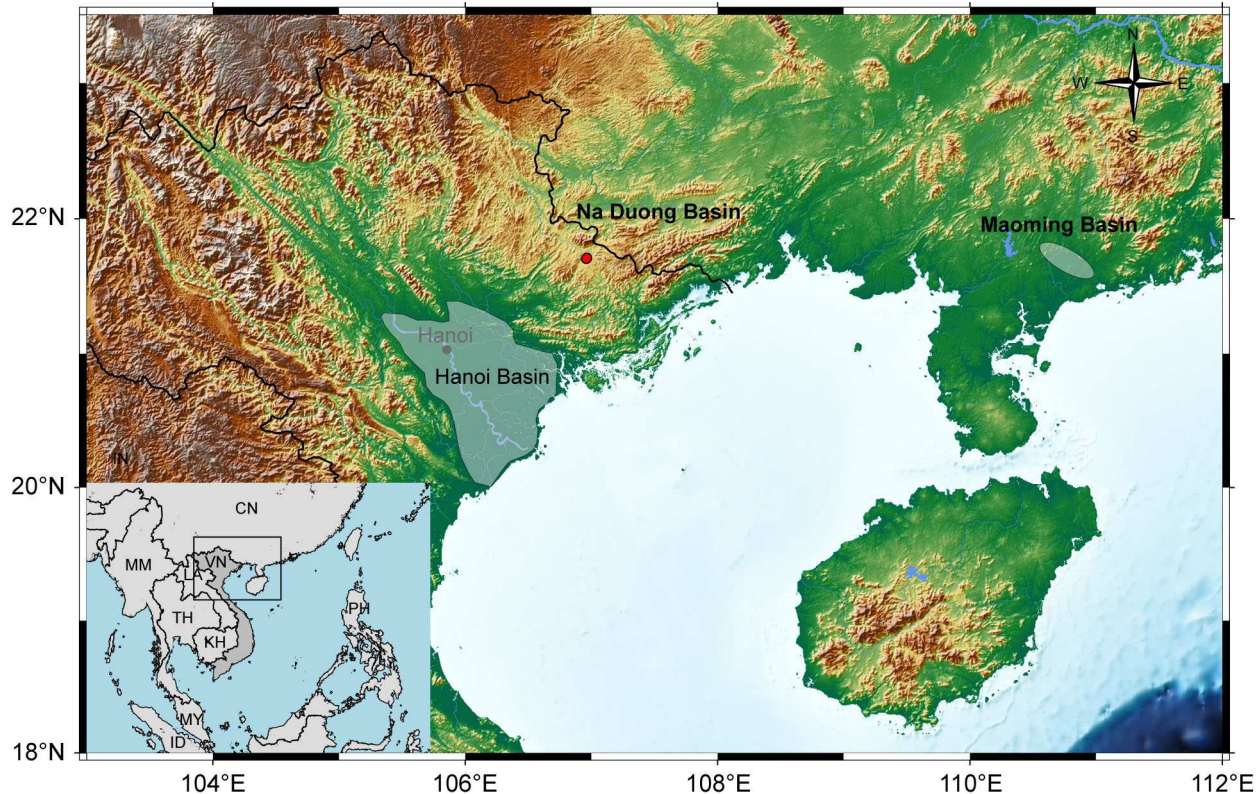


Figure 1. Map of northern Southeast Asia, showing the Na Duong Basin in north-east Vietnam and the Maoming Basin in southern China. The map was created using the Generic Mapping Tools program (Wessel et al., 2019).

of two almost complete carapaces with associated plastral elements and seven partial carapaces, some of them with associated plastral elements. Additionally, a highly weathered skull and pectoral girdle, as well as several isolated plastral elements were found, which, however, cannot be associated with any of the carapaces. The best-preserved specimen and designated holotype consists of an almost complete carapace, which was found associated with several plastral elements (entoplastron, both hypoplastra, the right hypoplastron and the left xiphoplastron), as well as additional postcranial material (one cervical vertebra, the left pectoral girdle and humerus, the right radius and ulna, and a phalanx). The holotype material can be confidently referred to a single individual because it was found semi-articulated.

The data set of Joyce et al. (2018) (see [Supplemental material File S1](#)) was used for the phylogenetic analysis with taxa and rescorings of Lyson et al. (2021) added. The data set is derived from multiple previous data sets including Brinkman et al. (2017), Joyce and Lyson (2010, 2011, 2017), Joyce et al. (2009) and Meylan (1987). Together with the new taxon, the data set consists of 40 taxa and 95 characters. *Adocus lineolatus* Cope, 1874 and *Carettochelys insculpta* Ramsay, 1887

were chosen as outgroup taxa. For the analysis, 11 characters (1, 3, 5, 16, 20, 22, 41, 54, 79, 81, 94) were treated as ordered. A total of 40 characters (42%) could be scored for the new taxon.

The maximum parsimony analysis was conducted as a traditional search in TNT v. 1.5 standard version updated on 13 July 2022 (Goloboff & Catalano, 2016). The multistate characters mentioned above were treated as ordered; the maximum trees were set to 999,999 and the tree replication to 1000. For the branch swapping, tree bisection and reconnection with 10 trees saved per replication was used. Additionally, we applied molecular constraints based on the phylogenetic tree for extant taxa after Le et al. (2014) and an extended implied weighting $k=12$ to decrease the impact of variable characters (Goloboff et al., 2018) as in the analysis of Lyson et al. (2021) and Joyce et al. (2018).

Institutional abbreviations

AMNH, American Museum of Natural History, New York, New York, USA; **FMNH**, Field Museum of Natural History, Zoology Department, Chicago, Illinois, USA; **GPIT**, Geologisch-Paläontologisches Institut Tübingen, Tübingen, Germany; **IVPP**, Institute of

Vertebrate Paleontology and Paleoanthropology, Chinese Academy of Sciences, Beijing, China; **NHMUK**, Natural History Museum, London, UK; **UCMVZ**, University of California Museum of Vertebrate Zoology, California, USA; **USNM**, National Museum of Natural History, Smithsonian Institution, Washington, DC, USA.

Taxonomic nomenclature

We follow the phylogenetic nomenclature of Joyce *et al.* (2021) and highlight all clade names defined herein in italics according to the PhyloCode.

Systematic palaeontology

Testudinata Klein, 1760, *sensu* Joyce *et al.*, 2020

Cryptodira Cope, 1868, *sensu* Joyce *et al.*, 2021

Pan-Trionyichidae Joyce *et al.*, 2004, *sensu* Joyce *et al.*, 2021

Diagnosis. Members of *Pan-Trionyichidae* can be diagnosed by the following shell features: (1) the presence of sculpturing that covers all metaplastic portions of the shell bones; (2) absence of scutes; (3) absence of peripherals; (4) absence of pygals; (5) absence of supra-pygals; (6) boomerang-shaped entoplastron; and (7) a plywood-like microstructure in the metaplastic portions of the shell (modified after Georgalis & Joyce, 2017).

Striatochelys gen. nov.

Diagnosis. *Striatochelys* can be differentiated from other pan-trionyichid genera by the combination of the following characters: (1) relatively small size, with a carapace length reaching an estimated maximum of 27 cm; (2) absence of a preneural; (3) strong straight ridges on the carapace, spanning from costal I to costal VIII; and (4) stronger ridges posteriorly.

Etymology. The genus name is female and derives from the Latin word ‘striatus’ meaning ‘streaked’ due to the multiple anteroposteriorly running ridges across the carapace, resulting in a furrowed surface, and ‘chelys’ meaning turtle in Greek.

Striatochelys baba sp. nov.

(Figs 2–7)

Diagnosis. *Striatochelys baba* can be differentiated from *Striatochelys impressa* comb. nov. by the combination of the following characters: (1) a larger costal VIII,

forming the posterolateral margin of the carapace; (2) presence of ridges on the neurals, which are straight anteriorly and sinusoidal posteriorly; and (3) entoplastron callosity in the shape of a bulge (unknown for *S. impressa* and possibly a synapomorphy for *S. baba* + *S. impressa*).

Etymology. The species name is derived from the Vietnamese word ‘Ba ba’, meaning softshell turtle, declared as substantive.

Holotype. GPIT-PV-112860, carapace, xiphiplastron, thoracic vertebrae (GPIT-PV-112860-1) and partial plastron (entoplastron, GPIT-PV-112860-2; hyoplastron right, GPIT-PV-112860-3; hyoplastron left, GPIT-PV-112860-4; hypoplastron right, GPIT-PV-112860-5) and further postcranial material (cervical vertebra, GPIT-PV-112860-6; left pectoral girdle, GPIT-PV-112860-7; left humerus, GPIT-PV-112860-8; right radius, GPIT-PV-112860-9; right ulna, GPIT-PV-112860-10; phalanx, GPIT-PV-112860-11).

Referred material. Additional material consists of: a nearly complete carapace missing only the nuchal with a right hyo- and hypoplastron (GPIT-PV-122867); a fragmentary carapace with a complete row of neurals and a nuchal (GPIT-PV-122879); the anterior part of a carapace associated with an entoplastron (GPIT-PV-122872); fragmented costals belonging to a larger individual (GPIT-PV-122875); fragmented costals and a right hypoplastron (GPIT-PV-122871); a costal fragment (GPIT-PV-122874); a medial part of a hypoplastron (GPIT-PV-122873); an anterior part of the carapace and right hyo- and hypoplastron (GPIT-PV-112861); a part of the carapace and plastron and a first thoracic vertebra (GPIT-PV-112862 and GPIT-PV-112863); multiple isolated costal fragments belonging to a single individual (GPIT-PV-112864); multiple carapace fragments belonging to a single individual (GPIT-PV-112865); left xiphiplastron and a right costal VIII (GPIT-PV-112866); and a single costal fragment (GPIT-PV-112867).

Additionally, an isolated pectoral girdle (GPIT-PV-122869) and skull (GPIT-PV-122870) putatively belonging to a single individual of a pan-trionyichid turtle, as well as additional postcranial material consisting of an isolated costal fragment (GPIT-PV-122877), a phalanx (GPIT-PV-122878) and a plastron fragment (GPIT-PV-112868) are tentatively referred to *S. baba*.

Type locality and horizon. The fossils were recovered from the base of layer 80 of the Na Duong coal mine (Böhme *et al.*, 2013) in northern Vietnam (21°42.2'N, 106°58.6'E); Na Duong Formation, Eocene, late Bartonian–Priabonian age (39–35 Ma).

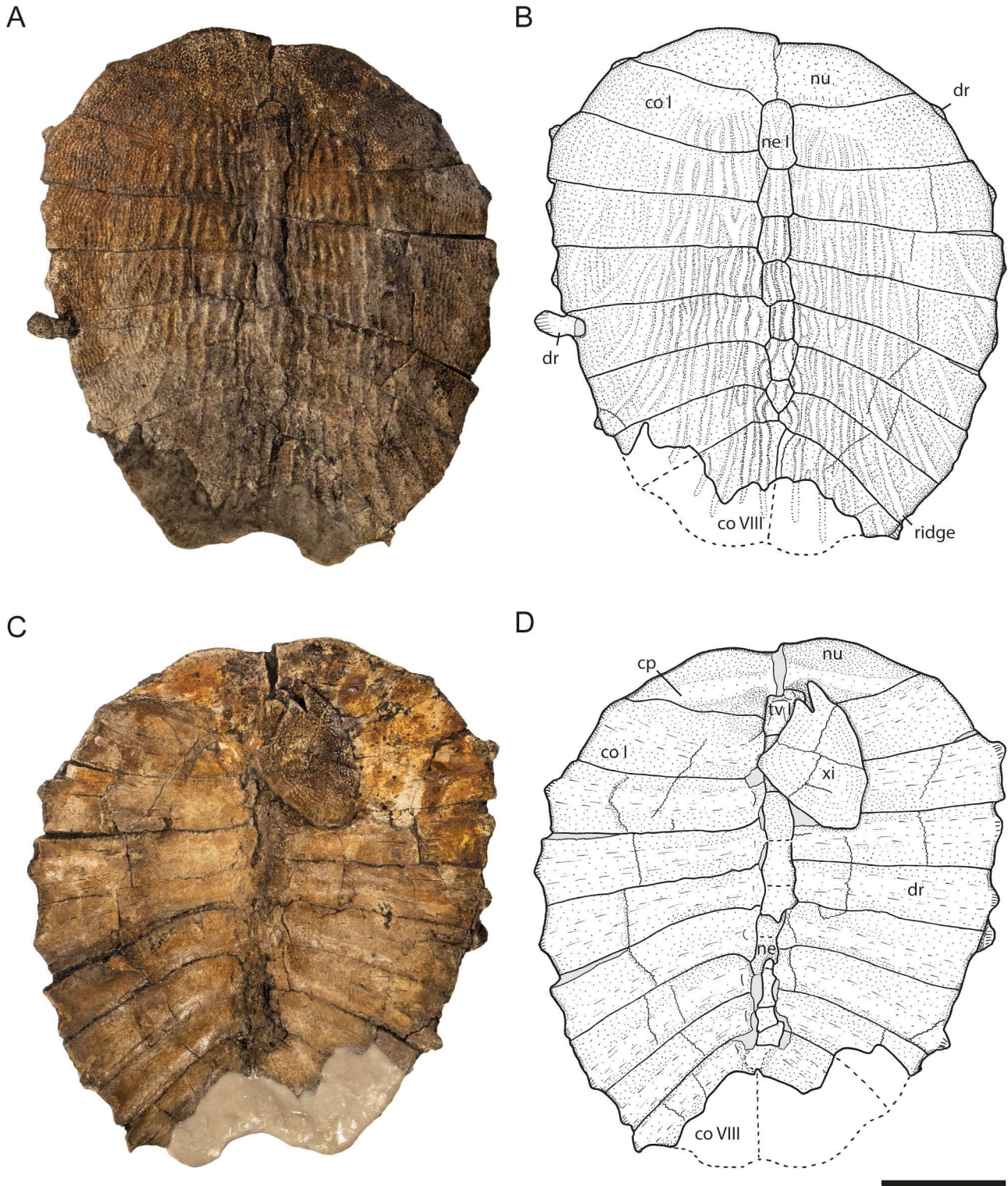


Figure 2. *Striatochelys baba*, holotype, GPIT-PV-112860-1, Na Duong Formation, middle–upper Eocene, Vietnam. Carapace in **A**, **B**, dorsal and **C**, **D**, ventral views. **Abbreviations:** **co**, costal; **cp**, costiform process; **dr**, dorsal rib; **ne**, neural; **nu**, nuchal; **tv**, thoracic vertebra; **xi**, xiphiplastron. Scale bar equals 5 cm.

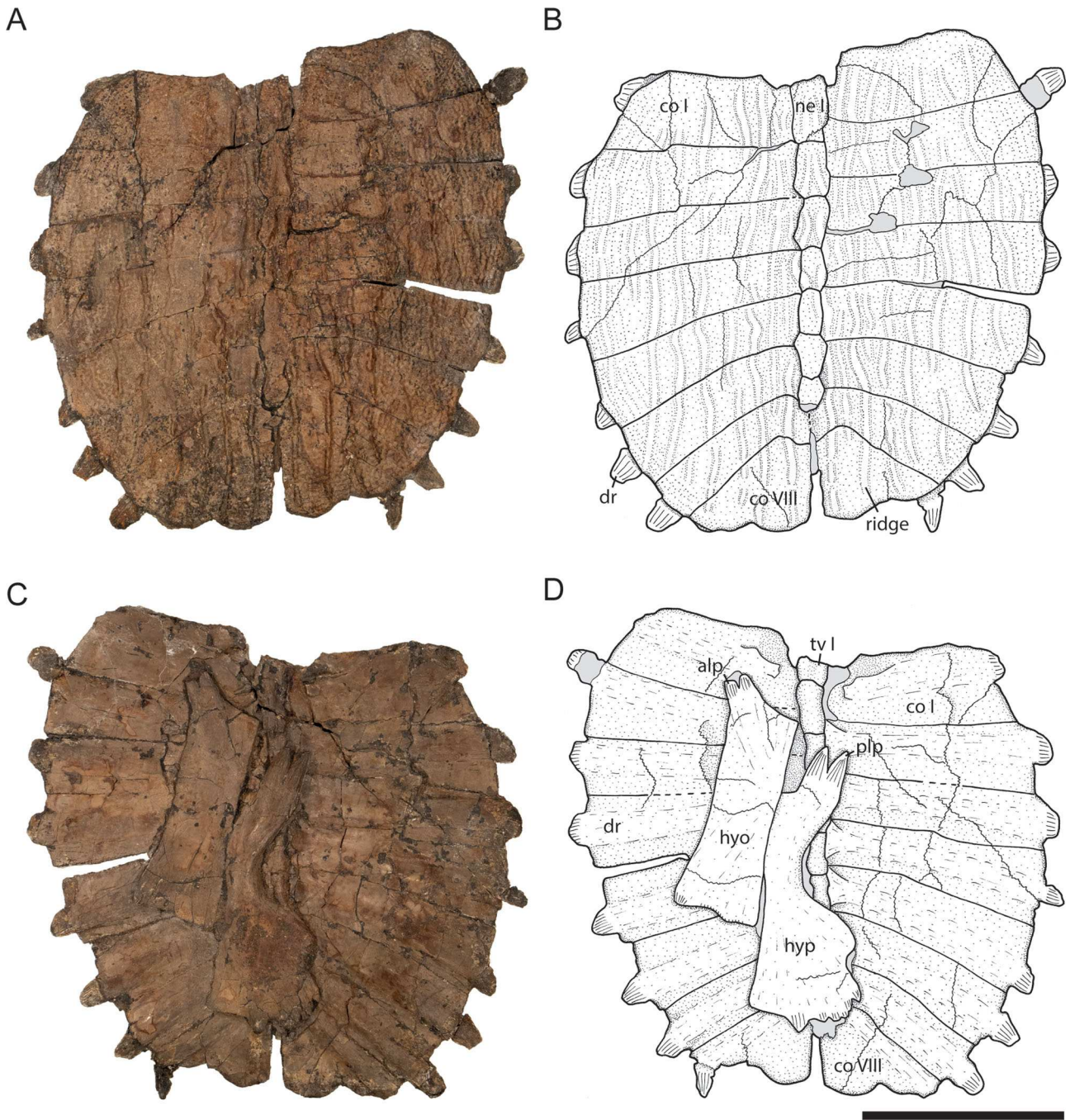


Figure 3. *Striatochelys baba*, GPIT-PV-122867, Na Duong Formation, middle–upper Eocene, Vietnam. Carapace in **A, B**, dorsal and **C, D**, ventral views. **Abbreviations:** **alp**, anterolateral process; **co**, costal; **dr**, dorsal rib; **hyo**, hyoplastron; **hyp**, hypoplastron; **ne**, neural; **plp**, posterolateral process; **tv**, thoracic vertebra. Scale bar equals 5 cm.

Remarks. The holotype carapace of *S. baba* was embedded with its ventral part facing upwards. This allowed for a negative relief of the dorsal carapace, especially the ridges, in the sediment below. Based on those ridges, a cast was modelled for the missing posterior most part, but does not cover the correct outline, as seen in the posteriorly complete specimen GPIT-PV-122867.

Additional species. *Striatochelys impressa* (Yeh, 1963).

Remarks. *Striatochelys impressa* (IVPP V1036) was originally described as *Aspideretes impressus* by Yeh (1963) from the late Eocene deposits of Maoming and was recombined as *Trionyx impressus* by Danilov *et al.* (2013). Georgalis & Joyce (2017) retained the taxon ‘*Trionyx*’

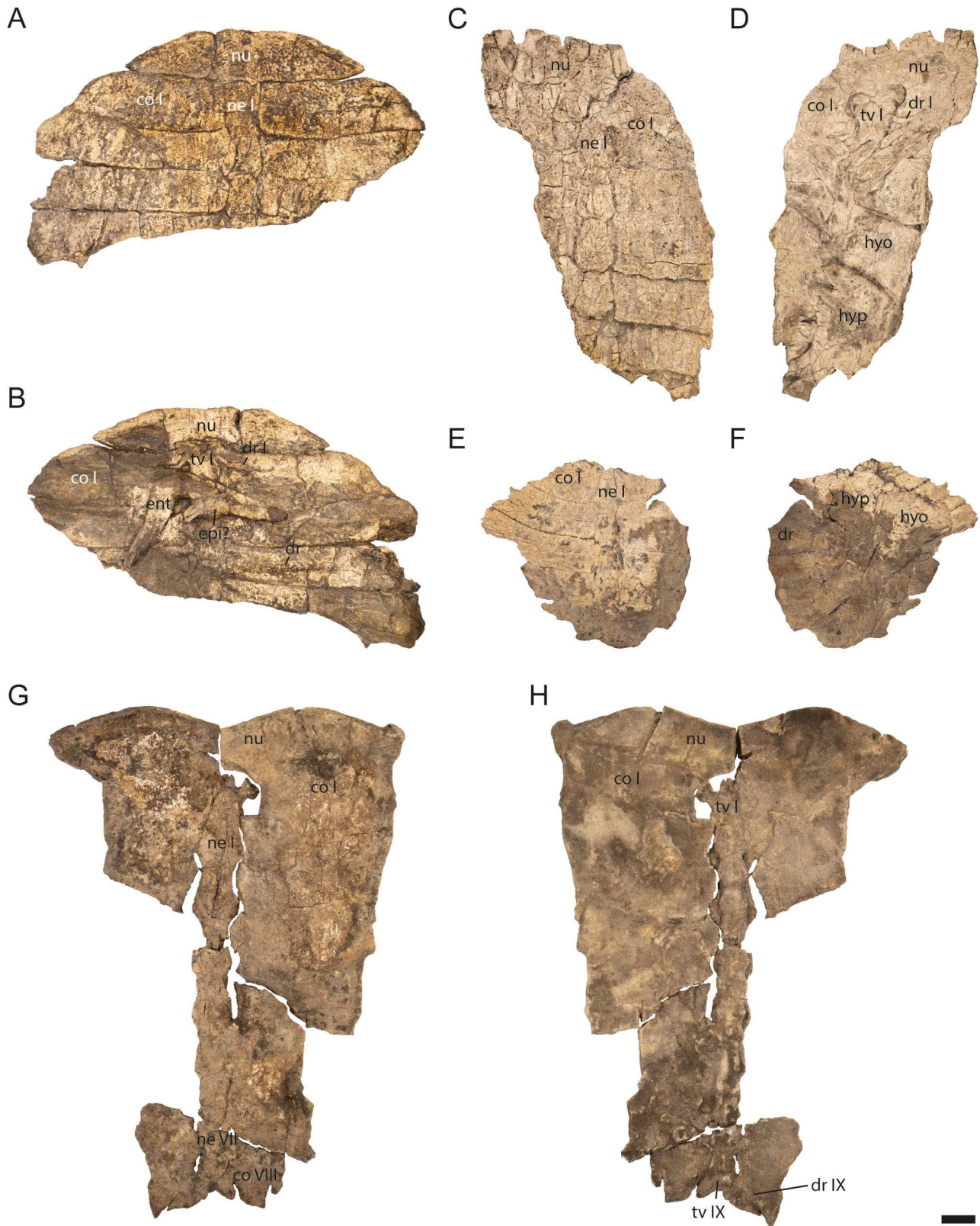


Figure 4. *Striatochelys baba*, Na Duong Formation, middle–upper Eocene, Vietnam. Carapace of GPIT-PV-122872 in **A**, dorsal and **B**, ventral views. Carapace of GPIT-PV-112862 in **C**, dorsal and **D**, ventral views. Carapace of GPIT-PV-112861 in **E**, dorsal and **F**, ventral views. Carapace of GPIT-PV-122879 in **G**, dorsal and **H**, ventral views. **Abbreviations:** **co**, costal; **dr**, dorsal rib; **ent**, entoplastron; **epi**, epiplastron; **hyo**, hyoplastron; **hyp**, hypoplastron; **ne**, neural; **nu**, nuchal; **tv**, thoracic vertebra. Scale bar equals 1 cm.

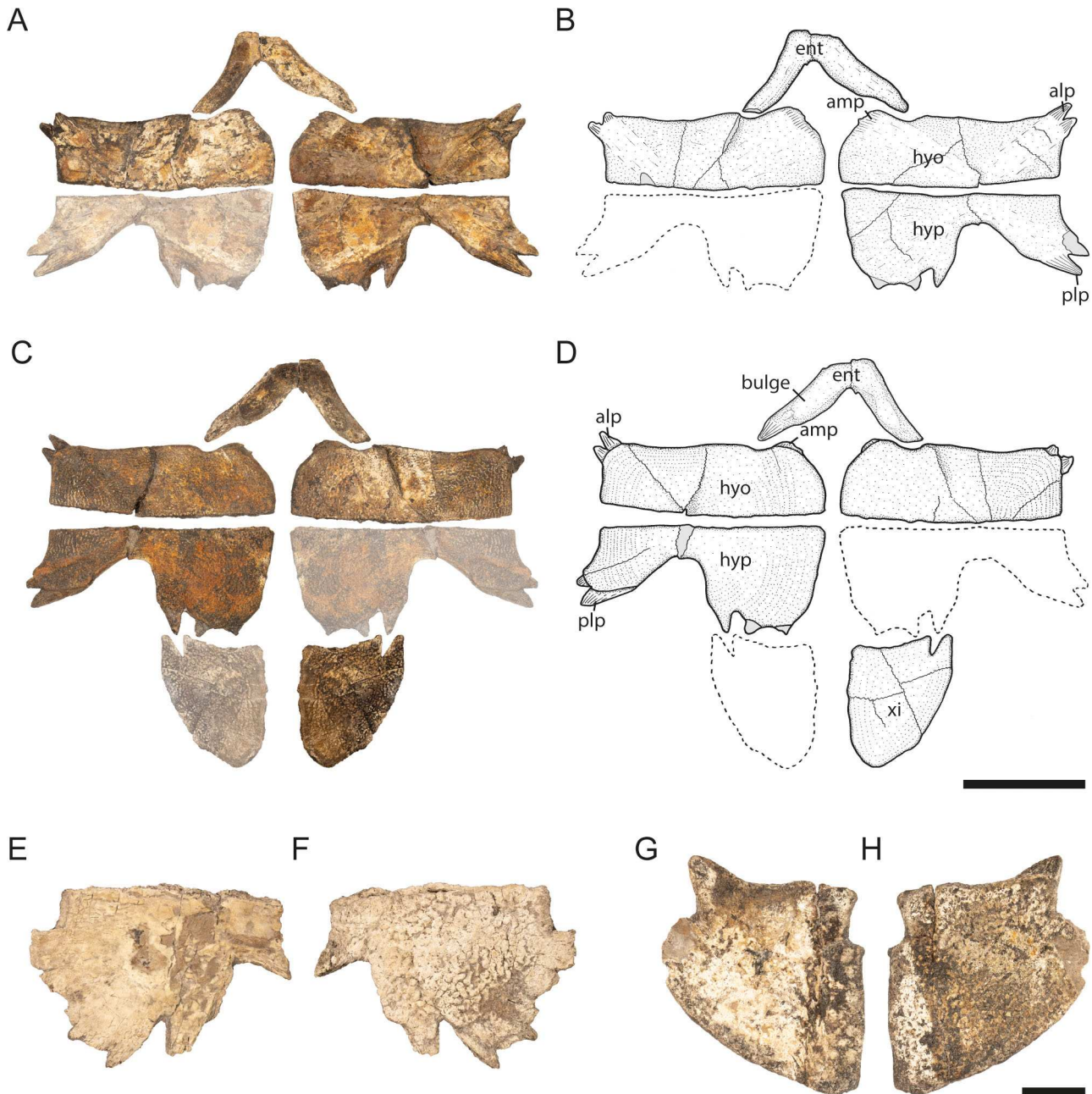


Figure 5. *Striatochelys baba*, Na Duong Formation, middle–upper Eocene, Vietnam. Plastron of holotype (GPIT-PV-112860-2, GPIT-PV-112860-3, GPIT-PV-112860-4, GPIT-PV-112860-5, GPIT-PV-112860-1) in **A**, **B**, dorsal and **C**, **D**, ventral views. Missing bones are mirrored and faded. Right medial hypoplastron fragment (GPIT-PV-122873) in **E**, dorsal and **F**, ventral views. Left xiphiplastron (GPIT-PV-122866) in **G**, dorsal and **H**, ventral views. **Abbreviations:** **alp**, anterolateral process; **amp**, anteromedial process; **ent**, entoplastron; **hyo**, hyoplastron; **hyp**, hypoplastron; **plp**, posterolateral process; **xi**, xiphiplastron. Scale bars equal **A–D**, 5 cm; **E–H**, 1 cm.

impressus as valid but treated its genus-level assignment as uncertain, pending a re-description of the holotype. Based on the high degree of similarity to the new material from Na Duong and a comparison to other relevant taxa, we unite *S. impressa* and the new species from Na Duong under a new genus name herein.

Description

Overall, most of the material is well preserved. It consists of two nearly complete carapaces with associated plastral elements, as well as vertebrae and appendicular elements. Additional postcranial material of the anterior



Figure 6. *Striatochelys baba*, holotype, Na Duong Formation, middle–upper Eocene, Vietnam. Left pectoral girdle (GPIT-PV-112860-7) in **A**, dorsal and **B**, ventral views. Cervical vertebra (GPIT-PV-112860-6) in **C**, dorsal and **D**, ventral views. Left humerus (GPIT-PV-112860-8) in **E**, dorsal, **F**, ventral, **G**, anterior and **H**, posterior views. Right radius (GPIT-PV-112960-9) in **I**, dorsal and **J**, ventral views. Left ulna (GPIT-PV-112860-10) in **K**, dorsal and **L**, ventral views. Phalanx (GPIT-PV-112860-11) in **M**, dorsal and **N**, ventral views. **Abbreviations:** **acd**, anterior condylus; **ap**, acromion process; **ca**, capitellum; **cor**, coracoid; **dp**, dorsal process; **gf**, glenoid fossa; **hh**, humerus head; **if**, intertubercular fossa; **lp**, lateral process; **mp**, medial process; **ph**, phalanx; **prz**, prezygapophysis; **pz**, postzygapophysis; **sc**, scapula. Scale bar equals 1 cm.

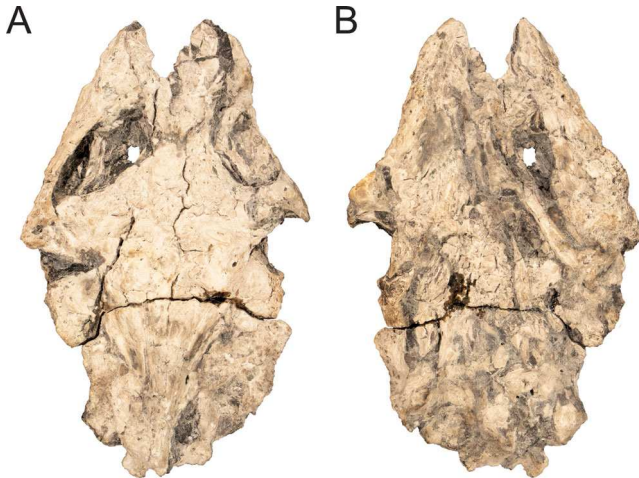


Figure 7. Skull of a *Pan-Trionychidae* referred to *Striatochelys baba*, Na Duong Formation, middle to upper Eocene, Vietnam. Skull of GPIT-PV-122870 in **A**, dorsal and **B**, ventral views. Scale bar equals 1 cm.

skeletal region, including partial carapaces, plastral elements, vertebrae and appendicular material can also be referred to *S. baba*, but are slightly deformed and less well preserved. A single skull referable to a trionychid (here assigned tentatively to *S. baba*) was found, but it is unfortunately highly weathered and no sutures are visible.

Carapace

Two well-preserved carapaces are available, GPIT-PV-112860 (holotype; Fig. 2) and GPIT-PV-122867 (Fig. 3). Other less well-preserved carapaces are also available (GPIT-PV-122872, GPIT-PV-122879, GPIT-PV-112861, GPIT-PV-112862; Fig. 4), together with multiple costal fragments from at least four individuals. *Striatochelys baba* is a medium-sized pan-trionychid. The carapace of the holotype (Fig. 2) is from an adult (or near-adult) specimen based on the very short free ends of the ribs and represents the second largest individual, with a carapace length of 20 cm. Another individual is larger than the holotype but only preserves isolated costal fragments. The best preserved costal III? is one-third larger than its holotype equivalent and leads to an estimated maximum carapace length of around 27 cm, likely representing the maximum carapace size for the species. The maximum width is 18.4 cm for the holotype and around 24.5 cm in the largest individual. The carapace is oval in outline with its maximum width at the level of costal III and tapers anteriorly to a width of 35% of the maximum width at the level of the nuchal and posteriorly to a width of 55% of the maximum

width at the level of costal VIII. The carapace consists of a single nuchal, seven neurals and eight pairs of costal bones. The dorsal ribs are only slightly visible in larger individuals (Fig. 2), whereas they are clearly pronounced in younger ones (Fig. 3).

The central part of the carapace exhibits up to 20 relatively straight prominent ridges with deep furrows in between. All ridges originate at costal I. The medial ridges extend mainly anteroposteriorly and reach costal VIII posteriorly, whereas the more laterally placed ridges diverge posteriorly and extend posterolaterally. However, even the rather straight medial ridges become more sigmoidal on neurals VI and VII (i.e. posteriorly). Approximately half of the ridges are continuous, while the other half become shallower or are even interrupted by the costal sutures. Generally, the medial ridges are more prominent than the lateral ones and become even stronger posteriorly. Two rows of ridges are further present on all neurals in large individuals (Fig. 2). In smaller individuals (e.g. GPIT-PV-122867; Fig. 3), ridges are only pronounced on the anterior neurals and are not visible on neurals VI and VII. This part (i.e. the anterior medial region) of the carapace becomes slightly domed in larger individuals. The lateral part of the carapace is, in contrast, narrower and flat and seems to develop only later in ontogeny and grows with age. Whereas, for example, in the holotype (Fig. 2) and costal III? of the largest individual this region is clearly defined, smaller individuals like GPIT-PV-122867 (Fig. 3) lack this region completely and the central ridged region fills out the complete size of the carapace.

Aside from the ridges, the overall sculpturing of the carapace comprises small pits, which is typical for pan-trionychids. The sculpturing pattern is sectioned into two regions. Towards the centre of the carapace, the sculpturing consists of multiple unordered pits, whereas towards the lateral margins the pits are ordered in lines following the outline of the carapace in multiple rows. The number of rows depends on the size and thus the age of the individual, with more rows being present in larger individuals.

Nuchal. The nuchal is an unpaired bone forming the anterior part of the carapace (Figs 2, 4). It is trapezoidal and around four times wider than long. In some specimens (e.g. GPIT-PV-122879; Fig. 4) there is a strong nuchal emargination, whereas in others, the anterior margin of the nuchal is only slightly convex. In dorsal view, the nuchal is strongly ornamented with many unordered pits anteriorly and shallow furrows posteriorly at the suture with costal I. Suprascapular fontanelles are not present between the nuchal and costal I of *S. baba*. As there is no trace of fontanelles even in the smallest preserved individuals (e.g. GPIT-PV-122872),

the fontanelles most likely close very early in ontogeny. In ventral view, the anterior and posterior costiform processes are united and situated close to the suture with costal I. A prenuchal is absent.

Neurals. In three individuals of *S. baba* (GPIT-PV-112860 [holotype], GPIT-PV-122872, GPIT-PV-122879), the complete set of neurals is preserved. In these individuals, seven neurals are present in total (Figs 2–4). The neurals span from the posterior margin of the nuchal to the middle of the costal VII, but do not reach costal VIII. The preneural is either absent or fused with the first neural. The first neural is the largest neural of the row spanning from the posterior margin of the nuchal to the anterior margin of the costal II. The anterior margin of the first neural is rounded (GPIT-PV-112860, holotype) to pointed (GPIT-PV-122879) in contrast to the straight margins of the more posterior neurals. The first four (GPIT-PV-112860 [holotype], GPIT-PV-122872) to five (GPIT-PV-122879) neurals are hexagonal with a long anterior side and a small posterior one. A reversal occurs on the fifth (GPIT-PV-112860 [holotype], GPIT-PV-122872) or sixth (GPIT-PV-122879) neural. The sixth neural in GPIT-PV-112860 (holotype), and GPIT-PV-122872 is again hexagonal with a short anterior side. The seventh neural in all specimens is much shorter than the others and pentagonal with a pointed posterior tip.

Costals. *Striatochelys baba* has a total of eight paired costals (Figs 2–4). Costals I–VII are similarly-shaped and have a rectangular outline with costal I the antero-posteriorly longest and costal III the lateromedially broadest. The first three costals have a relatively straight, mediolaterally extending suture. More posteriorly, the suture between the costals extends posterolaterally. Costal VIII is trapezoidal and only slightly wider than long. Costals VIII contact each other only anteriorly, whereas posteriorly they are separated by a narrow notch. The posterior margin is only well preserved in GPIT-PV-122872. Medial to the ninth dorsal rib, the costal VIII shows a shallow indentation followed by a convexity. In ventral view, the costals contact two adjacent thoracic vertebrae medially. Depressions for a contact with the ilium are absent on the costal VIII. The tenth thoracic vertebra is only poorly preserved and nothing can be said about its shape. It is also unknown whether a tenth dorsal rib is absent or not preserved.

Plastron

A nearly complete plastron is preserved in GPIT-PV-112860 (holotype; Fig. 5). As for other pan-trionychids the plastron consists of two epiplastra, a single entoplastron, two hyoplastra, two hypoplastra and two

xiphiplastra (Figs 2–5). For *S. baba*, the epiplastra are, however, unknown. A possible epiplastron is present in GPIT-PV-122872, located posteromedially to the entoplastron (Fig. 4B). The plastral bridge is short and only reaches less than half of the hyoplastron width. All plastral elements except for the entoplastron are sculptured with multiple small pits, similar to the carapace.

Entoplastron. The only well preserved entoplastron is GPIT-PV-112860-2 (holotype; Fig. 5). An additional, slightly weathered, entoplastron is preserved in GPIT-PV-122872 (Fig. 4B). The entoplastron is boomerang-shaped with two long posterolateral projecting branches. GPIT-PV-112860-2 (holotype) is asymmetrical, although this appears to be a preservation artefact with the left branch likely showing the correct morphology judging by the comparison with other pan-trionychids. The anterior part of the bone is lateromedially straight. The branches have a straight anterolateral margin and a convex posteromedial one. In lateral view, the entoplastron is slightly curved dorsally with the anterior part being more upturned than the posterior one. The dorsal surface of the bone is smooth, whereas the ventral surface has very prominent oval bulges, which likely represent entoplastral callosities, reaching from the anterior margin to the last third of the branches. The posterior part of the branches ends in a narrow process loosely contacting the hyoplastron.

Hyoplastron. The hyoplastron contacts the entoplastron anteriorly and the hypoplastron posteriorly (Figs 3–5). Four complete hyoplastra are preserved for *S. baba* (GPIT-PV-112860-3, holotype), GPIT-PV-112860-4 (holotype; Fig. 5), GPIT-PV-122867 (Fig. 3), and GPIT-PV-112861 (Fig. 4F). The hyoplastron is rectangular and three times broader than long. The lateral and anterior margins are straight, whereas the medial margin is convex. Posteriorly, it is sutured to the hypoplastron over its whole width. The connection appears, however, to be rather weak, as the two bones were found articulated in only one individual (GPIT-PV-112861). The ventral surface is sculptured with many small pits which are aligned in lines laterally and more diffusely ordered towards the centre of the bone and at its medial margin. The dorsal surface is smooth with the exception of the raised extension of the paired anterolateral processes. The anterior process is slightly longer than the posterior one. In contrast to the anterolateral processes, the anteromedial process is very short and consists of at least two short spikes, but the surface is abraded, making a correct assessment difficult. However, there is no sign of a strong serration. On the anterior margin, at the area of contact with the entoplastron, a shallow flap is developed in GPIT-PV-112860-3 (holotype) and GPIT-PV-

112860-4 (holotype; Fig. 5). In GPIT-PV-122867 (Fig. 3) and GPIT-PV-112861 (Fig. 4F), the anterior margin is, however, completely straight, which might be due to either intraspecific or ontogenetic variation.

Hypoplastron. The hypoplastron contacts the hyoplastron anteriorly and the xiphiplastron posteriorly (Figs 3–5). Three complete hypoplastra are preserved for *S. baba* (GPIT-PV-112860-5 [holotype; Fig. 5]; GPIT-PV-122867 [Fig. 3]; GPIT-PV-112861 [Fig. 4F]). The hypoplastron can be divided into a small lateral part and a much larger medial part, which are connected by a narrow bridge. Anteriorly, it is sutured to the hyoplastron over the whole width. The connection appears to be weak, however, as only one individual (GPIT-PV-112861) has the two bones articulated. The ventral surface is sculptured with many small pits, which are aligned in lines laterally and more irregularly arranged towards the centre and medially. The dorsal surface is smooth except for the raised extension of the paired posterolateral processes. The posterior process is slightly longer than the anterior one. Posteromedially, the hypoplastron has multiple processes. The lateral-most of these projects into a notch between the two anterolateral processes of the xiphiplastron. Medial to this single process is a shallow notch, followed by a posteromedial fan of four connected processes that direct ventromedially (best visible in GPIT-PV-122867 [Fig. 3]; worn away in GPIT-PV-112860-5 [holotype, Fig. 5]). The fan is followed, again, by a small gap and then a single slightly enlarged and medially projecting anterior process (best visible in GPIT-PV-122867; Fig. 3).

Xiphiplastron. The xiphiplastron contacts the hypoplastron anteriorly (Figs 2–5). Only two xiphiplastra are preserved for *S. baba* (GPIT-PV-112860-1 [holotype; Figs 2C, D, 5C, D]; GPIT-PV-112866 [Fig. 5G, H]). The xiphiplastron is triangular with a straight anterior and medial margin and a convex lateral margin. Anterolaterally, there are two prominent processes with a deep notch in between, which encompasses the lateral-most medial process of the hypoplastron. It is not discernible, in any of the preserved specimens, whether the left and right xiphiplastra are sutured to each other along the midline. Although the straight medial margin is somewhat indicative of such a contact, GPIT-PV-112866 (Fig. 5G, H) has two separate medial processes, which are seemingly worn away in GPIT-PV-112860-1 (holotype), and that could have prevented a continuous sutural contact between the xiphiplastra. The ventral surface is sculptured with multiple small pits. Although the arrangement is more irregular than that on the hyo- and hypoplastron, weakly developed rows can be

distinguished, roughly following the bone outline. In contrast to this, the dorsal surface is smooth (Fig. 5G).

Vertebrae

A single cervical vertebra is preserved (Fig. 6C, D), which is slightly deformed and weathered dorsally. Due to incomplete preservation, the bone cannot be assigned to an exact position in the neck. The anterior condyle is round. The prezygapophysis is larger than the postzygapophysis and closer to the centrum. The dorsal portion of the bone is heavily damaged and nothing can be said about the potential presence of a dorsal process. In ventral view, a midline keel projects from a point slightly posterior of the anterior condyle to the posterior end of the bone.

All thoracic vertebrae are fused to the carapace (Figs 2, 3). The first thoracic vertebra reaches anteriorly the level of the nuchal bone midlength. Its prezygapophyses are very broad. The first dorsal rib is not fused to the carapace and is short and slender (Fig. 4B, D; Supplemental material File S2). It originates at the anterolateral part of the first thoracic vertebra and projects posterolaterally until reaching the second dorsal rib. The more posteriorly positioned thoracic vertebrae are rather uniform in size and morphology. No caudal vertebrae of a pan-trionychid have thus far been recovered from Na Duong.

Pectoral girdle

The left pectoral girdle of the holotype GPIT-PV-112860 (Fig. 6A, B) was found in close association with the carapace. As in other pan-trionychids, the scapula and coracoid are tightly sutured at the glenoid fossa with the scapula forming the largest part of the fossa. The scapula has two processes: a dorsal process loosely contacting the carapace and a slightly shorter acromion process. The angle between the acromion process and the main body of the scapula is larger than the angle between the acromion process and the coracoid. The coracoid has a blade-like morphology and is larger than the dorsal process of the scapula. In GPIT-PV-112860-7 (holotype), the blade appears to be anteromedially convex, and thus differs from that of other pan-trionychids, in which the blade is convex posterolaterally. This is, however, likely an artefact stemming from taphonomic distortion.

Appendicular skeleton

Among the bones of the appendicular skeleton, only the left humerus (Fig. 6E–H), the right radius (Fig. 6I, J), the left ulna (Fig. 6K, L) and a single proximal phalanx

(Fig. 6M, N) are preserved, which were all found associated with the holotype carapace (GPIT-PV-112860) and are also referred to the holotype individual. The general morphology of the appendicular skeleton does not differ from that of other members of *Pan-Trionychidae*. The humerus is 'S'-shaped with a prominent medial process and a smaller lateral one. The humerus head is round to oval and the capitellum is small and round. The radius is slightly larger than the ulna and has an elongated morphology with a sloped proximal and a wide distal articulation surface. The ulna has a broad proximal and a narrower distal articulation surface. The phalanx is dumbbell-shaped with broader proximal and narrower distal articular surfaces.

Skull

Only a single, isolated pan-trionychid skull (GPIT-PV-122870; Fig. 7) has been recovered from Na Duong, which we refer tentatively to *Striatochelys baba*. It measures approximately 45 mm and, if corrected for the missing posterior part, it would have had a length of approximately 50 mm. The skull is dorsoventrally compressed, and its surface is highly weathered, to the extent that it is impossible to locate any sutures or other diagnostic traits. The material only allows for an assignment to *Pan-Trionychidae* based on its general slender outline, the anteriorly projecting snout region and the far posteriorly reaching supraoccipital crest. Although it was found isolated it most probably belongs to *S. baba*, as this is the only pan-trionychid currently known from the Na Duong Basin.

Intraspecific and ontogenetic variation

A high degree of intraspecific variation has been described in many pan-trionychid taxa (Meylan, 1987), and the same is true for *Striatochelys baba*. The carapace of the holotype (representing the largest nearly complete specimen) is almost planar laterally. In this area, ridges are absent or only weakly developed, although the typical trionychid ornamentation is present (Fig. 2). This lateral area is, however, almost absent in smaller individuals (Fig. 3), in which the ridges nearly reach the lateral margin of the carapace. The presence of this planar area, which is devoid of the otherwise prominent ridges, in isolated costals of another large individual therefore indicates ontogenetic variation in this feature. Interestingly, there is almost no variation in the number of ridges (up to 20) between individuals irrespective of their ontogenetic stage. Overall, the lateral part of the carapace changes much more during ontogeny than the central part, indicating growth from the lateral margin outwards,

as in the extant *Pelodiscus sinensis* (Wiegmann, 1835) (Sánchez-Villagra et al., 2009).

The position of the reversal of the neural orientation in *S. baba* varies between the fifth and sixth neural. The complete neural row is only visible in three individuals, two of which show a reversal on the fifth neural (Figs 2, 3) and one a reversal on the sixth neural (Fig. 4G). This feature does not seem to correlate with ontogenetic stage, as the individual showing reversal on the sixth neural is intermediate in size.

The hyoplastron has two distinct morphologies in *S. baba*. In the holotype, the hyoplastron forms an anterior notch, into which the posterior process of the entoplastron projects (Fig. 5). This notch is missing in two smaller individuals (Figs 3, 4F). It is conceivable that the stronger contact between the hyoplastron and the entoplastron in the holotype, formed by the notch and the process, is related to the greater robustness of the plastron generally developing later in ontogeny, as is the case for some other species like *P. sinensis* or *Apalone ferox* (Schneider, 1783). To verify this hypothesis, however, more individuals, especially of the same size as the holotype, are needed.

Comparisons

Asian taxa from the Palaeogene

According to Georgalis and Joyce (2017), only a few named *Pan-Trionychidae* from the Palaeogene of Asia are diagnostic and these were chosen for comparison with *Striatochelys baba*. These species are *Kuhnemys palaeocenica*, *Drazinderetes tethyensis*, '*Trionyx*' *linchuensis*, '*Trionyx*' *gregarius*, '*Trionyx*' *johnsoni*, '*Trionyx*' *minusculus*, '*Trionyx*' *ninae* and *Striatochelys impressa* (= '*Trionyx*' *impressus*). Whereas most of these species preserve a complete or nearly complete carapace, in '*T.*' *linchuensis* only the anterior right part of a carapace is known (Yeh, 1962, fig. 1.1), and '*T.*' *minusculus* only preserves a right hyo- and hypoplastron (Chkhikvadze, 1973, pl. 4.2). In addition, comparison with *K. palaeocenica* is complicated by the juvenile status of this species. Comparison with the plastron is even more challenging as it is only partially preserved in *K. palaeocenica* (Danilov et al., 2015, fig. 1), '*T.*' *gregarius* (Gilmore, 1934, fig. 3), '*T.*' *minusculus* (Chkhikvadze, 1973, pl. 4.2) and '*T.*' *ninae* (Vitek & Danilov, 2015, figs 2, 3).

Carapace. The carapace of *S. baba* reaches an estimated size of 27 cm in the largest individual (GPIT-PV-122875), which lies well within the range of '*T.*' *gregarius* and '*T.*' *linchuensis* (Gilmore, 1934; Yeh, 1962). *Drazinderetes tethyensis*, in contrast, is much

larger, with a carapace length of 80 cm (Head *et al.*, 1999). ‘*Trionyx*’ *johnsoni* and ‘*T.*’ *ninae* are only slightly larger than *S. baba*, with a carapace length of around 40 cm (Gilmore, 1931; Vitek & Danilov, 2015). *Kuhnemys palaeocenica* and *S. impressa* are each known from only one specimen and reach a carapace length of 12.5 cm and 14 cm, respectively (Danilov *et al.*, 2015, fig. 1; Ye, 1994, fig. 70). The general shape of the carapace is oval in *S. baba*, which is consistent with most of the other species. It is noteworthy, however, that in *D. tethyensis* the posterior part of the carapace becomes proportionately narrower than in *S. baba* (Head *et al.*, 1999, figs 3, 4), whereas in ‘*T.*’ *gregarius*, the carapace appears to be more rectangular (Gilmore, 1934, fig. 1). The most striking characteristics of *S. baba* are the pronounced ridges on the carapace, projecting in multiple, roughly parallel rows from costal I to costal VIII. In most of the species mentioned above, there are no such ridges, but they are present in *S. impressa* (Yeh, 1963, pl. XX) and, at least posteriorly, in ‘*T.*’ *gregarius* (Gilmore, 1934, fig. 1). Importantly, in both taxa, these ridges do not occur on the neurals as in *S. baba* (Fig. 2).

In *S. baba*, the nuchal is around four times broader lateromedially than long anteroposteriorly. This is also the case in *K. palaeocenica*, ‘*T.*’ *gregarius*, ‘*T.*’ *ninae* and *S. impressa*. In *D. tethyensis*, the nuchal is more robust and only three times broader than long (Head *et al.*, 1999, fig. 3). The nuchal is not preserved in ‘*T.*’ *linchuensis* and ‘*T.*’ *johnsoni*. A shallow nuchal emargination, similar to the one seen in *S. baba*, is also present in ‘*T.*’ *gregarius*, ‘*T.*’ *ninae* and *S. impressa*, whereas there is no such emargination in *K. palaeocenica* (Danilov *et al.*, 2015, fig. 1) or *D. tethyensis* (Head *et al.*, 1999, fig. 3). Suprascapular fontanelles are only present in *K. palaeocenica* (juvenile) (Danilov *et al.*, 2015: fig. 1) and ‘*T.*’ *ninae* (Vitek & Danilov, 2015, fig. 3), while they are absent in all other taxa considered here.

Striatochelys baba has seven neurals in total. This is also the case for *K. palaeocenica*, ‘*T.*’ *johnsoni* and ‘*T.*’ *ninae*. In *S. impressa*, there are eight neurals (Yeh, 1963, fig. 70) and the number of neurals is unknown in *D. tethyensis* and ‘*T.*’ *linchuensis*. A distinct preneural element is only present in *D. tethyensis* (Head *et al.*, 1999, fig. 3), whereas in the other Asian species, the preneural is absent. The last neural is always the smallest neural in the species considered here, except for *K. palaeocenica*, in which the last neural is slightly larger than the penultimate one (Danilov *et al.*, 2015, fig. 1). In *S. impressa*, the region around the first neural is not preserved, making a statement on the presence or absence of a preneural challenging. The reversal of the neural orientation in *S. baba* varies between the fifth

and sixth neural (Figs 2, 3, 4G), but intraspecific variation in the location of the reversal is common among *Pan-Trionychidae* (Meylan, 1987). A reversal on the fifth neural is also known for ‘*T.*’ *johnsoni*, ‘*T.*’ *ninae* and *S. impressa*, whereas it occurs on the sixth in ‘*T.*’ *gregarius*. In *K. palaeocenica*, the neurals are more uniformly shaped. The last neural does not reach costal VIII in *S. baba*, which is also true for the other species considered here, except for ‘*T.*’ *gregarius* and *S. impressa*, in which the additional eighth neural reaches costal VIII (Gilmore, 1934, fig. 1; Yeh, 1973, fig. 70).

Costals I–VII are almost uniformly shaped in *S. baba*. While this is true for most other species as well, in *D. tethyensis* and ‘*T.*’ *ninae* costal I is much shorter lateromedially and costal II much more expanded distally (Head *et al.*, 1999, fig. 3; Vitek & Danilov, 2015, figs 2, 3). In *S. baba*, the anteroposteriorly longest costal is the first, whereas in *K. palaeocenica*, *D. tethyensis*, ‘*T.*’ *gregarius* and ‘*T.*’ *ninae* the second costal is longer (Danilov *et al.*, 2015, fig. 1; Gilmore, 1934, fig. 1; Head *et al.*, 1999, fig. 3; Vitek & Danilov, 2015, figs 2, 3). In *S. baba*, costal VIII is triangular and anteroposteriorly longer than costal VI and VII together, which is unknown for the other species from Asia. An overall similar but proportionately slightly smaller costal VIII is, however, present in *D. tethyensis*, ‘*T.*’ *gregarius* and *S. impressa*, in which it barely reaches the size of costal VI and VII together (Gilmore, 1934, fig. 1; Head *et al.*, 1999, fig. 3; Ye, 1994, fig. 70). In *K. palaeocenica* and ‘*T.*’ *ninae*, costal VIII is much smaller and shorter than costal VII and only forms the posterior margin of the carapace (Danilov *et al.*, 2015, fig. 1; Vitek & Danilov, 2015, figs 2, 3), and in ‘*T.*’ *johnsoni* it is additionally also more ‘U’-shaped than triangular (Gilmore, 1931, pl. XI; Ye, 1994, fig. 74).

Plastron. *Striatochelys baba* has a relatively well-developed and robust plastron. The entoplastron is boomerang-shaped with relatively short branches, which project posteriorly into a notch of the hyoplastron. Based on the width of the carapace, the two hyo- and hypoplastra must have nearly contacted each other at midline; yet the medial processes of the hypoplastra present in *S. baba* indicate that they did not have a sutural contact. It is difficult to ascertain whether the xiphoplastra were sutured to each other along their midline (Fig. 5). Unfortunately, among the Asian taxa, only *K. palaeocenica* and ‘*T.*’ *gregarius* preserve a complete plastron, which, in both cases, shows a completely different morphology. In these two species, the hyo-, hypo- and xiphoplastra are much farther apart from their counterparts and the entoplastron is slenderer with longer branches, which do not project posteriorly into a notch of the hyoplastron (Danilov *et al.*, 2015, fig. 1; Gilmore, 1934, figs 3, 4). Furthermore, there is no

callosity in the shape of a bulging area in the central region of the bone in ventral view in those species, as is the case for *S. baba* (Fig. 5).

The hyoplastron of *S. baba* is relatively long antero-posteriorly and has a straight anterior margin and, at least in the holotype (Fig. 5), a well-developed notch anteriorly, in which the branches of the entoplastron fit. Additionally, the anterolateral process consists of two short spikes and the anteromedial processes consist of at least two short spikes, but assessment is difficult due to an eroded surface. In *K. palaeocenica*, the hyoplastron also possesses a straight anterior margin, but it differs in being very slender, having no notch anteriorly and having very long anterolateral and anteromedial processes (Danilov et al., 2015, fig. 1). The hyoplastron of ‘*T. ninae*’ is very similar to that of *K. palaeocenica*, but is slightly more robust and has a bowed anterior margin (Vitek & Danilov, 2015, figs 2, 3). ‘*Trionyx*’ *gregarius*, on the other hand, is more similar to *S. baba*, but the anterior margin is more rounded than straight and there is no notch for encompassing the branches of the entoplastron (Gilmore, 1934, fig. 3). The hyoplastron of ‘*T. minusculus*’ is, again, quite similar to that of *S. baba*, but also appears to have a more rounded anterior margin and no notch for encompassing the branches of the entoplastron (Chkhikvadze, 1973, pl. 4.2).

The hypoplastron of *S. baba* is divided into an antero-posteriorly short lateral part and a longer medial part, which are separated by a marked constriction. The lateral part possesses two small posterolateral processes, and on the medial part, there are more than three short posteromedial processes arranged in a fan-like manner (Figs 3, 5E, F); the exact number of processes on the medial part of the hypoplastron is difficult to assess, as they are broken (Figs 3, 4F) or nearly completely eroded (as in the holotype; Fig. 5). As is the case for the hypoplastron, the hypoplastron of *K. palaeocenica* is much slenderer and the processes are much longer (Danilov et al., 2015, fig. 1). From ‘*T. ninae*’, only fragments of a hypoplastron are preserved, but it is clear that the posterolateral process is much longer than in *S. baba* (Vitek & Danilov, 2015, fig. 2). In ‘*T. minusculus*’, the lateral and medial processes are not preserved, but the lateral part of the hypoplastron is as long anteroposteriorly as the medial part, a condition differing from *S. baba* (Chkhikvadze, 1973, pl. 4.2). The closest resemblance to *S. baba* with respect to the hypoplastron is shown again by ‘*T. gregarius*’. The only (small) differences are the slightly more robust hypoplastron of ‘*T. gregarius*’ and the larger paired posterolateral processes in this species (Gilmore, 1934, fig. 3).

The xiphiplastron of *S. baba* is triangular and robust. The xiphiplastra could have had a long sutural contact

with each other along the midline (Fig. 5), although this is difficult to ascertain (see above). As for the other Asian taxa, xiphiplastra are only preserved in *K. palaeocenica* and ‘*T. gregarius*’ (Danilov et al., 2015, fig. 1; Gilmore, 1934, fig. 3). The xiphiplastra of these two species are rather similar to each other but differ strongly from those of *S. baba*. They are much slenderer, rectangular as opposed to triangular, and have four long processes one at each corner.

***Gilmoremys* from the Cretaceous of North America**

Besides *S. impressa*, the closest resemblance to *S. baba* among *Pan-Trionychidae* is shown by some members of *Plastomenidae* from the Late Cretaceous of North America. The carapace and plastron of *Gilmoremys lancensis* (Gilmore, 1916) and especially of *Gilmoremys gettyspherensis* Joyce, Lyson and Sertich, 2018 are very similar in overall morphology to both species of *Striatochelys*.

Carapace. *Gilmoremys lancensis* has an overall carapace length of 34 cm and thus is larger than both *S. baba* and *S. impressa* (carapace lengths of 27 cm and 14 cm, respectively) as well as its sister taxon *G. gettyspherensis* (carapace length of 25 cm). The overall carapace shape is similar in *G. lancensis* and *G. gettyspherensis*, as well as in *S. baba* and *S. impressa*, all having an oval outline and a distinctive sculpturing on the dorsal surface of the carapace. *G. lancensis* differs from both *G. gettyspherensis* and the two species of *Striatochelys* in having sculpturing that consists of grooves (Joyce & Lyson, 2011, figs 8, 10). In *G. lancensis*, *S. baba*, and *S. impressa*, on the other hand, the sculpturing consists of well-developed longitudinal ridges, that reach from costal I anteriorly to costal VIII posteriorly (for *S. baba*, see Figs 2, 3; for *S. impressa* see Yeh [1963, pl. XIX, fig. 3, and pl. XX, fig. 1]; for *G. gettyspherensis* see Joyce et al. [2018, fig. 2]).

The nuchal of *G. lancensis* is as wide as it is in *Striatochelys*. It differs from the latter, however, in the absence of a nuchal emargination (Joyce & Lyson, 2011, figs 8, 10). Further differences occur in the number of neurals. *Striatochelys baba* and *G. lancensis* both have a total of seven neurals, whereas there are eight neurals present in *S. impressa* and *G. gettyspherensis*. Another difference lies in the presence of a preneural and a small first neural in the two species of *Gilmoremys* (Joyce & Lyson, 2011, figs 8, 10; Joyce et al., 2018, fig. 2). In *S. baba*, the preneural is absent (Figs 2, 3); in *S. impressa*, the region is not preserved. In *Gilmoremys*, costal II is laterally enlarged and projects anteriorly, reducing the lateral margin of costal I

(Joyce & Lyson, 2011, figs 8, 10; Joyce *et al.*, 2018, fig. 2). In *Striatochelys*, by contrast, the distal part of costal II is not enlarged and the distal margin of costal I and II are similarly-sized (Figs 2, 3; Ye, 1994, fig. 70). Costal VIII is, in all four species, triangular and enlarged. It is largest in *S. baba*, in which it is anteroposteriorly slightly longer than costal VI and VII together, whereas it is barely the size of costal VI and VII together in the other species.

Plastron. In contrast to the carapace, which shows many (small) differences despite its overall resemblance, the plastron is extremely similar in *Striatochelys* and *Gilmoremys*. The hyoplastron of *Gilmoremys* has a well-developed anterior notch for the entoplastron (Joyce & Lyson, 2011, figs 9, 11; Joyce *et al.*, 2018, fig. 3), a feature that is also present in one individual of *S. baba* (Fig. 5), but absent in two others (Figs 3, 4G, H). The posterolateral processes of the hypoplastron of *Gilmoremys* are slightly larger than in *S. baba*, while the fan-like posteromedial processes present in *Striatochelys* are only weakly developed or absent in *Gilmoremys* (Joyce & Lyson, 2011, figs 9, 11; Joyce *et al.*, 2018, fig. 3). The xiphoplastron in all three species has the same triangular morphology but is anteroposteriorly slightly longer in *Gilmoremys* (Joyce & Lyson, 2011, figs 9, 11; Joyce *et al.*, 2018, fig. 3) than in *S. baba* (Figs 5C, D, G, H).

Extant taxa from Southeast Asia

Southeast Asia has the highest diversity of extant trionychids. According to molecular data, most Asian taxa belong to a single monophyletic group, including five genera, i.e. *Pelodiscus*, *Palea*, *Dogania*, *Amyda* and *Nilssonina*, which likely originated between the Eocene and Miocene (Engstrom *et al.*, 2004; Le *et al.*, 2014; Pereira *et al.*, 2017; Thomson *et al.*, 2021). Based on the middle to late Eocene age and Southeast Asian distribution of *Striatochelys baba*, a comparison with selected members of this extant group is provided below.

Carapace. With a bony disc length (BDL) of 27 cm (GPIT-PV-122875), *S. baba* is far larger than the smallest *Pelodiscus* species, i.e. *Pelodiscus huangshanensis* and *Pelodiscus shipian*, which barely reach 10 cm BDL, but it is much smaller than the large *Nilssonina* and *Amyda* species (e.g. *Nilssonina leithi* [Gray, 1872], *Nilssonina gangetica* [Cuvier, 1825], *Amyda cartilaginea* [Boddaert, 1770]), with a BDL between 38 and 60 cm. In contrast to this, *Dogania subplana* (Geoffroy Saint-Hilaire, 1809) and *Palea steindachneri* (Siebenrock, 1906) have a roughly similar size, with 21.7 and 30 cm BDL, respectively (S. Gong *et al.*, 2022; Y. A. Gong

et al., 2021; Pritchard, 2001). The overall carapace morphology in different taxa of *Pan-Trionychinae* is very similar, but one notable difference is the presence or absence of multiple anteroposteriorly extending ridges across the carapace. Such ridges are prominent in *S. baba* (see above). In extant eastern Asian taxa, similar but weaker ridges are often found in early ontogenetic stages (e.g. in *Pelodiscus sinensis*; IVPP 525, USNM 539334). If such ridges are also present later in ontogeny (e.g. in *A. cartilaginea*; FMNH 11088, USNM 22522, 222521), they are much more weakly developed in comparison to *S. baba* and never appear as double rows on the neurals.

In *S. baba*, the nuchal is about four times wider than it is long. Among extant Eastern Asian taxa, this is only the case in the genus *Pelodiscus* (e.g. *P. sinensis* and *Pelodiscus jiangxiensis* Hou *et al.*, 2021) and in *D. subplana*, whereas in other taxa the nuchal is only two to three times wider than long. The absence of a preneural, as in *S. baba* (Figs 2, 3), is common in extant Eastern Asian taxa. Notable exceptions to this are two species of the genus *Nilssonina*, i.e. *Nilssonina hurum* (Gray, 1831) and *N. gangetica*, where a separated preneural is formed. *Striatochelys baba* has seven neurals (Figs 2, 3). In extant taxa, the number of neurals is often variable within a given genus or species, ranging from seven to eight. However, some taxa of the eastern Asian group (*D. subplana*, *A. cartilaginea*, *Nilssonina formosa* [Gray, 1869] and *N. hurum*) invariably have eight neurals. The point of reversal for the neural orientation is less variable in extant eastern Asian taxa and is usually at the fifth or sixth neural. Only *N. gangetica* and *N. hurum* show the same intraspecific variability as *S. baba* (Figs 2, 3, 4G), in which the reversal occurs at either the fifth or the sixth neural. In *S. baba*, costals I–VII are relatively uniformly shaped (Figs 2, 3). This is also the case for most extant eastern Asian taxa, but in *D. subplana* (FMNH 224111, USNM 222523, UCMVZ 95937) and *N. leithii* (FMNH 224231), costal II is distally expanded, similar to the morphology of *D. tethyensis* and ‘*T. ninae*’ (see above). Remarkably, *S. baba* has an enlarged triangular costal VIII, which is longer anteroposteriorly than costal VI and VII combined (Figs 2, 3). In *Nilssonina* spp. (NHMUK 86.8.26.2, FMNH 223231) and *A. cartilaginea* (FMNH 11088, USNM 22522), costal VIII is also triangular and thus shaped similarly, but somewhat smaller than in *S. baba*, while in *D. subplana*, costal VIII has the same elongated morphology as costals I–VII.

Plastron. As mentioned above, the plastron of *S. baba* is relatively well developed and robust. In some extant east Asian species, i.e. *A. cartilaginea* and *D. subplana*, the plastron is much thinner and the hyo- and

hypoplastra are much further apart from their counterparts. In other species, i.e. *Nilssonina* spp. and *P. sinensis*, however, the overall plastron morphology is very similar to that of *S. baba*.

The entoplastron of *S. baba* is relatively slender, it possesses a callosity in the shape of a bulge and its branches project into a notch of the hyoplastron (Fig. 5). In *P. sinensis* (IVPP 556, USNM 539335), the entoplastron is much larger and its branches are slenderer. Additionally, callosities are much less developed and the branches do not project into a hyoplastral notch. In *A. cartilaginea* (FMNH 11088, USNM 22522) and *D. subplana* (FMNH 224111, USNM 222523), the general shape of the entoplastron resembles the condition in *S. baba*, but callosities are much less developed and the branches do not extend into a hyoplastral notch. In *N. gangetica*, the entoplastron is either similarly shaped (FMNH 260430, USNM 293693) or slightly slenderer (NHMUK 86.8.26.1) than in *S. baba*, the callosities are much more weakly developed and the branches do not project into a hyoplastral notch. In *N. hurum* (NHMUK 86.8.26.2), the entoplastron has a shape similar to that in *S. baba* and also shows a callosity in the shape of a bulge. However, the bulge is much more weakly developed than that of *S. baba*. Furthermore, the branches do not project into a hyoplastral notch. In *N. leithi* (FMNH 224231), the shape is again similar to *S. baba*, but callosities are less developed. In contrast to the extant taxa mentioned above, *N. leithi* shows well-defined hyoplastral notches for the branches of the entoplastron.

The hyoplastron of *S. baba* has a moderately short pair of anterolateral processes and at least two short processes anteromedially, which appear to be even shorter than the lateral ones, but their surface is abraded (Figs 3, 5). The morphology of the hyoplastron differs from that found in *A. cartilaginea* (FMNH 11088, USNM 22522) and *D. subplana* (FMNH 224111, USNM 222523, UCMVZ 95937), in which the anterolateral processes are much longer and the anteromedial processes are both much longer and more numerous. In *P. sinensis* (IVPP 556, USNM 68476), the hyoplastron is much more similar to that of *S. baba*. The anterolateral and anteromedial processes are still longer than in *S. baba*, but much shorter than in the aforementioned two taxa. In *N. gangetica* (NHMUK 86.8.26.1, USNM 293693), *N. hurum* (NHMUK 86.8.26.2) and *N. leithi* (FMNH 224231), the processes are more or less identical to those of *S. baba*. Possible small differences in the anteromedial processes can easily be explained by the abraded processes of *S. baba*.

A similar picture emerges in the hypoplastron. The processes in *S. baba* are short and similar in length to those in the hyoplastron. As in the hyoplastron, *A.*

cartilaginea (FMNH 11088, USNM 22522) and *D. subplana* (USNM 222523, UCMVZ 95937) show a different morphology with much longer processes, whereas the morphology in *N. gangetica* (NHMUK 86.8.26.1, NHMUK 293693), *N. hurum* (NHMUK 86.8.26.2) and *N. leithi* (FMNH 224231) is almost identical to that found in *S. baba*. *Pelodiscus sinensis* (IVPP 556, USNM 68476) is again intermediate in this respect: its processes are shorter than in *A. cartilaginea* and *D. subplana*, but still longer than in *Nilssonina* spp. and *S. baba*.

The xiphoplastron of *S. baba* is relatively large, triangular and has short abraded processes (Figs 2, 5). As with the hyo- and hypoplastron the closest similarities are present within *Nilssonina* spp. and *S. baba*. In *N. gangetica* (NHMUK 86.8.26.1, USNM 293693) and *N. hurum* (NHMUK 86.8.26.2) the xiphoplastron looks almost identical to that found in *S. baba*. Small differences occur in the medial processes, which are slightly more pronounced and are not covered with callosities in *S. baba*. In *N. leithi* (FMNH 224231), the xiphoplastron is more massive than in *S. baba* and anteroposteriorly almost as long as the hyo- and hypoplastron combined, whereas in *S. baba* the xiphoplastron reaches only the anteroposterior length of the hypoplastron. In *P. sinensis* (IVPP 556, USNM 68476), the xiphoplastron is less triangular and more elongated. In addition, there is no direct medial contact between the left and right counterparts as is the case for *Nilssonina* spp. and probably also for *S. baba*. In *A. cartilaginea* (FMNH 11088, USNM 22522) and *D. subplana* (USNM 222523, UCMVZ 95937), the xiphoplastron is much slenderer and anterolaterally wider than in *S. baba*.

Discussion of the comparisons

Comparisons with the Palaeogene taxa from Asia underline a general issue concerning *Pan-Trionychidae*: despite many occurrences, the material in question often consists only of fragmentary shell remains, which are rarely diagnostic at the species level (for discussion of the issue, see also Georgalis & Joyce [2017]). Only eight Palaeogene Asian species were considered valid by Georgalis and Joyce (2017), but their preservation differs greatly. Whereas there are multiple complete individuals preserved for '*Trionyx*' *gregarius*, including at least one juvenile, only a single almost complete carapace has been described for *Drazinderetes tethyensis*, '*Trionyx*' *johnsoni*, '*Trionyx*' *ninae* (including some additional fragmentary material) and *Striatochelys impressa*. The only specimen of *Kuhnemys palaeocenica* is a nearly complete shell of a juvenile individual. On the other hand, '*Trionyx*' *linchuensis* only preserves an anterior carapace fragment, and for '*Trionyx*' *minusculus* only a hyo- and hypoplastron are known. *Pan-*

Trionychidae are, however, known for their high intra-specific variation (Meylan, 1987), making comparisons based on single individuals especially difficult.

Aside from the aforementioned Asian *Pan-Trionychidae*, we also provided a comparison with *Plastomenidae* due to it being the only group with prominent anteroposteriorly extending ridges as adults and a very similar plastron morphology; this is especially true for the Late Cretaceous genus *Gilmoremys*. However, plastomenids are so far known only from the Cretaceous and Palaeogene of North America (Joyce & Lyson, 2011; Joyce *et al.*, 2018).

Overall, three features of the carapace and plastron are potentially important for a discussion of the close relationship between *S. baba* and *S. impressa*, as well as to untangle the potential affinity of *Striatochelys* within either *Pan-Trionychinae* or *Plastomenidae*.

- Multiple anteroposteriorly projecting ridges on the carapace are rare in *Pan-Trionychidae*. They occur in some individuals of extant species (e.g. *Apalone ferox*, AMNH 57384, AMNH 65622; *Trionyx triunguis* (Forskål, 1775), AMNH 50723, AMNH 50724; *Amyda cartilaginea*, FMNH 11088, USNM 22522, 22521; *Pelodiscus sinensis*, IVPP 525, USNM 539334), but are much weaker, usually only present in juvenile/subadult individuals and only rarely present in adult specimens. In fossil taxa, however, they also sometimes occur in the shape of prominent ridges in adult specimens. Besides *Striatochelys*, they also appear in *Plastomenus*, e.g. *Plastomenus vegetus* (Gilmore, 1919), in *Gilmoremys gettyspherensis* and (in the form of a finer striation present only posteriorly) in '*T.*' *gregarius*. All species that have prominent carapacial ridges as adults thus belong to *Plastomenidae*. Although such ridges are absent in adult pan-trionychines, the appearance of such ridges in juveniles of several (not particularly closely related) trionychine species, indicates that some species might have retained this morphology in later ontogenetic stages as well.
- The difference in the number of neurals between *S. baba* and *S. impressa* is of low significance for separating these taxa. It is known that the number of neurals varies between individuals of a single species in *Pan-Trionychidae* (Meylan, 1987). Additionally, the number of individuals showing a complete row of neurals is too low in both taxa (three individuals in *S. baba*, one individual in *S. impressa*) to establish a clear difference in this regard. The absence of a preneural (first neural fused to the second neural in the character-taxon matrix of Meylan, 1987) is exclusively known for *Pan-Trionychinae*, with a reversal in *Nilssonina gangetica* and *Nilssonina hurum* and basal

trionychids. The absence of a preneural in *S. baba* hence strongly supports a position for *Striatochelys* inside *Pan-Trionychinae*. Costals I and II are similarly shaped in *S. baba* and *S. impressa*, as in other Asian *Pan-Trionychidae*, except for *D. tethyensis* and '*T.*' *ninae*. This stands in marked contrast to the condition present in *Gilmoremys*, in which costal II is strongly bowed anterolaterally, further pointing away from a close relationship between *Striatochelys* and *Gilmoremys*.

- The plastron of *S. baba* is remarkably similar to that of *Gilmoremys*, whereas there are many differences to most species of *Pan-Trionychinae*. The hyo- and hypoplastron are robust and the lateral and medial processes are short. Moreover, a notch is present at the anterior margin of the holotype, as in *Gilmoremys* (Fig. 5). The triangular xiphiplastra might have been sutured to each other along the midline, based on their straight medial margin; however, only two xiphiplastra are preserved in total and the most complete one (Figs 5G, H) has an anteromedial process that possibly prevented such a suture. In the majority of *Pan-Trionychinae*, on the other hand, the plastron is much more reduced and the lateral and medial processes are longer. Exceptions to this are several species of *Nilssonina* spp. In those species, the overall plastron morphology is very similar to that of *S. baba*, including very short lateral and medial processes on the hyo- and hypoplastron and triangular xiphiplastral. The overall plastron morphology thus indicates a closer relationship of *Striatochelys* either with *Plastomenidae* or to extant east Asian trionychines.

In conclusion, the carapace of *Striatochelys* strongly indicates affinities to *Pan-Trionychinae*. The absence of a preneural is known only in members of this clade, as well as in basal trionychids, and characters indicating a close relationship with *Plastomenidae* (like the strongly developed ridges on the carapace) can also be found in some juvenile/subadult individuals of *Pan-Trionychinae*. Additionally, differences in the shapes of costals I and II further support a distinction from *Plastomenidae*. The plastron of *S. baba* is very similar to that of *Nilssonina* spp. and possibly indicates a closer relationship of the former to members of this genus. The very similarly-shaped plastron of the plastomenid *Gilmoremys*, on the other hand, probably represents a convergence.

Phylogenetic analysis

For the maximum parsimony analysis, a total of 135 most parsimonious trees with lengths of 327 steps, a

consistency index (CI) of 0.361 and a retention index (RI) of 0.605 were recovered (Fig. 8).

Overall, the strict consensus tree is similar to that of most other recent analyses based on the same data set in recovering a monophyletic group, which consists of *Plastomenidae* and *Trionychinae*, as the sister group to *Pan-Cyclanorbinae* (Brinkman et al., 2017; Joyce & Lyson, 2017; Joyce et al., 2018). Alternatively, some analyses find *Plastomenidae*, *Pan-Trionychinae* and *Pan-Cyclanorbinae* in an unresolved polytomy (Joyce et al., 2016; Lyson et al., 2021), or *Plastomenidae*

nested inside *Pan-Cyclanorbinae* (Evers et al., 2023; Joyce & Lyson, 2011).

In the phylogenetic analysis performed here, *Striatochelys baba* is recovered within *Pan-Trionychinae* in a polytomy with *Nilssonina gangetica*, *Nilssonina hurum* and *Nilssonina formosa*. *Pan-Trionychinae* is supported by five synapomorphies, four of which are known exclusively for this group, i.e. characters 4(2), 20(2), 38(1) and 79(0) (if Early Cretaceous taxa are considered part of *Pan-Trionychinae*). A single additional character is found only as an autapomorphy

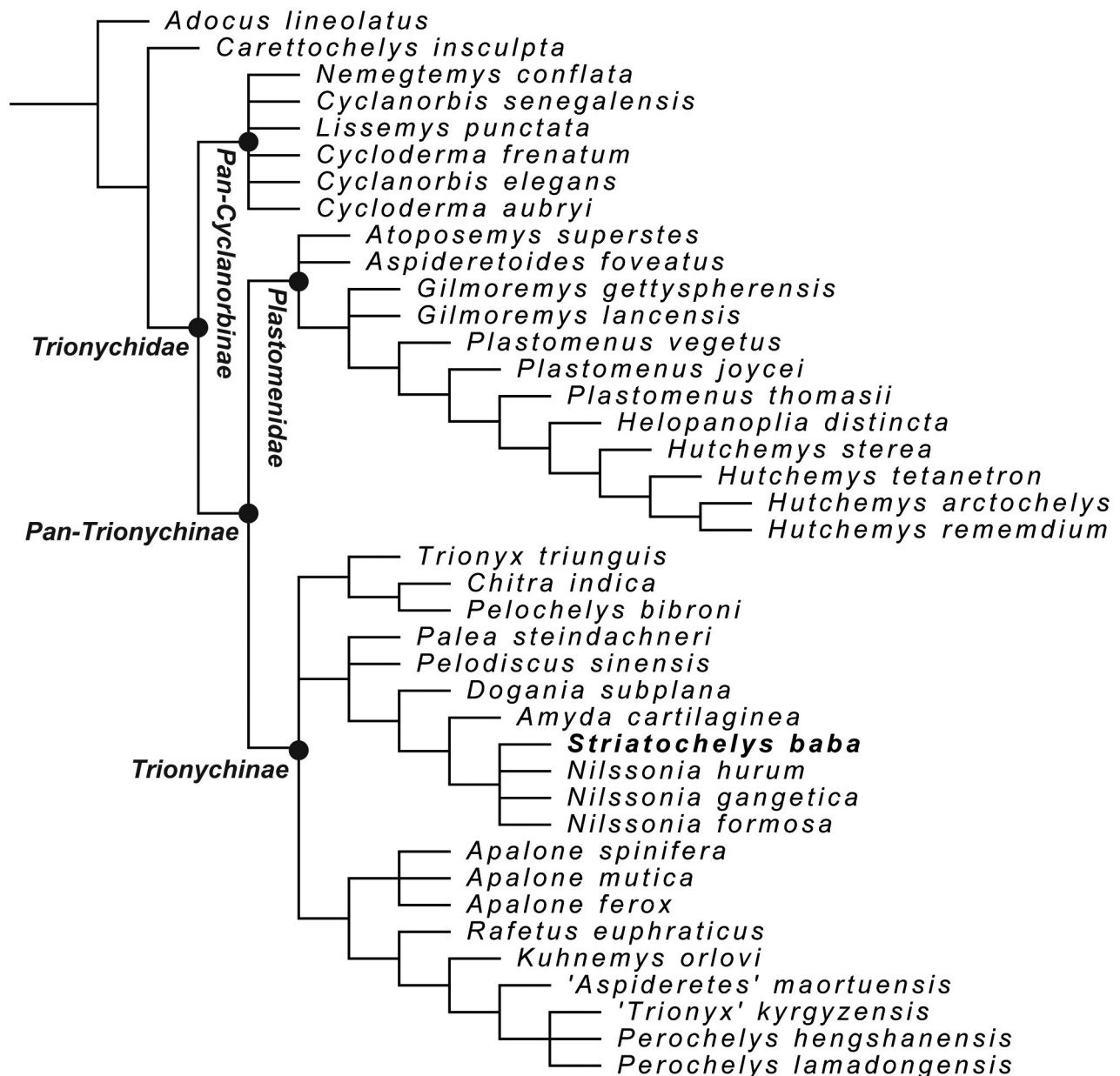


Figure 8. Strict consensus tree of 135 equally optimal trees, obtained from the maximum parsimony analysis of 40 taxa and 95 characters. Tree length = 327 steps; consistency index = 0.361; and retention index = 0.605.

for *Pan-Trionychinae*, if either *Aspideretoides foveatus* (Leidy, 1856) or *Atoposemys superstes* (Russell, 1930) is recovered as the basal-most taxon within *Plastomenidae*. For a complete list of synapomorphies for major groups and additional tree figures, see [Supplemental material File S2](#).

Only a single autapomorphy supports *Nilssonina* spp. + *S. baba* in all trees of our phylogenetic analysis: character 20(1) ‘suprascapular fontanelles closed at hatching’, which is a reversal of one of the autapomorphies outlined above for *Pan-Trionychinae*, in which the fontanelles only close very late in ontogeny. Two other characters (22[2] and 50[1]) are considered autapomorphies for the group only if *S. baba* and *N. gangetica* form a monophyletic sister group with *N. hurum* + *N. formosa* or if *N. gangetica* is the most basal taxon of the group. The relationships between *S. baba* and *Nilssonina* spp. are unresolved. A basal position of *S. baba* is recovered in 33/135 trees, whereas in another 33/135 trees, *S. baba* is found as the sister taxon to *N. gangetica*. A basal position for *N. gangetica*, with *S. baba* being the sister taxon to *N. hurum* + *N. formosa*, is recovered in 34/135 trees. In the remaining 35 trees, *S. baba* is recovered in a derived position inside *Nilssonina* spp., either as sister taxon to *N. formosa* (14/135 trees) or as sister taxon to *N. hurum* (21/135 trees).

However, not only is the position of *S. baba* inside *Nilssonina* spp. ambiguous, but also its position within *Pan-Trionychinae* in general is not stable. The interpretation of the medial edge of the hyoplastron (character 89) is crucial for the position of *S. baba* on the tree. The medial edge of the hyoplastron is worn away, but three small projections can be interpreted as part of a serrated anteromedial process. If they are interpreted as such, or if a more conservative approach is taken and the character is scored as questionable (as is the case for our analysis), *S. baba* is recovered as part of *Nilssonina* spp. However, if the small projections are interpreted as too small for such a serrated edge, *S. baba* is placed in a polytomy with *Gilmoremys getty-spherensis* and *Gilmoremys lancensis* at the base of *Plastomenidae* ([Supplemental material File S2, Fig. 2](#)).

Another problem with the current phylogeny is in the positions of five Early Cretaceous taxa (*Kuhnemys orlovi* Khosatzky, 1976, ‘*Aspideretes*’ *maortuensis* Yeh, 1965, ‘*Trionyx*’ *kyrgyzensis*, *Perochelys hengshanensis* and *Perochelys lamadongensis*) recovered deeply nested inside *Pan-Trionychinae*. If those taxa are forced to the base of *Pan-Trionychinae* in accordance with their age, *S. baba* is found at the base of this Early Cretaceous group, which is in strong contrast to its middle–upper Eocene age ([Supplemental material File S2, Fig. 3](#)).

However, if *K. orlovi* is allowed to float and thus recovered as a *Pan-Trionychinae*, *S. baba* is again nested within *Nilssonina* spp. ([Supplemental material File S2, Fig. 4](#)).

An additional phylogenetic analysis based on the matrix of Evers *et al.* (2023) yields a completely different result and instead places *S. baba* as the basal-most taxon of *Pan-Cyclanorbinae* ([Supplemental material File S2, Fig. 5](#)).

As highlighted above, *S. baba* can be recovered in several different positions on the tree based on only minor changes to the data set. There are two main reasons for this uncertainty. One is related to the problematic position of Early Cretaceous taxa within the crown of *Pan-Trionychinae* (see also Brinkmann *et al.*, 2017; Evers *et al.* 2023; Joyce *et al.*, 2021; Vitek *et al.*, 2018) and a re-evaluation of the characters placing these taxa within the crown seems necessary. The second reason is the preservation of *S. baba* or, more specifically, the poor preservation of its skull, rendering cranial scorings impossible. In the current data set 39/95 characters refer to the skull, while in the data set of Evers *et al.* (2023) the proportion is 62/116. With more than half of the possible scorings missing and high intraspecific variation in *Pan-Trionychinae* (Meylan, 1987), well-justified placement of *S. baba* in the tree is challenging. Until the issues outlined above are properly addressed, the position of *S. baba* within *Nilssonina* spp., as suggested here, should be treated with caution.

Palaeobiogeographical implications

Although the results of the phylogenetic analyses should be treated with caution (see above), the position of *Striatochelys baba* in a polytomy with *Nilssonina* spp. is unsurprising given its age and its occurrence in Southeast Asia. According to Pereira *et al.* (2017), the *Nilssonina* clade originated during the middle–late Oligocene in either East or Southeast Asia, and the split from *Palea steindachneri* and *Amyda cartilaginea* occurred sometime during the late Eocene in Southeast Asia. Based on these data, it seems possible that *S. baba* is more basal than extant *Nilssonina* spp. However, based on other analyses (Evers *et al.*, 2023; Thomson *et al.*, 2021), *Nilssonina* spp. originated much later, in the middle Miocene. These results would indicate a more basal position for *S. baba* within the extant eastern Asian trionychnines.

Unfortunately, the majority of taxa from the Paleogene of central and eastern Asia are only incompletely preserved, severely limiting direct comparisons. Consequently, they were also never included in a

phylogenetic analysis. Interestingly, those taxa do not show any close resemblances to *S. baba* based on our comparisons (see above), the only exception being *S. impressa* from the Maoming locality of southern China. This taxon, as outlined above, appears to be very closely related to *S. baba* from the Na Duong locality of north-eastern Vietnam, most likely representing its sister taxon.

A high degree of faunal similarity between the two localities is also indicated by the pan-geoemydid turtles. From Maoming, two species are known: *Guangdongnemys pingi* Claude, Zhang, Li, Mo, Kuang and Tong, 2012 (minimum number of individuals [MNI]=4) and *Isometremys lacuna* Chow and Yeh, 1962 (MNI = 6). From Na Duong, *Banhxeochelys trani* was recently described by Garbin et al. (2019), who concluded that *B. trani* was most similar to the species from Maoming. The high degree of faunal similarity between the two localities is further supported by the crocodylian fauna: the taxa known from Na Duong, *Orientalosuchus naduongensis* and *Maomingosuchus acutirostris*, are closely related to those from Maoming, *Dongnanosuchus hsui* Shan, Wu, Sato, Cheng and Rufolo, 2021 and *Maomingosuchus petrolicus* (Yeh, 1958), respectively (Massonne et al., 2019, 2021; Shan et al., 2021).

A third locality, which resembles the Na Duong fossil site in terms of its vertebrate assemblage, is the Krabi Basin of southern Thailand. As in Maoming, two pan-geoemydids have been described: *Hardella siamensis* Claude, Suteethorn and Tong, 2007 (MNI = 1) and *Mauremys thanhinensis* Claude, Suteethorn and Tong, 2007 (MNI = 11). Although Garbin et al. (2019) did not find a particularly close relationship between the Krabi taxa and *B. trani*, their phylogenetic analysis yielded a large polytomy including, among others, all five geoemydid taxa mentioned here. As for the crocodylian fauna, *Krabisuchus siamogallicus* Martin and Lauprasert, 2010 is closely related to *O. naduongensis* and *D. hsui*, while a specimen referred to as the ‘Krab-Maomingosuchus’ is closely related to *Maomingosuchus* spp. from Na Duong and Maoming (Martin et al., 2019; Massonne et al., 2019, 2021; Shan et al., 2021). However, no pan-trionychid has so far been described from the Krabi Basin, potentially indicating the prevalence of different environmental conditions that were not suitable for pan-trionychids.

Interestingly, pan-trionychids are rare in the Na Duong Basin compared to other turtles: only nine individuals of *S. baba* were excavated, which stands in marked contrast to the more than 100 individuals known for *B. trani* (Garbin et al., 2019). In Maoming, the pan-geoemydids are, in absolute numbers, less frequent than in Na Duong (*G. pingi*, MNI = 4 and *I.*

lacuna, MNI = 6), but still much more common than *S. impressa* with only a single known individual. Therefore, in both of these localities, pan-geoemydids are approximately 10 times more abundant than pan-trionychids. In Krabi, the number of pan-geoemydids is comparable to Maoming (*H. siamensis*, MNI = 11 and *M. thanhinensis*, MNI = 1). Based on these numbers (and the assumption that pan-trionychids are equally rare in Krabi as they are in Maoming and Na Duong), the absence of a pan-trionychid could also be explained by a sampling bias instead of unsuitable environmental conditions.

Conclusions

Striatochelys baba gen. et sp. nov. is a pan-trionychid from the middle–upper Eocene (late Bartonian–Priabonian, 39–35 Ma) of the Na Duong Basin of northern Vietnam. The taxon is known from extensive shell material of at least nine individuals. The best preserved of these specimens was selected as the holotype, consisting of a virtually complete carapace and plastron. In general, *S. baba* is a medium-sized species characterized by prominent ridges on the carapace (on both costals and neurals) in adult specimens, a larger costal VIII, forming the posterolateral margin of the carapace, and an entoplastron callosity in the shape of a bulge.

Comparison with plastomenids, other Palaeogene pan-trionychids from Asia and extant taxa from Southeast Asia, reveals a close resemblance of *S. baba* to the latter group, particularly to members of the genus *Nilssonina*. Some other characters seen in *S. baba* are otherwise unique to *Plastomenidae*. Our phylogenetic analysis supports the results of these comparisons and recovers *S. baba* in a polytomy with *Nilssonina* spp.

Striatochelys baba is morphologically very similar to a pan-trionychid from the upper Eocene of the Maoming Basin of southern China, which has previously been referred to as ‘*Trionyx*’ *impressus*. Accordingly, we assign ‘*T.*’ *impressus* to the new genus *Striatochelys*, as *S. impressa*. In the past, representatives of *Pan-Geoemydidae* among cryptodirans, as well as of *Orientalosuchina* and *Tomistominae* among crocodylians, have demonstrated a high degree of faunistic similarity between the Na Duong Basin in Vietnam and the Maoming Basin in China. The close resemblance between the two Southeast Asian pan-trionychids further supports this conclusion and provides additional evidence for the close similarity between the reptile faunas of the Na Duong Basin and Maoming Basin.

Acknowledgements

We thank the Editor-in-Chief Paul M. Barrett and Associate Editor Serjoscha Evers, as well as the reviewers Walter G. Joyce and Georgios L. Georgalis, for their comments, which helped us improve the manuscript. We thank our Vietnamese colleagues who facilitated and participated in the Na Duong palaeontological expeditions of 2009, 2011 and 2012: Nguyễn Việt Hưng, La Thế Phúc, Đặng Ngọc Trần, Đồ Đức Quang, and Phan Đông Pha. We further thank Gabriel Ferreira (SHEP), Márton Rabi and Erich Weber (both University of Tübingen) for stimulating discussions and Walter G. Joyce (University of Fribourg) for stimulating discussions and photographs of comparative material of fossil and extant species. Regina Ellenbracht and Henrik Stöhr (both University of Tübingen) are thanked for preparation and Gabriel Ferreira and Christina Kyriakouli (SHEP) for helping with a CT scan. Erich Weber and Ingmar Werneburg (both University of Tübingen) are thanked for granting access to specimens under their care. The Willi Hennig Society is thanked for providing access to the software TNT v. 1.5.

Supplemental material

Supplemental material for this article can be accessed here: <https://doi.org/10.1080/14772019.2023.2217505>

ORCID

Tobias Massonne  <http://orcid.org/0000-0002-6782-5280>

Felix J. Augustin  <http://orcid.org/0000-0002-7787-5601>

Madelaine Böhme  <http://orcid.org/0000-0003-2100-6164>

References

- Boddaert, P.** (1770). *Over de Kraakbeenige Schildpad*. Kornelis van Ton-gerlo.
- Böhme, M.** (1995). Eine Weichschildkröte (Trionychidae) aus dem Untermiozän vom Dietrichsberg bei Vacha (Rhön). *Mauritania (Altenburg)*, 15(3), 357–366.
- Böhme, M., Aiglstorfer, M., Antoine, P. O., Appel, E., Havlik, P., Métails, G., Phug, L. T., Schneider, S., Setzer, F., Tappert, R., Tran, D. N., Uhl, D., & Prieto, J.** (2013). Na Duong (northern Vietnam) – an exceptional window into Eocene ecosystems from Southeast Asia. *Zitteliana A*, 53, 121–167.
- Böhme, M., Prieto, J., Schneider, S., Hung, N. V., & Tran, D. N.** (2011). The Cenozoic on-shore basins of Northern Vietnam: Biostratigraphy, vertebrate and invertebrate faunas. *Journal of Asian Earth Sciences*, 40(2), 672–687. <https://doi.org/10.1016/j.jseae.2010.11.002>
- Brinkman, D., Rabi, M., & Zhao, L.** (2017). Lower Cretaceous fossils from China shed light on the ancestral body plan of crown softshell turtles (Trionychidae, Cryptodira). *Scientific Reports* 7, 1–11. <https://doi.org/10.1038/s41598-017-04101-0>
- Chavasseau, O., Chaimanee, Y., Ducrocq, S., Lazzari, V., Pha, P. D., Rugbumrung, M., Surault, J., Tuan, D. M., & Jaeger, J. J.** (2019). A new primate from the late Eocene of Vietnam illuminates unexpected strepsirrhine diversity and evolution in Southeast Asia. *Scientific Reports*, 9(1), 1–11. <https://doi.org/10.1038/s41598-019-56255-8>
- Chkhikvadze, V. M.** (1971). [New turtles from the Oligocene of Kazakhstan and the systematic position of some species of Mongolia]. *Soobshcheniya Akademii Nauk Gruzinskoi SSR*, 62, 489–492. [In Russian.]
- Chkhikvadze, V. M.** (1973). [Tertiary turtles of the Zaisan Depression]. Tbilisi, Georgia. [In Russian.]
- Chow, M. C., & Yeh, H. K.** (1962). A new emydid from Eocene of Maoming, Kwangtung. *Vertebrata Palasiatica*, 6(3), 225–229.
- Claude, J., Suteethorn, V., & Tong, H.** (2007). Turtles from the late Eocene–early Oligocene of the Krabi Basin (Thailand). *Bulletin de la Société géologique de France*, 178(4), 305–316. <https://doi.org/10.2113/gssgfbull.178.4.305>
- Claude, J., Zhang, J. Y., Li, J. J., Mo, J. Y., Kuang, X. W., & Tong, H.** (2012). Geoemydid turtles from the Late Eocene Maoming basin, southern China. *Bulletin de la Société géologique de France*, 183(6), 641–651. <https://doi.org/10.2113/gssgfbull.183.6.641>
- Cope, E. D.** (1868). On the origin of genera. *Proceedings of the Academy of Natural Sciences, Philadelphia*, 20, 242–300.
- Cope, E. D.** (1874). Review of the Vertebrata of the Cretaceous Period found west of the Mississippi River. *Bulletin of the United States Geological and Geographical Survey of the Territories, First Series*, 2, 3–48.
- Cuvier, G.** (1825). *Recherches sur les ossemens fossiles: où l'on rétablit les caractères de plusieurs animaux dont les révolutions du globe ont détruit les espèces. Contenant la description géologique des couches des environs de Paris parmi lesquelles se trouvent les gypses à ossemens* (Vol. 5,2). Dufour et d'Ocagne.
- Danilov, I. G., Hirayama, R., Sukhanov, V. B., Suzuki, S., Watabe, M., & Vitek, N. S.** (2014). Cretaceous soft-shelled turtles (Trionychidae) of Mongolia: new diversity, records and a revision. *Journal of Systematic Palaeontology*, 12(7), 799–832. <https://doi.org/10.1080/14772019.2013.847870>
- Danilov, I. G., Sukhanov, V. B., Obratzova, E. M., & Vitek, N. S.** (2015). The first reliable record of trionychid turtles in the Paleocene of Asia. *Paleontological Journal*, 49, 407–412. <https://doi.org/10.1134/S0031030115040061>
- Danilov, I. G., Syromyatnikova, E. V., Skutschas, P. P., Kodrul, T. M., & Jin, J.** (2013). The first ‘true’ *Adocus* (Testudines, Adocidae) from the Paleogene of Asia. *Journal of Vertebrate Paleontology*, 33(5), 1071–1080. <https://doi.org/10.1080/02724634.2013.768254>

- Danilov, I. G., & Vitek, N. S. (2013).** Soft-shelled turtles (Trionychidae) from the Bissekty Formation (Late Cretaceous: late Turonian) of Uzbekistan: shell-based taxa. *Cretaceous Research*, *41*, 55–64. <https://doi.org/10.1016/j.cretres.2012.10.003>
- Engstrom, T., Shaffer, H., & McCord, W. (2004).** Multiple data sets, high homoplasy, and the phylogeny of softshell turtles (Testudines: Trionychidae). *Systematic Biology*, *53*, 693–710. <https://doi.org/10.1080/10635150490503053>
- Ernst, C. H., & Barbour, R. W. (1989).** *Turtles of the world*. Smithsonian Institution Press.
- Evers, S. W., Chapelle, K. E. J., & Joyce, W. G. (2023).** Cranial and mandibular anatomy of *Plastomenus thomasi* and a new time-tree of trionychid evolution. *Swiss Journal of Palaeontology* *142*(1), 1–40. <https://doi.org/10.1186/s13358-023-00267-5>
- Forskål, P. (1775).** *Descriptiones animalium, avium, amphibiorum, piscium, insectorum, vermium: quae in itinere orientali observavit*. Hauniae, Copenhagen.
- Gaffney, E. S. (1979).** Description of a large trionychid turtle shell from the Eocene Bridger Formation of Wyoming. *Contributions to Geology, University of Wyoming* *17*, 53–57.
- Garbin, C. G., Böhme, M., & Joyce, W. G. (2019).** A new testudinoid turtle from the Middle to Late Eocene of Vietnam. *PeerJ* *7*(1), e6280. <https://doi.org/10.7717/peerj.6280>
- Geoffroy Saint-Hilaire, E. (1809).** Sur les tortues molles, nouveau genre sous le nom de *Trionyx* et sur la formation des carapaces. *Annales du Muséum national d'histoire naturelle, Paris*, *14*, 1–20.
- Georgalis, G. L. (2021).** First pan-trionychid turtle (Testudines, Pan-Trionychidae) from the Palaeogene of Africa. *Papers in Palaeontology*, *7*, 1919–1926. <https://doi.org/10.1002/spp2.1372>
- Georgalis, G. L., & Joyce, W. G. (2017).** A review of the fossil record of Old World turtles of the clade Pan-Trionychidae. *Bulletin of the Peabody Museum of Natural History*, *58*(1), 115–208. <https://doi.org/10.3374/014.058.0106>
- Gilmore, C. W. (1916).** Description of two new species of fossil turtles, from the Lance Formation of Wyoming. *Proceedings of the United States National Museum*, *50*, 641–646. <https://doi.org/10.5479/si.00963801.50-2137.641>
- Gilmore, C. W. (1919).** *Reptilian faunas of the Torrejon, Puerco, and underlying Upper Cretaceous formations of San Juan County, New Mexico (No. 119)* (pp. 68). US Government Printing Office.
- Gilmore, C. W. (1931).** Fossil turtles of Mongolia. *Bulletin of the American Museum of Natural History*, *59*, 213–257.
- Gilmore, C. W. (1934).** Fossil turtles of Mongolia: second contribution. *American Museum of Natural History Novitates*, *689*, 1–14.
- Goloboff, P. A., & Catalano, S. A. (2016).** TNT version 1.5, including a full implementation of phylogenetic morphometrics. *Cladistics*, *32*(3), 221–238. <https://doi.org/10.1111/cla.12160>
- Goloboff, P. A., Torres, A., & Arias, J. S. (2018).** Weighted parsimony outperforms other methods of phylogenetic inference under models appropriate for morphology. *Cladistics* *34*, 407–437. <https://doi.org/10.1111/cla.12205>
- Gong, S., Fritz, U., Vamberger, M., Gao, Y., & Farkas, B. (2022).** Disentangling the *Pelodiscus axenaria* complex, with the description of a new Chinese species and neotype designation for *P. axenaria* (Zhou, Zhang & Fang, 1991). *Zootaxa*, *5125*(2), 131–143. <https://doi.org/10.11646/zootaxa.5125.2.2>
- Gong, Y. A., Peng, L. F., Huang, S., Lin, Y. F., Huang, R. Y., Xu, Y. H., Yang, D. C. & Nie, L. W. (2021).** A new species of the genus *Pelodiscus* Fitzinger, 1835 (Testudines: Trionychidae) from Huangshan, Anhui, China. *Zootaxa*, *5060*(1), 137–145. <https://doi.org/10.11646/zootaxa.5060.1.7>
- Gray, J. E. (1831).** *Synopsis Reptilium, Pt. 1, Cataphracta. Tortoises, crocodiles, enaliosaurians*. London.
- Gray, J. E. (1869).** Notes on the families and genera of tortoises (Testudinata), and on the characters afforded by the study of their skulls. *Proceedings of the Zoological Society of London*, *37*(1), 165–225. <https://doi.org/10.1111/j.1469-7998.1869.tb07312.x>
- Gray, J. E. (1872).** Notes on the mud-tortoises of India (*Trionyx*, Geoffroy). *Journal of Natural History*, *10*(59), 326–340. <https://doi.org/10.1080/00222937208696710>
- Head, J. J., Raza S. M., & Gingerich, P. D. (1999).** *Drazinderetes tethyensis*, a new large trionychid (Reptilia: Testudines) from the marine Eocene Drazinda Formation of the Sulaiman Range, Punjab (Pakistan). *Contributions from the Museum of Paleontology of the University of Michigan*, *30*, 199–214.
- Hou, X. C., Lin, L., Li, M. M., Jiang, H., & HaiTao, S. (2022).** A new species of the genus *Pelodiscus* (Testudines, Trionychia) from Jiangxi China. *ARPHA Preprints*, *3*, e84618.
- Jasinski, S. E., Heckert, A. B., Sailer, C., Lichtig, A. J., Lucas, S. G., & Dodson, P. (2022).** A softshell turtle (Testudines: Trionychidae: Plastomeninae) from the uppermost Cretaceous (Maastrichtian) Hell Creek Formation, North Dakota, USA, with implications for the evolutionary relationships of plastomenines and other trionychids. *Cretaceous Research*, *135*, 105172. <https://doi.org/10.1016/j.cretres.2022.105172>
- Joyce, W. G., Anquetin, J., Cadena, E. A., Claude, J., Danilov, I. G., Evers, S. W., Ferreira, G. S., Gentry, A. D., Georgalis, G. L., Lyson, T. R., Perez-Garcia, A., Rabi, M., Sterli, J., Vitek, N. S., & Parham, J. F. (2021).** A nomenclature for fossil and living turtles using phylogenetically defined clade names. *Swiss Journal of Palaeontology*, *140*, 5, 1–45. <https://doi.org/10.1186/s13358-020-00211-x>
- Joyce, W. G., & Lyson, T. R. (2010).** A neglected lineage of North American turtles fills a major gap in the fossil record. *Palaeontology*, *53*, 241–248. <https://doi.org/10.1111/j.1475-4983.2009.00929.x>
- Joyce, W. G., & Lyson, T. R. (2011).** New material of *Gilmoremys lancensis* nov. comb. (Testudines: Trionychidae) from the Hell Creek Formation and the diagnosis of plastomenid turtles. *Journal of Paleontology*, *85*, 442–459. <https://doi.org/10.1666/10-127.1>
- Joyce, W. G., & Lyson, T. R. (2017).** The shell morphology of the latest Cretaceous (Maastrichtian) trionychid turtle *Helopanoplia distincta*. *PeerJ*, *5*, e4169. <https://doi.org/10.7717/peerj.4169>
- Joyce, W. G., Lyson, T. R., & Sertich, J. J. W. (2018).** A new species of trionychid turtle from the Upper Cretaceous (Campanian) Fruitland Formation of New Mexico, USA. *Journal of Paleontology*, *92*, 1107–1114. <https://doi.org/10.1017/jpa.2018.30>

- Joyce, W. G., Lyson, T. R., & Williams, S. (2016). New cranial material of *Gilmoremys lancensis* (Testudines, Trionychidae) from the Hell Creek Formation of southeastern Montana, USA. *Journal of Vertebrate Paleontology*, 36(6), e1225748. <https://doi.org/10.1080/02724634.2016.1225748>
- Joyce, W. G., Parham, J. F., Anquetin, J., Claude, J., Danilov, I. G., Iverson, J. B., Kear, B., Lyson, T. R., Rabi, M., & Sterli, J. (2020). Testudines. in K. de Queiroz, P. D. Cantino, & J. A. Gauthier (Eds.), *Phylonyms – A companion to the PhyloCode* (pp. 1049–1051). CRC Press.
- Joyce, W. G., Parham, J. F., & Gauthier, J. A. (2004). Developing a protocol for the conversion of rank-based taxon names to phylogenetically defined clade names, as exemplified by turtles. *Journal of Paleontology*, 78, 989–1013. [https://doi.org/10.1666/0022-3360\(2004\)078<0989:DAFPTC>2.0.CO;2](https://doi.org/10.1666/0022-3360(2004)078<0989:DAFPTC>2.0.CO;2)
- Joyce, W. G., Revan, A., Lyson, T. R., & Danilov, I. G. (2009). Two new plastomenine softshell turtles from the Paleocene of Montana and Wyoming. *Bulletin of the Peabody Museum of Natural History*, 50, 307–325. <https://doi.org/10.3374/014.050.0202>
- Khosatzky, L. I. (1976). A new representative of trionychids from the Late Cretaceous of Mongolia. *Gerpetologiya. Kubanskiy gosudarstvennyy universitet. Nauchnye trudy*, 218, 3–19. [In Russian.]
- Klein, I. T. (1760). *Klassifikation und kurze Geschichte der vierfüßigen Thiere* (translation by F. D. Behn). Lübeck: Jonas Schmidt.
- Le, M., Duong, H. T., Dinh, L. D., Nguyen, T. Q., Pritchard, P. C. H., & McCormack, T. (2014). A phylogeny of softshell turtles (Testudines: Trionychidae) with reference to the taxonomic status of the critically endangered, giant softshell turtle, *Rafetus swinhoii*. *Organisms Diversity & Evolution*, 14, 279–293. <https://doi.org/10.1007/s13127-014-0169-3>
- Leidy, J. (1856). Notices of the remains of extinct reptiles and fishes discovered by Dr. F.V. Hayden in the bad lands of the Judith River, Nebraska Territory. *Proceedings of the Academy of Natural Sciences of Philadelphia*, 8, 72–73.
- Li, L., Joyce, W. G., & Liu, J. (2015). The first soft-shelled turtle from the Jehol Biota of China. *Journal of Vertebrate Paleontology*, 35(2), e909450. <https://doi.org/10.1080/02724634.2014.909450>
- Lyson, T. R., Petermann, H., & Miller, I. M. (2021). A new plastomenid trionychid turtle, *Plastomenus joycei*, sp. nov., from the earliest Paleocene (Danian) Denver Formation of south-central Colorado, USA. *Journal of Vertebrate Paleontology*, 41(1), e1913600. <https://doi.org/10.1080/02724634.2021.1913600>
- Martin, J. E., & Lauprasert, K. (2010). A new primitive alligatorine from the Eocene of Thailand: Relevance of Asiatic members to the radiation of the group. *Zoological Journal of the Linnean Society*, 158(3), 608–628. <https://doi.org/10.1111/j.1096-3642.2009.00582.x>
- Martin, J. E., Lauprasert, K., Tong, H., Suteethorn, V., & Buffetaut, E. (2019). An Eocene tomistomine from peninsular Thailand. *Annales de Paléontologie*, 105(3), 245–253. <https://doi.org/10.1016/j.annpal.2019.03.002>
- Massonne, T., Augustin, F. J., Matzke, A. T., Weber, E., & Böhme, M. (2021). A new species of *Maomingosuchus* from the Eocene of the Na Duong Basin (northern Vietnam) sheds new light on the phylogenetic relationship of tomistomine crocodylians and their dispersal from Europe to Asia. *Journal of Systematic Palaeontology*, 19(22), 1551–1585. <https://doi.org/10.1080/14772019.2022.2054372>
- Massonne, T., Böhme, M., & Mayr, G. (2022). A tarsometatarsus from the late Eocene locality Na Duong – the first Palaeogene fossil bird from Vietnam. *Alcheringa: An Australasian Journal of Palaeontology*, 46(3–4), 291–296. <https://doi.org/10.1080/03115518.2022.2126010>
- Massonne, T., Vasilyan, D., Rabi, M., & Böhme, M. (2019). A new alligatoroid from the Eocene of Vietnam highlights an extinct Asian clade independent from extant *Alligator sinensis*. *PeerJ*, 7, e7562. <https://doi.org/10.7717/peerj.7562>
- Meylan, P. A. (1987). The phylogenetic relationships of soft-shelled turtles (family Trionychidae). *Bulletin of the American Museum of Natural History*, 186, 1–101.
- Nessov, L. A. (1995). On some Mesozoic turtles of the Fergana depression (Kyrgyzstan) and Dzhungar Alatau ridge (Kazakhstan). *Russian Journal of Herpetology*, 2(2), 134–141.
- Pereira, A. G., Sterli, J., Moreira, F. R., & Schrago, C. G. (2017). Multilocus phylogeny and statistical biogeography clarify the evolutionary history of major lineages of turtles. *Molecular Phylogenetics and Evolution*, 113, 59–66. <https://doi.org/10.1016/j.ympev.2017.05.008>
- Pritchard, P. C. H. (2001). Observations on body size, sympatry, and niche divergence in softshell turtles (Trionychidae). *Chelonian Conservation and Biology*, 4, 5–27.
- Ramsay, E. P. (1887). On a new genus and species of fresh water tortoise from the Fly River, New Guinea. *Proceedings of the Linnaean Society of New South Wales*, 1, 158–162.
- Russell, L. S. (1930). A new species of *Aspideretes* from the Paskapoo Formation of Alberta. *American Journal of Science*, 5(115), 27–32. <https://doi.org/10.2475/ajs.s5-20.115.27>
- Sánchez-Villagra, M. R., Müller, H., Sheil, C. A., Scheyer, T. M., Nagashima, H., & Kuratani, S. (2009). Skeletal development in the Chinese soft-shelled turtle *Pelodiscus sinensis* (Testudines: Trionychidae). *Journal of Morphology*, 270(11), 1381–1399.
- Schneider, J. G. (1783). *Allgemeine Naturgeschichte der Schildkröten: nebst einem systematischen Verzeichnisse der einzelnen Arten und zwey Kupfern*. Johann Gotfried Müllersche Buchhandlung.
- Shan, H. Y., Wu, X. C., Sato, T., Cheng, Y. N., & Rufolo, S. (2021). A new alligatoroid (Eusuchia, Crocodylia) from the Eocene of China and its implications for the relationships of Orientalosuchina. *Journal of Paleontology*, 95(6), 1321–1339. <https://doi.org/10.1017/jpa.2021.69>
- Siebenrock, F. (1906). Zur Kenntnis der Schildkrötenfauna der Insel Hainan. *Zoologischer Anzeiger*, 30, 578–586.
- Thomson, R. C., Spinks, P. Q., & Shaffer, H. B. (2021). A global phylogeny of turtles reveals a burst of climate-associated diversification on continental margins. *Proceedings of the National Academy of Sciences*, 118(7), e2012215118.
- Turtle Taxonomy Working Group (Rhodin, A. G. K., Iverson, J. B., Bour, R., Fritz, U., Georges, A., & Shaffer, H. B.) (2021). Turtles of the world annotated checklist and atlas of taxonomy, synonymy, distribution,

- and conservation status (9th ed.). *Chelonian Research Monographs*, 8, 1–472.
- Vitek, N. S., & Danilov, I. G. (2010).** New material and a reassessment of soft-shelled turtles (Trionychidae) from the Late Cretaceous of Middle Asia and Kazakhstan. *Journal of Vertebrate Paleontology*, 30(2), 383–393. <https://doi.org/10.1080/02724631003617548>
- Vitek, N. S., & Danilov, I. G. (2012).** New data on the soft-shelled turtles from the Upper Cretaceous Kyrkkuduk I locality of Southern Kazakhstan. *Proceedings of the Zoological Institute of the Russian Academy of Sciences*, 316(1), 50–56. <https://doi.org/10.31610/trudyzin/2012.316.1.50>
- Vitek, N. S., & Danilov, I. G. (2015).** New material of *Ultrionyx ninae* from the Oligocene of Kazakhstan, with a review of Oligocene trionychids of Asia. *Journal of Vertebrate Paleontology*, 35(5), e973570. <https://doi.org/10.1080/02724634.2015.973570>
- Vitek, N. S., Danilov, I. G., Nakajima, Y., & Hirayama, R. (2018).** Redescription of the skull of ‘*Trionyx*’ *kyrgyzensis* and improved phylogenetic taxon sampling of Cretaceous and Palaeogene soft-shelled turtles (Trionychidae) of Asia, including the oldest crown trionychids. *Journal of Systematic Palaeontology*, 16, 199–211. <https://doi.org/10.1080/14772019.2017.1283365>
- Vitek, N. S., & Joyce, W. G. (2015).** A review of the fossil record of New World turtles of the clade Pan-Trionychidae. *Bulletin of the Peabody Museum of Natural History*, 56(2), 185–244. <https://doi.org/10.3374/014.056.0204>
- Wang, Y., Li, Q., Bai, B., Jin, X., Mao, F., & Meng, J. (2019).** Paleogene integrative stratigraphy and timescale of China. *Science China Earth Sciences*, 62(1), 287–309. <https://doi.org/10.1007/s11430-018-9305-y>
- Wessel, P., Luis, J. F., Uieda, L., Scharroo, R., Wobbe, F., Smith, W. H. F., & Tian, D. (2019).** The generic mapping tools version 6. *Geochemistry, Geophysics, Geosystems*, 20(11), 5556–5564. <https://doi.org/10.1029/2019GC008515>
- Wiegmann, A. F. A. (1835).** Beitrage zur Zoologie gesammelt auf einer Reise um die Erde von Dr. F.J.F. Meyen. Siebente Abhandlung. Amphibien. *Nova Acta Physico-Medica Academia Caesarea Leopoldino-Carolina*, 17, 185–268.
- Ye, X. (1994).** *Fossil and recent turtles of China* (pp. 112). Science Press.
- Yeh, H. K. (1958).** A new crocodile from Maoming, Kwangtung. *Vertebrata Palasiatica* 2, 237–242. [In Chinese, with English summary.]
- Yeh, H. K. (1962).** Note on two fossil trionychid turtles from Shantung and Chekiang. *Vertebrata Palasiatica*, 6, 384–389.
- Yeh, H. K. (1963).** Fossil turtles of China. *Paleontologia Sinica*, 150, 1–112.
- Yeh, H. K. (1965).** New materials of fossil turtles of Inner Mongolia. *Vertebrata Palasiatica*, 9, 47–69.

Associate Editor: Serjoscha Evers